Politechnika Wrocławska

XXII Fluid Mechanics Conference

Book of abstracts

Słok near Bełchatów, 11–14 September 2016

Plan of XXII Fluid Mechanics Conference
11-14 September 2016, Słok near Bełchatów, Poland

<table>
<tr><th>11.09.2016
Sunday</th><th colspan="2">12.09.2016
Monday</th><th colspan="2">13.09.2016
Tuesday</th><th colspan="2">14.09.2016
Wednesday</th></tr>
<tr><td rowspan="8"></td><td colspan="2">8:00 – 13:00 - Registration</td><td colspan="2">8:00 – 13:00 - Registration</td><td colspan="2" rowspan="2">8:00 – 9:00 - Breakfast</td></tr>
<tr><td colspan="2">8:00 – 9:00 - Breakfast</td><td colspan="2">8:00 – 9:00 - Breakfast</td></tr>
<tr><td colspan="2">9:00 – 9:30 - Opening of XXII FMC

Invited lectures
9:30 – 10:15 – K. Moffatt
10:15-11:00 – M. Farge</td><td colspan="2" rowspan="2">Invited lectures
9:00 – 10:00 – G. N. Barakos
10:00-11:00 – A. Herczyński</td><td colspan="2" rowspan="2">Invited lectures
9:00 – 10:00 – J. Szmyd
10:00-11:00 – T. Kowalewski</td></tr>
<tr><td colspan="2">11:00 – 11:20 – Coffee break</td></tr>
<tr><td>11:20 – 13:00 - Session IA (room no. 1A)</td><td>11:20 – 13:00 - Session IB (room no. 2)</td><td>11:20 – 13:00 - Session IIA (room no. 1A)</td><td>11:20 – 13:00 - Session IIB (room no. 2)</td><td>11:20 – 13:00 - Session IIIA (room no. 1A)</td><td>11:20 – 13:00 - Session IIIB (room no. 2)</td></tr>
<tr><td colspan="2">13:00 – 14:20 - Lunch</td><td colspan="2">13:00 – 14:20 - Lunch</td><td colspan="2">13:00 – 14:20 - Lunch</td></tr>
<tr><td>14:20 – 16:00 – Session IC (room no. 1A)</td><td>14:20 – 16:00 – Session ID (room no. 2)</td><td>14:20 – 16:00 – Session IIC (room no. 1A)</td><td>14:20 – 16:00 – Session IID (room no. 2)</td><td colspan="2" rowspan="2">14:00 – 14:30 – Closing ceremony of XXII Fluid Mechanics Conference</td></tr>
<tr><td rowspan="3">Since 16:00 (Hall of the hotel) - Registration of participants of the Conference</td><td colspan="2">16:00 – 16:20 – Coffee break</td><td colspan="2">16:00 – 16:20 – Coffee break</td></tr>
<tr><td>16:20 – 17:40 – Session IE (room no. 1A)</td><td>16:20 – 17:40 – Session IF (room no. 2)</td><td>16:20 – 18:00 – Session IIE (room no. 1A)</td><td>16:20 – 17:40 – Session IIF (room no. 2)</td></tr>
<tr><td colspan="2">Sponsors' presentations - room 1A
18:15 – 18:45 – Intel
18:45 – 19:15 – SymKom
19:15 – 19:45 – UniSens</td><td colspan="2">Sponsors' presentations - room 1A
18:15 – 18:45 – Casp system
18:45 – 19:15 – Eurotek and Dantec</td></tr>
<tr><td>18:00 – 21:00 (Restauracja Zielona) - Welcome dinner</td><td colspan="2" rowspan="2">20:00 – 23:00 – Barbecue</td><td colspan="2" rowspan="2">20:00 – 20:45 – Jazz Quartet concert

20:45 – 23:00 – Banquet
(results of prof. Elsner competition)</td></tr>
<tr><td>19:00 – 20:30 (Sala Pastelowa) - Meeting of Scientific and Organizing Committees with invited speakers</td></tr>
</table>

XXII FLUID MECHANICS CONFERENCE

BOOK OF ABSTRACTS

Editors:
Henryk Kudela, Paweł Regucki, Katarzyna Strzelecka

Słok near Bełchatów, 11–14 September 2016

Oficyna Wydawnicza Politechniki Wrocławskiej
Wrocław 2016

Organizing Committee address
Wrocław University of Science and Technology
Faculty of Mechanical and Power Engineering
Wybrzeże Wyspiańskiego 27
50-370 Wrocław, Poland

The book has been printed in the camera ready form

OFICYNA WYDAWNICZA POLITECHNIKI WROCŁAWSKIEJ
Wybrzeże Wyspiańskiego 27, 50-370 Wrocław
http://www.oficyna.pwr.edu.pl
e-mail: oficwyd@pwr.edu.pl
zamawianie.ksiazek@pwr.edu.pl

SCIENTIFIC COMMITTEE

CHAIRMAN:

Tomasz Kowalewski,
Institute of Fundamental Technological Research,
Polish Academy of Sciences

MEMBERS

Janusz Badur, Szewalski Institute of Fluid-Flow Machinery Polish Academy of Sciences
Andrzej Bogusławski, Częstochowa University of Technology
Tadeusz Chmielniak, Silesian University of Technology
Michał Ciałkowski, Poznań University of Technology
Piotr Doerffer, Szewalski Institute of Fluid-Flow Machinery Polish Academy of Sciences
Stanisław Drobniak, Częstochowa University of Technology
Zbigniew Kosma, Kazimierz Pułaski University of Technology and Humanities in Radom
Anna Kucaba-Piętal, Rzeszów University of Technology
Henryk Kudela, Wrocław University of Science and Technology
Jan Kulczyk, Wrocław University of Science and Technology
Marek Morzyński, Poznań University of Technology
Zbigniew Peradzyński, University of Warsaw
Jacek Pozorski, Szewalski Institute of Fluid-Flow Machinery Polish Academy of Sciences
Romuald Puzyrewski, Gdańsk University of Technology
Jacek Rokicki, Warsaw University of Technology
Kazimierz Rup, Tadeusz Kościuszko Cracow University of Technology
Andrzej Styczek, Warsaw University of Technology
Janusz Szmyd, AGH University of Science and Technology
Jacek Szumbarski, Warsaw University of Technology
Ewa Tuliszka-Sznitko, Poznań University of Technology

ORGANIZING COMMITTEE

Henryk Kudela

Conference chairman,
Wrocław University of Science and Technology

Katarzyna Strzelecka

Conference secretary,
Wrocław University of Science and Technology

Paweł Regucki

Conference manager,
Wrocław University of Science and Technology

HONORARY PATRONAGE

RECTOR OF WROCŁAW UNIVERSITY
OF SCIENCE AND TECHNOLOGY

Wrocław
University
of Science
and Technology

PGE GÓRNICTWO I ENERGETYKA
KONWENCJONALNA S.A.

SPONSORS

Preface

This *Book of abstracts* contains extended summaries of papers that will be presented at XXII Fluid Mechanics Conference (XXII FMC) held in Słok near Bełchatów in Poland during 11th–14th September of 2016. The Conference is organized by Wrocław University of Science and Technology, Polish Academy of Sciences – Committee of Mechanics and Foundation for Development of Wrocław University of Science and Technology.

Let us recall some historical facts: Fluid Mechanics Conferences have been taking place every two years since 1974, which makes a total of forty-two years. The goal of this conference is to provide a forum for exposure and exchange of ideas, methods and results in fluid mechanics.

We have already met in Bełchatów 10 years ago (XXVII KKMP). It was a successful meeting. Since then National Conference on Fluid Mechanics has changed the title and started to be named as Fluid Mechanics Conference in the hopes that it will attract more participants from other countries. English became the Conference's first language and we started to invite world leading scientists – working in the field of fluid mechanics. At the 2006 conference we hosted for the first time prof. Keith Moffatt from the Cambridge University. In this year prof. Moffatt once again promised us to arrive to Bełchatów. The whole fluid mechanics community celebrates 9^2 anniversary of his birthday. So let us also wish happy anniversary to prof. Moffatt.

In the mean time we had to pay last respects to our collages. Prof. Prosnak who is regarded as a founder of Notational Conference on Fluid Mechanics and is well known through his books. Prof. Puzyrewski who was present at all conferences so far. He was providing by his discussions a special value to these conferences, and our colleague prof. Konrad Bajer who was intended to be the organizer and host of the present conference. Short memories to them will be given during the opening ceremony.

Conference topics include, but are not limited to aerodynamics, atmospheric science, bio-fluids, combustion and reacting flows, computational fluid dynamics, experimental fluid mechanics, flow machinery, general fluid dynamics, hydromechanics, heat and fluid flow, measurement techniques, micro- and nano-flow, multi-phase flow, non-Newtonian fluids, rotating and stratified flows and turbulence.

Within the general subjects of this conference, the Professor Janusz W. Elsner's Competition for the best fluid mechanics paper presented during the Conference is organized. Authors holding a M.Sc. or a Ph.D. degree and who are not older than 35 may enter the Competition. Authors with a Ph.D. degree must present individual papers; authors with a M.Sc. degree may present papers with their supervisors as coauthors, including original results of experimental, numerical or analytic research.

Six state-of-the-art keynote papers will be delivered by world leading experts. All contributed papers were peer reviewed. Recommendations were received from the Scientific Committee of the Conference; reviewers were from all Polish scientific-academic centres that are involved in fluid mechanics. Accordingly, of the 66 eligible extended abstracts submitted, after a review process by the Scientific Committee, all papers were selected for presentation at XXII Fluid Mechanics Conference. More than 40 papers were accepted for publishing in the *Journal of Physics: Conference Series*.

We hope that this *Book of abstracts* will be used not only as a guide through the conference's events but also help in the future to access people and topics in fluid mechanics research.

We would like to express grateful appreciation to our colleagues from the Polish Academy of Sciences – Committee of Mechanics, as well as to the Scientific Committee of this conference. Their advices and efforts have helped us to overcome the problems normally associated with organising international meeting. Special thanks goes to the reviewers for their work in encouraging the submission of papers. Their contribution cannot be overestimated.

Thank you very much.

Organizing Committee,
Faculty of Mechanical and Power Engineering,
Wrocław University of Science and Technology

Henryk Kudela
Katarzyna Strzelecka
Paweł Regucki

Professor
W.J. Prosnak
1925–2014

Professor Włodzimierz Juliusz Prosnak, dr h.c. – A Remembrance

S. Drobniak

Częstochowa University of Technology, The Faculty of Mechanical Engineering and Computer Science, Armii Krajowej Avenue 21, 42-200 Częstochowa, Poland. E-mail: drobniak@imc.pcz.czest.pl

Professor Włodzimierz Juliusz Prosnak was born on 21st April 1925 in Łask, later he moved with his parents to Łódź and then, after the outbreak of the 2nd World War to Cracow, where he continued education in technical high school. After the war he obtained maturity diploma (matura) at Mikołaj Kopernik Gymnasium in Łódź. In 1945 he enrolled at the Mechanical Faculty of Łódź Technical University. After the completion of the first year he moved to Warsaw, where he was admitted to Aeronautical Faculty of Warsaw Technical University. He graduated in 1950 as Mechanical and Aeronautical Engineer with MSc in technical sciences. While still a student, in 1948 he was invited by Prof. Jerzy Bukowski to become a Junior Assistant at the Chair of Hydro and Aerodynamics, where he began a scientific career under the guidance of Prof. Julian Bonder. In 1957 he obtained a PhD with distinction and his supervisor was Prof. J. Bonder. In the same year Prof. W. Prosnak obtained an academic appointment of docent and began a scientific career in the field of aerodynamics. Among his first achievements one should mention the design of the first in Poland supersonic wind tunnel. Prof. W. Prosnak spent a period of 1960–1961 as a "Visiting Professor" at Princeton University, USA, where he became fascinated by numerical research in the field, which is known today as CFD (Computational Fluid Mechanics). He continued this research at Warsaw Technical University and Polish Academy of Sciences, where he hold a post of Director of Computer Centre from 1968 to 1970. In 1980 Prof. W. Prosnak moved to Gdańsk, where he continued his scientific investigations in two research institutes of Polish Academy of Sciences, i.e. Institute of Fluid Flow Machinery and Institute of Oceanology. His outstanding achievements were rewarded by the membership of Polish Academy of Sciences. He published over a hundred papers and 18 monographs and textbooks. He will be remembered by his contribution to theory of aerodynamic profiles and conformal mapping, which was summarized in the book "Method of Integral Relations" published by Springer. He shared his knowledge with numerous MSc students and 17 PhD students, who graduated under his supervision.

Professor Włodzimierz Juliusz Prosnak was also a gifted organizer of Polish scientific community and for many years he was a Chairman of Fluid Mechanics Section of Polish Academy of Sciences Committee on Mechanics. The integration of Polish fluid mechanics scientific community was initiated by the 1st National Conference on Fluid Mechanics, which was organized in 1974 at Jaszowiec by the Institute of Aeronautics and Applied Mechanics of Warsaw University of Technology and chaired by Prof. W. Prosnak.

Professor Włodzimierz Juliusz Prosnak died on 24th August 2014 and was buried at Łostowice Cemetery in Gdańsk, mourned by his numerous pupils and friends.

Professor
R. Puzyrewski
1935–2016

Professor Romuald Puzyrewski – Obituary

J. Pozorski

IMP PAN, Fiszera 14, 80-231 Gdańsk, Poland

Romuald Puzyrewski was born on 3 March 1935 in Brasław. After the cruelties of WWII, his family moved to the West Pomerania region. In 1958 he graduated from the Shipbuilding Faculty of the Gdańsk University of Technology. Then, Professor Robert Szewalski offered him an assistantship position at the Institute of Fluid-Flow Machinery (IMP) of the Polish Academy of Sciences. The subject of work were flow path design methods for large output steam turbines, in cooperation with "Zamech" turbine works in Elbląg. The design problem involved a number of difficult partial tasks such as blade shape optimisation, transonic flow analysis, vapour condensation and droplets motion in low pressure turbine parts. In the early1960s, R. Puzyrewski went for a research stay at the Leningrad Politechnic Institute (USSR) where he met Professor L.G. Loitsianski, an outstanding specialist in fluid dynamics. In 1963 he accomplished his PhD on turbine blade losses. Then, he left for a post-doctoral stay in Caltech, Pasadena (USA), working on compressible, condensing vapor flows in Laval nozzles. For that research, he was presented with the award of the Polish Academy of Sciences. Experimental studies on vapor condensation and a theoretical description of nucleation processes were the basis of his DSc dissertation (1969). In1973 he was nominated to a professorship; in 1989, he became an ordinary professor.

At IMP, Professor Puzyrewski headed the multiphase flow group, doing experiments on condensation phenomena (using the Mie scattering theory) as well as on droplet deformation and break-up in the flow. He also directed various studies commissioned by the Polish power sector. He was a co-author of rotor blade design for steam turbine at Mertaniemi power station in Finland, as well as of a concept of nozzle guide vane with water suction. He also participated in the design of stator vane with a movable trailing edge flap, allowing for mass flow control in the adaptive stage. In the periods 1980–81 and 1989–91, he stayed at the R & D department of Brown Boveri corporation (later: ABB) in Baden, Switzerland. There, he worked on the computations of flow paths and on the concept of steam turbine admission system. He patented the idea of twin volute admission as an alternative inlet configuration. Moreover, he has given a series of lectures on turbomachinery theory and design for ABB staff. He has written a monograph on

fluid-flow machinery fundamentals in 1D approach and a series of papers on blading channel design using the inverse method with some fairly general assumptions on the stream surface shape.

In the 1970s, Professor Puzyrewski was the head of the Doctoral School at IMP and in the late 1990s he managed to establish the Conjoint Doctoral School of TU Gdańsk and IMP. In 1984, he was appointed as the head of Flow Machinery and Fluid Mechanics Chair at TU Gdańsk (till his retirement in 2005).

Aside of research and applied work, teaching was another passion of Professor Puzyrewski. He started at TU Szczecin and continued over the decades at TU Gdańsk with fluid mechanics courses, as well as seminars for PhD students at IMP. Also, he was the supervisor of 20 PhD theses. The textbook *Fundamentals on Fluid Mechanics and Hydraulics*, co-authored with J. Sawicki, was published in 1987 by PWN (Warsaw) and reprinted a few times with new material added (1998, 2000 and 2013).

He died in March 2016 at the age of 81, being professionally active till his last months. He will be fondly remembered by his students, co-workers, and the fluid mechanics community in Poland.

Dr Konrad Bajer – A Personal Tribute

H.K. Moffatt

Trinity College, Cambridge, UK

Konrad Bajer died on 29th August 2014 from a rare and virulent form of cancer, diagnosed only one week before his untimely death. He had been working earlier in the year, among many other responsibilities, on the Proceedings of two Workshops held during the 2012 programme on *Topological Dynamics in the Physical and Biological Sciences* at the Isaac Newton Institute in Cambridge UK. Konrad had been a key organiser of this programme, during which he was on leave from the University of Warsaw. He held a Visiting Fellowship during the programme at Trinity College, Cambridge University, where he had been a regular and welcome visitor ever since taking his PhD degree in Fluid Dynamics in 1984–1989, under my supervision. He had earlier graduated in Physics from the University of Warsaw in 1980.

Konrad was active in EUROMECH, having been a principal organiser of the European Turbulence Conference (ETC13) in Warsaw 2011, and of the meeting *Turbulence: the Historical Perspective* that immediately followed it. He has been equally active in IUTAM; his distinction was recognised by his election in August 2014 to the Congress Committee of IUTAM, an election that delighted him, but that sadly he was unable to take up. He had also recently been appointed an Associate Editor of *Fluid Dynamics Research*, and was (since 2009) a Member of the Programme Council of the Copernicus Science Centre (Poland).

Konrad's research interests were in magnetohydrodynamics and vortex dynamics in classical and quantum systems, in which he published many papers; also in problems of gasification, in which he played a coordinating role at the University of Warsaw. He impressed all with his great scientific integrity and commitment, and with his warm and friendly personality, coupled with a delightful sense of humour.

PROGRAMME OF THE XXII FLUID MECHANICS CONFERENCE

SUNDAY – 11th of September

Since 16:00 – Registration of Participants of the Conference
18:00–21:00 – Welcome dinner
19:00–20:30 – Meeting of Scientific and Organizing Committees with invited speakers

MONDAY – 12th of September

8:00–13:00 – Registration
8:00–9:00 – Breakfast
9:00–9:15 – Solemn opening of XXII Fluid Mechanics Conference
9:15–9:30 – A Remembrances of prof. Włodzimierz Juliusz Prosnak, prof. Romuald Puzyrewski and dr hab. Konrad Bajer
9:30–11:00 – Invited Lectures, chairmen: J. Rokicki and S. Drobniak
9:30–10:15 – **Keith Moffatt**, University of Cambridge, UK Department of Applied Mathematics and Theoretical Physics, "Magnetic relaxation and structure formation in highly conducting fluids"
10:15–11:00 – **Marie Farge**, LMD–IPSL-CNRS Ecole Normale Supérieure, Paris, France "Revisiting d'Alembert's paradox"
11:00–11:20 – Coffee break
11:20–13:00 – Sessions IA (room no. 1A) **and IB** (room no. 2)
13:00–14:20 – Lunch
14:20–16:00 – Sessions IC (room no. 1A) **and ID** (room no. 2)
16:00–16:20 – Coffee break
16:20–17:40 – Sessions IE (room no. 1A) **and IF** (room no. 2)
18:15–18:45 – Presentation of Intel company (room no. 1A) P. Gepner and R. Adamski, "Intel Scalable System Framework the foundation for computational fluid dynamics simulations"
18:45–19:15 – Presentation of SymKom company (room no. 1A) A. Piechna and L. Rudniak, "Optymalizacja topologiczna oraz inżynieria odwrotna w zastosowaniach przepływowych"
19:15–19:45 – Presentation of UniSens company (room no. 1A) H. Stańczyk, "TE connectivity pressure and temperature scanning solutions for wind tunnel, flight and turbomachinery testing"
20:00–23:00 – **Barbecue**

TUESDAY – 13th of September

8:00–13:00 – Registration
8:00–9:00 – Breakfast
9:00–11:00 – Invited Lectures, chairmen: K. Moffatt and H. Kudela
9:00–10:00 – **G. N. Barakos,** University of Liverpool, UK "Unsteady shock-boundary layer interaction: applications and challenges"
10:00–11:00 – **A. Herczyński,** Boston College, Physics Department, USA "Two variations on normal modes: sloshing in free vessels & Bragg resonance"

11:00–11:20 – Coffee break
11:20–13:00 – Sessions IIA – **prof. Elsner Competition** (room no. 1A)
11:20–13:00 – Sessions IIB (room no. 2)
13:00–14:20 – Lunch
14:20–16:00 – Sessions IIC – **prof. Elsner Competition** (room no. 1A)
14:20–16:00 – Sessions IID (room no. 2)
16:00–6:20 – Coffee break
16:20–18:00 – Sessions IIE – **prof. Elsner Competition** (room no. 1A)
16:20–17:40 – Sessions IIF (room no. 2)
18:15–18:45 – Presentation of Casp system company (room no. 1A) A. Głodek, "Laser Imaging Systems"
18:45–19:15 – Presentation of Eurotek and Dantec companies (room no. 1A) K. Dörner and A. Antonowicz, "The latest development in planar, volumetric and point measurements techniques for fluid mechanics"
20:00–20:45 – Jazz Quartet concert
20:45–23:00 – Banquet

WEDNESDAY – 14th of September

8:00–9:00 – Breakfast
9:00–11:00 – Invited Lectures, chairmen: M. Farge and A. Herczyński
9:00–10:00 – **J. Szmyd,** AGH University of Science and Technology, Cracow, Poland "Influence of a strong magnetic field on convection processes in paramagnetic fluids"
10:00–11:00 – **T. Kowalewski,** Institute of Fundamental Technological Research, Polish Academy of Sciences "New experimental tools in microfluidics"
11:00–11:20 – Coffee break
11:20–13:00 – Sessions IIIA (room no. 1A) and **IIIB** (room no. 2)
13:00–14:00 – Lunch
14:00–14:30 – Closing ceremony of XXII Fluid Mechanics Conference

SESSION IA (room no. 1A) – Monday

Chairman: **E. Tuliszka-Sznitko** – Poznań University of Technology
(presentations in English: 12 min. – lecture and 3 min. – discussion)

11:20 – D. Asendrych, G. Kanik and S. Drobniak "Modelling liquid flow structure on a flat inclined surface"
11:40 – J. Pozorski and M. Knorps "Subfilter-scale modelling in particle-laden turbulent flows"
12:00 – A. Bartosik "Simulation of Reynolds number influence on heat exchange in turbulent flow of medium slurry"
12:20 – R. Szwaba and T. Ochrymiuk "Transpiration effects in perforated plate aerodynamics"
12:40 – M. Księżyk and A. Tyliszczak "LES-IB analysis of a flow in channel with an adverse pressure gradient"

SESSION IB (room no. 2) – Monday

Chairman: **P. Doerffer –** Szewalski Institute of Fluid-Flow Machinery Polish Academy of Sciences
(presentations in English: 12 min. – lecture and 3 min. – discussion)

11:20 – J. Badur, S. Kornet, D. Sławiński and P. Ziółkowski "Analysis of unsteady flow forces acting on the thermo-well in a steam turbine control stage"
11:40 – S. Kornet and J. Badur "Evaporation level of the condensate droplets on a shock wave in the IMP PAN nozzle depending on the inlet conditions"

12:00 – **M. Olejnik, K. Szewc and J. Pozorski** "Smoothed Particle Hydrodynamics modelling of the shear driven gas-liquid interface deformation"

12:20 – **A. Szymański, S. Dykas, W. Wróblewski, M. Majkut and M. Strozik** "Experimental and numerical study on the performance of the smooth-land labyrinth seal"

12:40 – **D. Frączek and W. Wróblewski** "Validation of the numerical models for flow simulation in labyrinth seals"

SESSION IC (room no. 1A) – Monday

Chairman: **A. Kucaba-Piętal** – Rzeszów University of Technology
(presentations in English: 12 min. – lecture and 3 min. – discussion)

14:20 – **E. Tuliszka-Sznitko and K. Kiełczewski** "The numerical simulation of Taylor-Couette flow with radial temperature gradient"

14:40 – **A. Kraszewska, Ł. Pyrda and J. Donizak** "Influence of a strong magnetic field on a paramagnetic fluid's convection in systems with different aspect ratios"

15:00 – **A. Kraszewska, Ł. Pyrda and J. Donizak** "Influence of a strong magnetic field on paramagnetic fluid's flow in cubical enclosure"

15:20 – **F. Tejero, P. Flaszyński, R. Szwaba and J. Telega** "Unsteady conjugate heat transfer analysis for impinging jet cooling"

15:40 – **P. Niegodajew and D. Asendrych** "Modelling liquid spreading in porous zone – modification of 3D approach to efficient 2D axisymmetric algorithm"

SESSION ID (room no. 2) – Monday

Chairman: **J. Pozorski** – Szewalski Institute of Fluid-Flow Machinery Polish Academy of Sciences
(presentations in English: 12 min. – lecture and 3 min. – discussion)

14:20 – **M. Wacławczyk and M. Oberlack** "Symmetry analysis and invariant solutions of the multipoint infinite systems describing turbulence"

14:40 – **W. Stankiewicz, M. Morzyński, K. Kotecki and W. Szeliga** "Complex Dynamic Response Modes for Fluid Model Order Reduction"

15:00 – **M. Mierzwiczak, J.K. Grabski and J.A. Kołodziej** "Comparison of different approaches in the Trefftz method for analysis of fluid flow between regular bundles of cylindrical fibres"

15:20 – **M. Wichrowski** "Robust preconditioners and stabilization for Fluid-Structure Interaction problem in saddle-point formulation"

15:40 – **K. Urbanowicz, A. Tijsseling and M. Firkowski** "Comparing convolution integral models with analytical pipe flow solutions"

SESSION IE (room no. 1A) – Monday

Chairman: **M. Morzyński** – Poznań University of Technology
(presentations in English: 12 min. – lecture and 3 min. – discussion)

16:20 – **A. Kucaba-Piętal and A. Kordos** "Molecular Dynamic simulation of water flows in nanochannels with nanocavities. Vortices formation."

16:40 – **S. Pawłowska** „Highly deformable nanofilaments in flow"

17:00 – **K. Kaczorowska and K. Tesch** "Modelling of Blood Flow: From Macro to Micro-scales"

17:20 – **J.K. Grabski, M. Mierzwiczak and J.A. Kołodziej** "Analysis of non-Newtonian fluid flow in porous media by means of the global radial basis function collocation method"

SESSION IF (room no. 2) – Monday

Chairman: **J. Badur –** Szewalski Institute of Fluid-Flow Machinery Polish Academy of Sciences
(presentations in English: 12 min. – lecture and 3 min. – discussion)

16:20 – **O. Szulc, P. Doerffer and F. Tejero** "Passive control of rotorcraft high-speed impulsive noise"

16:40 – **W. Wróblewski and D. Homa** "Numerical research on unsteady cavitating flow over a hydrofoil"

17:00 – **A. Pawłowska, S. Drobniak and P. Domagała** "Spectral analysis of self-sustained oscillations for the free jet under variable outlet conditions"

17:20 – **Z. Nosal and B. Olszański** "Experimental research of an airfoil cascade in varying air humidity conditions"

18:15–18:45 – **Presentation of Intel company** (room no. 1A) **P. Gepner and R. Adamski,** "Intel Scalable System Framework the foundation for computational fluid dynamics simulations"

18:45–19:15 – **Presentation of SymKom company** (room no. 1A) **A. Piechna and L. Rudniak,** "Optymalizacja topologiczna oraz inżynieria odwrotna w zastosowaniach przepływowych"

19:15–19:45 – **Presentation of UniSens company** (room no. 1A) **H. Stańczyk,** "TE connectivity pressure and temperature scanning solutions for wind tunnel, flight and turbomachinery testing"

SESSION IIA (room no. 1A) – Tuesday

Prof. Elsner Competition – Supervisor: **S. Drobniak** – Częstochowa University of Technology
Chairman: **W. Elsner** – Częstochowa University of Technology
(presentations in English: 12 min. – lecture and 3 min. – discussion)

11:20 – **A. Rosiak and A. Tyliszczak** "Impact of numerical method on auto-ignition in a temporally evolving mixing layer at various initial conditions"

11:40 – **M. Lewandowski and J. Pozorski** "Assessment of turbulence-chemistry interaction models in the computation of turbulent non-premixed flames"

12:00 – **W. Regulski** "Simulations of particle suspensions in viscoplastic fluids using a combined Discrete Element - Lattice Boltzmann Method"

12:20 – **A. Roszko and E. Fornalik-Wajs** "Nanofluids convective flow structure modified by the magnetic field"

12:40 – **M. Piotrowicz and P. Flaszyński** "Numerical investigations of shock wave interaction with laminar boundary layer on compressor profile"

SESSION IIB (room no. 2) – Tuesday

Chairman: **W. Wróblewski** – Silesian University of Technology
(presentations in English: 12 min. – lecture and 3 min. – discussion)

11:20 – **T. Kozłowski and H. Kudela** "Generation of the vorticity field by the flapping profile"

11:40 – **P. Strzelczyk and P. Gil** "Properties of velocity field in the vincity of synthetic jet generator"

12:00 – **W. Szeliga, M. Morzyński, W. Stankiewicz and K. Kotecki** "Incompressible mean-field model with modal closure"

12:20 – **M. Remer, K. Gumowski, J. Rokicki, G. Sobieraj, M. Kaliusz, M. Psarski, G. Celichowski and D. Pawlak** "Investigation of droplet impact spreading angle"

12:40 – **T. Seredyn and R. Rowiński** "Simulating the trajectory of droplets in an aircraft wake"

SESSION IIC (room no. 1A) – Tuesday

Prof. Elsner Competition – Supervisor: **S. Drobniak** – Częstochowa University of Technology
Chairman: **T. Kowalewski -** Institute of Fundamental Technological Research, Polish Academy of Sciences (presentations in English: 12 min. – lecture and 3 min. – discussion)

14:20 – **P. Kaczyński and R. Szwaba** "Cooling intensity influence on shock wave boundary layer interaction region in turbine cascade."
14:40 – **T. Kura and E. Fornalik-Wajs** "Near-blade flow structure modification"
15:00 – **K. Wawrzak and A. Bogusławski** "Impact of numerical method on a side jets formation in a round jet"
15:20 – **P. Szałtys and J. Majewski** "High-order hybrid grid generation for simulation of high-Reynolds number flows"
15:40 – **F. Wasilczuk and P. Flaszyński** "Numerical investigations of flow structure in gas turbine shroud gap"

SESSION IID (room no. 2) – Tuesday

Chairman: **J. Szmyd –** AGH University of Science and Technology
(presentations in English: 12 min. – lecture and 3 min. – discussion)

14:20 – **B. Engler, P. Regucki and Z. Szeliga** "Analysis of water management at a closed cooling system of a power plant"
14:40 – **M. Marek** "A study of geometrical structure of packed beds using flow simulation with the immersed boundary method"
15:00 – **M. Marijnissen and J. Rojek** "Particle-fluid interaction inside a beater mill"
15:20 – **K. Smołka, S. Dykas, M. Majkut and M. Strozik** "Application of a single-fluid model for prediction of the steam condensing flow"
15:40 – **P. Konderla, K. Patralski and J. Lewandowski** "Modelling of wet fumes condensation process in industrial stacks"

SESSION IIE (room no. 1A) – Tuesday

Prof. Elsner Competition – Supervisor: **S. Drobniak** – Częstochowa University of Technology
Chairman: **A. Bogusławski** – Częstochowa University of Technology
(presentations in English: 12 min. – lecture and 3 min. – discussion)

16:20 – **P. Ziółkowski and J. Badur** "On the unsteady Reynolds thermal transpiration law"
16:40 – **Ł. Pleskacz and E. Fornalik-Wajs** "Momentum budget of the paramagnetic fluid flow influenced by magnetic force"
17:00 – **A. Grucelski** "LBM estimation of the thermal conductivity coefficient in a granular bed"
17:20 – **S. Gepner** „ Stability of flow in a corrugated channel"
17:40 – **J. Martinez Suarez and P. Flaszyński** "Streamwise vortex generator for separation reduction on wind turbine profile"

SESSION IIF (room no. 2) – Tuesday

Chairman: **Z. Kosma** – Kazimierz Pułaski University of Technology and Humanities in Radom
(presentations in English: 12 min. – lecture and 3 min. – discussion)

16:20 – **A. Dróżdż and W. Elsner** "Study of Reynolds number effect on turbulent boundary layer near the separation"
16:40 – **A. Dróżdż and W. Elsner** "An attempt to scale streamwise veocity fluctuations near turbulent boundary layer separation"

17:00 – **N. Yadav, S. Gepner and J. Szumbarski** "Instability in a channel with grooves parallel to the flow"

17:20 – **P. Regucki and S. Goujon-Durand** "Influence of holding on second onset of instability for a sphere"

18:15–18:45 – **Presentation of Casp system company** (room no. 1A) **A. Głodek,** "Laser Imaging Systems"

18:45–19:15 – **Presentation of Eurotek and Dantec companies** (room no. 1A) **K. Dörner and A. Antonowicz,** "The latest development in planar, volumetric and point measurements techniques for fluid mechanics"

SESSION IIIA (room no. 1A) – Wednesday

Chairman: **A. Bartosik** – Kielce University of Technology
(presentations in English: 12 min. – lecture and 3 min. – discussion)

11:20 – **D. Pavlík, P. Procházka and V. Kopecký** "Reconstruction of three-dimensional velocity vector maps from two-dimensional PIV data"

11:40 – **S. Kordel, T. Nowak, R. Szkoda and J. Hussong** "Combined Differential Interferometry and Long-range μPIV measurements of a temperature driven boundary layer flow"

12:00 – **P. Procházka and V. Uruba** "Three-dimensional structures behind Glauert-Goldschmied profile under control of plasma actuation"

12:20 – **K. Kurec and J. Piechna** "Numerical and experimental investigations of flow within a pressure exchanger with rotating valves"

12:40 – **M. Firkowski, K. Urbanowicz and Z. Zarzycki** "Modelling water hammer in viscoelastic pipelines"

SESSION IIIB (room no. 2) – Wednesday

Chairman: **P. Flaszyński –** Szewalski Institute of Fluid-Flow Machinery Polish Academy of Sciences
(presentations in English: 12 min. – lecture and 3 min. – discussion)

11:20 – **J. Broniszewski and J. Piechna** "Ground vehicle dynamics in the presence of unsteady aerodynamics loads"

11:40 – **P. Leśniewicz, M. Kulak and M. Karczewski** "Vehicle wheel drag coefficient in relation to travelling velocity – CFD analysis"

12:00 – **D. Wójcik, Z. Piotrowski, B. Rosa and M. Ziemiański** "Application of anelastic and compressible EULAG solvers for limited-area numerical weather prediction in the COSMO consortium"

12:20 – **R. Rowiński** "Bio-aviation"

INVITED LECTURES
– ABSTRACTS

Magnetic relaxation and structure formation in highly conducting fluids

K. Moffatt

Trinity College, Cambridge, UK. E-mail: H.K.Moffatt@damtp

I will take this opportunity firstly to pay tribute to my former student, colleague and close friend, Konrad Bajer, who died on 29 August 2014 after a brief illness. This was a grievous loss to our community. Konrad was then at the height of his career. Just two weeks previously, he had been elected by the General Assembly of IUTAM to its Congress Committee, an indication of the very high esteem in which he was held by the whole international community of Theoretical and Applied Mechanics.

The first part of my lecture will be devoted to work that Konrad and I did following the 2012 Newton Institute programme "Topological Dynamics in the Physical and Biological Sciences", of which Konrad had been a Principal Organizer, and a moving spirit. This work, published in the Astrophysical Journal in 2013, concerned the relaxation of a unidirectional magnetic field in an extremely tenuous plasma contained between perfectly conducting boundaries, such that the fluid pressure is negligible compared with the magnetic pressure. In the perfect conductivity limit, the magnetic field seeks a minimum energy state, resisted only by the viscosity of the medium. During an initial rapid stage of relaxation, the plasma is driven towards null points (or null curves) of the magnetic field, the magnetic pressure becoming nearly uniform, with current sheets forming at the nulls. During the subsequent slow diffusive stage, the field diffuses in the neighborhood of these current sheets, and the magnetic energy slowly decreases. Plasma continues to be drawn into the current sheets, until limited by growing plasma pressure (or by ultimate diffusive decay).

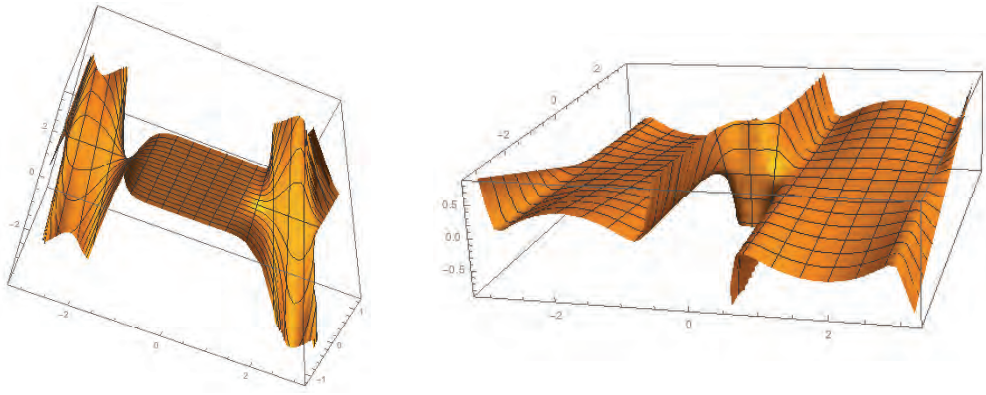

(a) (b)

Fig. 1. Ruled surface containing the **B**-lines of the field **B** = (0, $B_y(x, t)$, $B_z(x, t)$) in a typical relaxation process; (a) initial field; (b) field after initial rapid relaxation phase, during which the magnetic pressure becomes uniform

Stimulated by discussions with Konrad, I have more recently considered an extension of this model to the relaxation of a two-component but still rectilinear magnetic field, which in general does not have null points. Nevertheless, the magnetic pressure still tends to rapidly equalise (or "uniformatise"), and the subsequent slow diffusive decay proceeds under the constraint of uniform

magnetic pressure (i.e., the force-free condition in the simple geometry considered). The motivation for studying this problem is in part to understand the process by which a "Taylor state" may be attained; this state, obtained by minimising energy subject to the single constraint of prescribed global magnetic helicity, is a Beltrami state in which current **j** and magnetic field **B** are related by $\mathbf{j} = \gamma\,\mathbf{B}$, where γ is a constant related to the helicity. But in fact, under the assumed condition of perfect conductivity, the helicity density divided by fluid density is a Lagrangian invariant, and this exerts profound control over the relaxation process; the force-free condition $\mathbf{j} = \gamma(\mathbf{x})\,\mathbf{B}$ is indeed realised, but with $\gamma(\mathbf{x})$ seriously non-uniform, and determined in principle, by the initial magnetic field and density distributions.

It may be that turbulence arising from instability of current sheets within the plasma may give rise to a non-uniform non-isotropic turbulent diffusivity and α-effect (i.e., mean electromotive force linearly related to mean field, $E_i = \alpha_{ij}B_j$) which will undoubtedly affect the relaxation process. Work on this aspect of the problem is in progress, in collaboration with Krzysztof Mizerski.

Revisiting D'alembert's paradox

Marie Farge[1], Romain Nguyen van Yen[1], Kai Schneider[2]

[1] LMD-CNRS-IPSL, Ecole Normale Supérieure Paris, France
[2] IMM, Aix-Marseille Université, France. E-mail: Marie.Farge@ens.fr

We propose to revisit the problem posed by Euler in 1748 for the Mathematics Prize of the Prussian Academy in Berlin, that lead d'Alembert to formulate his paradox and address the following problem: does, in the limit of very large Reynolds numbers (i.e., $Re \to \infty$), energy dissipate when the boundary layer detaches from the wall? For trying to answer this question we consider a vortex dipole impinging onto a wall and compare the numerical solutions of the Euler, Prandtl, and Navier–Stokes equations integrated from the same initial condition. We first observe the formation of a boundary layer, whose thickness scales in $Re^{-1/2}$, as predicted by Prandtl in 1904.

But, after a certain time, Prandtl's solution becomes singular, while the boundary layer obtained for the Navier–Stokes solution collapses down to a much finer thickness, scaling in Re^{-1} as predicted by Kato in 1984. This very thin boundary layer then rolls up into vortices, which detach from the wall while dissipating a finite amount of energy, in accordance with Kato's 1984 theorem.

References

[1] PRANDTL L., *Über Flüssigkeitsbewegung bei sehr kleiner Reibung*, Proc. 3rd Inter. Math. Congr., Heidelberg 1904, 484–491, 1237.

[2] KATO T., *Remarks on zero viscosity limit for nonstationary Navier-Stokes flows with boundary*, Seminar on Nonlinear Partial Differential Equations, 1984, 85–98, MSRI Berkeley.

[3] NGUYEN VAN YEN R., FARGE M., SCHNEIDER K., *Energy dissipative structures in the vanishing viscosity limit of two-dimensional incompressible flow with boundaries*, Phys. Rev. Lett., 2011, 106(8), 184502, 1–4.

Unsteady shock-boundary layer interaction: applications and challenges

G.N. Barakos

School of Engineering, University of Glasgow, Glasgow G12 8QQ, Scotland, U.K.
E-mail: George.Barakos@Glasgow.ac.uk

Abstract: This work presents some recent efforts related to the numerical simulation of the unsteady, transitional interaction between a shock-wave and a boundary layer. In contrast to earlier works where the simulation has been attempted considering fully turbulent flow, this work shows results for transitional interactions. The flow mechanism and the origin of the unsteadiness are examined suggesting a possible flow mechanism and strategies for flow control.

1. Introduction – the buffet envelope

High speed aircraft, especially military, can experience shock oscillations on their wings and control surfaces. These oscillations are not desirable since they cause large variations in lift and moment loads as well as substantial drag increase. The unsteady shock oscillation, known as transonic buffet is a challenging problem for aerodynamicists that are asked to predict not only when the phenomenon occurs, and what its implications are on unsteady loads, but should also suggest mechanisms for countering the growth of the shock oscillations and pacify the flow without affecting the overall performance of the aircraft. In this work, turbulence models of the URANS framework are used and for transition, models based on the transport equation of flow intermittency (γ) are exploited (Menter and Langtry, 2009).

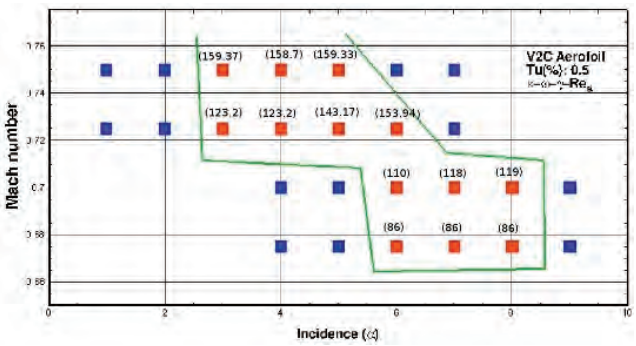

Fig. 1. Region of shock oscillation for the V2C aerofoil using the κ-ω-γ-Re_θ model.
The frequencies indicated in brackets are at Hz

A first result can be seen in Figure 1 where the boundary of the shock oscillations is bracketed using a repeat of computations. This is a time-consuming process but can be used with modern CFD codes since a strategy for re-starting one computation from another can be set-up to reduce the required CPU time.

2. Buffet control

The flow mechanism established via URANS simulations for buffet includes an interaction between two flow separation regions. The first is formed at the foot of the shock on the aerofoil and the second at the trailing edge (Figure 2). Any flow control should aim to reduce the interaction and/or remove one of the flow separation regions. In general, tripping the upstream boundary layer reduces the separation at the foot of the shock and can be an effective flow control method. A trailing edge device like a flap could be used for trailing edge control. Both

methods can be effective and have been used in this work. A draw-back of the flow control methods is that they appear to affect the amount of lift and drag produced by the aerofoil. For this reason, care is needed to avoid excessive flow separation by applying too much control.

The flow separation can be seen by the extent of the negative skin friction coefficient region in Figure 2. As part of this work upstream flow control was attempted using vortex generators or air-jet vortex generators as well as trailing edge flaps. For each of the cases, the upstream flow control was found to be more beneficial if the location of the vortex generators was carefully selected with low drag penalties and no penalties in terms of aerodynamic moment. On the other hand, the trailing edge flap was the most convenient way for buffet control. The device exists in many aircraft (ailerons, and spoilers can be used for this purpose). Using the flap incurred a penalty in the aerodynamic model but it also resulted in re-trimming of the lifting surface so that the required overall amount of lift is maintained while the control is still applied.

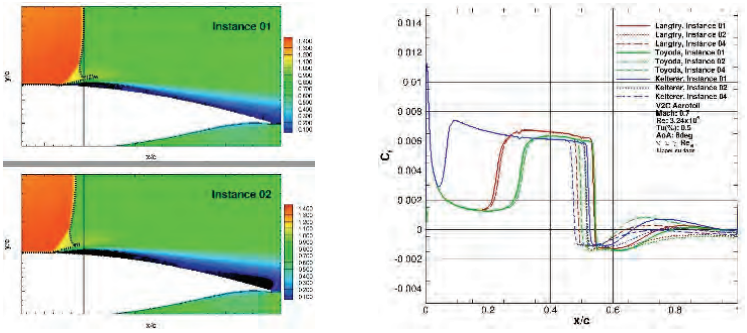

Fig. 2. Flow visualization during buffet and corresponding skin friction coefficient

3. Aerodynamic loads during buffet

Another area of interest is the prediction of the exact loads during buffet. In general, 2D configurations result in large load variations in lift and drag while smaller variations can be seen for 3D cases due to the localized effect of buffet. Indicative results are shown in Figure 3 while a detailed account is presented in the final paper.

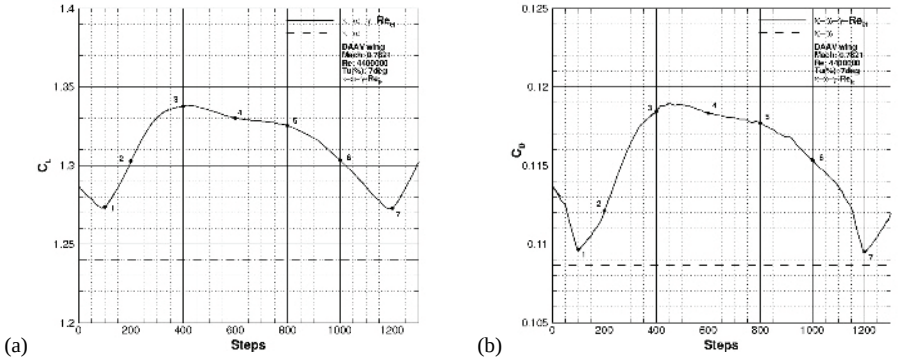

Fig. 3. History of lift (a) and drag (b) coefficients versus time
(Mach = 0.7821, $Re = 4.4\times10^6$, a = 7 deg, Tu(%) = 2.58, κ-ω-γ-Re_θ)

References

[1] MENTER F.R., LANGTRY R.B., 2009, AIAA J., 2009, 47, 2894–2906.

Two variations on normal modes: sloshing in free vessels and Bragg resonance

A. Herczyński[1], P. Weidman[2]

[1] Boston College, Department of Physics, 140 Commonwealth Avenue, Chestnut Hill, Ma 02467, USA
[2] University of Colorado, Department of Mechanical Engineering,
1111 Engineering Drive, Boulder, CO 80309, USA. E-mail: andrzej@bc.edu

Abstract: Standing waves in a container partially filled with water and free to move horizontally are investigated. In the simplest case, the vessel oscillates out-of-phase with the liquid sloshing within. Experimental results for containers of various shapes are found to be in excellent agreement with the potential flow theory. A separate study concerns forced waves in a container of corrugated bottom. The theory of Howard and Yu, which predicts the existence of resonant "Bragg" modes, wherein the amplitude grows exponentially in one of two possible ways, is confirmed experimentally.

1. Introduction

Two variations on the classical theme of standing waves in a stationary container of uniform depth are presented. The first problem treats the case when the container is no longer stationary and is itself free to oscillate. The second problem concerns a fixed container whose bottom is no longer flat but takes the form of an undulating bed. For both problems, a linear theory leading to solutions in the form of sum of normal modes is outlined, and results from new experiments designed specifically to test theoretical predications are discussed.

2. Sloshing in free containers

The hydrodynamic coupling between containers free to move in some manner, and liquid sloshing within, has been studied extensively. The problem arises, in particular, out of concern with the impact of liquid propellant oscillations on the stability of space vehicles, and with the disturbances of trucks or ships transporting partially filled fuel tanks subject to external forcing (due, for example, to a corrugated pavement or ocean waves). Faltinsen & Timokha [1] provide an extensive summary of such parametrically forced liquid transport problems.

In the present investigation the focus is on a motion of a rigid container constrained to move horizontally along a straight line and subject only to hydrodynamic forces of the liquid sloshing inside. A variety of complicated rectilinear motions can arise depending on the initial conditions. In the simplest case, the container oscillates in a periodic fashion about a fixed position, out-of-phase with the liquid oscillating within [2]. This oscillatory motion can be considered a limit of the motion of a partially filled container suspended as a bifilar pendulum [3] whose length is infinite.

The counter-synchronous sloshing-oscillation is analysed using linearized potential flow theory for containers of symmetric shapes, which are amenable to analytical solutions: rectangular boxes, upright cylinders, wedges and cones of 90° apex angles, and cylindrical annuli. While the wedge and cone exhibit only one mode of oscillation, the boxes, cylinders and annuli have an infinite number of modes. Experiments were carried out using containers made of Plexiglas, filled with water, and attached to a low-friction cart. In most cases, it was possible to collect data corresponding to the first two modes. Oscillation frequencies were measured at various relative fillings, $M = m/m_o$ (m is the mass of water and m_o of the dry container).

There was generally a very good agreement between experiments and theory. Damping, while clearly noticeable in time-series data, had negligible effect on the measured frequencies. Notably,

for containers with vertical walls, oscillation frequencies rise with M up to some critical value and then begin to gently decline. For the cone and the wedge, however, the frequencies decrease monotonically with increasing M.

3. Waves over an undulating bed

Another problem with a long history is that of waves passing over variable topography. When the wavelength of the fluid motion is large compared to the water depth, models based on the shallow-water approximation are appropriate. If the waves are short compared to the depth, bottom variations can be ignored. The intermediate case, where the wavelength, depth and bottom variations have comparable scales, is more complex. Initial studies have revealed that propagating surface waves can be amplified by a corrugated seabed, particularly when the free-surface wavelength is approximately double that of the bottom corrugations. This phenomenon, and the resulting beach erosion, has been observed in some shallow bays and has come to be known as the fluid dynamical Bragg resonance.

The first complete theory for the idealized scenario of waves propagating in a stationary rectangular tank of sinusoidal bottom has been provided by Howard and Yu [4] and later generalized to arbitrary periodic and non-periodic beds. The linear analysis, based on a conformal mapping technique, predicted the existence of resonant normal modes – Bragg modes – wherein the amplitude grows exponentially, either from one end of the channel to the other or from the centre out, depending on the phases of the corrugations at the two end-walls.

Experiments designed to test the theory were carried out in a rectangular tank, with an adjustable length between 450 and 490 cm, width 13 cm, and height 30 cm, fitted with a sinusoidal bottom (made of polyurethane foam) of wavelength 52 cm and peak-to-peak amplitude 5 cm [5]. The two lengths noted above corresponded to symmetric and asymmetric configuration with respect to corrugation phases at the ends. Waves were excited by oscillating the container in a periodic horizontal motion with a very small stroke (~ 2 mm). The amplitude of the standing waves was recorded using two sensitive pressure probes and also observed and filmed through the transparent acrylic walls of the tank. Experimental results were in essential agreement with the theory, with the measured resonant frequencies very close to the theoretical values, and waveforms of the predicted amplitude variations except near the end-walls. For smaller depths wave distortions were observed, presumably a manifestation of nonlinear effects.

References

[1] FALTINSEN O., TIMOKHA A.N., *Sloshing*, Cambridge University Press, 2009.
[2] HERCZYŃSKI A., WEIDMAN P., J. Fluid Mech., 2012, 693, 216.
[3] WEIDMAN P., TURNER M., J. Fluids and Struct., 2016, (in press).
[4] HOWARD L.N., YU J., J. Fluid Mech., 2007, 593. 209.
[5] WEIDMAN P., HERCZYŃSKI A., YU J., HOWARD L., J. Fluid Mech., 2015, 777, 122.

Influence of a strong magnetic field on convection processes in paramagnetic fluid

J.S. Szmyd

Dept. of Fundamental Research in Energy Engineering, AGH University of Science and Technology, 30 Mickiewicza Ave., 30-059 Krakow, Poland. E-mail: janusz.szmyd@agh.edu.pl

Abstract. The magnetic convection of paramagnetic fluid is studied in the different systems. With different strengths of magnetic field, the convection of paramagnetic fluid is enhanced depending on angle of magnetic coil inclination. Depending on the level of the coil, the convection and heat transfer rates can be controlled extensively. By applying the superconducting magnet with imposed magnetic field up to 10 T, the initially stable laminar-like flow regime is extended to its transient and fully turbulent states.

1. Introduction

Super conducting materials at high temperature were found in 1986 and then various new oxides to represent super-conductivity at 100 K or more have been reported extensively. Probably due to these new findings, a compact type super conducting electro magnet becomes available commercially and various new phenomena in a strong magnetic field have been reported recently. For example, Wakayama and coworkers have reported various phenomena such as nitrogen jet flow in an atmospheric air in a direction of decreasing magnetic field [1], promotion of combustion in a micro-gravity field [2], breathing enhancement with a small magnet placed in a nose [3], enhancement of oxygen supply toward fuel cells using magnets [4]. Kitazawa's group has also been working on the phenomena associated with magnetic force. Kitazawa et al. have reported floating of water droplet in the magnetic field [5], curved water surface at a strong magnetic center, enhanced water vaporization, magneto thermal wind tunnel, separation of particles from a mixture [6]. By the application of the magneto-Archimedes levitation technique, they realized a new separation method for the weakly magnetic materials, which are, dia- and paramagnetic [7]. Braithwaite et al. [8] used the magnetic field both to enhance and suppress the Rayleigh–Benard convection in a solution of gadolinium-nitrate and showed that the effect depends on the relative orientation of the magnetic force and the temperature gradient. Group of Ozoe has studied effect of the magnetic field on various convective phenomena. Tagawa et al. [9] derived model equations for magnetic convection using a method similar to Boussinesq approximation and carried out numerical calculations. Kaneda et al. [10] studied the effect of gradient magnetic field with four poles electro-magnet. They placed a cubic enclosure filled with air inside and heated from above and cooled from below at the center of four poles magnet. The stagnant conduction of air in the cube was disturbed and the convection of air was visualized with incense smoke to go downward from the hot top center plane toward the cold bottom plate against the gravitational buoyancy force. Maki et al. [11] measured the average heat transfer rate of air in a shallow cylindrical enclosure heated from below and cooled from above which was placed in the bore of a super-conducting magnet at 1.6 Tesla. They obtained the declined or enhanced heat transfer rates which were in agreement with their numerical analyses and with the classical experimental data by [12].

The magnetic (magnetization, magnetizing or Kelvin) force to induce these various phenomena is strong enough in comparison to the gravitational acceleration. For example, the air receives almost 9 times larger acceleration than gravity in a strong magnetic field of 10 Tesla. It is expected that this magnetic force may be employed for some new engineering processes in

the near future and the related transport phenomena is expected to be quantitatively described with appropriate model equations and be able to be numerically computed. This is the motivation of the present work and we have reported a number of heat and mass transfer processes. In the present report, we would like to introduce some of our recent works of convection of fluids with and without gravitational acceleration.

The first one is for the natural and magnetic convection of paramagnetic fluid (for example, air) in a cubic enclosure heated and cooled from opposing walls [13]. The heat transfer rate is affected by the shift of the coil center from a cubic center. The combinations of a shifted distance and the angle of inclination provide the general configuration between the magnetic coil and the enclosure. The second system is a vertical cylindrical enclosure whose upper side wall is cooled and lower one is heated with intermediate one thermally adiabatic [13]. A magnetic coil is placed around the cylinder coaxially at various levels. Depending on the level of the coil, the convection and heat transfer rates may be affected. The third system presents an experimental and numerical analysis of a thermo-magnetic convective flow of paramagnetic fluid in a concentric annuli under a strong magnetic field gradient. The inner cylindrical surface was heated and the outer cylindrical surface was cooled. The applied superconducting magnet was able to achieve 10 T of magnetic induction [14]. The results show that magnetising force affects the heat transfer rate and that a strong magnetic field can control the magnetic convection of a paramagnetic fluid in a concentric annuli. Finally, for the magnetization forces, we analyze the flow reorganization and wall-heat transfer of the non-conductive paramagnetic working fluids in a differentially heated cubical enclosure subjected to the strong non-uniform magnetic fields of different orientations, [15], [16]. Here, by applying the superconducting magnet with imposed magnetic field up to 10 T, the initially stable laminar-like flow regime is extended to its transient and fully turbulent states.

References

[1] WAKAYAMA N.I., Chem. Phys. Letters, 1991, 185, 449.
[2] WAKAYAMA N.I., Combustion and Flame, 1993, 93, 207.
[3] WAKAYAMA M., WAKAYAMA N.I., Japanese J. Applied Physics, 2000, 39, 262.
[4] WAKAYAMA N.I., OKADA T., OKANO J., OZAWA T., Jpn. J. Appl. Phys., 2001, 40, 269.
[5] IKEZOE Y., HIROTA N., NAKAGAWA J., KITAZAWA K., Nature, 1998, 393, 749.
[6] KITAZAWA K., IKEZOE Y., UETAKE H., Physica B, 2001, 294–295, 709.
[7] HIROTA N., IKEZOE Y., UETAKE H., KAIHATSU T., TAKAYAMA T., KITAZAWA K., RIKEN Rev., 2002, 44, 159.
[8] BRAITHWAITE D., BEAUGNON E., TOURNIER R., Nature, 1991, 354, 134.
[9] TAGAWA T., SHIGEMITSU R., OZOE H., Int. J. Heat and Mass Transfer, 2002, 45, 267.
[10] KANEDA M., TAGAWA T., OZOE H., Int. J. Heat Transfer, 2002, 124, 17.
[11] MAKI S., TAGAWA T., OZOE H., Experimental Thermal and Fluid Science, 2003, 27, 891.
[12] SILVESTON P.L., Forsch. Ing.Ves., 1958, 24, 29.
[13] OZOE H., SZMYD J.S., I. J. Trans. Phenomena, 2006, 8, 197.
[14] WROBEL W., FORNALIK-WAJS E., PLESKACZ L., KENJERES S., SZMYD J.S., Proc.15 Int. Heat Transfer Conference, Begell House, Danbury 2014, 1.
[15] KENJERES S., PYRDA L., WROBEL W., FORNALIK-WAJS E., SZMYD J.S., Phys. Rev. E, 2012, 85, 1.
[16] KENJERES S., PYRDA L., FORNALIK E., SZMYD J.S., Flow, Turbulence and Combustion, 2014, 92, 371.

New experimental tools in microfluidics

T.A. Kowalewski

IPPT PAN, Dep. of Mechanics and Physics of Fluids,
Pawińskiego 5B, 02-106 Warszawa, Poland. E-mail: tkowale@ippt.pan.pl

Abstract: Contemporary experiment in fluid mechanics evidently moves from large scale problems to micro or even nanoscale phenomena, to accomplish our desire to elucidate mechanisms driving living nature. Experiments at such scales found new exciting approaches, some of them touching molecular limits, where assumption of continuous and deterministic description becomes questionable. At short time and length scales diffusion governed by Brownian motion becomes the most efficient transport mechanism. Whereas its analysis is apparently simple in case of ideal spherical objects, understanding complex behavior of long, deformable objects is far from being complete. Examples of experimental techniques allowing us to monitor and control behavior of single micro objects conveyed by flow will be given.

1. Introduction

It is generally understood, that the main difference between macro- and nano-scale mechanics originates from rapidly increasing surface to volume ratio along with the decreasing of object size. The fluid phenomena that dominate liquids at this length scale are measurably different from those that dominate at the macroscale [1]. Some experimental examples we my gain observing the mother nature, some of them has been recently proposed using completely new for fluid mechanics techniques, like fluorescent microscopy, atomic force microscopy, and optical tweezers.

Most of microfluidic problems concern multiphase flow, suspensions of micro and nanoparticles, cells or macromolecules (proteins, DNA, etc). Understanding and properly interpreting fluid-particle interaction is crucial for interrogating such systems [2]. One of the basic optical tools is based on Brownian motion. The local and bulk mechanical properties of a complex fluid can be obtained by analyzing thermal fluctuations of probe particles embedded within it.

Thermal fluctuations generated by molecules are not only noises, it has been demonstrated that such fluctuations are fundamental to the function of biological systems. Preferential binding of ligands to one of the spontaneously fluctuating structures of proteins leads to activation or deactivation. This mechanism appears essential for a long scale evolutionary development of leaving species, and at short time scale to create signaling paths for early immune response of individual cells. Hence, looking at the “bottom” of our fluid mechanics, there is no place for steady, unique and predictable modelling. Rather, by analogy to quantum mechanics, we have to talk about the most probably evolution of the analyzed system. As an illustration of the difficulties, in the following we cope with two intriguing problems, kinematic boundary conditions in micro and nano scales flow, and mobility of nano-objects suspended in liquids.

New experimental tools largely help in understanding transport phenomena at nanoscales. In the presentation we give few examples of problems appealing for new theoretical and numerical models embracing continuous flow modelling with molecular scale phenomena.

2. Slip velocity

The physics of hydrodynamic slip may have different origins. Purely molecular slip is clearly relevant in case of gases and relatively easy to demonstrate there. Its observation in liquids became challenging. Classical microscopy used for nanoscale observation has resolution

limited by the light wavelength of about 500 nm micrometers. Evaluating diffraction disks the measured position of particle coordinates in plane perpendicular to the optical axis can be improved by order of magnitude. However, resolution in depth, along optical axis, remains very low (tenths of micrometer), and is defined solely by focal depth of the microscope lens. Total Internal Reflection Microscopy (TIRF) helps to bypass some of these limitations offering possibility to locate objects position with resolution of about 20 nm. Laser light illuminating object undergoes total internal reflection at an interface between investigated medium (liquid) and the wall (glass), and part of the light penetrates into the medium parallel to the interface with an intensity that decays exponentially with the normal distance from the interface. This evanescent wave illumination has been used extensively in the life sciences. Recently it was rediscovered in microfluidics for near wall flow measurements. The main advantage of the method is possibility to reduce the depth of focus of the acquisition system [3]. Hence, it became possible to obtain images of particles, which are in the direct vicinity of the wall. In our recent study of the Brownian motion of fluorescent particles observed close to the wall, the deviation of the particle diffusion rate has been interpreted as an evidence of the hydrodynamic slip.

3. Tackling particle in flow

Detailed experimental analysis of interactions of individual particle conveyed in flow is very difficult. Recently, a new optical tool, so called Optical Tweezers (OT) expanded our traditional instrumentation creating possibility for undisturbed measurements of forces and position for suspended micro particles in picoNewton and nanometer scales. Dragging, towing single particle allows to perform precise analysis of forces involved by liquid environment, wall interactions, and particle-particle interactions. One of the fundamental problems of single particle mobility, namely ballistic regime and effects of inertia creating time dependent recirculation of surrounding liquid molecules, could be proven using OT. Electronic way of signal analysis allows for thermal motion of particle trapped by OT to be evaluated with MHz sampling frequency and displacements below 1 nanometer. In our preliminary study OT developed at IPPT have been used to analyze Brownian motion of trapped polystyrene particle [4]. It appears that already at sampling times of 10 kHz diffusion becomes influenced by ballistic regime of molecular interactions.

References

[1] KOWALEWSKI T.A. et al., *Micro and nano fluid mechanics Adv. in Mech.*, Theoretical, Computational and Interdisciplinary Issues, ed. M. Kleiber et al., CRC Press, 2016, 27–34.
[2] ZEMBRZYCKI K. et al., J. of Physics: Conference Series, 2012, 392.
[3] NAKIELSKI P. et al., PLOS ONE, 2015, 10(6).
[4] PIERINI F. et al., Measurement Science and Technology, 2016, 27(2).

ABSTRACTS OF THE CONFERENCE PRESENTATIONS

Modelling liquid flow structure on a flat inclined surface

D. Asendrych, G. Kanik, S. Drobniak

Częstochowa University of Technology, Faculty of Mechanical Engineering and Computer Science,
Armii Krajowej 21, 42-200 Częstochowa, Poland. E-mail: darek@imc.pcz.czest.pl

The paper presents a numerical simulation of a liquid flow on a flat inclined surface using a 3-dimensional 2-fluid Volume of Fluid model. Application of a surface tracking method allowed to reconstruct a flow structure and estimate surface wettability revealing their dependence on the flow rate and the surface tension. The critical Reynolds number value corresponding to the transition from the rivulet flow to the fully wetted surface was found to agree quite well with the experimental observations.

1. Introduction

Packed bed columns are commonly used in chemical, petrochemical and process industries, where the chemical and/or thermal interactions between gas and liquid phases take place. Drying, distillation, absorption or rectification could be mentioned as the examples of these processes [1, 2]. Their performance is dependent on a number of factors including packed bed characteristics (porosity, specific surface area, liquid spreading ability), gas and liquid properties as well as their loads. The most important role of the packed is to enlarge the contact area between phases to enhance the mass, momentum and heat transfer processes. However, the actual gas-liquid interface surface area depends also on surface wettability, which is expected to be high enough. In order to achieve that goal the research efforts are undertaken aimed at investigating the wetting abilities of structured packing designs [3]. The models are first developed and tested for simple geometries (like flat surfaces) [2, 3] what allows for their verification with available experimental data [4].

2. Numerical model

The liquid flow structure is simulated with the use of a 3-dimensional (3D) Eulerian 2-fluid model. A surface tracking was accomplished by application of a Volume of Fluid (VOF) method. The flow was considered as unsteady, isothermal and laminar, with water as liquid phase and air as the surrounding medium. Thus the system of governing equations consisted of mass and momentum conservation laws in their classical forms.

The computational domain was designed in a way allowing to compare the simulation results with the available experimental and numerical data. The plate inclination angle (with respect to horizontal direction) was set to 60°. The dimensions of a plate were as follows: length – 60 mm, width – 50 mm. The model was completed with the relevant boundary conditions. At inlet a parabolic velocity profile and film thickness were set according to the liquid film theory [2] and a pressure outlet boundary condition was applied at the outlet. At walls the non-slip and slip conditions were set for the plate and the side domain boundaries, respectively.

3. Results and discussion

The simulations were started from test calculations with the use of a 2D model. It is obvious that in this case either rivulet or droplet flow structure could not be simulated because of their 3D character. So the simulations were conducted for Reynolds number exceeding the critical value ensuring the formation of a liquid film covering entirely the plate. The simulated

liquid layer thickness as well as the velocity profiles were found to be in a very good agreement with the liquid film theory [2] and thus proving the model relevance. The verified model was then used for the 3D simulations in the low Re range, i.e., corresponding to the non-perfect wetting conditions. As the solution was initiated with the uniform liquid distribution (liquid film) with constant thickness the flow had to evolve to reach the steady-state conditions. This is illustrated in Fig. 1, where the surface wetting (corresponding to black color) is shown for 3 different time moments. As can be easily seen the film flow is first qualitatively replaced by the rivulet flow pattern (Fig. 1, left) which is then consecutively reduced by the surface tension force (Fig. 1, center) and finally arrives to the steady-state rivulet-droplet flow (Fig. 1, right).

Fig. 1. Rivulet flow structure formed at the subcritical Reynolds number regime – temporal evolution

The simulations were conducted for the varying Reynolds number so the flow structure and the surface wettability (i.e., the portion of the surface wetted by the liquid) could be obtained. The results were found to be in a good qualitative and quantitative agreement with the reference experimental [4] and numerical [2, 3] data. The critical Re value equal to approx. 200 was determined as the upper limit of partial surface wetting. The preliminary tests have also shown significant influence of Weber number on liquid flow structure proving the importance of surface tension on the wettability.

References

[1] WANG Y., CHEN J., LARACHI F., *Modelling and simulation of trickle-bed reactors using computational fluid dynamics: A state-of-the-art review*, Can. J. Chem. Eng., 2013, 91, 136.
[2] XU Y., ZHAO M., PASCHKE S., WOZNY G., *Detailed investigations of the countercurrent multiphase (gas-liquid and gas-liquid-liquid) flow behavior by three-dimensional computational fluid dynamics simulations*, Ind. Eng. Chem. Res., 2014, 53, 7797.
[3] HAROUN Y., RAYNAL L., ALIX P., *Prediction of effective area and liquid hold-up in structured packings by CFD*, Chem. Eng. Res. Des., 2014, 92, 2247.
[4] HOFFMANN A., AUSNER I., REPKE J.-U., WOZNY G., *Detailed investigation of multiphase (gas–liquid and gas–liquid–liquid) flow behaviour on inclined plates*, Chem. Eng. Res. Des., 2006, 84, 147.

Subfilter-scale modelling in particle-laden turbulent flows

J. Pozorski, M. Knorps

Institute of Fluid-Flow Machinery, Polish Academy of Sciences,
Fiszera 14, 80-231 Gdańsk, Poland. E-mail: jp@imp.gda.pl

We consider large-eddy simulations of two-phase turbulent flows. The Lagrangian description is used for the dispersed phase in the point-particle approximation and also for the modelling of fluid dynamics along the particle trajectories. We discuss stochastic approaches for particle dispersion in turbulence, including the specific features of the near-wall regions. First, we apply the model formulation based on the instantaneous fluid velocity sampled by the particles as compared to more popular approaches where the velocity fluctuations are followed. Second, we propose an extension with the fluid acceleration as an additional model variable. The results for the particle-laden, fully-developed channel flow are presented and discussed.

1. Introduction

Two-phase turbulent flows with the dispersed phase are present in various practical applications, including pulverised coal or liquid fuel combustors, cyclone separators, atmospheric aerosols, etc. Such flows still represent a challenge for the Reynolds-averaged Navier–Stokes (RANS) approaches and also for increasingly popular flow solvers based on the large-eddy simulations (LES) with sub-grid-scale closures. For the latter, the problem remains open, in particular at smaller particle inertia.

The particles are advected as $d\mathbf{x}_p/dt = \mathbf{V}_p$; the equation of motion (drag only), $d\mathbf{V}_p/dt = (\mathbf{U}_s - \mathbf{V}_p)/\tau_p$, includes the inertia parameter (the time scale τ_p) and the fluid velocity sampled (or seen) along the particle trajectory, denoted by $\mathbf{U}_s = \mathbf{U}(\mathbf{x}_p, t)$. Except for the direct numerical simulation (DNS) where $\mathbf{U}_s$ is known (to within an interpolation error) from the fluid flow field, it has to be modelled, using the hints from the single-phase turbulence closures, often in terms of the Lagrangian stochastic approaches.

2. Models for the fluid velocity sampled by particles

In LES, models of two-phase flows need to account for subfilter-scale effects. Various proposals have been formulated, usually in analogy with closures developed for RANS in the environmental fluid dynamics (dispersion of pollutants as passive tracers) with most interest in free-shear flows. In studies of inertial particle dispersion, these models were often simply adopted without much further insight [1]. Basically, given that only the filtered fluid velocity $\overline{\mathbf{U}}$, is solved for in LES, the remaining

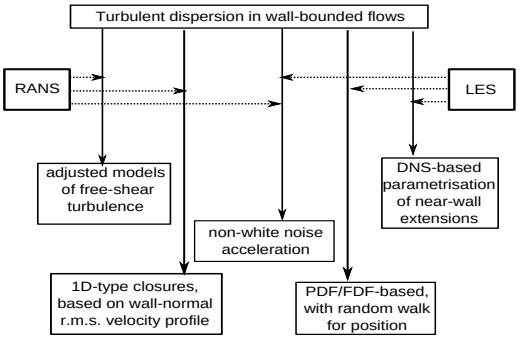

Fig. 1. A classification of models for turbulent dispersion of particles

subfilter contribution $\boldsymbol{u}_s = \mathbf{U}_s - \overline{\mathbf{U}}(\mathbf{x}_p, t)$ has to be either neglected or modelled (e.g., as a stochastic process).

In the Eulerian–Lagrangian approach to dispersed flows, the prediction of the velocity and concentration statistics of the dispersed phase (in particular in wall-affected, viscosity–dominated flow regions with strong turbulence inhomogeneity) requires a suitable modelling of the fluid velocity sampled, or seen, along the particle trajectory. In the talk, stochastic models for particle dispersion are presented and tentatively classified, with a particular emphasis on their behavior near the wall (Fig. 1). Some are specific, but acceleration (below) and random-walk [2] seem useful both for RANS and LES.

Our previous proposal of a simple stochastic diffusion process for the subfilter fluid velocity seen by particles [3] has been extended to an anisotropic variant with correlations of velocity components [4]:

$$\mathrm{d}\boldsymbol{u}_s = [(-u_s \cdot \nabla)\overline{U} + \nabla \cdot \boldsymbol{\tau}]\mathrm{d}t - \frac{\boldsymbol{u}_s}{\tau_{sg}}\mathrm{d}t + \boldsymbol{\sigma} \cdot \mathrm{d}\mathbf{W} \tag{1}$$

where $\boldsymbol{\tau}$ is the subfilter stress tensor, $\boldsymbol{\sigma}$ is the diffusion matrix, τ_{sg} is a characteristic time scale of the subfilter velocity correlations. One of the issues is a better parametrisation of the time scale. We have gathered usuful hints from *a priori* DNS studies. Moreover, we established a formulation in terms of the full velocity "seen", $\boldsymbol{U}_s$. One of the advantages is that, unlike (1), the gradients of the subfilter stresses are no longer computed; only the flow pressure gradient is provided at the particle location. Results will be shown for particle concentration and velocity statistics in fully-developed channel flow.

3. Model extension: the fluid acceleration

Both for RANS and LES, several attempts have been made to modify the diffusion term in (1) and replace the increment of the Wiener process $\mathrm{d}\boldsymbol{W}$ by a non-white noise. This amounts to introducing a specific acceleration model of the fluid elements. We advanced such idea for RANS (see [1]). Near-wall extensions have been developed in the fluid PDF approach [2]. Akin to a stochastic fluid acceleration model proposed for LES [5], we formulated a closure for the subfilter acceleration of the fluid "seen" by inertial particles. Tests of the improved model application to particle-laden channel are in progress.

Acknowledgement

The work has been supported by the National Science Centre (NCN, Poland) through the research project 2011/03/B/ST8/05677.

References

[1] MINIER J.P., *On Lagrangian stochastic methods for turbulent polydisperse two-phase reactive flows*, Prog. Energy Combust. Sci., 2015, 50, 1–62.
[2] WACŁAWCZYK M., POZORSKI J., MINIER J.P., *Probability density function computation of turbulent flows with a new near-wall model*, Phys. Fluids, 2004, 16, 1410–1422.
[3] POZORSKI J., APTE S.V., *Filtered particle tracking in isotropic turbulence and stochastic modelling of subgrid-scale dispersion*, Int. J. Multiphase Flow, 2009, 35, 118–128.
[4] KNORPS M., POZORSKI J., *An inhomogeneous stochastic subgrid scale model for particle dispersion in Large-Eddy Simulation*, Direct and Large-Eddy Simulation IX, 2015, 671–678.
[5] ZAMANSKY R., VINKOVIC I., GOROKHOVSKI M., *Acceleration in turbulent channel flow: universalities in statistics, subgrid stochastic models and application*, J. Fluid Mech., 2013, 721, 627.

Simulation of Reynolds number influence on heat exchange in turbulent flow of medium slurry

A. Bartosik

Kielce University of Technology, Faculty of Management and Production Engineering,
al. Tysiąclecia P.P. 7, 25-314 Kielce, Poland. E-mail: artur.bartosik@kielce.pl

The paper deals with numerical simulation of mass and heat exchange in turbulent flow of solid-liquid mixture, in which averaged solid particle diameter various from 0.1 mm to 0.8 mm, named further as the medium slurry. Physical model assumes that dispersed phase is fully suspended and a turbulent flow is hydro-dynamically, and thermally developed in a straight horizontal pipeline. On the base of the assumptions the slurry is treated as a single-phase flow with increased density and with viscosity, which is equals to carrier liquid viscosity, as no one can measure rheology in such slurries. The mathematical model constitutes time averaged momentum equation in which turbulent stress tensor was designated using two-equation turbulence model, which makes use of the Boussinesq eddy-viscosity hypothesis. The wall turbulence damping function, which appears in the turbulence model, was especially designed for medium slurries [1]. In addition, the energy equations have been used in which a convective term was determined from the energy balance acting on the unit pipe length, assuming that the temperature in the main flow direction varies linearly. Finally, the mathematical model of non-isothermal medium slurry flow comprises four partial differential equations, namely momentum and energy equations, and equations for kinetic energy of turbulence and its dissipation rate. The equations were solved by finite difference scheme using own computer code. The objective of the paper is to examine the influence of Reynolds number on Nusselt number and temperature profiles in turbulent flow of medium slurries in the range of solids concentration from 0% to 30% by volume. The effect of influential factors on the heat transfer between the pipe and the slurry were analysed. The paper demonstrates substantial influence of Reynolds number and solids volume fraction on velocity profiles and as a consequence the temperature profiles too. The results of numerical simulation are discussed.

1. Introduction

A solid-liquid flow exists comprehensively in nature and engineering and belongs to main challenges of computational fluid dynamics [2, 3]. Many approaches have been investigated to predict a solid–liquid mechanism during turbulent flow, however mixture theory models are the most promising and are based on a rigorous fluid mechanics framework. If slurry with averaged solid particle diameter in the range from 0.1 to 0.8 mm is considered, named further as medium slurry, it is well known there appears damping of turbulence, which depends mainly on particle size and solids concentration [4]. The damping of turbulence is a result of thickening of a viscous sublayer, which tends to increase throughput velocity and thus promotes a drag reduction. Simulation of turbulent flow of medium slurry requires a proper approach in predicting velocity distribution. The velocity distribution and the viscous sublayer are closely related to temperature distribution, which is a special interest in a food industry, medicine, mining industry, and pipeline erosion.

The objective of the paper is to examine the influence of Reynolds number on Nusselt number and temperature profiles in turbulent flow of medium slurry in the range of solids concentration from 0% to 30% by volume.

2. Simulation results

All prediction presented in the paper have been made for slurry with averaged particle diameter equals to 0.24 mm. Simulation of heat exchange process in turbulent flow of medium slurry indicates substantial influence of Reynolds number and solids concentration. Fig. 1 presents influence of Reynolds number on Nusselt number in flow without solids (C = 0%) and in flow with solids concentration equal to 10%, 20% and 30% by volume.

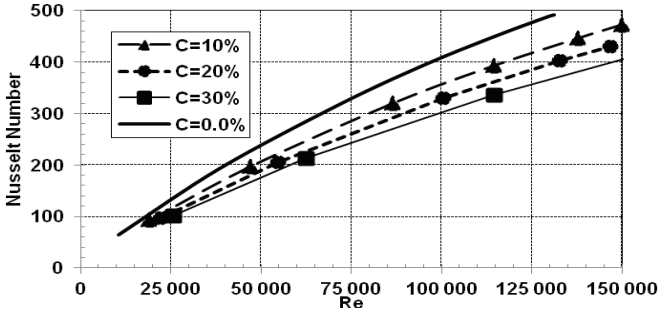

Fig. 1. Dependence of Nusselt number on Reynolds number: D = 0.0127 m

The paper presents several figures emphasising substantial influence of Reynolds number and solids concentration on Nusselt number and temperature profiles in turbulent flow of medium slurry in which the sand was used as dispersed phase. Results of numerical simulation are discussed and major conclusions have been made.

References

[1] BARTOSIK A., *Mathematical modelling of slurry flow with medium solid particles*, Monograph: *Mathematical Models and Methods in Modern Science*, Int. Conf. Mathematical Models for Engineering Science, Spain, 10–12.12.2011. Editor of Institute for Environment, Engineering, Economics and Applied Mathematics; ed. Mastorakis N, Mladenov V, Travieso-Gonzalez C M, Kohler M, 124–129.

[2] HETSRONI G., ROZENBLIT R., *Heat transfer to a solid-liquid mixture in a flume*, Int. J. Multiphase Flow, 1994, 20, 671–689.

[3] ROZENBLIT R., *Heat transfer in horizontal solid-liquid pipe flow*, Int. J. Multiphase Flow, 2000, 26, 1235–1246.

[4] SUMNER R.J., MCKIBBEN M., SHOOK C.A., *Concentration and velocity distribution in turbulent vertical slurry flow*, J. Solid Liquid Flow, 1991, 2, No. 2, 33–42.

Transpiration effects in perforated plate aerodynamics

R. Szwaba, T. Ochrymiuk

Institute of Fluid Flow Machinery Polish Academy of Sciences, Fiszera 14, 80-231 Gdańsk, Poland
E-mail: tomasz.ochrymiuk@imp.gda.pl

Perforated walls find a wide use as a method of flow control and effusive cooling. Experiments of the gas flow past perforated place with microholes (110 μm) were carried out. The wide range of pressure difference between outlet and inlet were investigated. Two distinguishable flow regimes were obtained: laminar and turbulence transitional regime. The results are in good agreement with theory, simulations and experiments on large scale perforated plates and compressible flows in microtubules. Formulation of the transpiration law was associated with the porous plate aerodynamics properties. Using model of transpiration flow "aerodynamic porosity" are determined for microholes.

1. Introduction

This paper is focusing on the investigation of the microscale effects on the global macroscale characteristics. For that purpose the experiments in air were per formed on the perforated plated with perforation of 5.2% and holes of 110 μm diameter. Various range of pressure differences were studied and this has allowed to obtain characteristics of two distinguishable regimes: laminar and transition to turbulence in around Re = 60. The studies were performed for all Mach numbers up to the critical conditions (chocking flow in the microholes). From the phenomenological point of view this problem could be analyzed using transpiration law and porous media properties to determine "aerodynamic porosity" [1].

2. Measurement technique

The experimental investigations were carried out in the test section shown in Figure 1. The flow direction is from left to right indicated in figure by an arrow. The flow is caused by pressure difference between the ambient condition and the vacuum which was created behind the valve 7. The air from ambient flow through the flowmeter 1, next trough the control valve 2 and compensatory chamber 3 to frame 4, where is mounted membrane with microholes. Downstream of the membrane the flow goes through another chamber 5, second valve 6 (which control the flow condition downstream of the microholes) and cut-off valve 7 to the vacuum tanks. The change of stagnation parameters (pressure and density) was realized by means of control valve 2, but the pressure downstream of microholes was controlled by means of valve 6. One can able to measure the particular characteristics throughout adequate manipulation of these two control valves.

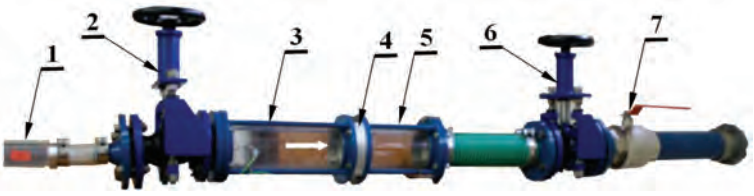

Fig. 1. View of the test section. 1 – flow meter; 2 – control valve; 3 – compensatory chamber; 4 – membrane location; 5 – second chamber, 6 – second valve; 7 – cut-off valve to the vacuum tanks

3. Perforated plate aerodynamics

Perforated plate aerodynamics has been studied for many years, mostly focusing on plates with large holes [2]. Both the laminar and turbulent regimes have been considered. Some specific examples can be found in the literature; for example: the pressure loss coefficient over plate thickness, the turbulent flow over a perforated plate and a very high Reynolds number (Re > 10 000). For the comparison also for our experiment we chose to plot the nondimensional values.

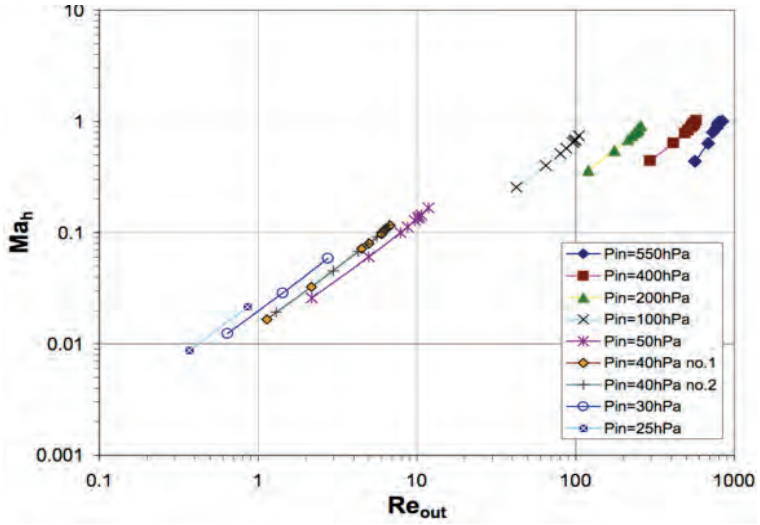

Fig. 2. Nondimensional number dependencies, the Mach number as a function of the Reynolds number

As can be seen in Fig. 2 there are two distinguishable flow regimes: one for low Reynolds numbers (Re < 10) and one for high Reynolds numbers (Re > 10). The latter is related to the turbulence transition. Development of this topic and many others interesting results obtained from these study will be include in the paper.

References

[1] DOERFFER P., BOHNING R., *Modelling of perforated plate aerodynamics performance*, Aerospace Science and Technology, 2000, 4(8), 525–534
[2] ZIEREP J., BOHNING R., DOERFFER P., *Experimental and Analytical Analysis of Perforated Plate Aerodynamics*, Journal of Thermal Science, 2003, 12(3), 193–197

LES-IB analysis of a flow in channel with an adverse pressure gradient

M. Księżyk, A. Tyliszczak

Częstochowa University of Technology, Faculty of Mechanical Engineering and Computer Science,
Al. Armii Krajowej 21, 42-201 Częstochowa, Poland. E-mail:ksiezykm@imc.pcz.pl

This paper presents results of Large Eddy Simulation (LES) of flow in a channel with adverse pressure gradient. The applied computational code (SAILOR) is based on a high order compact finite difference scheme combined with an Immersed Boundary (IB) method. The obtained results agree well with experimental data. It is shown that by changing a shape of the channel or by application of suction on its wall, the pressure gradient and occurrence of separation regions can be effectively controlled.

1. Introduction

Understanding flow separation phenomena in a channel with adverse pressure gradient is an important and ambitious task. Wide range of turbulent structures and influence of high-energy large-scale motion on turbulence production near the walls makes this flow difficult to analyze experimentally. In this view the LES method not only complements the measurements but also gives deep insight into every detail of the flow.

The LES requires the use of non-dissipative high order methods [1] and compact finite difference method used in the SAILOR code belongs to this family. The weak point of these methods is that they can be applied in cases with rather simple flow domains. To avoid this limitation in the present work we combine LES with an Immersed Boundary [2] method, which enables simulations in almost arbitrary domain shapes.

2. Governing equations and solution algorithm

For incompressible Newtonian fluid flow in the LES framework momentum and continuity equations are given as:

$$\frac{\partial \overline{u}_j}{\partial x_j} = 0 \tag{1}$$

$$\frac{\partial \overline{u}_i}{\partial t} + \overline{u}_j \frac{\partial \overline{u}_i}{\partial x_j} = -\frac{1}{\rho}\frac{\partial \overline{P}}{\partial x_i} + \frac{\partial}{\partial x_j}\left((\upsilon + \upsilon_t)\left(\frac{\partial \overline{u}_i}{\partial x_j} + \frac{\partial \overline{u}_j}{\partial x_i} \right) \right) + \overline{f}_i^{IBM} \tag{2}$$

where symbol ¯ denotes spatially filtered variables; u – velocity components; P – pressure; ρ, υ_t – density and turbulent viscosity. The term $\overline{f}_i^{IBM}$ is a body-force term, which is used in IB method based on a direct forcing approach [3]. The spatial discretization is performed using 6th order scheme on half-staggered meshes. The time integration is performed with 2nd order Adams-Bashfort/Adams-Moulton schemes with the projection method for pressure-velocity coupling. The subgrid viscosity is modeled by the model proposed be Vreman [4]. The correctness of applied discretization and temporal integration methods and their combination with the IB method was confirmed in laminar and turbulent flow problems [5–7].

3. Case setup and preliminary results

The computational domain is presented in the Fig. 1. The flow is from the left to right side and the adverse pressure gradient is caused by curved upper wall. The size of the channel cor-

respond to experimental set-up: length is equal to 1.80 m, the inlet and outflow heights are equal to 0.32 m and 1.09 m, respectively. In the computations the periodic boundary condition are used in the transversal direction. The Reynolds number based on friction velocity is equal to $Re_\tau = 2000$. The computation domain above the upper wall is modelled by the IB method.

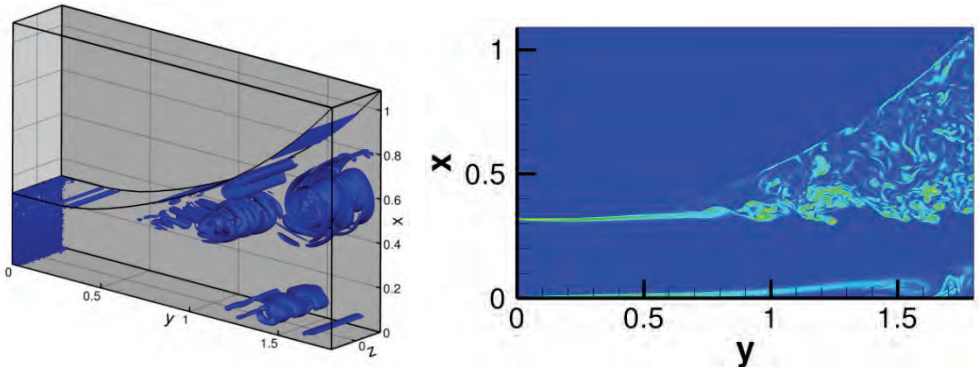

Fig. 1. Isosurface of Q-parameter and vorticity contours in the central plane

Sample results presented in Fig. 1 shows isosurface of Q-parameter and contours of vorticity in the main cross-section plane. These results illustrate complexity of this seemingly simple configuration. Large vortices generated on curved wall and near-wall separation regions in the boundary layer close to the bottom wall are apparent. The latter phenomenon is the effect of the pressure gradient caused by the expansion of the channel.

Acknowledgment

The investigation was supported by Polish National Science Center under Grant no. DEC-2012/07/B/ST8/03791.This research was also supported in part by PL-Grid (Poland).

References

[1] WANG J. et al., Int. J. Numer. Meth. Fl., 2013, 72, 811–845.
[2] PESKIN C., J. Comput. Phys. 1972, 10, 252–271.
[3] MOHD-YUSOF J., CTR Annual ResearchBrief Ames/Stanford University, 1997.
[4] VREMAN A.W., Phys. Fluids. 2004, 16, 3670–3681.
[5] TYLISZCZAK A., J. Comput. Phys. 2014, 276, 438–467.
[6] KSIĘŻYK M., TYLISZCZAK A., J. Phys. Conf. Ser. 2014, 530, 012066.
[7] KSIĘŻYK M., TYLISZCZAK A., *Progress in Wall Turbulence 2*, Springer, 2016, 191.

Analysis of unsteady flow forces acting on the thermo-well in a steam turbine control stage

J. Badur, S. Kornet, D. Sławiński, P. Ziółkowski

Energy Conversion Department, The Szewalski Institute of Fluid-Flow Machinery PAS-ci,
Fiszera 14, 18-231 Gdansk, Poland. E-mail: skornet@imp.gda.pl

In the present paper, the phenomenon of unsteady flow forces acting on the thermo-well for measuring steam temperature in a steam turbine control stage is presented. The non-stationarities of fluid acting on the thermo-well such as: Strouhal frequency, pressure amplitude, pressure peaks, pressure field, velocity field etc. are studied analytically and numerically. There have been examined two cases of flow with changing temperature, pressure and mass flow rate in the control stage chamber. The problem is also described in the ASME standard PTC19.3 TW-2010 providing detailed guidelines for thermo-well calculations. The possibility of operation in resonance has been examined too.

1. Introduction

From the scientific and engineering point of view, unsteady flow forces acting on a solid structure are a very important issue. Therefore, in the paper, in order to specify the similarity between periodical phenomena and to take into account the case of non-stationary flows forces acting on the thermo-well, a novel CFD (Computational Fluid Dynamics) + CSD (Computational Solid Dynamics) approach has been used.

However, it should be underlined that the presence of a cylindrical element in the steam flow is a reason of occurrence of the vortex shedding phenomenon, where the flowing steam detaches from the cylinder surface creating downstream a vortex structure [1]. The accompanying pressure pulsations generate flow-induced vibrations which may lead to thermo-well damage due to high-cycle fatigue [2, 3]. The problem is described in the ASME standard PTC19.3 TW-2010 [4] providing detailed guidelines for thermo-well calculations.

2. Results and discussion

In order to confirm the correctness of the results, some resultant points from [2] were marked on the diagram showing dependence of the Strouhal number on the Reynolds number (Fig. 1), taken from ASME norm [4]. The position of points in Fig. 1 should be considered as satisfactory, because they are within the area defined experimentally. It is worth mentioning that the diagram from *ASME PTC 19.3 TW-2010* refers to the obstacles completely embedded in the channel of a uniform cross-section. In our case of the thermo-wells the flow was only partially disturbed, and additionally the thermo-well has the shape of a truncated cone.

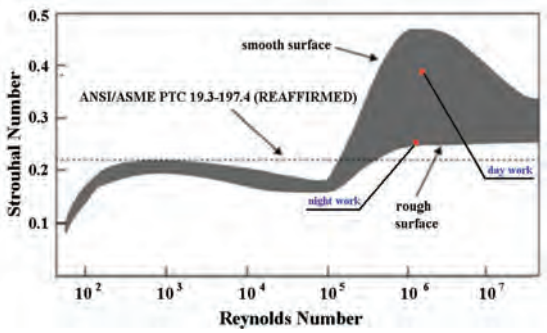

Fig. 1. Comparison of *St*(*Re*) from ASME PTC 19.3 TW-2010 to numerical results

Figure 2 presents distributions of the total pressure around the thermo-well at 180 MW (partial load) and 380 MW (full load). The pressure distribution changes both its values and shapes with changing load, which means that both the pressure amplitude and the resultant force direction vary with turbine load. It can be thus concluded that direction of the pressure force acting on the thermo-well depends on the operation regime (Fig. 2).

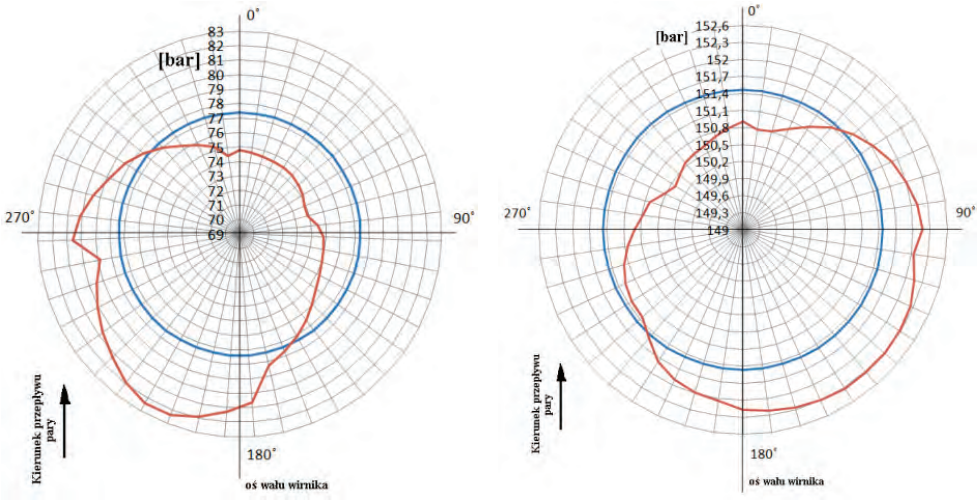

Fig. 2. Plots of total pressure distribution around thermo-well
(bottom parts correspond to the upstream side): left – for 180 MW; right – for 380 MW

3. Conclusions

Operation with partial load is characterized by larger pressure amplitudes acting on the thermo-well. The total pressure amplitude reaches 5.6 bar while at full load is equal to maximum 2 bar. Pressure distribution curve around the thermo-well changes both its shape and values bringing about a variation of not only the pressure amplitude but also the load direction.

Two major excitations from the steam flow in the control stage chamber can be distinguished, namely due to non-uniform steam supply to the nozzle boxes and due to aerodynamic wakes of rotor blades trailing edges. The excitation frequency due to non-uniform steam supply to the nozzle boxes is 100 Hz for 180 MW load and 50 Hz for 380 MW load. The excitation frequency due to aerodynamic wakes is 3200 Hz in the entire load range.

At steady state operation the natural frequencies of the thermo-well lie outside the range of excitation frequencies from the steam forces and the thermo-well is free of resonance.

References

[1] EL-BATAHGY A., FATHY G., Case Stud. Eng. Fail., 2013, Vol 1, 79.
[2] KORNET S., SŁAWIŃSKI D., ZIÓŁKOWSKI P., BADUR J., Trans. IFFM, 2015, Vol. 129, 25.
[3] HASLINGER K.H., J. Fluid Struct., 2003, Vol. 18, 425.
[4] ASME PTC19.3 TW-2010: performance test codes: thermowells. ASME 2010.

Smoothed particle hydrodynamics modelling of the shear driven gas-liquid interface deformation

M. Olejnik[1,2], K. Szewc[1], J. Pozorski[1]

[1] Institute of Fluid-Flow Machinery, Polish Academy of Sciences, Fiszera 14, 80-231 Gdańsk, Poland
[2] Gdańsk University of Technology, Conjoint Doctoral School of GUT and IFFM PAS,
Narutowicza 11/12, 80-233 Gdańsk, Poland. E-mail: michal.olejnik@imp.gda.pl

Smoothed Particle Hydrodynamics (SPH) is a meshless, particle based method for fluid flow computations. In recent years it has been successfully applied to multi-phase flow modelling, where no need of numerical grid is a huge advantage. In the present study we apply SPH to simulations of the formation and break-up of liquid film. This phenomenon is of importance in technical applications (lubrication) as well as in sea research (wave generation).

1. Introduction

Smoothed Particle Hydrodynamics (SPH) is a particle based method for the fluid flow modelling. It was proposed independently by Gingold and Monaghan [1] and Lucy [2] to simulate some astrophysical phenomena at the hydrodynamic level. Because of its Lagrangian nature the SPH method found application in modelling a wide range of problems involving large deformations like different kinds of fluid-flow or granular and solid mechanics [3].

Simulations of multiphase flows are branch of fluid dynamics where SPH is particularly useful. Contrary to Eulerian methods there is no necessity for interface reconstruction. Since there is no numerical grid and different phases are represented by particles, the shape of interface can be explicitly obtained from their positions. While the SPH gives accurate results for single bubbles/droplets, e.g., [4], its performance in more complex and realistic cases still needs to be assessed. In the present work we focus on formation and rupture of liquid film. The entrainment of droplets due to the shearing caused by the gas flow along the liquid layer, their behaviour and properties require an accurate method of modelling of the interface and influence of the surface tension.

2. SPH method

General idea behind the SPH approach is to introduce kernel interpolants for field values and solve governing equations by calculating interactions between particles representing continuous medium. Detailed description of the SPH formalism can be found in [5].

Depending on purpose and assumptions different formulations of SPH for fluid dynamics may be obtained. For a viscous, incompressible fluid flow set of governing equations consists of the Navier–Stokes equation, the continuity equation, the equation of state and the advection equation. In our work we use the SPH formalism proposed by Hu and Adams [6]. To the best of our knowledge, their approach is well suited for modelling multiphase flows with high density ratios, which is crucial for gas-liquid flows. Surface tension is modelled with Continuum Surface Force (CSF) method [4]: it is calculated from the local curvature of the interface and then converted into force per unit volume. To avoid unphysical mixing of different phases we use interface sharpness correction procedure proposed in [4] and discussed in [7].

3. Numerical experiments

In order to test applicability of SPH to modelling of liquid film formation we performed simulation of flow in a two-dimensional rectangular channel of width D and length $L = 5D$ with

periodic boundary conditions along the streamwise direction. Initially the channel is filled with gas G, except layers of liquid L on both walls. The layers were set to be of $0.1D$ thickness. The density and viscosity ratios were similar to those of water and air, i.e., $\rho_L/\rho_G = 100$ and $\mu_L/\mu_G = 100$. The fluid motion in the channel is induced by applying mass force g along its length. Dimensionless numbers describing this case are Reynolds number for gaseous phase and fluid film, and Weber and Bond number for influence of surface tension. The accuracy of SPH simulation is assessed by comparing liquid film thickness and moment of entrainment with experimental correlations [8].

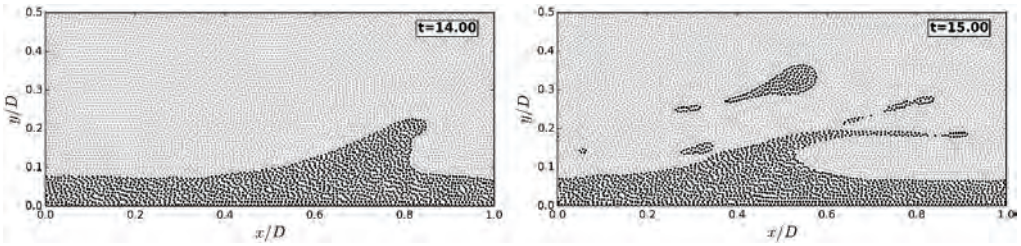

Fig. 1. SPH simulation of liquid film evolution with formation of disturbance waves on liquid layer (left plot) and entrainment of droplets at the later stage (right plot)

Acknowledgements

This research was supported by the project PB NCN 2013/11/B/ST8/03818 of the National Science Centre (NCN, Poland) and the EU FP7 project Nugenia Plus.

References

[1] GINGOLD R.A., MONAGHAN J.J., Mon. Not. R. Astron. Soc., 1977, 181, 375–389.
[2] LUCY L.B., Astron. J., 1977, 82, 1013–1024.
[3] MONAGHAN J.J., Annu. Rev. Fluid Mech., 1977, 44, 323–346.
[4] SZEWC K., POZORSKI J., MINIER J.P., Int. J. Multiphas. Flow, 2013, 50, 98–105.
[5] VIOLEAU D., *Fluid Mechanics and the SPH Method: Theory and Applications*, Oxford University Press 2012.
[6] HU X.Y., ADAMS N.A., J. Comput. Phys., 2006, 213, 844–861.
[7] SZEWC K., POZORSKI J., MINIER J.P., Int. J. Numer. Meth. Eng., 2015, 103, 625–649.
[8] BERNA C., ESCRIVÁ A., MUÑOZ-COBO J.L., HERRANZ L.E., Prog. Nucl. Energ., 2014, 74, 14–43.

Experimental and numerical study on the performance of the smooth-land labyrinth seal

A. Szymanski, S. Dykas, W. Wróblewski, M. Majkut, M. Strozik

Silesian University of Technology, Institute of Power Engineering and Turbomachinery,
ul. Konarskiego 18, 44-100 Gliwice, Poland. E-mail: Artur.Szymanski@polsl.pl

In turbomachinery the secondary flow system includes flow phenomena occurring outside the main channel, where the gaseous medium performs work on blades. Secondary air distribution constitutes a very complex and closely interrelated system that affects most of the gas turbine components. One of the most important examples of the secondary flow is leakage occurring in seals, e.g., at the rotor and stator tips, on the shaft or on the sides of the blade rim. Owing to its simplicity, low price, easy maintenance and high temperature capability, the labyrinth seal is a prime sealing solution that may be selected from numerous types of sealing structures applied in turbomachinery. For this reason, an experimental study of this particular structure has been carried out. The paper presents leakage performance of the smooth-land labyrinth seal.

1. Introduction

Turbomachinery labyrinth seals have been the focus of interest of numerous academic and research centres for many years. The works undertaken in them, both experimental and numerical [1], have concentrated mainly on determining the impact of geometrical parameters on leakage, distribution of pressure [2], temperature or propagation of aeroacoustic phenomena. This paper presents the approach and results of experimental testing carried out on an in-house stationary (the labyrinth does not move) measuring test rig of the Institute of Power Engineering and Turbomachinery of the Silesian University of Technology. The aim of the tests was to establish the impact of the clearance size on leakage and the static pressure distribution along the labyrinth structure.

2. Research methodology

In order to determine the performance characteristic of the seal under analysis, experimental tests were performed on a measuring stand supplied by a vacuum pump (Fig. 1). The installation makes it possible to achieve a maximum value of pressure ratio π of about 2. The mass flow is measured using a thermo-anemometer probe measuring the velocity, calibrated against the velocity profile determined by means of the LDA method, for velocity ranges under consideration. Additionally, the static pressure distribution was measured along the seal land over the

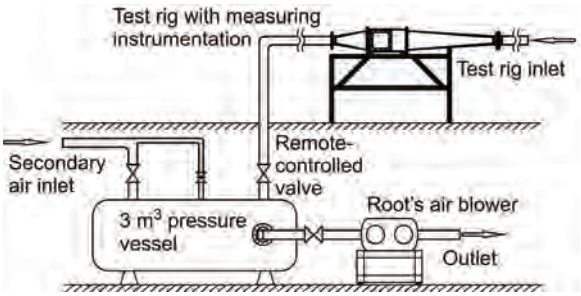

Fig. 1. Experimental installation intended for the turbine seal testing in the IPET of the SUT

sealing. The obtained results were compared to CFD calculations performed by means of the Ansys CFX v.16.2 commercial code using a flow model based on the RANS equations. Fig. 2 presents the investigated seal structure with the arrangement of impulse holes for the pressure measurement. Pressure ratio π is determined in relation to ambient pressure and static pressure from the last hole – as shown in Fig. 2.

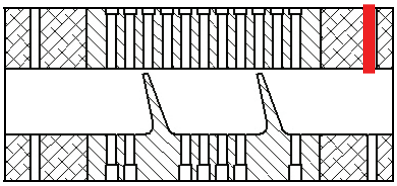

Fig. 2. The investigated labyrinth seal cross section

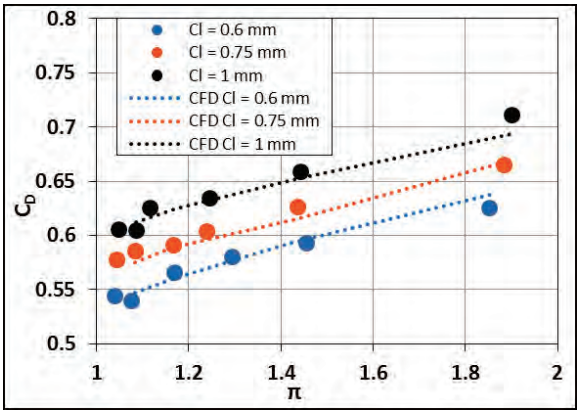

Fig. 3. Discharge coefficient depending on the pressure ratio and clearance

3. Results

The labyrinth seal operation is described in literature using dimensionless parameters [1, 2]. One of the most common ones is discharge coefficient C_D, which is the ratio of the current mass flow – measured or being the result of numerical calculations – to the mass flow resulting from ideal expansion in a nozzle with a surface area equal to that of the clearance. It takes account of total pressure and total temperature at the inlet, as well as the pressure ratio forcing the flow:

$$C_D = \frac{\dot{m}}{m_{id}}$$

$$m_{id} = \frac{p_{0,in} \cdot A}{\sqrt{T_{0,in}}} \sqrt{\frac{2\kappa}{R(\kappa-1)}\left[\left(\frac{1}{\pi}\right)^{\frac{2}{\kappa}} - \left(\frac{1}{\pi}\right)^{\frac{\kappa+1}{\kappa}}\right]}$$

Figure 3 presents the flow characteristic of the labyrinth seal characterized by the geometry presented in Fig. 1. The analysis was conducted for three values of clearance c between the fin tip and the wall. CFD calculation results are also presented.

References

[1] KIM T.S., KANG Y., MOON H.K., *Aerodynamic Performance of Double Sided Labyrinth Seals*, 4th International Symposium on Fluid Machinery and Fluid Engineering, 2008, 377.
[2] MASSINI D., FACCHINI B., MICIO M., BIANCHINI C., CECCHERINI A., INNOCENTI L., *Analysis of flat plate honeycomb seals aerodynamic losses: effects of clearance*, 68th CITMEA, 2014, 502.

Validation of numerical models for flow simulation in labyrinth seals

D. Frączek, W. Wróblewski

Silesian University of Technology, Institute of Power Engineering and Turbomachinery,
Gliwice Konarskiego Street 18, Poland. E-mail: daniel.fraczek@polsl.pl

CFD results were compared with the results of experiments for the flow through the labyrinth seal. RANS turbulence models (k-epsilon, k omega, SST and SST-SAS) were selected for study. Steady and transient results were analysed. ANSYS CFX was used for numerical computation. The analysis included flow through sealing section with the honeycomb land and smooth land. Leakage flows and velocity profiles in the seal were compared. In addition to the comparison of computational models ranges divergence of modeling and experimental results have been determined. Tips for modeling these problems were formulated.

1. Introduction

Flow in the labyrinth seal channel is very complex. Strong flow jets, flow detachment, and vortex structures appear in such a flow. Their modeling is very important for evaluation of the seal because the effectiveness of the labyrinth seal is a direct result of the possibility of dissipation of kinetic energy in seals chambers. Selection of seals using optimization methods requires the flow computation model to identify a solution with the greatest possible precision. CFD calculations are used to resolve the flow structures calculate the optimization of various flow channels. Numerical modelling has special appreciation for the design of labyrinth turbines and compressors seals due to the high construction costs of the test rig. The study [1] shows that the use of RANS models can give solutions which are incompatible with the experimental data. The other cases results of CFD calculations will be with the results of the experiment [2], [3] contrasted. This paper presents the comparison of results obtained using different turbulence models and type of calculations (steady or transient). RANS models (*k*-epsilon, *k*-omega, SST, SST-SAS) common used for the industrial calculation were selected for analysis.

2. Results

The analyzed problem deals with straight-through labyrinth seals model with honeycomb or smooth land. The geometrical data were selected based on the literature sources, experimental data availability and reference frequency. The preliminary study indicated that seal pitch can be limited to two honeycombs cells (Figure 1). Depending on the selected turbulence model and parameters the independent results may occur. Therefore, the grid independence study was performed for each of the three turbulence models in the steady-state case. The comparison of steady and transient solutions for selected grid was presented. The leakage flow is a global parameter whose minimization is of one of the important feature in seal performance assessment. Computational results are compared with the available experimental data obtained for different seal configurations and for different pressure ratios.

The results averaged over successive time steps and instantaneous distributions of the velocity field depending on the model of turbulence were analyzed. This section also rated the impact of using a transient model SST-SAS on the calculation results.

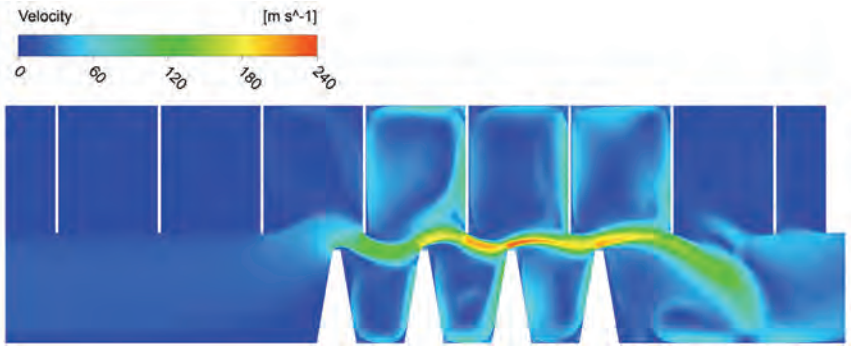

Fig. 1. Honeycomb seal velocity

3. Summary

The use of CFD for modelling of flow through the seal is associated with a lack of full compliance with the results of the experiment. Discrepancies amounted to more than few percent which could be too high to predict the seal performance. Also, differences between solutions were observed. It is possible to predict global trends. The analysis can be useful in justifying the decision on the use of numerical simulation flow through the channels.

References

[1] TYACKE J., JEFFERSON-LOVEDAY R., TUCKER P.G., *On the Application of LES to seal geometries*, Flow, Turbulence and Combustion, 2013, 91(4), 827–848.
[2] STOCKER H.L., COX D.M., HOLLE G.F., *Aerodynamic performance of conventional and advanced design labyrinth seals with solid-smooth abradable, and honeycomb lands*, NASA-CR-135307, 1977.
[3] WEINBERGER T., *Einfluss geometrischer Labyrinth- und Honigwabenparameter auf das Durchfluss- und Wärmeübergangsverhalten von Labyrinthdichtungen*, Stutensee 2014.

Evaporation level of the condensate droplets on a shock wave in the IMP PAN nozzle depending on the inlet conditions

S. Kornet, J. Badur

The Szewalski Institute of Fluid-Flow Machinery PAS-ci, Energy Conversion Department,
Fiszera 14, 18-231 Gdansk, Poland. E-mail: skornet@imp.gda.pl

In the present paper we have focused on the phenomena of condensate re-vaporation in the shock wave zone. Having observed the finishing of a foggy flow within the shock wave, according to Puzyrewski's observations, we would like to analyse the critical inlet conditions which cause total evaporation of condensate droplets on the shock in the IMP PAN nozzle. In the paper some original mechanistic model of droplet evaporation is involved, numerically implemented and compared with the IMP PAN experiment.

1. Introduction

In the space between the turbine blades, which resembles the shape of the de Laval nozzle, the shock wave can appear, which has a negative impact on the flow of the steam. Shock wave is the result of interaction between a normal shock wave and the boundary layer, which produces a λ-foot structure. According to Puzyrewski's observations, partial or total evaporation of the condensate droplets in the shock wave zone is possible and depends on the boundary conditions and the thermodynamic conditions in divergent part of the nozzle [1, 2].

In this paper we have focused on the precise prediction of the critical inlet temperature above which occurs total evaporation of condensate on the shock. In our model, the evaporation is governed not only by mass transport but also by internal structure energy that is based on balance of heat energy transported into a droplet. Numerical analysis was performed on the IMP PAN nozzle. The present work includes simulations results of the critical inlet temperatures which determine the border between total and partial evaporation on the shock wave. Calculations were performed for set of various inlet pressures with keeping the same value of pressure ratio for each case.

2. Evolution equation of dryness fraction

A wet steam model include governing equations which are based on balance of liquid-vapour mixture. For a consistent non-equilibrium condensation model a set of nine transport equations can be written in general form [3, 4]:

$$\partial_t(\rho\phi) + \mathrm{div}(\rho\phi\,\mathbf{v}) = \mathrm{div}(\mathbf{J}_\phi) + \rho S_\phi \tag{1}$$

where: $\phi = \{1, \mathbf{v}, e, k, \varepsilon, x, a\}$ represents the relevant conserved variable. Process of growth of individual droplet is governed by mass, momentum and energy transport mechanism between gas and liquid phases. Droplet growth can be described by an evolution of radius of droplet that moves in the wet steam field. Evolution equation of dryness fraction is given by:

$$\partial_t(\rho x) + \mathrm{div}(\rho x\,\mathbf{v}) = \mathrm{div}(\mathbf{J}_x) + \rho S_x \tag{2}$$

The dryness fraction sources S_x (in equation (2)) can be divided into homo- and heterogeneous sources of the mass generation rate due to condensation and evaporation. Homogenous source includes part responsible for inception of droplets and part responsible for growth and evaporation of droplets:

$$S_x = \frac{4}{3}\Pi\rho_1 \mathrm{I} r_*^3 + 4\Pi\rho_1 \alpha\, \bar{r}^2 \frac{\partial \bar{r}}{\partial t} \tag{3}$$

where: $\bar{r}$ – an average radius of droplet, ρ_1 – density of condensed phase, r_* – the critical radius of droplet, I – a volumetric rate of nucleation, α – volume fraction of condensate [3, 4].

3. Results, discussion and conclusions

For a given de Laval nozzle geometry authors have conducted calculations for wet steam model. Our numerical investigation has shown that for inlet temperatures lower than the critical temperature (which value depend on inlet pressure, pressure ratio, shape of the channel etc.) the condensate is partial evaporated during passage through the shock wave (Fig. 1). The increase of steam temperature at the inlet to values bigger than the critical temperature leads to full evaporation of the water drops in the shock wave zone – according to Puzerewski's observation (Fig. 2). Both results were obtained for the same value of inlet pressure and for the same value of pressure ratio.

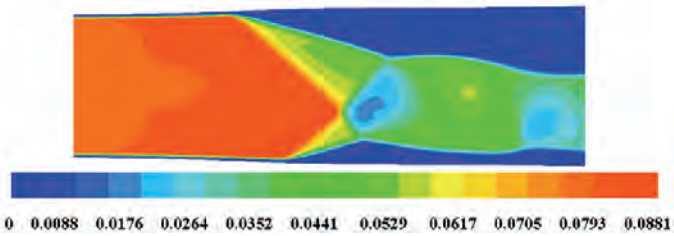

Fig. 1. Partial evaporation of condensate on the shock wave

Utilized to calculations wet-steam model, describing both condensation and re-vaporization, applied to de Laval nozzle gives satisfactory results that agree well with experimental data (very well describes both partial and complete condensate evaporation in the shock wave zone) [2].

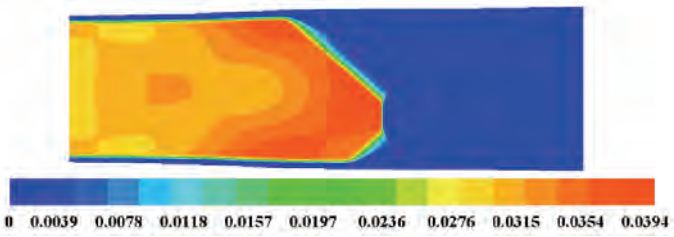

Fig. 2. Total evaporation of condensate on the shock wave

References

[1] PUZYREWSKI R., GARDZILEWICZ A., BAGIŃSKA M., Archives of Mechanics, 1973, Vol. 25, 393.
[2] KORNET S., BADUR J., 3rd Polish Congress of Mechanics and 21st Computer Methods in Mechanics, Vol 2, ed. M. Kleiber et al., 2015, 523.
[3] BILICKI Z., BADUR J., Journal of Non-Equilibrium Thermodynamics, 2003, Vol. 28, 145.
[4] KORNET S., BADUR J., Trans. IFFM, 2015, Vol, 128, 119.

The numerical simulation of Taylor-Couette flow with radial temperature gradient

E. Tuliszka-Sznitko, K. Kiełczewski

Poznań University of Technology, Faculty of Working Machines and Transportation,
Institute of Thermal Engineering, Poland. E-mail: Ewa.Tuliszka-Sznitko@put.poznan.pl

In the paper the authors present the results obtained during a numerical investigations (Direct Numerical Simulation/Spectral Vanishing Viscosity method – DNS/SVV) of the Taylor-Couette flow in the cavity of aspect ratio $\Gamma = 3.76$ and different radii ratios $\eta = 0.375 - 0.82$ with asymmetric boundary conditions. The computations are obtained for isothermal and non-isothermal fluid flow. In the paper attention is focused on the laminar-turbulent transition process. The main purpose of the research is to investigate the influence of the thermal boundary conditions and radii ratio η on the flow structure and on the flow characteristics. The transverse current J^{ω} is computed from the velocity field. The λ_2 criterion has been used for numerical visualization.

1. Introduction

In the paper we present the results obtained during a numerical investigation (Direct Numerical Simulation/Spectral Vanishing Viscosity method – DNS/SVV) of the Taylor–Couette flow in cavities of aspect ratio $\Gamma = H/(R_2–R_1) = 3.76$ and curvature parameter from the range $Rm = (R_2+R_1)/(R_2–R_1) = 2.2–10.2$ ($\eta = R_1/R_2 = 0.375–0.82$). The computations are obtained for the isothermal and non-isothermal fluid flows. In the considered cavities the end-wall boundary conditions are asymmetric, i.e., the outer cylinder and the top disk are stationary, and, the inner cylinder and the bottom disk rotate (the outer cylinder and the rotating bottom disk are heated). The Taylor–Couette flow is a model flow very useful from numerical and experimental points of view, among others, because of the simplicity of its geometry. Simultaneously, the Taylor–Couette flows appear in numerous machines in the field of mechanics and chemistry, e.g., in ventilation, desalination tanks and waste water tanks, in cooling systems, in gas turbines and axial compressors. The Taylor–Couette flow is ruled by the following dimensionless parameters: Reynolds number $Re = (R_2–R_1)R_1\Omega/\nu$, aspect ratio Γ, radii ratio $\eta = R_1/R_2$ and thermal Rossby number $B = \beta(T_2–T_1)$ in the non-isothermal fluid flow cases (where R_2 and R_1 are radii of the outer and inner cylinders, respectively). We focus on the influence of the radial temperature gradient on the flow structure and the flow characteristics (we study the local heat transfer, distributions of the local Nusselt numbers along cylinders and disks). The results are discussed in the light of the paper written by Fénot et al. [1], where the previously published results obtained for different gap thickness, axial and radial ratios, and Reynolds numbers are compared. We also study the dependence of the laminar-turbulent process on radii ratio η in the cavity with asymmetric end-wall boundary conditions (results obtained for small Reynolds number are compared with these obtained in [2]). We observe the transition from the three-cell structure (typical structure for the Taylor–Couette flow with asymmetric end-wall boundary conditions) to one-cell structure with increasing Reynolds numbers in the cavities of lower curvature parameter Rm, [2]. For higher Rm we observe typical laminar-turbulent transition process for the Taylor–Couette flow: consecutive bifurcations to Taylor vortex flow, wavy vortex flow, modulated waves state, turbulent Taylor vortex flows. The exemplary structure obtained for $\eta = 0.82$ and $Re = 967$ is presented in Figure 1, in which we observe 10 regular spiral vortices originating from the Ekman layer (the wave length in azimuthal direction is $\lambda_a/(H/2) = 1.7$). In Figure 1 the iso-surfaces of the λ_2 obtained near the inner cylinder are presented. The development of

boundary layers along cylinders and disks is the main object of our interest. We analyse the radial and axial distributions of the angular velocity, angular momentum, the local transverse angular momentum current $j^{\omega}(R, \varphi, Z, t) = R^3[v_r v_\varphi/R - \nu\partial(v_\varphi/R)/\partial R]$, the Reynolds stress tensor components and many structural parameters. In connection with the analysis carried out in [3] we consider j^{ω} averaged over concentric cylindrical surface $J^{\omega} = < j^{\omega}(R, \varphi, Z, t) >_{A(R),t} = R^3[<v_r v_\varphi/R>_{A(R),t} - \nu\partial(<v_\varphi/R>_{A(R),t})/\partial R]$. We analyse the thickness of the boundary layers.

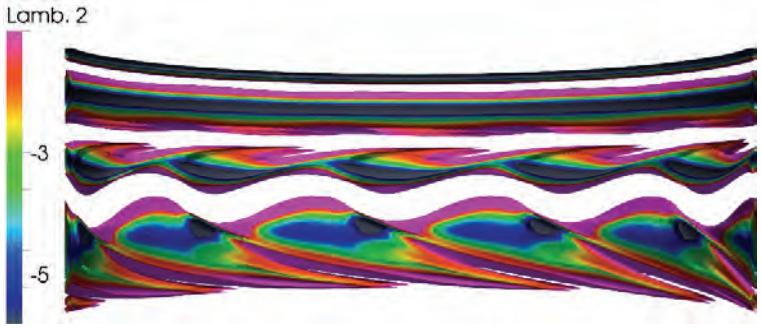

Fig. 1. The iso-surfaces of λ_2 obtained near the inner cylinder of the cavity of aspect ratio $\eta = 0.82$ ($Rm = 10.2$), $Re = 967$, $B = 0.1$, the outer stationary cylinder and the bottom rotating disk are heated, the top disk is stationary and the inner cylinder rotates

All presented numerical results are obtained with the use of DNS/SVV method with meshes of 2–12 million collocation points. In the numerical approach the time scheme is second-order semi-implicit, which combines an implicit treatment of the diffusive term and an explicit Adams–Bashforth scheme for the non-linear convective terms. The spatial scheme is based on a pseudo-spectral Chebyshev–Fourier–Galerkin collocation approximation. All dependent variables have been obtained by solving Helmholtz equation. In the DNS/SVV method an artificial viscous operator is added to the Laplace operator to stabilize the computational process for higher Reynolds numbers, [4]. The precision of computation is verified by analysing the total torque $J^{\omega} / J^{\omega}_{lam}$ for different resolutions [3] and by analysing parameters $(z)^{+}_{2/1}, (r)^{+}_{2/1}, (\Delta\varphi, R_{2/1})^{+}$ along the inner and outer cylinders.

References

[1] FÉNOT M., BERTIN Y., DORIGNAC E., LALIZEL G., *A review of heat transfer between concentric rotating cylinders with or without axial flow*, Int. J. Thermal Sciences, 2011, 50, 1138–1155.
[2] MULLIN T., BLOHM C., *Bifurcation phenomena in a Taylor-Couette flow with asymmetric boundary conditions*, Phys. Fluids, 2001, 13, 136.
[3] BRAUCKMANN H., ECKHARDT B., *Direct numerical simulations of local and global torque in Taylor–Couette flow up to Re D 30000*, J. Fluid Mech., 2013, 718, 398.
[4] SEVERAC E., SERRE E., *A spectral viscosity LES for the simulation of turbulent flows within rotating cavities*, J. Comp. Phys., 2007, 226, 2, 1234.

Influence of a strong magnetic field on a paramagnetic fluid's convection in systems with different aspect ratios

A. Kraszewska, L. Pyrda, J. Donizak

AGH University of Science and Technology, Faculty of Energy and Fuels,
Al. Mickiewicza 30, 30-059 Kraków. Poland. E-mail: kraszka@agh.edu.pl

The main purpose of proposed research was to investigate the influence of a magnetic field on a natural convection of a paramagnetic fluid in enclosures with aspect ratios (*AR* = height/width) 0.5 and 2.0. Performed experiments allowed to determine the impact of strong magnetic field on heat transfer and the nature of the flow, showing that strong magnetic field enhances Nusselt number and rapidly changes the character of the flow. Conducted analysis also allowed to determine the aspect ratio influence on investigated systems.

1. Introduction

In many industrial situations, control of convection processes is a very crucial aspect. One of the possible ways to control convection processes is to apply strong magnetic field to convection of fluids with magnetic properties. In early 90s both suppression and enhancement of convective motion using strong magnetic field on paramagnetic fluid was achieved. Pleskacz [1] investigated impact of magnetic field on low and high Reynolds flows and Roszko [2] studied thermomagnetic convection of low concentration nanofluids. Turan [3] investigated influence of enclosure's aspect ratio on heat transfer for natural convection. He concluded that enclosure dimensions have great influence on Nusselt number. To the authors best knowledge, there is no experimental data available in literature stating the influence of *AR* on thermomagnetic convection, and so the purpose of reported research is to investigate the natural and thermomagnetic convection in enclosures with aspect ratios 0.5 and 2.

2. Experimental setup

The super conducting magnet and experimental apparatus used in presented research are shown in Figure 1 and Figure 2. Experimental enclosure was composed of two copper plates (one for cooled top and the second one for heated bottom), a rectangular cavity from plexiglass and

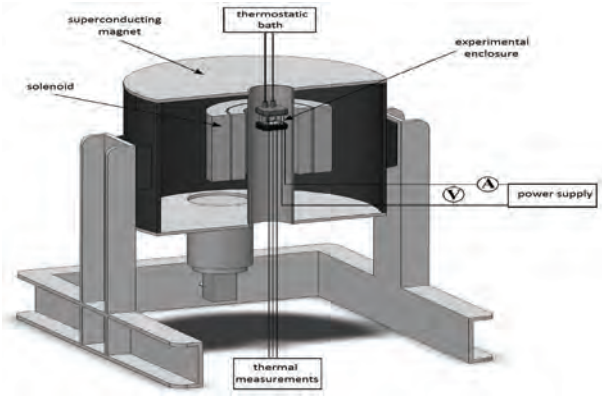

Fig. 1. Experimental setup and location of rectangular enclosure in the magnet

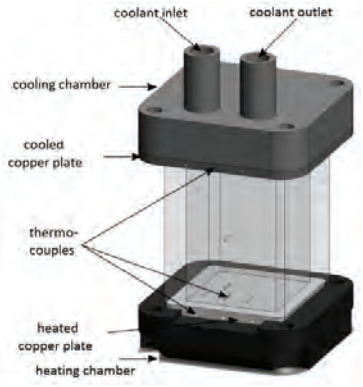

Fig. 2. Schematic view of experimental enclosure

cooling and heating chambers. Enclosure was filled with working fluid, which was a water-glycerol solution with an addition of gadolinium nitrate hexahydrate ($Gd(NO_3)_3 \cdot 6H_2O$) to make it paramagnetic. The enclosure was positioned in upper half of the magnet, so that gravitational and magnetization forces acted in the same direction causing an enhancement of the heat exchange.

3. Results

Conducted research enabled fast Fourier Transform analysis of fluid flow, which showed that magnetic field rapidly changes character of the flow.

Example of the heat transfer analysis in the enclosures with aspect ratios 0.5 and 2 for $\Delta T = 3°C$ between heated and cooled walls is shown in Figure 3. For natural convection case, without external magnetic field, Nusselt number for enclosure with $AR = 0.5$ is significantly higher than for $AR = 2.0$ and with increasing magnetic field, Nusselt number is three times higher for magnetic induction of 10T.

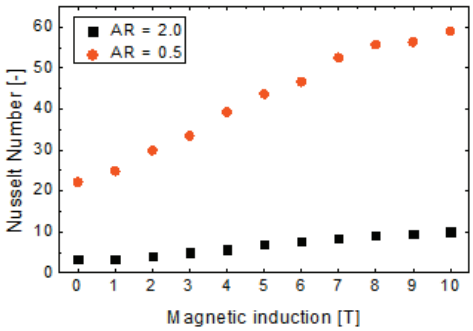

Fig. 3. Nusselt number versus magnetic field induction

Acknowledgements

The present work was financially supported by the Polish Science Centre (Project No. 12/07/B/ ST8/03109).

References

[1] PLESKACZ L., FORNALIK-WAJS E., J. Phys. Conf. Ser., 2014, Vol. 530, 012062.
[2] ROSZKO A., FORNALIK-WAJS E., DONIZAK J., WAJS J., KRASZEWSKA A., PLESKACZ L., KENJERES S., MATEC Web. Conf., 2014, Vol. 18, 03006.
[3] TURAN O., POOLE R.J., CHAKRABORTY N., Int. J. Heat Fluid Flow, 2012, Vol. 33, No. 1, 131–146.

Influence of a strong magnetic field on paramagnetic fluid's flow in cubical enclosure

A. Kraszewska, L. Pyrda, J. Donizak

AGH University of Science and Technology, Faculty of Energy and Fuels,
Al. Mickiewicza 30, 30-059 Kraków, Poland. E-mail: kraszka@agh.edu.pl

The fluid behaviour in thermo-magnetic convection of paramagnetic fluid in a strong magnetic field was studied. The fluid was 50% volume aqueous solution of glycerol with an addition of gadolinium nitrate hexahydrate ($Gd(NO_3)_3 \cdot 6H_2O$). Experimental enclosure – a vessel with aspect ratio (AR = height/width) equal to 1.0 – was heated from the bottom, and cooled from the top. Temperature difference between top and bottom walls was kept constant at $\Delta T = 5$ and 11 [°C]. The magnetic induction was increased stepwise from 1 to 10 [T] and thermocouples placed inside the enclosures measured temperature changes of the fluids. On the basis of temperature measurements, analysis of the fluid flow was performed.

1. Introduction

Natural convection control is crucial in many industrial, astrophysical and environmental applications. Utilization of magnetic convection phenomenon gives additional tool to control convection processes of non-electrically conducting fluids. Combined gravitational and magnetic force allow to enhance or suppress convection process, depending of fluid magnetic properties and configuration of system. Moreover, magnetic field significantly changes the behavior of the fluid flow, which can be showed by calculating spectral functions with the utilization of Fast Fourier Transform.

2. Experimental setup

Experimental apparatus used in conducted research consisted of superconducting magnet (HF10-100VHT-B, *Sumito Heavy Industries,* Ltd. Japan), an enclosure with aspect ratio 1 shown in Figure 1, DC supply, multimeter, thermo-static bath and data acquisition system. Cubical enclosure was made of cooling chamber, a vessel from plexiglass filled with experimental fluid, and heating chamber. Thermocouples inserted into one wall measured changes of the temperature during experiments.

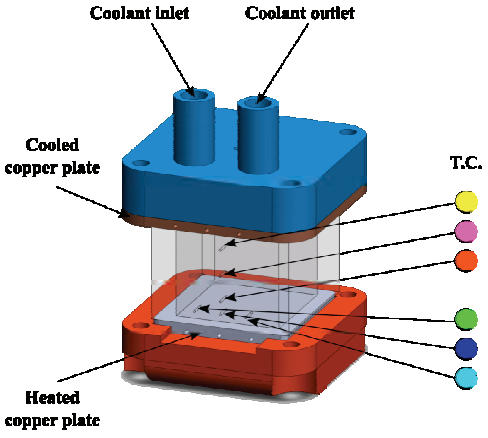

Fig. 1. Experimental enclosure

3. Measurements

Experiments were conducted for temperature difference between heated bottom wall and cooled top wall equal to 5 and 11 [°C], without magnetic induction and for magnetic induction from 1 [T] to 10 [T]. Working fluid was water-glycerol solution with addition of gadolinium nitrate hexahydrate. Experimental enclosure were placed in the upper half of superconducting magnet, and that position enabled strengthening of fluid motion by magnetic force.

4. Results

Conducted measurements allowed to perform Fast Fourier analysis on recorded temperature signals. Figure 2 shows sample results as power spectrum versus frequency for $\Delta T = 5$ [°C].

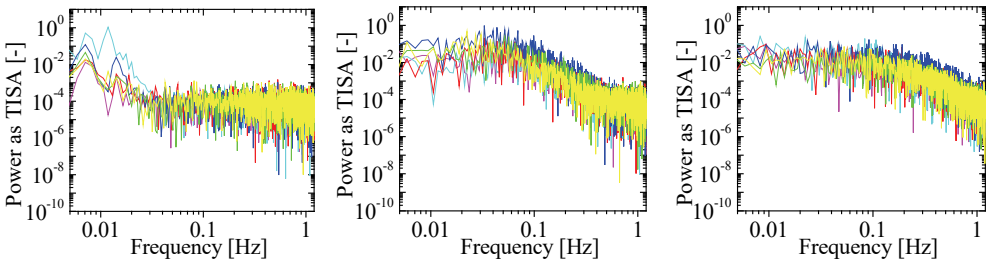

Fig. 2. Power spectrum for $\Delta T = 5$ [°C] and magnetic induction in the centre of the magnet $|b_0|_{max}$: a) 0 [T], b) 5 [T], c) 10 [T]

Spectral analysis showed that strong magnetic field heavily influence the fluid behaviour – in higher values of magnetic induction, temperature fluctuations are smaller and temperature field is more uniform. Spectral analysis also allowed to determine the transition point from laminar, to turbulent convection.

Acknowledgements

The present work was financially supported by the National Science Centre (Project No. 12/07/B/ST8/03109).

Unsteady conjugate heat transfer analysis for impinging jet cooling

F. Tejero, P. Flaszynski, R. Szwaba, J. Telega

Institute of Fluid Flow Machinery Polish Academy of Sciences,
Fiszera 14, 80-231 Gdansk, Poland. E-mail: fernando.tejero@imp.gda.pl

Abstract: The paper presents the numerical investigation of the heat transfer on flat plate under a single impingement jet. The CFD model is validated against the experimental data from the Institute of Fluid Flow Machinery Polish Academy of Sciences. Conjugated Heat Transfer simulations for unsteady flow above the plate and temperature evolution inside allows to validate the model and then to analyze heat transfer coefficient on the investigated wall. Numerical simulations are carried out by means of Ansys/Fluent and k-ω SST model. Geometry and the mesh were created according to the test section configuration. Unsteady simulations have been done for the geometry including metal and PMMA plates.

1. Introduction

Heat transfer from impinging jets is being investigated by several researchers recently. This approach for heat transfer enhancement is convenient in applications where the convention fails or is reduced (e.g., leading edge of a turbine blade). It was during the 50's when Freidman and Mueller [1] reported the first research conducted on this topic. Among other purposes, there has been a big effort on turbine cooling applications [2] where the impinging jets might cool several sections of the engine such as the combustor, the turbine case and/or the turbine blades.

The influence of plate material and thickness on heat transfer by impingement jets is investigated in the present paper. Two different material properties were studied for a plate thickness of 2 mm. The thermal conductivity of the plate was modified from a high thermal case (steel) to a low one (steel alloy – Inconel). The unsteady simulations allow for a better understanding of the flow physics when an impinging jet is applied. Besides, the temperature evolution on the investigated plate is successfully compared with the available experimental data (Transient Liquid Crystal measurements).

2. Computational domain and numerical results

The CFD investigation was carried out by means of the Ansys/Fluent code which solves the Unsteady Reynolds–Averaged Navier–Stokes (URANS) equations with various turbulence models. From the difference turbulent closures available in the solver, the two equation k-ω SST was chosen. The numerical algorithm is based on a semi-discrete approach with finite-volume of 2nd order of accuracy for the spatial discretization as well as a 2nd order for the time-stepping scheme. The computational domain was simplified to an axisymmetric approach reducing considerably the number of volumes and the computational resources.

Figure 1 presents a snapshot of the unsteady simulation with the single impinging jet. After certain time, the heat penetrates the investigated plate and travels in radial direction. At the bottom, the plate metal plate is isolated by the PMMA plate with very low thermal conductivity. Transient Liquid Crystal measurements were carried out on the lower side of metal plate.

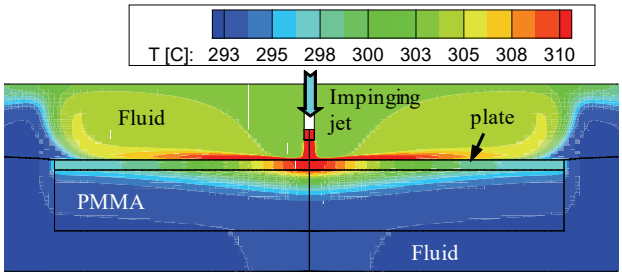

Fig. 1. Snapshot of the temperature distribution

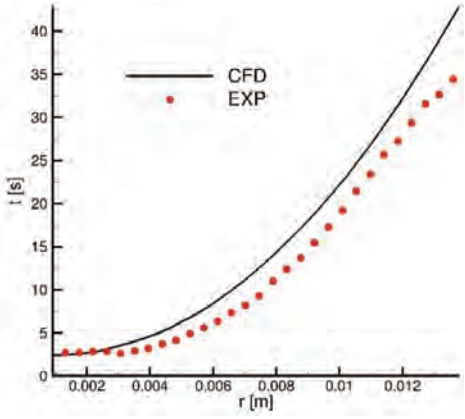

Fig. 2. Comparison of the temperature propagation in the plate

As exemplary comparison of the measurements and numerical results, Figure 2 presents the temperature propagation (value of 308 K) in the radial direction. Numerical results and experimental data show the same slope and the only difference arises from the different response of the plate to heat at the beginning (faster in the numerical results).

References

[1] FREIDMAN S.J., MUELLER A.C., Proc. Gen. Disc. on Heat Transfer, Institution of Mech. Engineers, 1951, 138–142.
[2] ZUCKERMAN N., LIOR N., Advances in Heat Transver, 2006, Vol. 39, 565–631.

Modelling liquid spreading in porous zone – modification of 3D approach to efficient 2D axisymmetric algorithm

D. Asendrych, P. Niegodajew

Częstochowa University of Technology, Institute of Thermal Machinery,
ul. Dąbrowskiego 69, 42-201, Częstochowa, Poland. E-mail: niegodajew@imc.pcz.pl

A 3-dimensional Eulerian 2-fluid model was applied to resolve a 2-phase gas-liquid flow in a trickle-bed reactor. A liquid spreading was simulated by the source term in the momentum equation that could additionally reconstruct a random character of the flow hydrodynamics in the packed bed. The paper presents a development of a 2-dimensional axisymmetric algorithm allowing for huge savings of computational efforts without losing model relevance and functionality.

1. Introduction

Trickle-bed reactors (TBR) are widely used in chemical and process engineering, e.g., in distillation, absorption or cooling columns [1]. Their efficiency is dependent on a number of parameters like the packed bed type and size, media properties and their loads and 2-phase flow regime [1]. The research studies of liquid flow hydrodynamics with the use of available experimental techniques are limited due to complex geometry of packed beds and their opacity [2]. That is why computational fluid dynamics (CFD) is more and more widely used to overcome these disadvantages allowing to investigate the liquid flow behaviour with sufficient relevance. An Eulerian two-fluid model, treating statistically the flow, is the most efficient approach as shown in review paper of Wang et al. [3]. Although it does not provide a detailed insight into the flow structure (e.g., gas-liquid interface cannot be tracked as with the use of VOF – Volume of Fluid method), the pressure drop, liquid holdup and flow redistribution can be predicted with satisfactory accuracy. With this approach the momentum equation is extended by the Ergun-type source term describing the liquid phase flow resistance (see, e.g., [3]).

2. Description of a 3D model

In the present simulation strategy the Ergun-type model is replaced by the corresponding expression coming from the solution of the VOF simulation. Such an approach was used to resolve a 2-phase countercurrent flow in a random packed bed composed of Raschig rings. At first, the exact geometry of the TBR was generated [4] allowing to find a flow structure with the use of conventional conservation laws and the liquid free surface tracking by VOF. The flow statistics obtained in this way allowed to determine the probability density function (pdf) of the velocity vector orientation φ [5] as

$$pdf(\varphi) = \frac{A\varphi}{1 + B\varphi^2} \tag{1}$$

where A and B are the fitting constants. Using expression (1) the relevant source term was derived of the form [5]

$$M_r = f(u_{x,B}, \varphi, \overline{\varphi}) \tag{2}$$

where $u_{x,B}$ is the mean axial velocity of liquid phase determined according to [1] and reflecting the axial flow resistance whereas $\overline{\varphi}$ stands for the average orientation angle value. In order to simulate the liquid spreading the local angle φ was generated in a random manner, however,

satisfying its pdf distribution (1). Such a procedure was implemented into the Ansys Fluent software allowing for joint modelling of the axial flow resistance and the liquid spreading [5].

3. Development of a 2D axisymmetric model

The presented model was applied to conduct a series of simulations showing reasonable liquid behaviour [5]. However, its 3D character made the CFD simulations computationally very expensive, That is why a 2D axisymmetric algorithm was developed. However, the numerical procedure could not be directly adopted to the 2D approach as it would lead to the unexpected liquid transfer and even unphysical behaviour. The mass and momentum transfer in transverse directions is governed by the velocity generated in a way satisfying the expression (1) and in principle it is proportional to the transverse velocity component. This transfer mechanism works correctly for 3D model and the simulated liquid spreading is fully consistent with the advection-diffusion model [6]. However, in a 2D axisymmetric formulation mass and momentum transferred to the neighbouring regions is additionally related to the radial position. Consequently the inward transfer statistically exceeds the outward one what leads to the liquid accumulation in the centre of the column. In order to overcome this undesired behaviour an adequate correction function had to be introduced into the source term (2). For that reason a virtual experiment was performed simulating the mass transfer process in a column cross section with initially uniformly distributed liquid phase. The domain was divided into cells of a sufficiently small size Δr. From the centre of each cell a series of elementary mass fluxes

$$\Delta \dot{m} = pdf(\varphi_i) \cdot u_r \cdot \rho \cdot \alpha \cdot 2\pi \cdot r \cdot \Delta r \tag{3}$$

was ejected with a radial velocity u_r for the angle φ_i varied with a constant step within its domain. The procedure was repeated for all the cells. Because of the undesired correlation $\dot{m} \sim r$ the mass flux distribution was modified from its initial state leading to its artificial accumulation at the centre with the local maximum at $r = 0$. The inverse of the obtained distribution was then applied as a correction function in the source term (2) responsible for the liquid spreading modelling.

The test simulations carried out for the CFD model with the use of a modified 2D algorithm provided the results clearly showing its full consistency with the reference 3D approach. The spatial distributions of liquid volume fraction obtained for both cases agree with very good accuracy, although with the 2D model no circumferential variation can be resolved. Summing up, the 2D modified liquid spreading approach allows for huge savings of computational effort without losing model relevance. With its application it is now possible to conduct parametric calculations of the 2-phase gas-liquid flow in TBR and the detailed analysis of the liquid redistribution in various flow condition, also including complex transfer processes in reacting systems like CO_2 chemical absorption.

References

[1] BILLET R., *Packed Towers*, Weinheim, FRG: Wiley-VCH Verlag GmbH & Co. KgaA, 1995.
[2] YIN F., AFACAN A., NANDAKUMAR K., CHUANG K.T., *Liquid holdup distribution in packed columns: gamma ray tomography and CFD simulation*, Chem. Eng. Proc., 2002, 41, 473.
[3] WANG Y., CHEN J., LARACHI F., *Modelling and simulation of trickle-bed reactors using computational fluid dynamics: A state-of-the-art review*, Can. J. Chem. Eng., 2013, 91, 136.
[4] MAREK M., *Numerical generation of a fixed bed structure*, Chem. Process Eng., 2013, 34, 347.
[5] NIEGODAJEW P., ASENDRYCH D., MAREK M., DROBNIAK S., *Modelling liquid redistribution in a packed bed*, J. Phys. Conf. Ser., 2014, 530, 1.
[6] CIHLA Z., SCHMIDT O., *Studies of the behaviour of liquids when freely trickling over the packing of cylindrical tower*, Collect. Czech. Chem. Commun., 1958, 23, 569.

Symmetry analysis and invariant solutions of the multipoint infinite systems describing turbulence

M. Wacławczyk[1], M. Oberlack[2]

[1] Warsaw University, Faculty of Physics, Pasteura 7, 02-093 Warsaw, Poland
[2] Technische Universität Darmstadt, Strömungsdynamik, Otto-Berndt-Str. 2, 64287 Darmstadt, Germany
E-mail: marta.waclawczyk@igf.fuw.edu.pl

The present work concerns multipoint description of turbulence in terms of the probability density functions (PDF's) and the characteristic Hopf functional. Lie symmetries of infinite systems of equations for the PDF's and the Hopf functional equation are derived. Based on symmetries, invariant solutions for turbulence statistics are calculated.

1. Introduction

With respect to turbulence research three complete statistical descriptions of turbulence, treated as a stochastic field, are known, namely the infnite hierarchy of the multi-point correlation equations (so-called Friedmann-Keller (FK) hierarchy, the infnite hierarchy of the multipoint probability density functions (PDF's) equations (Lundgren–Monin–Novikov (LMN) equations, [1]) and finally the Hopf functional approach, [2]. The two latter approaches will be discussed below.

The n-point velocity PDF $f_n(\boldsymbol{v}_{(1)}, \boldsymbol{x}_{(1)}; ...; \boldsymbol{v}_{(n)}, \boldsymbol{x}_{(n)}, t)$ contains information about all statistics up to n-point statistics of infinite order which can be calculated from the PDF by integration over the sample space variables for example $\langle U_{i_{(1)}}(\boldsymbol{x}_{(1)}, t) \cdots U_{i_{(n)}}(\boldsymbol{x}_{(n)}, t)\rangle = \int v_{i_{(1)}} \cdots v_{i_{(n)}} f_n d\boldsymbol{v}_{(1)} \cdots d\boldsymbol{v}_{(n)}$.

The infinite hierarchy of equations for multipoint PDF's was derived in [1]. E. Hopf introduced another very general approach to the description of turbulence. He considered the case where the number of points in PDF goes to infinity, so that the probability density function becomes a probability density functional and one deals with a continuous set of sample space variables $\boldsymbol{v}(\boldsymbol{x})$. It is more convenient to consider a functional Fourier transform of the probability density functional, called the characteristic functional $\Phi([\boldsymbol{v}(\boldsymbol{x})], \boldsymbol{t})$. The approach of Hopf was later generalised in Ref. [3] where the full space-time functional formalism was introduced and the functional $\Phi([\boldsymbol{v}(\boldsymbol{x})], \boldsymbol{t})$ was defined as $\Phi([\boldsymbol{v}(\boldsymbol{x}, \boldsymbol{t})]) = \left\langle \exp \iint \boldsymbol{U}(\boldsymbol{x},\boldsymbol{t}) \cdot \boldsymbol{y}(\boldsymbol{x},\boldsymbol{t}) d\boldsymbol{x}d\boldsymbol{t} \right\rangle$. With this definition moments of the velocity can be calculated as the functional derivatives of the characteristic functional at the origin [3]

$$\left. \frac{\delta^n \Phi}{\delta y_{i_{(1)}} \cdots \delta y_{i_{(n)}}} \right|_{\boldsymbol{y}=0} = i^n \left\langle U_{i_{(1)}}(\boldsymbol{x}_{(1)}, t_{(1)}) \ldots U_{i_{(n)}}(\boldsymbol{x}_{(n)}, t_{(n)}) \right\rangle$$

Evolution equation for the characteristic functional was derived in Ref. [3]. It is only one equation (not a hierarchy) which embodies the statistical properties of the fluid flow in a very concise form.

The objectives of the present work are to discuss the classical and new statistical Lie symmetries that were first found for the FK hierarchy [4] and are also present in the LMN hierarchy [5] and find corresponding symmetries for the Hopf equation. Lie one-point symmetry transformation is such transformation of the independent and dependent variables, which does not change the functional form of a considered equation [6]. The transformed variables $\boldsymbol{x}^* = g(\boldsymbol{x}, \boldsymbol{y}(\boldsymbol{x}), \varepsilon)$ and $\boldsymbol{y}^*(\boldsymbol{x}^*) = h(\boldsymbol{x}, \boldsymbol{y}(\boldsymbol{x}), \varepsilon)$ are functions of $\boldsymbol{x}, \boldsymbol{y}$ and depend on a group parameter ε. The transformations can also be written in infinitesimal forms after a Taylor series expansion about ε: $\boldsymbol{x}^* = \boldsymbol{x} + \chi(\boldsymbol{x}, \boldsymbol{y})\, \varepsilon$

+ $\mathcal{O}(\varepsilon^2)$ and $\boldsymbol{y}^* = \boldsymbol{y} + \eta(\boldsymbol{x}, \boldsymbol{y})\varepsilon + \mathcal{O}(\varepsilon^2)$. It follows from the Lie's first theorem that knowing the infinitesimal forms χ and η uniquely determines the global form of the group transformation $g(\boldsymbol{x}, \boldsymbol{y}(\boldsymbol{x}), \varepsilon)$ and $h(\boldsymbol{x}, \boldsymbol{y}(\boldsymbol{x}), \varepsilon)$. With the use of infinitesimals invariant solutions of the considered equation may be derived [6]. In fluid mechanics these solutions often represent attractors of the instantaneous fluctuating solutions of the Navier–Stokes equations, i.e. the characteristic turbulent scaling laws.

From the Lie symmetry analysis of the LMN hierarchy it followed that, suprisingly, the new symmetries are connected with intermittent laminar/turbulent flows [5]. The outcome of the symmetry analysis are invariant solutions for turbulence statistics and new possibilities to improve turbulence closures, such that invariance under the whole set of symmetries is accounted for.

2. Symmetries of the LMN hierarchy and Hopf equation

Symmetries of the LMN hierarchy were investigated in Ref. [5]. Therein, it was shown that the hierarchy is invariant under the classical symmetries of the Navier–Stokes, equations, in particular, time and space translations, Galilean invariance and, for non-zero viscosity, one scaling group. Moreover, it was shown that two additional symmetries of the LMN hierarchy exist which transform a PDF of a turbulent signal into the PDF of an intermittent laminar-turbulent flow. With the use of new symmetries series of invariant solutions for turbulence statistics can be derived from the characteristic equation [6]. As an example, for the plane Poiseuille channel flowthe following solution for the mean velocity can be derived

$$\langle U_1 \rangle = \frac{C_1}{k_2} \ln y + \frac{C_1}{2k_2}\left(1 - \frac{y^2}{H^2}\right) + \mathbb{C}$$

where C_1, k_2, and $\mathbb{C}$ are constants and y is the wall-normal coordinate. This solution follows from a first principle mathematical analysis of the governing equations, hence, it is not a modelling assumption. It is valid in the logarithmic region and is a sum of the turbulent and laminar velocity profiles.

In contrast to the LMN system which has all symmetries of the Navier–Stokes equations, in the original equation for the space functional, as introduced by E. Hopf [2], the Galilei invariance is broken. This follows from the integral formulation of this equation where the integration bounds must remain constant. For this reason another, space-time functional formalism from Ref. [3]will be considered. It will be shown that the Galilei invariance, as well as other symmetries of the Navier–Stokes equations are preserved and the corresponding forms of the new statistical symmetries will derived. Invariant solutions for the Hopf functional, in a form of the infinite series of moments will be derived.

Acknowledgements

The financial support of the National Science Centre, Poland (project No./2014/15/B/ST8/00180) is acknowledged.

References

[1] LUNDGREN T.S., Phys. Fluids, 1967, 10, 969.
[2] HOPF E., J. Rational Mech. Anal., 1952, 1, 87.
[3] LEWIS R.M., KRAICHNAN R., Comm. Pure Appl. Math., 1962, 15, 397.
[4] OBERLACK M., ROSTECK A., Disc. Cont. Dyn. Sys. Ser S, 2010, 3, 451.
[5] WACŁAWCZYK M., STAFFOLANI N., OBERLACK M., ROSTECK A., WILCZEK M., FRIEDRICH R., Phys. Rev. E, 2014, 90, 013022.
[6] BLUMAN G., CHEVIAKOV A., ANCO S., *Applications of Symmetry Methods to Partial Differential Equations*, Springer, New York 2009.

Complex dynamic response mode for fluid model order reduction

W. Stankiewicz[1], M. Morzyński[1], K. Kotecki[1]. W. Szeliga[1,2]

[1] Poznań University of Technology, Institute of Combustion Engines and Transport,
Piotrowo 3, 60-965 Poznań, Poland
[2] Poznań Supercomputing and Networking Center, Jana Pawła II 10, 61-139 Poznań, Poland
E-mail: Witold.Stankiewicz@put.poznan.pl

The method of reduced order modelling of the flow with the use of physical modes is presented. These modes are generated using frequency response functions in complex domain. As opposed to empirical, modal decomposition methods, Complex Dynamic Response modes are computed without time-consuming unsteady simulations. In this paper, these modes will be used in Galerkin projection to reduce the dimension (order) of fluid model.

1. Introduction

Flow control is one of the most challenging areas of present fluid mechanics. The need of the reduction of emissions and generated noise in both aerospace and automotive industries, imposed by regulations like ACARE or EURO, lead to the requirement of continuous optimization of vehicles. While traditional approaches, based on geometrical changes, seem to be reaching their limits, active, feedback flow control might be the choice for future improvements.

Among the flow modeling techniques for flow control, low dimensional Galerkin modeling is one of the most promising. While it is strongly dependent on the chosen modal expansion basis, big effort is made to find the approach allowing to compute modes valid for flow modeling and control.

Most popular, empirical approaches are based on the decomposition of numerical or experimental data containing the velocity (and pressure) fields from consecutive time steps, like Proper Orthogonal Decomposition (POD) [1], Dynamic Mode Decomposition (DMD) [2, 3] and their modifications, like Snapshot POD [4], Balanced POD [5] and many others.

Unfortunately, empirical modes reproduce the dynamics in the very close vicinity of operating conditions, for which they were captured. That is a serious limitation for flow control applications, where operating and/or boundary conditions change due to actuation process.

2. Complex Dynamic Response

As an alternative to empirical decomposition methods, physical approach, called Complex Dynamic Response [6], is proposed as a source of global, physical modes for flow modeling and control.

In this method, we assume that the unsteady solution of the Navier–Stokes equation is expressed as a sum of some base solution $\overline{V}$ and the time-varying fluctuation $\widetilde{V}$. With additional assumptions of small value of fluctuation and it's periodicity, and further linearization, this leads to generalized eigenvalue problem:

$$\lambda\widetilde{V}_i + \widetilde{V}_j\overline{V}_{i,j} + \overline{V}_j\widetilde{V}_{i,j} + \widetilde{P}_i - \frac{1}{Re}\widetilde{V}_{i,jj} = 0 \tag{1}$$

or:

$$\lambda Bx + Ax = 0 \tag{2}$$

Instead of direct solution of (2) we investigate frequency response function having form:

$$\begin{aligned} Ax_{Re} + \lambda_{Re}Bx_{Re} + \lambda_{Im}Bx_{Im} &= F_{Re} \\ Ax_{Im} + \lambda_{Re}Bx_{Im} + \lambda_{Im}Bx_{Re} &= F_{Im} \end{aligned} \tag{3}$$

The use of complex shift in the matrices A and B enables continuous choice of frequency and growth of the searched structures and their computation without the need of unsteady simulation. Example solutions of these equations for a flow past a sphere and two different growth rates (real parts of the complex shift) are presented in Fig. 1.

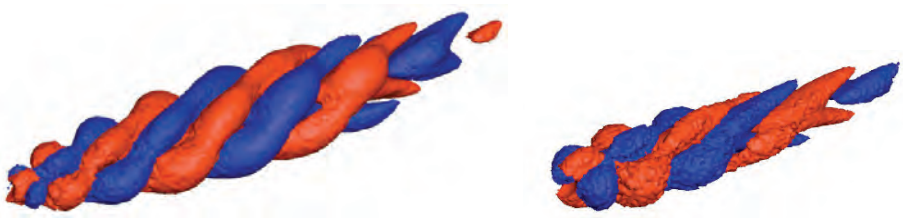

Fig. 1. Real parts of Complex Dynamic Response modes for a time-averaged flow past a sphere at Re = 400, St = 0.134 and two different real parts of complex shift

3. Applications to model order reduction

Obtained CDR modes are used to reduce fluid model's dimension, using well-known Galerkin method [7]. Residuum $R^{[n]}$ of incompressible Navier–Stokes equations, approximated with n expansion modes U are projected onto the space spanned by these modes:

$$(U_i, R^{[n]})_\Omega = \int_\Omega U_i R^{[n]} d\Omega = 0 \tag{4}$$

Resulting system of ordinary differential equations (Galerkin system), using CDR modes, will enable more precise modeling of flow phenomena, especially in the transition between steady and unsteady flow.

References

[1] HOLMES P., LUMLEY J.L., BERKOOZ G., *Turbulence, coherent structures, dynamical systems and symmetry*, Cambridge University Press, 1998.
[2] SCHMID P.J., *Dynamic mode decomposition of numerical and experimental data*, Journal of Fluid Mechanics, 2010, 656(1), 5–28.
[3] ROWLEY C.W., MEZIC I., BAGHERI S., SCHLATTER P., HENNINGSON D.S., *Spectral analysis of nonlinear flows*, Journal of Fluid Mechanics, 2009, 641, 115–127.
[4] SIROVICH L., *Turbulence and the dynamics of coherent structures*, Quarterly of Applied Mathematics, 1987, 45, 561–571.
[5] ROWLEY C.W., *Model reduction for fluids using balanced proper orthogonal decomposition*, Int. J. Bifurcat. Chaos, 2005, 15(3), 997–1013.
[6] MORZYŃSKI M., NOWAK M., STANKIEWICZ W., *Novel Method of Physical Modes Generation for Reduced Order Flow Control-Oriented Models*, Vibrations in Physical Systems, 2014, 26, 189–194.
[7] NOACK B.R., MORZYŃSKI M., TADMOR G. (eds.), *Reduced-Order Modelling for Flow Control*, CISM Courses and Lectures 528, Springer–Verlag, Vienna 2011.

Comparison of different approaches in the Trefftz method for analysis of fluid flow between regular bundles of cylindrical fibres

M. Mierzwiczak, J.K. Grabski, J.A. Kołodziej

Poznań University of Technology, Institute of Applied Mechanics,
Jana Pawła II 24, 60-965 Poznań, Poland. E-mail: magdalena.mierzwiczak@put.poznan.pl

In the paper three different approaches for the Trefftz method are compared in analysis of fluid flow between regular bundles of cylindrical fibres. The approximate solution is a linear combination of such trial functions which fulfil exactly the governing equations. The trial functions can be defined in the Cartesian coordinate system (the first approach), in the cylindrical coordinate system (and can fulfil also some boundary conditions – the second approach) or be defined as fundamental solutions (the third approach – the method of fundamental solutions).The average velocity and the product of friction factor f and Reynolds number Re are compared for selected parameters of the considered region.

1. Introduction

The Trefftz method was proposed in 1926 by Erich Trefftz [1]. In the method the approximate solution is a linear combination of trial functions which fulfil exactly the governing equation. The trial functions in the method are called the Trefftz functions or the T-functions. The unknown coefficients of the approximate solution are determined using the boundary collocation technique [2].

Sometimes the T-functions can fulfil also some of the boundary conditions. In such case the method is often called the Trefftz method with special purpose Trefftz functions. Then the boundary collocation technique is applied only for unfulfilled boundary conditions. This approach was successfully applied for different problems in applied mechanics, e.g., conductive heat flow [3].

The method of fundamental solution (MFS) was proposed in 1964 by Kupradze and Aleksidze [4]. It is a kind of the Trefftz method because the fundamental solutions which are the trial functions in the method fulfil exactly the governing equation.

The purpose of the present paper is to compare these three approaches in analysis of longitudinal fluid flow between bundles of cylindrical fibres.

2. Formulation of the problem

The governing equation for longitudinal fluid flow in the dimensional takes the form:

$$\nabla^2 W(X,Y) = -1, \tag{1}$$

where $W(X, Y)$ is the dimensional axial velocity. The above equation can be solved using the method of particular solution in which the general solution $W_g(X, Y)$ fulfills the Laplace equation and can be solved using the Trefftz method.

3. Application of the Trefftz method

The approximate solutions in all three approaches in the Trefftz method fulfill the governing equation. The detailed differences are presented in this section.

3.1. The Trefftz method

The approximate solution using the Trefftz method can be written in the following form:

$$W_g(X,Y) = \sum_{n=0}^{M} c_n F_n(X,Y) + \sum_{n=1}^{M} d_n G_n(X,Y), \tag{2}$$

where $F_n(X, Y)$ and $G_n(X, Y)$ are the trial functions defined in the Cartesian coordinate system:

$$F_n(X,Y) = \sum_{k=0}^{\left[\frac{n}{2}\right]} (-1)^k \frac{X^{n-2k}Y^{2k}}{(n-2k)!(2k)!}; \quad G_n(X,Y) = \sum_{k=0}^{\left[\frac{n-1}{2}\right]} (-1)^k \frac{X^{n-2k-1}Y^{2k+1}}{(n-2k-1)!(2k+1)!} \tag{3}$$

The above trial functions fulfils the Laplace equation in 2D. The unknown coefficients are calculated by fulfilling the boundary conditions [2].

3.2. The Trefftz method with special purpose Trefftz functions

As the general solution of the Laplace in 2D also the following expression in the polar coordinate system can be used:

$$\begin{aligned} W_g(R,\theta) = {} & A_0 + A_1\theta + A_2\theta \ln R + A_3 \ln R + \\ & \sum_{n=1}^{M} (B_n R^{\lambda_n} + C_n R^{-\lambda_n}) \cos(\lambda_n \theta) + \sum_{n=1}^{M} (D_n R^{\lambda_n} + E_n R^{-\lambda_n}) \sin(\lambda_n \theta). \end{aligned} \tag{4}$$

Applying it for the specific region some boundary conditions can be fulfilled by calculating some constants in the above solution. After that the approximate solution fulfils the governing equation and some of the boundary conditions. The remaining constants are calculated using the boundary collocation technique [2].

3.3. The MFS

In the MFS the approximate solution is assumed as a linear combination of fundamental solutions. The fundamental solution fulfils exactly the governing equation and it is a function of distance between the point inside the considered region and the source point which is located outside the region (because of singularity in fundamental solutions for $r = 0$). Using the MFS the approximate solution for the Laplace equation takes the form:

$$W_g(X,Y) = \sum_{j=1}^{M} c_j \ln(r_j), \tag{5}$$

where c_j ($j = 1, 2, ..., M$) are unknown coefficients to calculate by fulfilling the boundary conditions and r_j is the distance between the point (X, Y) and the j-th source point.

References

[1] TREFFTZ E., Proc. 2nd Int. Cong. Appl. Mech., 1926, Zurich, 131–134.
[2] KOŁODZIEJ J.A., ZIELIŃSKI A.P., *Boundary Collocation Techniques and their Application in Engineering*, WIT Press, Southampton 2009.
[3] KOŁODZIEJ J.A., STRĘK T., Int. J. Heat Mass Transfer, 44, 999–1012.
[4] KUPRADZE V.D., ALEKSIDZE M.A., USSR Comput. Math. Math. Phys., 1964, 4, 82–126.

Robust preconditioners and stabilization for Fluid-Structure Interaction problem in saddle-point formulation

M. Wichrowski

Institute of Fundamental Technological Reaserch,
Adolfa Pawińskiego 5b, 02-106 Warsaw, Poland. E-mail: mwichro@ippt.pan.pl

Fluid-Structure Interaction problem is considered. Semi-implicit time integration scheme is used, allowing to decouple momentum and geometry. Monolithic approach is reformulated as saddle-point problem. Finite element discretization of system is used and new nonuniform stabilization is proposed. Robust block preconditioners based on uniform well-posedness are discussed and experimentally verified. Convergence of presented method is verified numerically on Turek benchmark.

1. Introduction

In the case where the elastic body immersed in a fluid is flexible enough, interaction between flow and structure has crucial influence on the physics of the phenomenon. Therefore, it is not possible to neglect influence of (not known *a priori*) variable domain geometry or to solve decoupled flow and structure equations. In this paper we analyze preconditioners for arbitrary Lagrangian–Eulerian (ALE) formulation of FSI.

Numerical models for simulating FSI problems can be divided in two separate approaches: partitioned, where solid and fluid equations are solved separately, and monolithic, where complete set of coupled equations is solved at once. Partitioned approach requires coupling algorithm to enforce coupling conditions but allows reusing existing codes. Monolithic approach needs specialized code, but it is more favorable for its stability.

In this paper monolithic approach is considered [1]. Semi-implicit algorithm is used for time integration: momentum equation is solve implicitly, while geometry is treated explicitly (*Geometry-convective explicit* scheme). The resulting scheme exhibits good temporal stability, allowing time steps of order 0.01 at $Re = 200$ for Turek's benchmark [2]. Moreover, problem solved on each time step is linear. We propose optimal block preconditioners [3, 4] for iterative solvers.

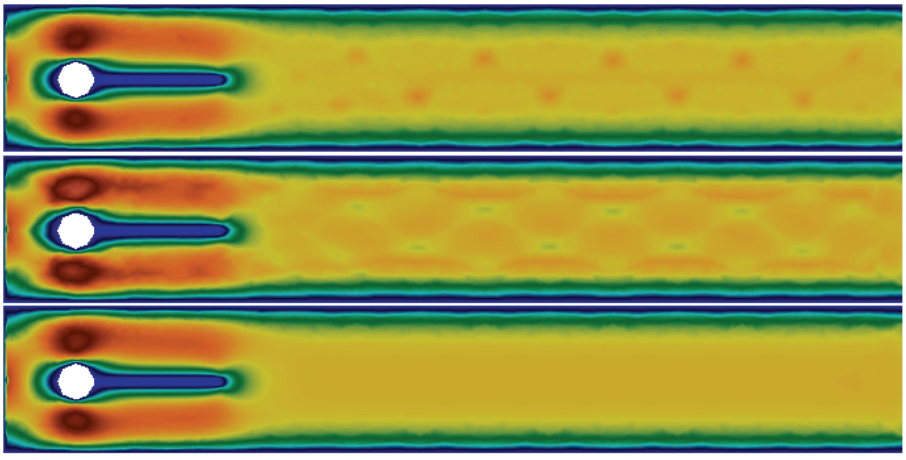

Fig. 1. Comparison of stabilization methods, from above: no stabilization, constant proposed by Xu [1] and variable on Turek benchmark problem

2. Saddle point formulation of FSI problem

As shown in [1] time-discrete system of FSI equation can be reformulated to Stokes-like problem with variable viscosity. Obtained equation can be considered as saddle point problem and uniform well-posedness of problem solved on one time step is proven in [1] for specially chosen norms by verification of *inf-sup* conditions.

2.1. Discretization and stabilization

Finite element discretized equations require stabilization to remain well-posed independent from problem parameters. Two variants of *grad-div* stabilization are considered: constant used in [1] and variable, introduced in this paper. Both are proven to result in uniformly well-posed discrete problem. Variable stabilization improves quality of solution while block preconditioners can be reused without greater effect on iteration number.

3. Solution of linear system

Optimal preconditioning for Krylov subspace methods (GMRES and MinRes) are shown from well-posedness of linear system. Block methods are employed [3, 4], that are proven to be independent from problem parameters and mesh size. We extend results in [1] for block-diagonal precondtioners on other block methods (like block-upper-triangular) in order to accelerate covergence. This result is verified numerically. Performed test show convergence in 2–12 iterations when each block is solved directly. However, iterative methods can be also used for inverting smaller sub-blocks.

References

[1] XU J., YANG K., *Well-posedness and robust preconditioners for discretized fluid–structure interaction systems*, Computer Methods in Applied Mechanics and Engineering, 2015, 292, 69–91.
[2] TUREK S., HRON J., *Proposal for numerical benchmarking of fluid-structure interaction between an elastic object and laminar incompressible flow*, Fluid-Structure Interaction, 2006, 71–385.
[3] KRZYŻANOWSKI P., *On block preconditioners for saddle point problems with singular or indefinite (1, 1) block*, Numerical Linear Algebra with Applications, 2011, 18(1), 123–140.
[4] MARDAL K.A., WINTHER R., *Preconditioning discretizations of systems of partial differential equations*, Numerical Linear Algebra with Applications, 2011, 18(1), 1–40.

Comparing convolution integral models with analytical pipe flow solutions

K. Urbanowicz[1], A.S. Tijsseling[2], M. Firkowski[1]

[1] West Pomeranian University of Technology Szczecin, Faculty of Mechanical Engineering and Mechatronics, Al Piastów 19, 70-310 Szczecin, Poland
[2] Eindhoven University of Technology, Department of Mathematics and Computer Science, PO Box 513, 5600 MB Eindhoven, The Netherlands
E-mail: kamil.urbanowicz@zut.edu.pl, a.s.tijsseling@tue.nl, mateusz.firkowski@zut.edu.pl

Extended abstract

This year, 134 years have passed since the first publication of the analytical solution for the accelerated pipe flow of an incompressible viscous fluid in a long hydraulic line or mammal blood vessel:

$$v(r,\hat{t}) = 2v_{\infty}\left[\left[1-\left(\frac{r}{R}\right)^2\right] - 8\sum_{n=1}^{\infty}\frac{J_0\left(\lambda\cdot\frac{r}{R}\right)}{\lambda^3\cdot J_1(\lambda)}\cdot e^{-\lambda^2\hat{t}}\right] \quad \text{where} \quad v_{\infty} = \frac{R^2\Delta p}{8\mu L} \tag{1}$$

and: r – the radial coordinate, R – inner radius of pipe, $\hat{t}$ – dimensionless time, λ – n-th zero of J_0, v_{∞} – final average (cross-sectional) velocity, Δp – pressure gradient suddenly applied at time $t = 0$, L – pipe length, μ – dynamic viscosity.

This solution was presented in 1882 by the Russian professor Gromeka (Fig. 1) at the University of Kazan in their scientific materials [1]. Gromeka developed a solution that was based mainly on earlier work in the field of unsteady heat transfer in cylinders by professors from France and Italy respectively, namely Poisson [2] and Betti [3]. Due to the local nature of the publication and the absence of English, French or German translations, this solution remained unknown for a long time after the death of its author in 1889. Many years later, a similar problem was focused upon and studied by a young Polish scientist named Szymański (Fig. 1). While in 1928 staying in Paris on an internship, Szymański derived his solution which was based mainly on Hankel transforms. The final work [4] was published in the prestigious Journal de Mathématiques Pures et Appliquées in 1932 (although preceded by a conference paper in 1930) and contained a range of mathematical proofs on convergence and asymptotic behaviour of the analytical solutions. Yet another approach to find exactly the same solution was published in 1951 by Gerbes [5], who used the Laplace transform. Gerbes, beside showing the solution to accelerated flow, also proposed a solution for decelerated flow (after the complete and rapid disappearance of the pressure gradient in the pipe considered).

The current study will also deal with other known analytical solutions, such as those presented in 2002 by Ghidaoui and Kolyshkin [6] and in 2008 by Volodko and Koliskina [7], that analyze decelerated velocity profiles occurring after the sudden closure of a valve.

The main objective of this study is the comparison of the classic analytical solutions with solutions obtained by applying efficient numerical methods to the corresponding convolution integrals. Integral convolution models are widely used to introduce unsteady friction in numerical methods (especially the method of characteristics) based on a mesh with fixed time steps.

The results of numerical simulations show that an improved conventional numerical solution [8] and a corrected more effective solution [9] are entirely consistent with the classic analytical results.

Fig. 1. On left picture Prof Gromeka and on the right Prof Szymański

References

[1] GROMEKA I.S., *Theory of the motion of fluid in narrow cylindrical tubes*, Uch. Zap. Kazan Inst., No. 112, 41, Kazan, Russia, 1882, 1–19; collected works, USSR Academy of Sciences, Moscow, 1952, 149–171 (in Russian).
[2] POISSON S.D., *Théorie mathématique de la chaleur*, Paris 1835 (in French).
[3] BETTI E., *Sopra la determinazione delle temperature variabili di un cilindro*, Annali delle Universita Toscane, t. X, Pisa, 1868, 145–158 (in Italian).
[4] SZYMAŃSKI P., *Quelques solutions exactes des équations de l'hydrodynamique du fluide visqueux dans le cas d'un tube cylindrique*, Journal de Mathématiques Pures et Appliquées, 1932, 11(9), 67–107 (in French).
[5] GERBES W., *Zur instationären, laminaren Strömung einer inkompressiblen, zähen Flüssigkeit in kreiszylindrischen Rohren*, Zeitschrift für angewandte Physik, 1951, 3(7), 267–271 (in German).
[6] GHIDAOUI M.S., KOLYSHKIN A.A., *A quasi-steady approach to the instability of time-dependent flows in pipes*, J. Fluid. Mech., 2002, 465, 301–330.
[7] VOLODKO I., KOLISKINA V., *Transient flows in pipes and channels: analytical solutions*, 4th IASME/WSEAS International Conference on Energy, Environment, Ecosystems and Sustainable Development (EEESD'08) Algarve, Portugal, June 11–13, 2008, 265–268.
[8] VARDY A.E., BROWN J.M.B., *Evaluation of unsteady wall shear stress by Zielke's method*, J. Hydraulic. Eng., 2010, 136, 453–456.
[9] URBANOWICZ K., *Simple modelling of unsteady friction factor*, BHR Group, Proceedings 12th International Conference on Pressure Surges, Dublin, Ireland, November 18–20, 2015, 113–130.

Molecular dynamic simulation of water flows in nanochannels with nanocavities. Vortices formation

A. Kucaba-Piętal, A. Kordos

Rzeszów University of Technology, Faculty of Mechanical Engineering and Aeronautics,
al. Powstańców Warszawy 8, 35-959 Rzeszów, Poland.
E-mail: anpietal@prz.edu.pl, a-kordos@prz.edu.pl

A series of molecular dynamic simulation have been performed to investigate the vortex formation in nanocavities. Water nanoflow in a quartz nanochannel with nanocavities extending perpendicularly from the main nanochannel wall was studied. Two nanocavities 50 Å and 70 Å wide were taken into consideration. The study aims on answer the question how vortex formation and flow morphology is affected by the various nanocavity width.

1. Introduction

The phenomenon of mass transport into micro- and nano-cavities is crucial in understanding the nature of numerous biological and physical processes. For last ten years the flows through microchannels with microcavities have been studied intensively due to the growing interest of engineers in applicability of microcavity vortices formation in microtechnology. Obtained results showed that the flow pattern at the microcavity entrance are key for the mass transfer into the cavity [1] and that velocity decreases with the distance from microcavity entrance [2]. It allowed successful constructions of numerous modern microdevices and microchips for which vortices in microcavity are the core for its operations, for instance cell sorter, equipment for cultivation of cells, etc.

The small size of nanocavities makes it difficult to study, because classical (Cauchy) continuum mechanics methods are inapplicable to handle it. For this reason flows in nanocavities remain a challenging task and are not recognised yet and should be treated only by atomistic method. Results of [3, 4] showed that in nanocavities vorticity appears. The present study focuses on examination of the influence of the nanocavity width on the flow morphology and vortex formation.

The molecular dynamic (MD) method is used. In the simulation, the computer representation of molecules of real materials (water and quartz) were used in the simulation performed by LAMMPS program. Bulk quantities (velocity and density of water) are obtained applying the binning method to simulation data and sketched across the fluid field.

2. Simulation details

Water flows through quartz nanochannels with nanocavities extending perpendicularly from the main nanochannel were investigated by use of the MD method. The computer representation of molecules of real materials: hydroxylated alpha-quartz [5] and TIP4P/2005 [6] were used. In Cartesian coordinates water was flowing in the in the x – direction between two plane walls perpendicular to the z-axis. The flow was induced by an application of the constant force F_x to the mass center of every water molecule in the main channel. Periodic boundary conditions are considered in the x and y directions. The details concerned elementary cells domain used in simulations are presented in Fig. 1 and Tab. 1. The parameters of the simulation for water were: temperature T = 300 K, density ρ = 997 kg/m^3. The time step for integration of the equations of motion 1 fs. For quartz the values of the density was ρ = 2650 kg/m^3.

The system reaches the equilibrium state after a run of 100000 time steps. Then, a number of molecular dynamics simulations were performed, each with duration of 15000000 time steps. The simulation time was equal 15 ns of real flow.

Table 1. Elementary cells domain dimensions

Nanocavity width [Å]	H1 [Å]	H2 [Å]	H3 [Å]	L1 [Å]	L2 [Å]	Number of water molecules	Number of quartz molecules
50	265	250	515	172	65	64942	44756
70	265	250	515	192	65	49257	49257

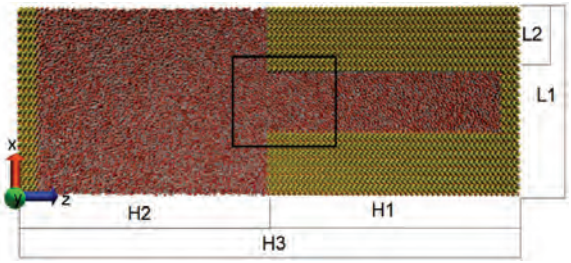

Fig. 1. Elementary cells domain view

3. Results

The hydrodynamic bulk parameters of the water flow were obtained by averaging the data from 15 000 000 time steps with the bin method. The data were binned in one hundred layers in both, the wider and the narrower channels.

Velocity vectors across the fluid field marked in Fig. 1. are presented in Fig. 2. The water vortex formation in the entrance part to the nanocavity 50 Å and 70 Å can be observed.

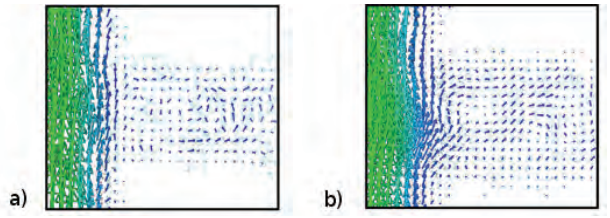

Fig. 2. The view of water vortex formation in the entrance part to the nanocavity
a) 50 Å b) 70 Å

Results obtained for water flows through quartz nanochannels with nanocavities extending perpendicularly from the main nanochannel shows that nanocavity width affect the flow morphology.

Acknowledgements

The calculations were performed in ICM UW, Grant G45-8.

References

[1] YEW A.G., PINERO D., HSIEH A.H., ATENCIA J., Appl. Phys. Lett., 2013, 102, 084108.
[2] YU Z.T.F., LEE Y.K, WONG M., ZOHAR Y., J. Microelectromech. Syst., 2005, 14, 1386–1398.
[3] KORDOS A., KUCABA-PIĘTAL A., Proceedings of the 35th IC ITI, 2013, ISBN 978-953-7138-31-8.
[4] KORDOS A., *Modeling of hydrodynamics and mass transport in chromatographic columns using molecular dynamics simulation*, PhD thesis, Rzeszów University of Technology, 2015.
[5] SKELTON A.A., FENTER P., KUBICKI J.D., WESOLOWSKI D.J., J. Phys. Chem. C, 2011, 115, 2076.
[6] ABASCAL J.L.F., VEGA C., J. of Chem. Phys., 2005, 123.

Highly deformable nanofilaments in flow

S. Pawłowska

Institute of Fundamental Technological Research PAS, Department of Mechanics and Physics of Fluids, Pawińskiego 5B, 02-106 Warszawa, Poland. E-mail: spaw@ippt.pan.pl

Experimental analysis of hydrogel nanofilaments conveyed by flow is conducted to help in understanding physical phenomena responsible for transport properties and shape deformations of long bio-objects, like DNA or proteins. Investigated hydrogel nanofilaments exhibit typical for macromolecules behavior, like spontaneous conformational changes and cross-flow migration. Results of the experiments indicate critical role of thermal fluctuations behavior of single filaments.

1. Introduction

Predicting behavior of long, deformable objects carried by the flowing fluid is needed for a full understanding of the physics of macromolecular suspensions. Such knowledge is important in a variety of biological processes responsible for transport, aggregation and structure formation at the cellular level [1]. Most hydrodynamic models are based on classical complex systems of interconnected identical spherical particles (*worm-like chain*) or *dumbbell models* that describe the two particles configurations of two ends of the polymer which form the filament connected by short springs. Other molecular models are focused on experimental studies of the dynamics of DNA molecules or another bio-objects like actin filaments. However, their experimental validation is doubtful, as the mechanical properties of their components are unknown *a priori*, hence they have to be estimated or matched to very inaccurate molecular scale observations. Here, we propose *synthetic experimental model* of molecular chain, i.e., long, highly flexible nanofilaments exhibiting Brownian deformability, and still large enough to be directly observed and analyzed using optical methods.

2. Experiment

We have developed a coaxial electrospinning technique for producing highly deformable filaments [1]. They are elongated objects characterized by typical diameter of 100 nm and contour length ranging from one micrometer to millimeters. A microfluidic system for observation and analysis the dynamics of the hydrogel nanofilaments movement was made using PDMS polymer. The experiment was performed in a 500 μm long and 60 μm deep channel. The movement of nanofilaments was recorded using high-gain EM-CCD camera. The experiment is based on observation of the behavior of hydrogel nanofilament under the influence of a pulsating motion generated by the syringe pump. The instantaneous velocity profile in the channel is measured by particle tracking technique (PTV) using small amount of fluorescent tracers. For each of the analyzed filaments the stiffness was determined by calculating the Young's modulus. For this purpose we analyzed their Brownian mobility, and we have applied the cosine correlation method in order to evaluate their persistence length [1].

3. Results

Analysis of the monofilament dynamics confirms that their mechanical properties are resemble that of long biomolecules (Tab. 1). Our study shows that mobility of our filaments strongly depends on their length. Longer filaments exhibit high bending flexibility. For short

pieces (10–20 μm) translational and rotational diffusion coefficients could be evaluated from Brownian motion. We can observe similar effects in pulsating flow. Short filaments move along the channel and rotate while long filaments have a tendency to coil and form knots. This effect remains prevalent for objects conveyed by Poiseuille flow (Fig. 1).

Table 1. Typical experimental parameters: mean flow velocity (*Vm*), contour length (*L*), radius (*R*), persistence length (*Lp*), and Young modulus (*E*) of the analyzed filament. Flow Reynolds number (*Re*) is based on the channel width (200 μm)

No.	*Vm* [μm/s]	*L* [μm]	*R* [nm]	*Re*	*Lp* [μm]	*E* [kPa]
1	59.02	71.91	0.081	1.51E-02	17.62	2.17
2	77.78	72.87	0.081	1.98E-02	12.38	1.53
3	39.65	34.49	0.045	1.01E-02	3.44	4.45
4	68.87	54.31	0.045	1.76E-02	7.51	9.72
5	250.43	75.58	0.045	6.39E-02	9.56	12.37
6	199.64	82.90	0.081	5.09E-02	14.34	1.77

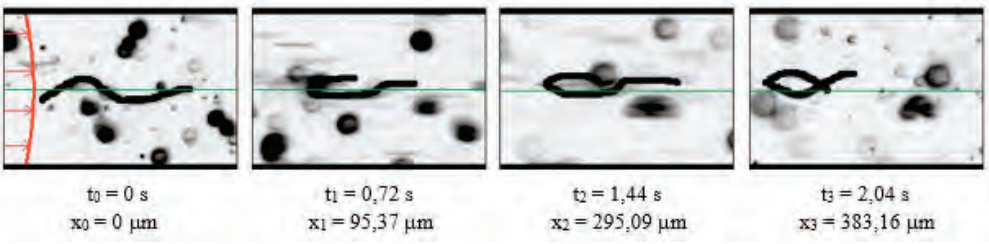

Figure 1. Sequence of images for a single flexible nanofilament conveyed by Poiseuille flow (no. 6 in Table 1), green line is a center of the channel, *t* – time stamp, *x* – distance traveled from the channel entry (picture frame moves with the object), image height 77 μm

One of the more interesting phenomena observed during the experiments is the cross-flow migration of filaments into the center of channel.

Highly deformable hydrogel nanofilaments have demonstrated the possibility to be used to study the hydrodynamic interactions for such long objects. The study of the flow characteristics in presence of highly deformable nano-objects is of fundamental importance for the understanding and prediction of the rheological properties of biological fluid environment (cytoplasm, plasma). This data can be a base to create biocompatible nano-objects that can become tools for the regeneration of biological tissues, e.g., neural tissue.

Acknowledgement

The support of NCN grant no. 2015/17/N/ST8/02012 is acknowledged. Author gratefully acknowledge her supervisors Tomasz Kowalewski and Filippo Pierini and colleagues Paweł Nakielski and Krzysztof Zembrzycki for their help.

References

[1] NAKIELSKI P. et al., PLOS ONE 2015, 10(6).

Modelling of blood flow: from macro to microscales

K. Kaczorowska, K. Tesch

Gdańsk University of Technology ul. G. Narutowicza 11/12 80-233 Gdańsk, Poland
E-mail: krzyte@pg.gda.pl

The aim of this paper it to review various scale approaches to blood flow modelling. Blood motion may be described by three types of mathematical models according to the observed scales or resolutions, namely microscopic, mesoscopic and macroscopic description. The above approaches are discussed together with their advantages and disadvantages. Several results of mesoscopic approach are presented together with well-known macroscopic results.

1. Introduction

Blood is a suspension of blood cells in the plasma. Presence of red blood cells is responsible for the non-Newtonian blood nature. A proper approach allowing for complete or nearly complete blood flow behaviour modelling should take under consideration red blood cells presence, flexibility and aggregation. Furthermore, influence of temperature on viscosity, membrane thermal fluctuations and yield stress are also important.

2. Macro-, micro- and mesoscale descriptions

Typically, macroscale approach is not accurate enough in order to satisfy all of these features. This method, however, is useful in order to simulate blood flow for large space (arteries), see Figure 1. Continuum methods is applicable for vessels larger than 100 μm. One has to keep in mind that within the range 0.1–1 mm non-Newtonian constitutive equations are required.

When it comes to capillaries, i.e. diameters smaller than 100 μm, explicit modelling of red blood cells is required. This is because the continuum models prediction break down entirely. The average diameter of red blood cells is about 8 μm. This means that at least mesoscopic modelling is necessary, see figure 1, involving methods like Lattice Boltzmann [2, 6], Dissipative [5] and Smoothed Particle Dynamics [3].

Methods involving modelling of red blood cells motion may be divided into rigid and flexible. The latter, being the most interesting and advanced, can be further classified into spring/mass like models [1] and spectrin network models [4].

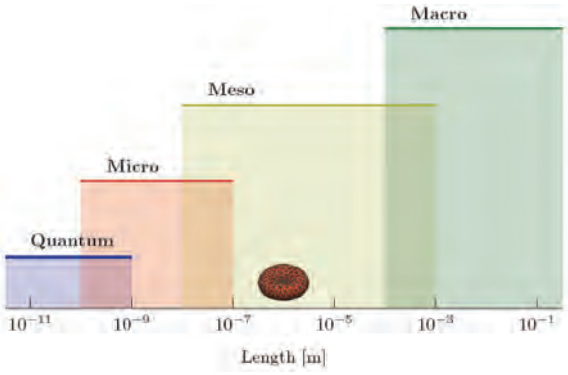

Fig. 1. Length scales

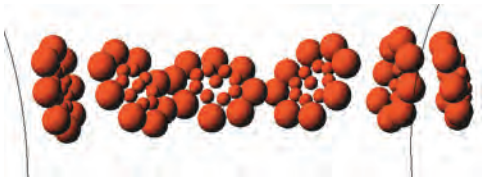

Fig. 2. Spring-mass model of a single RBC simulation

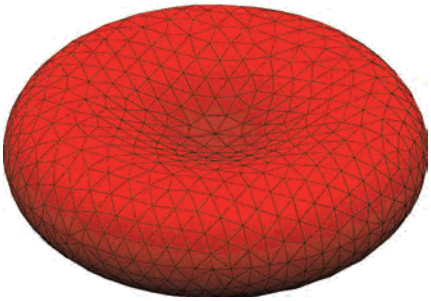

Fig. 3. Spectrin network

The individual vertex i of the red blood cell membrane surface moves according to

$$m\frac{\mathrm{d}^2 r_i}{dt^2} = \mathbf{G}_i + \mathbf{F} \tag{1}$$

The force exerted on a molecule consists of the external force such as gravity $\mathbf{G}_i$ and additional force $\mathbf{F}$ according to specific models. For spring/mass like models (Fig. 2) we have $\mathbf{F} = \mathbf{f}_{is} + \mathbf{f}_{id} + \mathbf{f}_{ib}$, where $\mathbf{f}_{is}$ is spring forces, $\mathbf{f}_{id}$ – damper forces and $\mathbf{f}_{ib}$ – bending forces. Also, local and global conservative forces may be applied if the spring/mass network represents a closed surface.

For spectrin (Fig. 3) network method the force exerted on a vertex consists of $\mathbf{F} = \mathbf{f}_i^{FS} + \mathbf{f}_i^{PP} + \mathbf{f}_i$. The external forces due to the fluid-structure interaction on the vertex are denoted as $\mathbf{f}_i^{FS}$, $\mathbf{f}_i^{PP}$ represents forces due to particle-particle interaction. Forces due to the Helmholtz free energy contribution are calculated as $\mathbf{f}_i = -\frac{\partial E}{\partial \boldsymbol{x}_i}$ where potential energy of the network is $E = E_{i-p} + E_b + E_a + E_v$. Potential energy of the network consists of in-plane energy E_{i-p} (elastic + dissipative forces), bending energy E_b, area conservation forces (global + local) E_a, volume conservation forces E_v.

References

[1] CIMRAK I., GUSENBAUER M., JANCIGOVA I., *An ESPResSo implementation of elastic objects immersed in a fluid*, Computer Physics Communications, 2014, 185, 900–907.
[2] MACMECCAN R.M., CLAUSEN J.R., NEITZEL G.P., AIDUN C.K., *Simulating deformable particle suspensions using a coupled lattice-Boltzmann and finite-element method*, J. Fluid Mech., 2008, 618, 13–39.
[3] MORENO N., VIGNAL P., LIC J., CALO V.M., *Multiscale modeling of blood flow: Coupling finite elements with smoothed dissipative particle dynamics*, Procedia Computer Science, 2013, 18, 2565–2574.
[4] REASOR J.D.A., CLAUSEN J.R., AIDUN C.K., *Coupling the lattice-Boltzmann and spectrin-link methods for the direct numerical simulation of cellular blood flow*, Int. J. Numer. Meth. Fluids, 2012, 68, 767–781.
[5] YE T., PHAN-THIEN N., KHOO B.C., LIM C.T., *Dissipative particle dynamics simulations of deformation and aggregation of healthy and diseased red blood cells in a tube flow*, Physics of Fluids, 2014, 26, 111902.
[6] ZHANG J., JOHNSON P.C., POPEL A.S., *Red Blood Cell Aggregation and Dissociation in Shear Flows Simulated by Lattice Boltzmann Method*, J. Biomech., 2008, 41(1), 47–55.

Analysis of non-Newtonian fluid flow in porous media by means of the global radial basis function collocation method

J.K. Grabski, M. Mierzwiczak, J.A. Kołodziej

Poznań University of Technology, Institute of Applied Mechanics,
Jana Pawła II 24, 60-965 Poznań, Poland. E-mail: jakub.grabski@put.poznan.pl

The porous media play an important role in the modern engineering applications. In many theoretical works on this subject the porous medium is modelled as a regular array of cylindrical fibres. In the present paper longitudinal flow of non-Newtonian fluid in such bundle of fibres (in triangular, square or hexagonal arrays) is solved numerically by means of the global radial basis collocation method. The longitudinal component of the permeability is calculated based on the velocity field and compared with results obtained from other methods.

1. Introduction

The porous media and structures are very common in the nature and engineering, e.g. rocks, soil, biological tissue (bone) and many others. Many engineering applications are related with fluid flow through such structures, e.g., the resin transfer molding process. Therefore theoretical description of these phenomena is very important.

The purpose of the present paper is application of the global radial basis function collocation method (GRBFCM) for analysis flow in a regular array of fibers. The method is quite new and was proposed by Edward Kansa in 1990 [1]. It is an example of meshless methods which means that there is no need of mesh generation. The approximate solution is assumed as a linear combination of radial basis functions (RBF) [2]. The governing equation and boundary conditions in the method are fulfilled approximately. Recent developments and examples of applications of the method was described in details in [3].

2. Formulation of the problem

Fluid flow in the porous medium is often described by the Darcy equation:

$$\mathbf{q} = -\frac{\mathbf{K}}{\mu}\nabla p, \tag{1}$$

where $\mathbf{q}$ is the filtration velocity, $\mathbf{K}$ is the permeability tensor, p is the pressure, and μ is the fluid velocity.

In order to determine the longitudinal component of the permeability firstly a microstructural fluid problem is considered. The problem is solved in the repeated element of a regular array of cylindrical fibers and the governing equation has the following form:

$$\frac{\partial}{\partial x}\left(\eta(\gamma)\frac{\partial w(x,y)}{\partial x}\right)+\frac{\partial}{\partial y}\left(\eta(\gamma)\frac{\partial w(x,y)}{\partial y}\right)=\frac{\mathrm{d}p}{\mathrm{d}z}, \tag{2}$$

where $\eta(\gamma)$ is the viscosity function, γ is the shear rate and $w(x,y)$ is the axial velocity. The problem is solved with non-slip boundary condition. The viscosity function $\eta(\gamma)$ depend on the non-Newtonian fluid model.

In order to transform the nonlinear problem into the sequence of inhomogeneous problems the Picard iteration method is applied. Then at each iteration step the GRBFCM can be applied to solve the inhomogeneous problems.

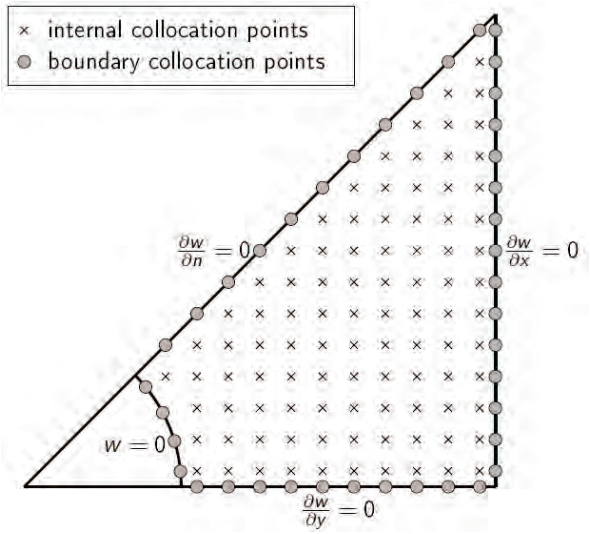

Fig. 1. The repeating element of the considered region

3. Application of the GRBFCM

In the method the approximate solution is a linear combination of the RBF:

$$w(x,y) = \sum_{j=1}^{N} c_j \varphi(r_j), \tag{3}$$

where c_j (j = 1, 2, ..., N) are unknown coefficients, and N is the number of the collocation points. The solution do not fulfill either the governing equation as well as the boundary conditions. Thus the unknown coefficients c_j (j = 1, 2, ..., N) are calculated by fulfilling the governing equation inside the considered region and the boundary conditions on the boundary.

References

[1] KANSA E.J., Computers Math. Appl., 1990, 19, 147.
[2] BUHMANN M.D., Acta Numer., 2000, 9, 1.
[3] CHEN W., FU Z.-J., CHEN C.S., *Recent Advances in Radial Basis Function Collocation Method*, Springer, 2014.

Passive control of rotorcraft high-speed impulsive noise

O. Szulc, P. Doerffer, F. Tejero

Institute of Fluid-Flow Machinery, Polish Academy of Sciences,
Fiszera 14, 80-231 Gdańsk, Poland. E-mail: Oskar.Szulc@imp.gda.pl

A strong, normal shock wave, terminating a local supersonic area located at the tip of a helicopter blade, not only limits aerodynamic performance, but also constitutes an origin of the High-Speed Impulsive (HSI) noise. The application of a passive control device (a shallow cavity covered by a perforated plate) just beneath the interaction region weakens the compression level, thus reducing the main source of the HSI noise. The numerical investigation based on the URANS approach and Bohning/Doerffer transpiration law confirms a large potential of the new method. The normal shock wave is effectively eliminated by the wall ventilation exerting a positive impact on the generated level of the HSI noise.

1. Introduction

Impulsive noise, described as a series of intense, low-frequency impulses, is believed to be one of the most annoying and loud sounds that can be generated by a helicopter rotor. The HSI noise phenomenon develops when the advancing tip Mach number is sufficiently high to give rise to transonic conditions and strong compressibility effects in high-speed forward flight. Additionally, the shock wave delocalization may arise emitting intense thumping, harsh sounds heard for many kilometers compromising the detection distance of an approaching helicopter and increasing community annoyance. Delaying appearance of the HSI noise and shock wave delocalization is still one of the fundamental considerations in the early design and development process of rotor systems. The target is often met by a passive tip shape alteration relying on combined sweep, taper and thinning. Such a major modification of the blade's most important part effectively damps the HSI noise. Unfortunately, the achieved benefits in the acoustic signature may be outbalanced by a decreased aerodynamic performance. On the contrary, the proposed type of a passive control device does not require any alteration of the outer shape (section) of the blade, assuring a beneficial effect on the radiated HSI noise without degradation of the retreating side performance [1–4].

Two exemplary implementations adapted to model helicopter rotors tested at NASA Ames facility in transonic conditions: Caradonna–Tung (lifting hover) and Caradonna–Laub (non-lifting, high-speed forward flight) demonstrate the possible gains in terms of the reduction of acoustic pressure fluctuations in the near-field of the blade tip. The CFD results are validated against the experimental data obtained for the reference configurations (no control), while the analysis of the passive control arrangement is based on a purely numerical research.

2. Mechanism of passive control of shock wave by wall perforation

At the beginning of the 90's W. Braun (University of Karlsruhe, Germany) investigated experimentally passive control of the shock wave terminating a local supersonic area – a flow configuration commonly found on airfoils or helicopter rotor blades in transonic conditions [5]. It was shown for the first time that when the cavity covered by a perforated plate is sufficiently prolonged (called here "extended" passive control) a strong, normal shock wave may be interchanged with a system of oblique waves reflecting between the wall and the edge of the supersonic region (see the experimental interferograms in Figure 1). In contrast to the fixed wing

applications, the "extended" passive control may constitute a basis of a new method designed for the HSI rotorcraft noise reduction.

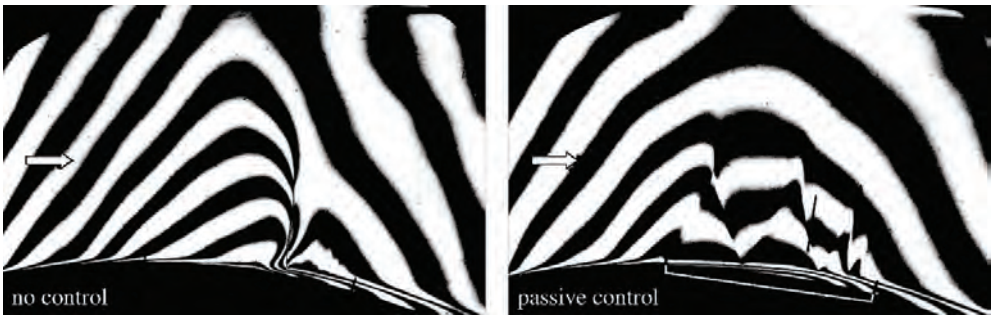

Fig. 1. "Extended" passive control of shock wave at the convex wall (Ma = 1.32) [5]

3. Exemplary results of transonic hover of the Caradonna-Tung rotor

The exemplary numerical results are presented for a well-known transonic hover of the Caradonna–Tung, 2-bladed, NACA 0012 untwisted and untappered rotor blades (Ma_T = 0.877, Re_T = 3.93 ·10^6 and collective θ = 8^o) – see Figure 2. The acoustic pressure fluctuations p' are averaged at the plane that is intersected with the moving blades. The resulting ΔOASPL (drop of Overall Sound Pressure Level due to passive venting) is presented together with the signals recorded at point p_1 and the resulting amplitude spectra are A-weighted. The negative peak of p' is reduced by 27%, while the rms of the is damped by 21%. The duration time is increased limiting the impulsive character as well. The ΔOASPL of 2 dB was identified, while the A-weighted value was found to be 4 dBA. At certain parts of the spectrum the difference was even more pronounced (>10 dBA).

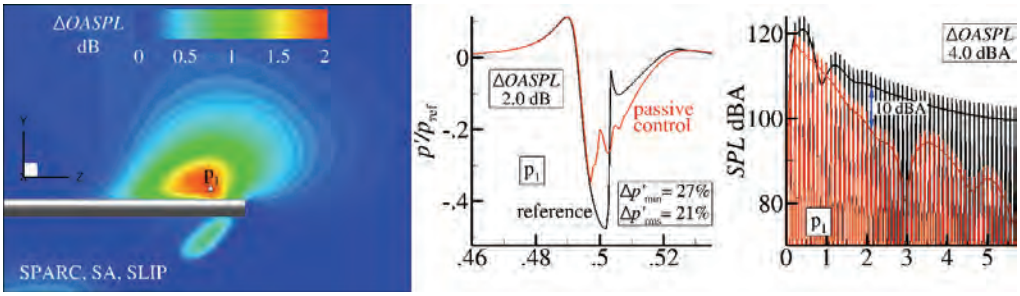

Fig. 2. Effect of "extended" passive control on acoustic pressure fluctuations

References

[1] DOERFFER P., SZULC O., BOHNING R., J. of Thermal Science, 2005, 15(1), 43–48.
[2] DOERFFER P., SZULC O., Arch. of Mechanics, 2006, 58(6), 543–573.
[3] DOERFFER P., SZULC O., J. of Thermal Science, 2007, 16(2), 97–104.
[4] DOERFFER P., SZULC O., Int. J. of Eng. Systems Modelling and Simulation, 2011, 3(1–2), 64–73.
[5] BRAUN W., PhD Dissertation, University of Karlsruhe, 1990.

Numerical research on unsteady cavitating flow over a hydrofoil

W. Wróblewski, D. Homa

Silesian University of Technology, Faculty of Energy and Environmental Engineering,
Konarskiego 18, 44-100 Gliwice, Poland. E-mail: dorota.homa@polsl.pl

Cavitation is a widely known phenomenon in pumps and water turbines installations. It can lead to significant damage of blades and walls of the rotor therefore it is crucial during pump designing and exploitation to avoid working in flow conditions, that enabled cavitation to occur. Nowadays numerical simulations of flow can provide valuable information concerning pressure and velocity distribution and can indicate if there is a risk of cavitating flow appearance. There are a few mathematical models which describe cavitating flow. The Schnerr & Sauer model was chosen for simulation. Aim of this paper is to verify its utility in case of different cavitating flow regimes over a foil. The investigated case included flow over a Clark – Y hydrofoil. After performing the grid independence study four different cavitation regimes were investigated. The vapour areas appearance, their shapes and dynamic changes were observed. The assumption of isothermal, two-phase flow was made. The calculations were performed using Open FOAM and FLUENT software and were compared to the available measurements data.

1. Introduction

Cavitation includes vapour bubbles formation in the flow due to the local pressure drop. After passing to the area of higher pressure the bubbles collapse rapidly. The collapse generates pressure wave which can seriously damage the walls of the rotor's channel. Working on cavitating flow also leads to break of flow continuity, noise, vibration, erosion and change of pump's characteristics. Performing experiments on pumps to determine if cavitation occurs is expensive and time-consuming. Numerical simulation of flow can indicate if under the specific conditions (pressure, velocity of flow) cavitation will appear, without necessity of building measurement circuit. The crucial concern is to use the mathematical model of cavitation that provides the results as compatible with the measurement data as possible. For flow over the foil, which is typical flow occurring in case of pumps' rotors, the characteristic variable is called cavitation number σ, which is defined as [1, 2]:

$$\sigma = \frac{p - p_s}{0.5\rho u_\infty^2} \tag{1}$$

where: p – pressure, Pa; p_s – saturation pressure, Pa; ρ – free stream density, kg/m^3; u_∞ – free stream velocity, m/s.

With decrease of cavitation number the following cavitation regimes can be observed: incipient, sheet, cloud and supercavitation [1].

2. The description of mathematical model

In numerical simulation Schnerr & Sauer cavitation model was used. It is widely used in both commercial and open source codes. No slip between the phases (liquid water and vapour) was assumed. The fraction of vapour phase was calculated from following formulas [2, 3]:

$$\frac{\partial \alpha \rho_v}{\partial t} + \nabla(\alpha \rho_v u) = R_e - R_c \tag{2}$$

$$R_e = \frac{\rho_l \rho_v}{\rho} \alpha(1-\alpha) \frac{3}{r_B} \sqrt{\frac{2}{3} \frac{p_s - p}{\rho_l}} \tag{3}$$

$$R_c = \frac{\rho_l \rho_v}{\rho} \alpha(1-\alpha) \frac{3}{r_B} \sqrt{\frac{2}{3} \frac{p - p_s}{\rho_l}} \tag{4}$$

where: α – vapour volume fraction; $\rho_{v/l}$ – vapour/liquid density, kg/m^3; r_B – radius of bubble, m.

The radius of bubble r_B is derived from vapour volume fraction and number of bubbles per volume of liquid n_B, as shown in equation 5 [3]:

$$r_B = \left(\frac{\alpha}{1-\alpha} \frac{3}{4\pi} \frac{1}{n_B} \right)^{\frac{1}{3}} \tag{5}$$

3. Results of the simulation

Four main cavitation regimes were observed during the performed numerical simulations. For each of them the frequency of cavitation clouds formation and collapse was determined and the shape of structures was described. The maximum dimension of cavitation structure also was stated. To be able to compare the results with available measurement data [3], the location of beginning of the cavitation structure was also investigated. Moreover, the monitor points over the foil were created and vapour volume fraction as well as pressure in these points were analysed. The selected cloud structures in the case of cloud cavitation are depicted in Figure 1. All calculations were transient ones.

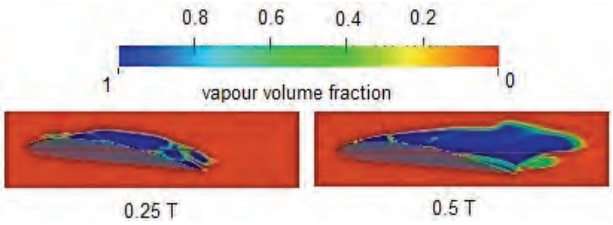

Fig. 1. Cavitation structure (cloud cavitation) T – period of changes

References

[1] WANG G., SENOCAK I., SHYY W., IKOHAGO T., CAO S., Progress in Aerospace Sciences, 2001, 37, 551.
[2] PUFFARY B., *Design and Analysis of High Speed Pumps. Educational notes*, RTO-EN-AVT-143, 2006, 3, 3.1.
[3] SCHNERR G.H., SAUER J., Fourth International Conference on Multiphase Flow, New Orleans, Louisiana, 2001.

Spectral analysis of self-sustained oscillations for the free jet under variable outlet conditions

A. Pawłowska, S. Drobniak, P. Domagała

Częstochowa University of Technology, The Faculty of Mechanical Engineering
and Computer Science, Institute of Thermal Machinery,
Armii Krajowej Avenue 21, 42-200 Częstochowa, Poland. E-mail: pawlowska@imc.pcz.czest.pl

The paper presents results of research devoted to the experimental verification of the self-sustained oscillations in the axisymmetric free jet. The new regime were found by Bogusławski et al. [1]. Appearance of self-sustained oscillations requires the fulfilment two initial conditions – the exit shear layer should be sufficiently thin and the level of turbulence intensity at the nozzle outlet should be sufficiently low. Presented results shows unusual free jet behaviour similar to the forced one. The CTA and LDA measurements were performed to verify the results of numerical modelling.

1. Introduction

Motivation for the present research comes from the paper published by members of our team, this paper presents the evidence of self-sustained oscillations in free jet. For thick exit shear layer the dominant frequency scales on the shear layer thickness and LES calculations and linear stability theory agree. However if shear layer becomes sufficiently thin then the new phenomenon appears, the Strouhal number no longer scales on the shear layer thickness, one obtains the constant value of Strouhal number and the dominant mode is self-exciting due to pressure feedback at the exit. It is a nonlinear phenomenon and of course the linear theory is not able to predict the jet behavior, so only LES simulation performed within the quoted paper could explain the phenomenon. It is a new finding, so the experiment was needed to prove that it was true. However, as it results from the paper [1] the experimental evidence was very limited, just two measurements were obtained, that is why in the present experiment it was decided to develop an experimental rig that will enable to perform a reliable verification of the finding from JoT paper [1].

2. Experimental conditions

Measurements had to be performed for sufficiently wide range of exit shear layer thickness, so a special design of jet nozzle was applied, it uses the third order polynomial profile and a high surface contraction ratios equal 144 and 225 for two nozzle designs tested. The thickest layer is characterized by R/θ ratio equal 12 (where R is the exit nozzle radius and θ is the momentum thickness of the exit shear layer), it was obtained for the lowest Re number, the thinnest layer has R/θ ratio over 80, LES simulations suggest that for the shear layer that is sufficiently thin for self -sustained oscillations to be developed, the critical ratio should be of the order of 25. The second important parameter of the experiment was the turbulence intensity Tu, which also had to be sufficiently low, Tu level in present experiment is evidently lower than in the preliminary experiment. The profiles of mean velocity and turbulence intensity Tu and values of shape parameter (not shown here) support the evidence that shear layer is laminar.

3. Results and discussion

In present experiment measurements have been taken for Reynolds number equal Re = 5 000, 10 000, 20 000, respectively. Four different cylindrical nozzle extensions were used

with lengths equal L/d = 1, 7, 15, 25, which vary the exit shear layer thickness. The CTA and LDA measurements were performed. Comparison of the two methods of measurement shows that the presence of the CTA probe does not disturb the flow (see Fig. 1) and the CTA and LDA results are equivalent not only for velocity and turbulence intensity flow fields but also in spectral analysis. The preliminary results in isothermal jet are not fully convincing and this is why the measurements in non-isothermal jet were undertaken.

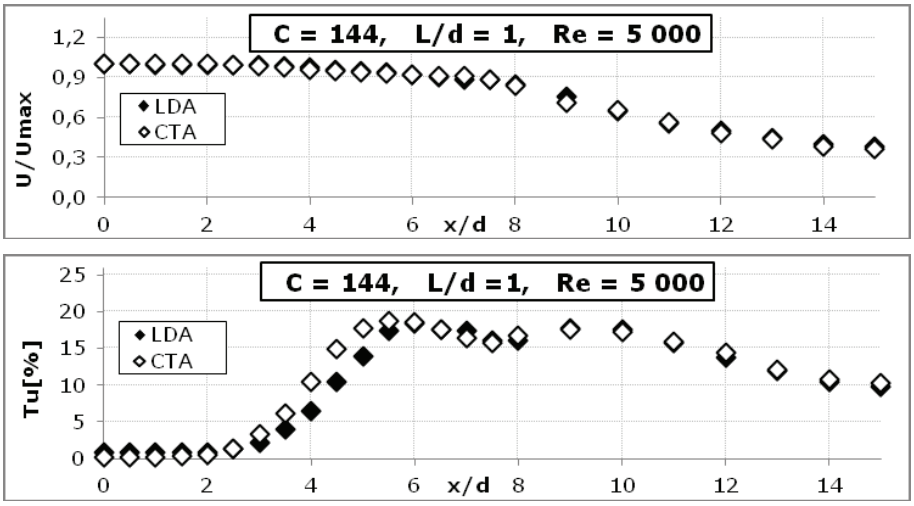

Fig. 1. The exemplary comparison CTA and LDA results

The measurements in non-isothermal jet are still being performed, but in this moment uniform temperature profile with thin thermal insulation layer has already been achieved, see Fig. 2.

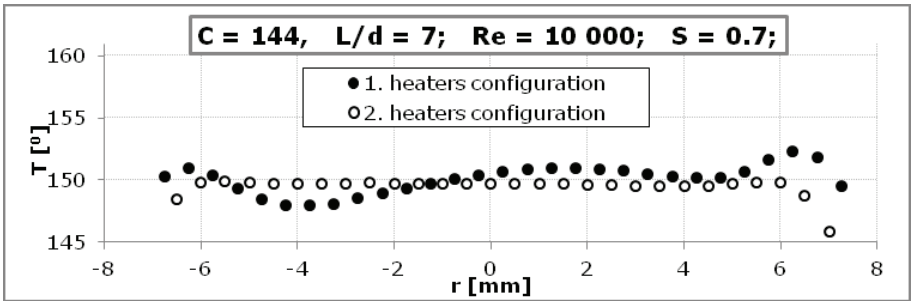

Fig. 2. Initial and after some heaters modification temperature profile

Acknowledgements

The investigations presented in this paper have been obtained with funding from Polish National Centre of Science within the grant DEC 2011/03/B/ST8/06401.

References

[1] BOGUSŁAWSKI A., TYLISZCZAK A., DROBNIAK S., ASENDRYCH D., *Self-sustained oscillations in a homogenous-density round jet*, Journal of Turbulence, 2013, 14(4), 25–52

Experimental research of an airfoil cascade in varying air humidity conditions

Z. Nosal, B. Olszański

Warsaw University of Technology, Faculty of Power and Mechanical Engineering,
Institute of Aeronautics and Applied Mechanics, Nowowiejska 24, 00-665 Warsaw, Poland
E-mail: bolszanski@meil.pw.edu.pl

Abstract: This paper shows the experimental study results for an exemplary turbine blade cascade mounted in a linear cascade wind tunnel in the varying air humidity conditions. The research consisted of pressure measurements from two inner blades of a cascade and the Schlieren flow visualization of selected region between the inner blades with its wake. The influence of angle of incidence, vacuum tank pressure along with humidity was examined. The shock wave pattern and condensation shock were identified.

1. Introduction

The development of the increased efficiency low pressure turbine (LPT) is one of the most popular and emerging topics in current turbomachinery flow research. The more ambitious requirements regarding to NOx emission, noise pollution and fuel economy for modern turbofan engines encourages to development of advanced, multi-stage LPT module. As the LPT provides the power to drive the fan, that diameter is gradually increasing effectively boosting the bypass ratio and engine thrust-to-weight ratio in new designs such as GEnx-2B, the more focus are put on the design of LPT. More sophisticated aerodynamics of a fan means that the load of LPT is also substantially increased so there is a strong need for minimization of secondary flow losses from one side, and the development of a new, high lift blades to reduce blade numbers for weight, manufacturing and operating cost savings from another to maintain the improved engine performance.

Nowadays, the design and optimization process of blade is carried out by using specialized, in-house codes and commercial CFD software, such as CFX or Fluent. However, every complex numerical simulation needs a calibration and validation data, usually obtained from wind tunnel tests. Routinely, the fluid medium in computations is assumed as a dry air. In fact, the air has a small fraction of water vapor which alter the properties of a perfect, dry gas. The latent heat in water vapor is released to surrounding non-condensed gas when the phase change occurs, increasing local temperature and pressure. This obviously non-adiabatic effect induces a nonlinear phenomenon, the so-called “condensation shock” [1], that can be easily captured by flow visualization techniques.

The main purpose of current work is to estimate the air humidity influence on turbine blade cascade performance. The experimental study of custom turbine cascade consisting of 4 separate blades with a chord of approximately 80 mm for various humidity was carried out in Department of Aerodynamics, Institute of Aeronautics and Applied Mechanics (IAAM) cascade wind tunnel. It was an initial phase research before further investigation of more advanced, modern blade geometries. Among the other important parameters taken into consideration were vacuum tank pressure as well as inlet angle of attack (AoA). The additional task were to identify the intake Mach number of test section in turbine configuration in a function of vacuum tank pressure and throttle valve opening width and qualitative evaluation of the flow field near the rounded trailing edge of turbine blade for the separation shock wave pattern identification.

2. Experimental setup

2.1. Cascade wind tunnel

All experiments were carried out using stationary, linear high-speed cascade wind tunnel. It is an open circuit, intermittent, in-draft (suction) type of wind tunnel designed to test turbine and compressor blade cascades as well in cold-gas conditions. The test section has 100 mm depth so it is mainly used for approx. 2-D flow examination. The cascade is mounted between two circular discs – aluminum for pressure acquisition and optical grade glass for flow visualization in order to adjust the inlet AoA.

2.2. Instrumentation

Static pressure distribution from cascade blades was retrieved by 3 miniature electronic differential pressure measurement units with 32 piezoresistive pressure sensors each. Single pressure tap has the 0.3 mm diameter. The flow visualization was prepared by using a Schlieren photograph optical system with 270 mm diameter mirrors.

3. Results and Discussion

Figure 1 shows a series of Schlieren photographs for various air humidity. The vacuum tank pressure in all three cases was approximately 250 mbar and AoA was 0°.

The light area between blades for (b) and (c) cases corresponds to high pressure gradient. Pressure distribution evaluation on a suction side of a upper blade and wind tunnel walls revealed, that the velocity changes according to a same trend – increasing, but this trend is less marked for high humidities, so the density change appears to be a result of a condensation shock.

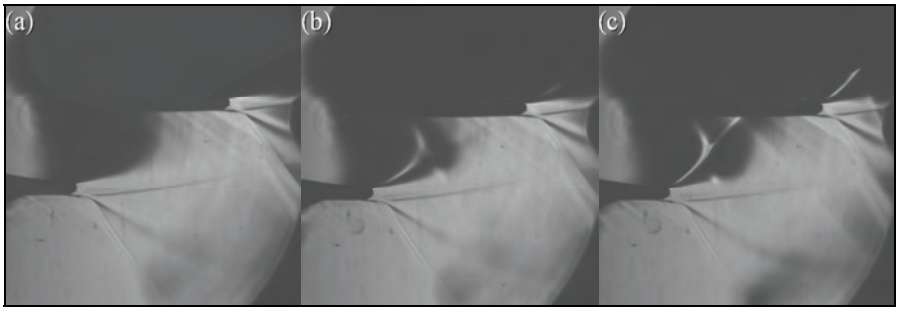

Fig. 1. Schlieren photographs of inner blades trailing edge region for 3 different humidities: (a) H = 13%, (b) H = 40%, (c) H = 72%

The study proved that the favorable pressure gradient along blade is negatively influenced when humidity rise, due to the presence of condensation. The evolution of condensation shock position in function of humidity was observed. For a low humidity (below 20–25% for a standard experiment temperature 20 degrees Celsius), when the partial vapor pressure cannot exceed equilibrium vapor pressure in a lowest pressure point, the flow can be treated as a dry air case.

References

[1] SASAO S., YAMAMOTO S., *Numerical Prediction of Humid Effect to Transonic Flows in Turbomachinery*, Proc. Int. Gas Turbine Congress (Tokyo), ed. T. Watanabe (Tokyo: Gas Turbine Society of Japan), chapter 21, 2003.

Impact of numerical method on auto-ignition in a temporally evolving mixing layer at various initial conditions

A. Rosiak, A. Tyliszczak

Częstochowa University of Technology, Faculty of Mechanical Engineering and Computer Science,
Al. Armii Krajowej 21, 42-200 Częstochowa, Poland. E-mail: rosiaka@imc.pcz.czest.pl

Numerical analysis of the auto-ignition of turbulent mixing layer between the cold fuels (hydrogen, methane) and hot air is presented. The research were performed using Direct Numerical Simulation (DNS) and Implicit-Large Eddy Simulation (ILES) methods with attention on auto-ignition time, flame kernel localisation and propagation. The results obtained showed that numerical approach plays an important role and to some extent may falsify the results, especially for low oxidiser temperatures.

1. Introduction

Generally the turbulent combustion process being a result of the two-way interaction of chemical reactions and turbulent structures is characterized by significant oscillations of all flow variables. The flame interacting with the turbulent flow leads to its modification caused by strong accelerations through the flame front and because of large changes of density and viscosity associated with temperature changes. Opposite impact is equally important, i.e. the turbulence affects the combustion process by enhancing the chemical reactions or inhibiting them, which may lead to a spontaneous ignition or flame extinction, respectively. The fact that accuracy of modelling of turbulent flows is directly related to applied model and numerical method indicates that simulations of reacting flow are very complex problem regarded as ones of the most difficult tasks in contemporary CFD. They need involvement of computational methods capable to accurately represent a wide range of strongly, unsteady phenomena occurring in the combustion process.

The present work concerns both Direct Numerical Simulation (DNS) and Implicit Large Eddy Simulation (ILES) of non-premixed combustion in a temporally evolving mixing layer between cold fuel (hydrogen, methane) and hot oxidiser (air). The analysis is focused on the auto-ignition and the flame propagation phenomena, which are very important from the point of view of an improvement of existing technical applications. We analyse influence of numerical approach (chemical kinetics, discretisation method, mesh density, turbulence model) on occurrence of auto-ignition, ignition time, localisation of an ignition kernel and its propagation.

2. Numerical methods

2.1. Solution algorithm

The computations are carried out using an in-house numerical code (SAILOR) based on the low Mach number approach which was previously well verified in gaseous shear layer flows with/without chemical reactions (see [1–3]). The spatial discretisation is performed on a half-staggered meshes by high-order (6th) compact difference approximation for the Navier–Stokes and continuity equations while for the chemical transport equations two different schemes are examined: 2nd order TVD (Total Variation Diminishing) with van Leer's limiters and the 5th order WENO (Weighted Essentially Non-Oscillatory). The governing equations are integrated in time using the 2nd order predictor-corrector approach combined with the projection method for pressure-velocity coupling. In the half-staggered approach the velocity components and scalar quantities are stored in the same spatial locations (nodes) while the pressure nodes are

shifted to the cell centres. Compared to the fully staggered grid arrangement, where the pressure and all scalar variables are shifted to the cell centres and the velocity components are placed on different cell corners, the use of half-staggered meshes facilitate the solution algorithm as the velocity needs to be interpolated only within the projection method [2].

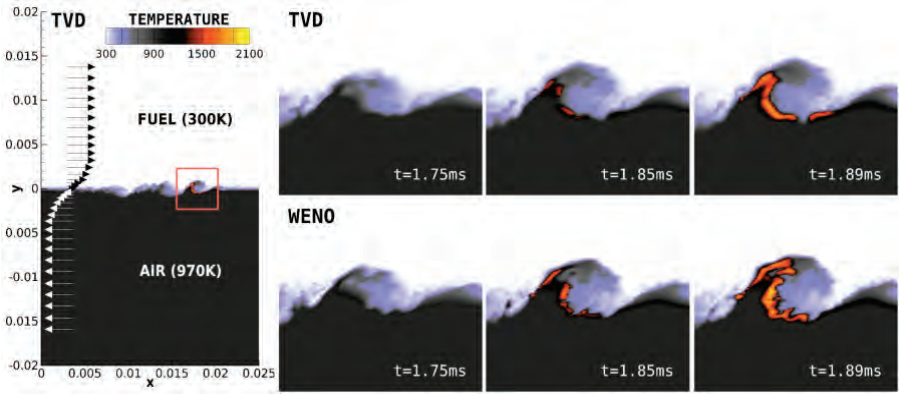

Fig. 1. Sample DNS results. Instantaneous temperature contours

2.2. Simulation details

The DNS and ILES calculations are performed to study the auto-ignition in the temporally evolving mixing layer between two separate streams (cold fuel/hot air) moving with opposite velocities or being stagnant. The initial isotropic turbulence prescribed by a three dimensional kinetic energy spectrum [4] was combined with the Gaussian function and superimposed on the initial flow field providing the largest velocity fluctuations in region of fuel/oxidiser contact zone. The analysis is performed for a wide range of the initial conditions (e.g., size of the shear layer, oxidiser temperature), however the main attention is put on the influence of the numerical method on the auto-ignition process.

3. Results and discussion

Sample DNS results, presenting a time evolution of temperature in 2D cross-section located in the centre of 3D computational domain, are shown in Fig. 1. The subfigures show enlarged regions where the flame starts to propagate along the vortex. These results were obtained using TVD and WENO schemes. It is found that in cases when the oxidizer temperature is low (here the case with 970K) the numerical approach significantly affects the ignition and growth of the flame. On the other hand, when the oxidiser temperature is large (e.g., 1000K) the numerical method does not play such an important role and it seems that in this case the chemical kinetics is a crucial part of simulation.

References

[1] TYLISZCZAK A., Combust. Flame, 2015, 162, 3864–3883.
[2] TYLISZCZAK A., J. Comp. Phys., 2014, 276, 438–467.
[3] TYLISZCZAK A., GEURTS B.J., Flow Turbul. Combust., 2014, 93, 221–247.
[4] DOOM J., MAHESH K., Proc. 47th AIAA Aerospace Sciences Meeting, 2009, AIAA2009-240.

Assessment of turbulence-chemistry interaction models in the computation of turbulent non-premixed flames

M.T. Lewandowski[1, 2], J. Pozorski[1]

[1] Institute of Fluid-Flow Machinery, Polish Academy of Sciences,
Fiszera 14, 80-231 Gdańsk, Poland
[2] Gdańsk University of Technology, Conjoint Doctoral School of IFFM PAS and GUT,
Narutowicza 11/12, 80-233 Gdańsk, Poland. E-mail: michal.lewandowski@imp.gda.pl

The present work reports on the assessment of different turbulence-chemistry interaction closures for the modelling of turbulent non-premixed combustion. Two dimensional axisymmetric simulations have been carried out based on three different laboratory flames. The methane fuelled, piloted jet flame Sandia D, the simple jet syngas flame and the so-called Delft Jet-in-Hot Coflow flame are studied. All the flames can be characterized as non-premixed but differ by some features which are discussed in terms of appropriate modelling approach.

1. Introduction

Turbulent combustion is an interdisciplinary and broad topic. It combines turbulent flow, described by the fluid dynamics equations, and complex chemical kinetics. Turbulence enhances mixing of the reactants; on the other hand, the chemical reactions, mainly due to the temperature rise and its impact on density and viscosity changes, affect the flow itself. Therefore, aside of mass and heat transfer including radiation, the coupling between turbulence and chemistry plays a crucial role in the turbulent reactive flows. Due to the multi-scale character of the phenomena in space and time [1], combustion appears as a challenging task for the numerical predictions. Apparently, nowadays computational tools are of huge importance for the design of modern fluid-flow machinery [2].

The accurate control of turbulent flames is required, e.g., to meet the environmental restrictions on the air pollution emissions, for optimal combustion chamber design, and for the safety issues. Development of various alternative technologies can be observed in the fields of combustion systems in the energy industry. Examples are fluidized bed combustors, oxy-fuel combustion, Moderate and Intense Low Oxygen Dilution (MILD) combustion or technologies based on production and utilization of low calorific gas from biomass or different kind of waste [3].

The need for comprehensive understanding of combustion leads to the study of chemical reactions in the flames using experimental and numerical tools. Experimental investigations that aim for numerical models validation are often conducted on the flames issuing from the laboratory burners with the use of laser diagnostic techniques. Attention is directed on capturing modelling challenges such as local extinction and re-ignition, detached or lifted reaction zones, auto-ignition, flow recirculation, and swirl [5]. In the present work we present a numerical study of three different non-premixed flames and an assessment of four turbulence-chemistry interaction models.

2. Experimental flames

Turbulent Non-premixed Flames Workshop [5] provides a library of well documented flames from which we have taken the following two: Sandia flame D and CHN flame B. The third one is a flame issuing from the Delft-Jet-in-Hot-Coflow burner that emulates the MILD combustion.

Table 1. The characteristic parameters of the flames

	Fuel	Reynolds number	Comment
Sandia D	Methane	22400	Piloted jet flame
CHN B	Syngas	16700	Simple jet flame
DJHC	Natural Dutch Gas	4100	Jet in Hot Coflow

3. Modelling

The simulations have been carried out with the Reynolds-averaged Navier–Stokes turbulence closure and with four turbulence-chemistry interaction models. Different versions of the two equation $k - \varepsilon$ model have been applied to test their impact on the behaviour of reactive jet flow. We have used two codes: commercial software AnsysFluent and open source code OpenFOAM, both based on finite volume method. The following closures for turbulence-chemistry interactions were applied: (i) presumed beta PDF and steady laminar flamelet model [2] in AnsysFluent, (ii) Partially Stirred Reactor (PaSR) and Eddy Dissipation Concept (EDC) [4] in OpenFOAM.

4. Preliminary results and comments

A number of simulations have been performed to have an opportunity for a broad comparative study. We have focused on the impact of turbulence closure and turbulence-chemistry interaction modelling on the results of multiscalar and velocity distributions. Not only the difference of fuel or flow conditions but also the specific regime (MILD) have been taken into consideration to assess the models' quality. Considerable discrepancies between EDC results for DJHC flame obtained with Fluent and OpenFOAM have been observed and their cause will be discussed.

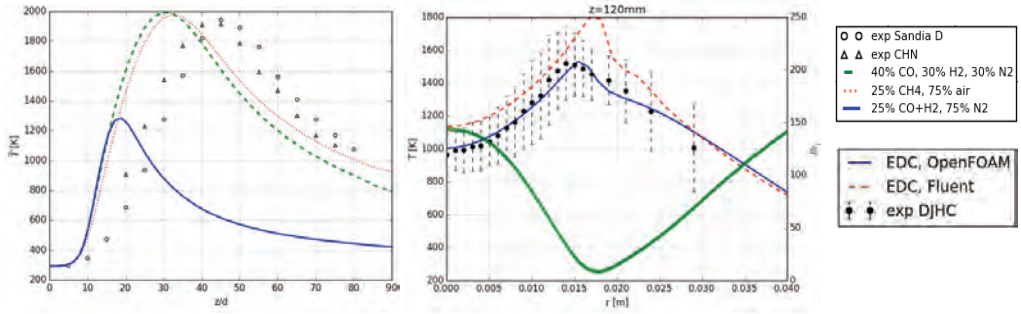

Fig. 1. a) The mean temperature profiles along the axis of methane and syngas flames in the configuration of Sandia D. The assumed PDF method was used (left figure); b) The radial distribution of temperature (left axis) and turbulent Reynolds number (right axis, green line) in the DJHC flame. Symbols represents experimental data (the RMS as the error bar) and lines are predictions

References

[1] PETERS N., P. Combust. Inst. 2009, 32, 1–25.
[2] VEYNANTE D., VERVISCH L., Prog. Energ. Combust. Sci., 2002, 28, 193–266.
[3] LEWANDOWSKI M.T., POZORSKI J., P. Eur. Combust. Meet., 2015, art. P4-58, Budapest 30.03–2.04.
[4] GRAN I.R., MAGNUSSEN B.F., Combust. Sci. Technol., 1996, 119, 191–217.
[5] http://www.sandia.gov/TNF/abstract.html

Simulations of particle suspensions in viscoplastic fluids using a combined discrete element-lattice Boltzmann method

W. Regulski

Warsaw University of Technology, Institute of Aeronautics and Applied Mechanics,
Nowowiejska 24, 00-665 Warsaw, Poland. E-mail: wregulski@meil.pw.edu.pl

This work presents the development of a numerical model capable of simulating particle suspensions in viscoplastic fluids. The fluid phase is modelled with a locally implict construction of the lattice Boltzmann method (LBM) which is capable of capturing the viscoplastic rheology of the fluid without regularisation. Solid particles are represented using the discrete-element method (DEM) and hydrodynamic coupling between the fluid and particles is handled using an immersed moving boundary condition.

1. Introduction

Generalized Newtonian fluids with particle suspensions are encountered at various length-scales in nature, industry as well as in everyday experience. Ranging from blood and mud with debris flows in the first case to specially designed hydraulic fracturing fluids in the latter, such suspensions always pose significant challenges from modelling point of view. However, an ever increasing demand for research in this field is observed.

This paper presents progress on the extension of the LBM-DEM framework [1, 2], in particular, the development of a computational material model which captures the rheology of viscoplastic fluids. The model employs the DEM to represent a range of particle geometries, while the fluid phase is captured using a specially constructed formulation of the LBM [3]. Full hydrodynamic coupling of the LBM and DEM is achieved using an immersed moving boundary condition [4].

2. The modelling approach

2.1. The lattice Boltzmann Method

In contrast to the classical methods (such as finite element or finite volume method), the LBM approach for modeling fluid flow relies on a simplified form of the Boltzmann transport equation for the mesoscopic particle populations:

$$f_i(x_j + c_i\Delta t, t + \Delta t) - f_i(x_j, t) = \Omega(f)\,. \tag{1}$$

Some of the advantages of the LBM over traditional approaches to computational fluid dynamics are its ability to handle complex geometrical shapes, its lack of a compressibility constraint, and the relative ease of parallelization.

A special kind of the LBM method able to directly capture the non-trivial zero-strain finite-stress nature of viscoplastic fluids is used. Due to the implicit nature of the LBM, it is possible to solve for the strain and stress at the same time step. The superiority over some standard techniques relying on regularization [5] is demonstrated on a range of benchmark cases. Some technical aspects such as the choice of a proper lattice stencil and presence of spurious currents are also discussed.

2.2. The solid-particle coupling

A two-way coupling is provided by an immersed moving boundary method (IMB). The standard LBM equation is modified with a special IMB source term:

$$f_i(x_j + c_i\Delta t, t + \Delta t) - f_i(x_j, t) = (1 - \Sigma B_d)\Omega(f) + \Sigma B_d \Omega^d_{IMB}. \quad (2)$$

The additional term, Ω_{IMB}, provides two way coupling since it carries information about the nodal force between the particle element and fluid. Some aspects of this approach such as Galilean invariance and behavior in the limiting cases of colliding particles are discussed.

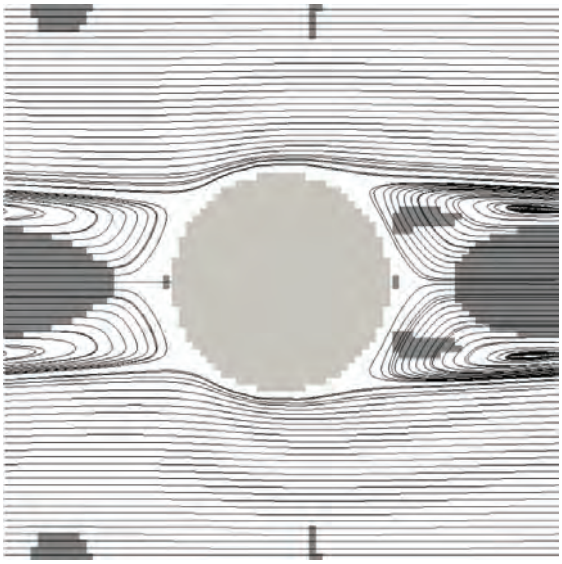

Fig. 1. Flow of a viscoplastic fluid past a periodic array of cylinders in the inertial regime, *Re* = 202. Unyielded zones are marked with dark grey

References

[1] OWEN D.R.J., LEONARDI C.R., FENG Y.T., Int. J. Num. Meth. Enging., 2011, Vol. 87, 66–95.
[2] LEONARDI C.R., OWEN D.R.J., FENG Y.T., J. Non-Newton. Fluid, 2011, Vol. 385, 628–638.
[3] NOBLE D.R., TORCZYŃSKI J.R., Int. J. Mod. Phys. C, 1998, Vol. 9, 1189.
[4] VIKHANSKY A., Can. J. Chem. Eng., 2012, Vol. 90, 1081–1091.
[5] PAPANASTASIOU T.C., J. Rheology, 1987, 385–404.

Nanofluids convective flow structure modified by the magnetic field

A. Roszko, E. Fornalik-Wajs

AGH University of Science and Technology, Department of Fundamental Research
in Energy Engineering, al. Mickiewicza 30, 30-059 Kraków, Poland. E-mail: roszko@agh.edu.pl

The main purpose of this paper was to find, to which extend the strong magnetic field is able to influence the diamagnetic nanofluid flow structure. Studied nanofluid consisted of the distilled water and silver particles of 0.1 vol.% concentration. The nanofluids diamagnetic components and particular location of cubical enclosure were chosen to gain the strongest effect of magnetic field on the flow structure. Presented results confirmed the changes in flow. The periodic structures of characteristic frequencies appearing without magnetic field were reorganized or damped in the magnetic field.

1. Introduction

Nowadays, due to the properties of nanofluids utilization in the industry, daily life or even medicine the extensive research work is going on various aspects of this topic. There were conducted numerous experimental and numerical investigations concerning the nanofluids properties [1, 2]. The engineering interests in heat transfer enhancement by nanofluid application were reported in [3]. However, in the publications a lot of inconsistences in the description of phenomena can be found, therefore there is still need of further investigations.

The influence of magnetic field on nanofluids is also a topic being widely discussed. However, the main direction of undertaken research is toward the numerical analysis [4]. The previous Authors research concerning experimental investigation of nanofluid in magnetic field was published in [5]. The main goal of presented studies was to define the range of magnetic field influence on the diamagnetic nanofluid flow. The attention was paid to the flow reorganization in dependence on the magnetic induction value.

2. Experimental equipment

Experimental set-up consisted of the superconducting magnet generating up to 10 T of magnetic induction, cubical enclosure, with the bottom wall heated and the top one cooled (both of them were made of copper), data acquisition system and personal computer to store thermocouples' signals. Detailed description can be found in [5]. The experimental enclosure was filled with silver nanofluid and placed in the magnet test section. The nanofluid consisted of the base fluid (distilled water) and 0.1 vol.% concentrations of silver particles (50–60 nm) was examined. The working nanofluid was prepared by two-step method, based on the ultrasonic mixing. In the one of the experimental enclosure side walls, six thermocouples were inserted, their signals were recorded and used to analysis of the flow structure. For this purpose the Fast Fourier Transform and the spectral analysis were applied.

3. Exemplary results

Examples of spectral analysis are presented in Fig. 1. The thermal power spectrum versus the frequency for nanofluid without magnetic field influence (Fig. 1(a)) and under the magnetic field of 10 T magnetic induction are shown (Fig. 1(b)).

On both diagrams characteristic peaks, representing the flow structures of particular frequencies could be seen. On left-side graph two clear peaks above a lot of smaller ones are noticeable without magnetic field utilization, which could point out on two large vortical struc-

tures present in the experimental enclosure. Whereas, on the right-side figure one of the maximum vanished, what could be interpreted as attenuation of the convection by strong magnetic field. The frequency of remaining maximum on both diagrams is the same. It should be noted that, the discussed signal came from the same thermocouple – t4, situated in vicinity of the cube left corner. The presented data are in agreement with heat transfer analysis, which also proved the attenuation of convection at high values of magnetic induction.

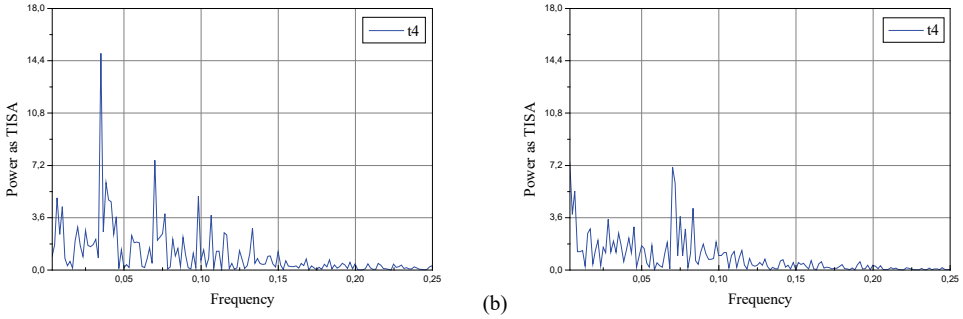

Fig. 1. The power spectrum versus frequency for $\Delta T = 15$ (a) without magnetic field and (b) at 10 T of magnetic induction

4. Summary

In the paper the experimental analysis of thermo-magnetic convection of nanofluid with Ag particles was described. Influence of magnetic field on the diamagnetic nanofluids behaviour was checked and presented. Estimation of the flow structure changes was able due to the signal analysis.

The components of nanofluid, as well as location of experimental enclosure in the magnetic field, were selected to obtain the strongest effect on the flow structure. Due to the FFT and spectral analysis the reorganization of the flow was found. It strongly depended on the magnetic induction, since grad $\mathbf{B}^2$ is one of the main factors defining the magnetic force.

Acknowledgment

The present work was supported by the Polish Ministry of Science (Grant AGH No. 15.11.210.328).

References

[1] GODSON L., RAJA B., LAI D.M., WONGWISES, Renew. Sustain. Energy Rev., 2010, 14, 629.
[2] CHANDRASEKAR M., SURESH S., CHANDRA BOSE A., Exp. Therm. Fluid Sci., 2010, 34, 210.
[3] VADASZ J.J., GOVENDER S., VADASZ P., Int. J. Heat Mass Transf., 2005, 48, 2673.
[4] ASHORYNEJAD H.R., MOHAMAD A.A., SHEIKHOLESLAMI M., Int. J. Therm. Sci., 2013, 64, 240.
[5] ROSZKO A., FORNALIK-WAJS E., Trans. IFFM, 2015, 128, 29.

Numerical investigation of shock wave interaction with laminar boundary layer on compressor profile

M. Piotrowicz, P. Flaszyński

Institute of Fluid-Flow Machinery, Polish Academy of Sciences,
Fiszera 14, 80-231 Gdańsk, Poland. E-mail: Michal.Piotrowicz@imp.gda.pl

The shock wave boundary layer interaction on suction side of transonic compressor blade is one of main objectives of TFAST project (Transition Location Effect on Shock Wave Boundary Layer Interaction). In order to investigate the flow structure on suction side of a profile, a generic test section in linear transonic wind tunnel was designed. The numerical investigation based on the RANS simulations with EARSM (Explicit Algebraic Reynolds Stress Model) turbulence model including transition modelling. The result are compared with the oil flow visualisation, schlieren picture, and static pressure measurements (Pressure Sensitive Paint).

1. Introduction

The shock wave boundary layer interaction (SWBLI) [1–2] on the suction side of the transonic compressor blade is one of the main objectives of TFAST project (Transition Location Effect on Shock Wave Boundary Layer Interaction). The test section was designed and assembled in IMP PAN in laboratory in order to reconstruct the flow structure existing in the real transonic compressor cascade [3–5].

The paper presents the comparison of numerical simulations results with measurements for the laminar boundary layer interaction with the shock wave. The investigated case is very challenging for the numerical simulations, because the shock wave location and flow structure is strongly dependent on the corner flow separation and interaction with the sidewalls. On the other hand, the secondary flows are very sensitive to the turbulence models.

2. Numerical results

The complex structure of the shock waves and corner separation occurring in the test section for transonic compressor profile investigations was predicted properly. As shown in Figure 1, the numerical simulation results represented by the density gradient magnitude (CFD) are compared with schlieren picture (EXP). The paper presents the influence of the upstream boundary layer on the shock wave and secondary flows as the effect of shock wave boundary layer interaction.

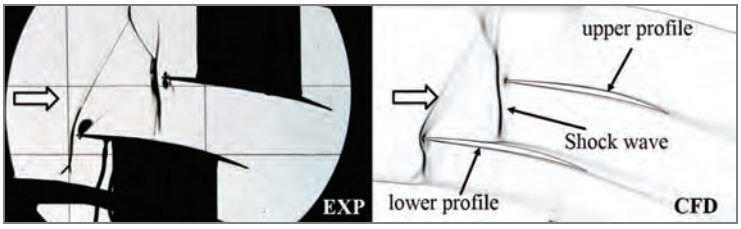

Fig. 1. Comparison of the structures of shock waves

Another example of the flow structure investigations is shown in Fig. 2. Oil flow visualization picture presented on the left side. One can observe interaction between the main flow and corner vortex. Such picture is considered as the reference for the streamlines distribution close

to the suction side of the profile. On the right side (Figure 2), streamlines are shown together with iso-surface of secondary flows represented by negative value of X component of velocity.

Numerical results and experimental data show that the flow structure is highly three-dimensional and strongly affected on the boundary layer upstream of the shock wave.

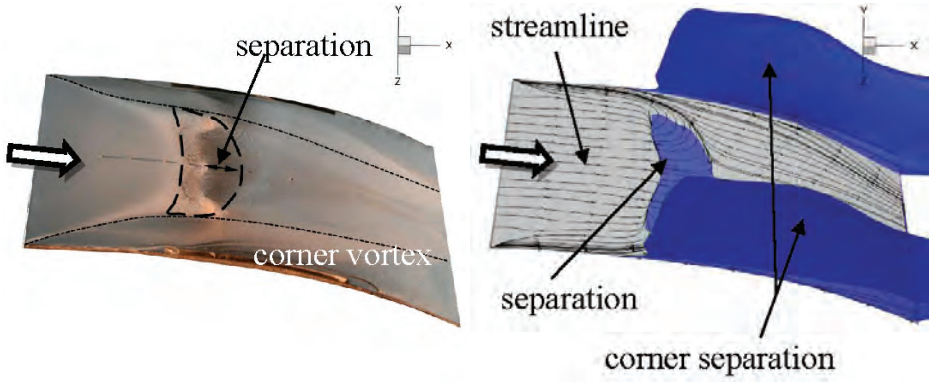

Fig. 2. Oil flow visualisation comparing to streamlines near the surface

References

[1] DOERFFER P., *UFAST Experiments Data Bank: Unsteady Effects of Shock Wave Induced Separation*, IMP PAN Publishing, 2009.

[2] DOERFFER P., HIRSCH M., DUSSAUGE J., BABINSKY H., BARAKOS G., *Unsteady Effects of Shock Wave Induced Separation*, Springer 2010.

[3] PIOTROWICZ M., FLASZYŃSKI P., DOERFFER P., *Investigation of Shock Wave Boundary Layer Interaction on Suction Side of Compressor Profile*, Journal of Physics: Conference Series, 2014, Vol. 530.

[4] PIOTROWICZ M., FLASZYŃSKI P., SZWABA R., *Influence of Limiting Walls on Shock Wave Strucure in Single Passage Test Section with Compressor Profile Task Quarterly*, Scientyfic Bulletin of Academic Computer Centre in Gdańsk, 2015, 19(2), 141–152.

[5] FLASZYŃSKI P., DOERFFER P., SZWABA R., KACZYŃSKI P., PIOTROWICZ M., *Shock Wave Boundary Layer Interaction on Suction Side of Compressor Profile in Single Passage Test Section*, Journal of Thermal Science, 2015, 24(6), 510–515.

Generation of the vorticity field by the flapping profile

T. Kozłowski, H. Kudela

Wrocław University of Science and Technology, Faculty of Mechanical and Power Engineering,
Wybrzeże Wyspiańskiego 27, 50-370 Wrocław, Poland. E-mail: tomasz.kozlowski@pwr.edu.pl

Birds and insects moved due to flapping of the wings. In the paper we presented the unsteady effects led to the lift and thrust force generation on the flapping foil. It was assumed the two dimensional flow. We demonstrated that flapping motion with low Reynolds number, low Strouhal number and small amplitude of plunging produced the well-ordered vorticity around the profile. The large enough amplitude of plunging motion may cause disordered vorticity distribution around the profiles that was led to the loss of the lift force and excluded the possibility of the fly.

1. Introduction

In contrast to classical airplanes, most of the insect and birds operate in low Reynolds number regime, below, 10^4 [1]. The flow is dominated by unsteady effect caused by the vorticity dynamics. Although flight in nature is naturally three-dimensional, the two-dimensional simplification is widely used and seems to be appropriate to capture the essence of flapping flight aerodynamics [2]. For the study of moving object in fluid we choose vortex particle method – Vortex-in-Cell method. The method was carefully tested for problems with known analytical solution and problems with well documented experimental data.

2. Vortex particle method

The Navier–Stokes equations of the incompressible viscous fluid in primitive variables ($\boldsymbol{u}$, p) can be transformed to the Helmholtz equations in vorticity-stream function formulation:

$$\frac{\partial \omega}{\partial t} + \boldsymbol{u} \cdot \nabla \omega = \upsilon \Delta \omega, \quad \Delta \psi = -\omega \tag{1}$$

$$\boldsymbol{u} = \nabla \times (0,0,\psi) = -\omega\,. \tag{2}$$

where $\mathbf{u} = (u, v)$ means vector velocity, ψ stream function and υ viscosity. In the vortex particle method the continuous vorticity field is approximated by the discrete particles distribution. For solution of the vorticity equations the viscous splitting algorithm is used. First, the inviscid fluid motion equation was solved ($\upsilon = 0$). In the second step the viscosity is introduced by the solution of the diffusion equation. The realized the non-slip condition for the velocity on the wall the suitable portion of vorticity had been added. The velocity field was obtained by the solution of the Poisson equation on the numerical grid using the finite difference method. To fit the numerical grid to the solid boundary we used conformal mapping.

3. Flapping simulation

On the figure 1 we presented the results that are related to the flapping motion that in literature is called as incline hovering. One can noticed the generation of dipolar vortex structures and got off that structure.

To capture the essence of vorticity role in the flapping motion we simplified the motion of the foil to simple harmonic motion: $y = A\cos(\omega t)$ that was perpendicular to the main flow direction (it is called as a plunging motion). When the amplitude A was large enough the vortex

wake could be reversed (change topology) or could be reversed and deflected. That caused arising the thrust and lift force on the profile, (see Figure 2 with different amplitude of plunging). For large enough amplitude *A* the vortex wake became disordered what resulted in the disordered aerodynamic forces that acted on the profiles.

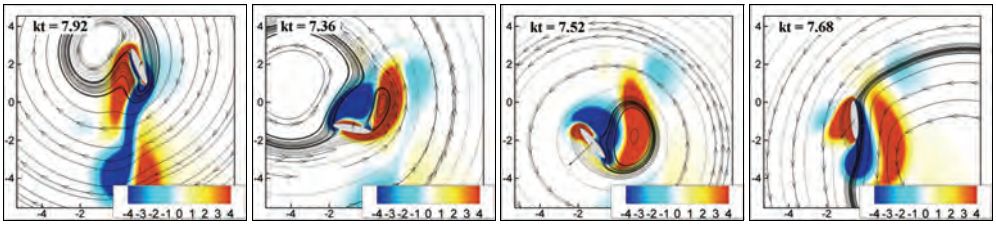

Fig. 1. Vorticity field and stream lines around profile after third the back-stroke flapping wing, *Re* = 125. The stream lines are plotted for fixed to wing coordinates

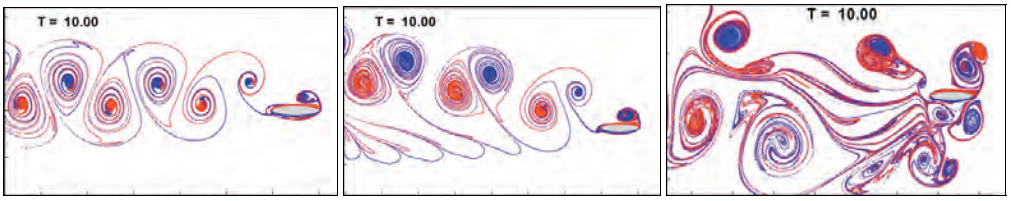

Fig. 2. The wing wake observed in flapping motion. Visualisation was done using passive markers

We checked how disordered vorticity field can affect the free flapping flight. The profile was replaced by the mass point which moved according to the second Newton law. The forces was calculated from action of the fluid on the profile. We noticed that the stable, predictable flight was only possible, when the profile generated periodic and well-ordered vorticity field, Figure 3.

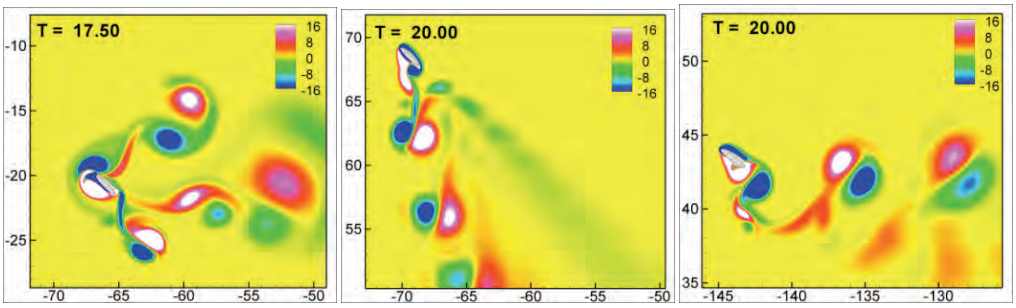

Fig. 3. Vorticity field generation in free flapping flight. Profile started from the origin. By a small modification of flapping parameter we can simply control the flight angle

References

[1] SHYY W., LIAN Y., TANG J., VIIERU D., LIU H., *Aerodynamics of Low Reynolds Number Flyers*, Cambridge University Press, Dover Publications, 2008.
[2] WANG Z.J., BIRCH J.M., DICKINSON M.H., J. Exp. Biol., 2007, Vol. 207.

Properties of velocity field in the vicinity of synthetic jet generator

P. Strzelczyk, P. Gil

Rzeszów University of Technology, al. Powstańców Warszawy 12, Rzeszów, 35-959, Poland
E-mail: piotstrz@prz.edu.pl

The paper presents the results of experimental investigation of velocity field in the vicinity of synthetic jet actuator as a function of Stokes number and for constant Reynolds number. A constant temperature hot-wire anemometer with tungsten–platinum coated single wire probe used for the velocity measurements. Synthetic jet velocity profiles were compared with a solution to fully-developed pipe flow with an oscillating pressure gradient.

1. Introduction

Since the end of the last century, the synthetic jet has been the subject of both experimental and numerical investigations, usually under the name "SJ" synthetic jet or "ZNMF" zero net mass flux. A synthetic jet actuator consists of an oscillating driver and cavity that contains one or more orifice. This driver may be for example a loudspeaker, piezoelectric diaphragm or a mechanical piston. The device is called ZNMF because the integration of the mass flow rate across the orifice over an integer number of cycles is equal to zero. Although there is no net mass transfer to ambient fluid, the ZNMF device has the interesting property of causing a finite amount of momentum transfer to ambient fluid [2].

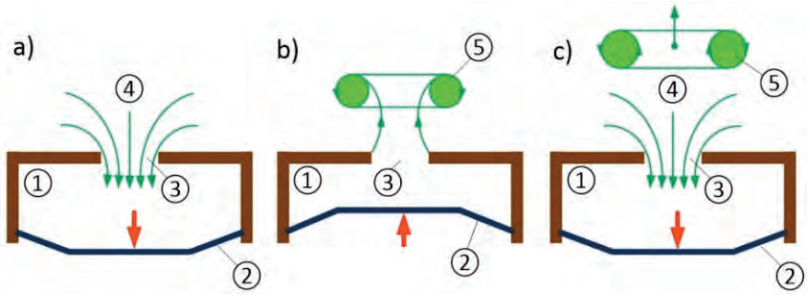

Fig. 1. Schematic of a device producing a synthetic jet: a) suction stroke, b) production a vortex ring during ejection stroke c) vortex ring propagates away from the orifice:
1 – cavity, 2 – diaphragm, 3 – orifice, 4 – ingested fluid, 5 – vortex ring

Figure 1 illustrates a typical ZNMF device being operated to producing a synthetic jet. If the diaphragm amplitude 2 is high enough, as fluid is expelled through the orifice 3 the boundary layer separates from the wall and, at edge of the orifice, it rolls up to produce a vortex ring 5. This vortex ring propagates away from the orifice under its own self-inducted velocity. During the subsequent suction stroke, fluid 4 is drawn into the cavity 1 from the surrounding, but the vortex ring has moved sufficiently far from the orifice so as to be relatively unaffected. A new vortex ring is then ejected and the cycle continues, producing a train of vortex rings.

2. Results

The problem of fully-developed pipe flow with an oscillating pressure gradient is the most reasonable exact solution available to model flows emanating from the orifice of synthetic jet actuator.

The non-dimensional solution for the velocity profile [1]:

$$\frac{u}{u_{\max}} = -i \cdot \frac{16}{Stk^2}\left[1 - \frac{J_0\left(\frac{r}{d}\cdot Stk\cdot\sqrt{-i}\right)}{J_0\left(0.5\cdot Stk\cdot\sqrt{-i}\right)}\right]\cdot e^{i\omega\tau} \tag{1}$$

where: u – velocity, Stk – Stokes number, τ – time, r – radial coordinate, d – orifice diameter, J_0 – zero order Bessel function

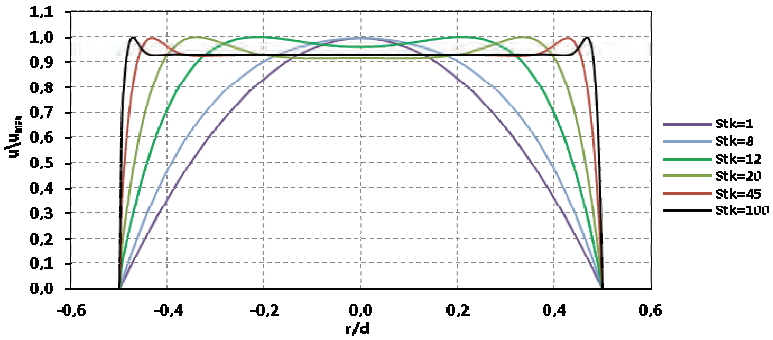

Fig. 2. Normalized velocity profile vs. normalized radius calculated for several Stokes number

3. Discussion

Tang et al. [3] made experimental and numerical investigation of flows result from the orifice of synthetic jet actuator. The results of measurements obtained in the present paper were obtained by use constant temperature hot wire anemometer. The measurement of velocity fields were made employing assumption of axial symmetry of the flow. The present measurements shows good with theoretical predictions. For low Stokes number a near parabolic radial distribution is obtained, while for high Stokes number it is more uniform for described solution. Experimentally obtained velocity profile behave similarly but only for low Reynolds number. For high Reynolds number the similarity of velocity distribution between theoretical prediction and experimental results is only qualitatively.

References

[1] HOLMAN R., UTTURKAR Y., MITTAL R., SMITH B.L., CATTAFESTA L., *Formation criterion for synthetic jets*, AIAA Journal, 2005, 43(10), 2110–2116.
[2] SMITH B.L., GLEZER A., *The Formation and evolution of synthetic jets*, Physics of Fluids, 1998, Vol. 10, No. 9, 2281–2297.
[3] TANG H., ZHONG S., *Incompressible flow model for synthetic jets actuators*, AIAA Journal, 2006, 44(4), 908–912.

Incompressible mean-field model with modal closure

W. Szeliga[1,2], M. Morzyński[1], W. Stankiewicz[1], K. Kotecki[1]

[1] Poznań University of Technology, Institute of Combustion Engines and Transport, Piotrowo 3, 60-965 Poznań, Poland
[2] Poznań Supercomputing and Networking Center, Jana Pawła II 10, 61-139, Poznań
E-mail: wojciech.s.szeliga@doctorate.put.poznan.pl

In this paperwork an attempt of 3D application of modal closure of Navier–Stokes equations is done for a flow past a sphere. There were coupled steady flow fields and 2 dominating flow modes. Mentioned data was computed numerically with usage of UNS3 solver based on the finite element method. Analysis of the dynamics and stability of received flow fields was described. Examination covered also the influence of adjustments of modal kinetic energy.

1. Introduction

Numerical examination of a fluid flow is still a challenge regarding to time and computational demands. Applicability of direct numerical simulation approach resolving full and complete set of governing equations, is still limited to low Reynolds number flows, because of required virtual model complexity sufficient for smallest scales phenomena. For multiple purposes there are widely employed methods of reduction of resolved scales range, including semi-empirical models like Reynolds averaged Navier–Stokes equations. Also the usage of eigenvectors of a flow, called also modes in fluid flow modelling receives much attention. Exemplary methods of fluid flow eigenvectors generation for purposes of reduced order modelling are POD (proper orthogonal decomposition) [1, 2, 3] and DMD (dynamic mode decomposition) described by Schmid [4]. It is also possible to perform a query of base solution, without a need of performing numerical simulation. Such method was characterized by Morzyński et al. [5, 6], where received eigenvectors are known as CDR (complex dynamic response). However, modal approach is also affected by mentioned restrictions related to high resolution methods. Nevertheless, modelling fluids in the range of high Reynolds number values is possible on the one hand by modification of the modes, as described by Östh et al. [7] or on the other hand with usage of modal closure hypothesis initially proposed by Rempfer et al. [8, 9]. Application of the last is shown in this investigation.

2. Presented idea

The general idea presented in this study covers the approach of modal closure realized by expansion of steady state with modes of fluid flow inserted into modified Reynolds stress tensor of Navier–Stokes momentum equation. Steady solutions received for several flows which are above critical Reynolds number were used to generate mean field solution of multiple Reynolds number configuration without need of solving multiple, long lasting unsteady simulations.

3. Examined configurations

Tested geometry was a sphere with dimensionless diameter equal to unity. Discrete model was built with second order tetrahedral mesh. The flow was resolved in cuboidal domain. Steady solutions and modes were calculated for several Reynolds numbers.

4. Numerical approach

The solver used in described investigation was UNS3 [10, 11]. It is based on the finite element method. Solver is capable of performing parallel direct numerical simulations in time and frequency domain, modal analysis of a flow and it also allows global stability analysis with subspace iteration method (with usage of mixed formulation or penalty). Integration of matrices is realised with symbolic manipulation software. Nonlinear problems are solved with Newton–Raphson method coupled with incomplete LU decomposition.

5. Performed investigation

The examination was divided to separate tasks. At first, steady solutions of flows around a sphere for considered Reynolds numbers were computed. From mentioned results sets of orthogonalized modes were extracted. After the analysis of their dynamics, harmonic parameters, shapes and level of kinetic energy, they were fit into modified Navier-Stokes momentum equation. Such action was possible by implementing modal closure hypothesis where Reynolds stress tensor in momentum balance was rebuilt with the dominating pair of eigenvectors. It allowed to extract mean flow fields with a new approach and reduced time costs. This methodology was tested and verified on 2D flow around infinite cylinder, and its application on 3D flow around a sphere is also going to be validated and presented.

References

[1] AUBRY N., HOLMES P., LUMLEY J.L., STONE E., *The dynamics of coherent structures in the wall region of a turbulent boundary layer*, J. Fluid Mech., 1988, 192, 115–173.
[2] HOLMES P., LUMLEY J.L., BERKOOZ G., *Turbulence, Coherent Structures, Dynamical Systems and Symmetry*, Cambridge University Press, Cambridge 1998.
[3] SIROVICH L., *Turbulence and the dynamics of coherent structures*, Part I: *Coherent structures*, Quart. Appl. Math., XLV, 1987, 561–571.
[4] SCHMID P., *Dynamic Mode Decomposition of Numerical and Exporimental Data*, Journal of Fluid Mechanics, 2010, 656, 5–28.
[5] MORZYŃSKI M., NOWAK M., STANKIEWICZ W., *Novel Method of Physical Modes Generation for Reduced Order Flow Control-Oriented Models*, Vibrations in Physical Systems, 2014, 26, 189–194.
[6] MORZYŃSKI M., STANKIEWICZ W., SZELIGA W., KOTECKI K., NOWAK M., *Physical mode basis design for the flow past a Delta wing*, Proceedings of International Conference on Innovative Technologies, IN-TECH, 2015, 362–365.
[7] ÖSTH J., NOACK B.R., KRAJNOVIĆ S., BARROS D., BORÉE J., *On the need for a nonlinear subscale turbulence term in POD models as exemplified for a high-Reynolds-number flow over an Ahmed body*, Journal of Fluid Mechanics, 2014, 747, 518–544.
[8] REMPFER D., FASEL H.F., *Dynamics of three-dimensional coherent structures in a flat-plate boundary layer*, Journal of Fluid Mechanics, 1994, 275, 257–283.
[9] REMPFER D., FASEL H.F., *Evolution of three-dimensional coherent structures in a flat-plate boundary layer*, Journal of Fluid Mechanics, 1994, 260, 351–375.
[10] MORZYŃSKI M., THIELE F., *3D FEM Global Stability Analysis of viscous flow*, [in:] *Lecture Notes in Computer Science, Parallel Processing and Applied Mathematics*, Verlag, Springer, 2008, Vol. 4967, 1293–1302.
[11] MORZYŃSKI M., THIELE F., *Finite Element Method for Global Stability Analysis of 3D Flows*, AIAA Paper, number 2008–3865, 38th AIAA Fluid Dynamics Conference and Exhibition, 23–26 June, Seattle, Washington, USA, 2008.

Investigation of droplet impact spreading angle

M. Remer[1], K. Gumowski[1], J. Rokicki[1], G. Sobieraj[1], M. Kaliusz[2], M. Psarski[3], G. Celichowski[3], D. Pawlak[3]

[1] Warsaw University of Technology, Faculty of Power and Aeronautical Engineering, Nowowiejska 24, 00-665 Warsaw, Poland
[2] Ukraine
[3] University of Łódź, Department of Materials Technology and Chemistry
E-mail: sob@meil.pw.edu.pl

Presented work focuses on study of the water droplet impingement on surfaces having various wetting angle – hydrophilic, hydrophobic and superhydrophobic. The process of water droplet impacting the surface was observed by fast Photron SA5 camera with speed of 50 000 fps. The image analysis was carried out using an in-house software based on LabView® that allowed to determine the parameters shown in the figure beside. Exemplary results of the contact angle Θ_x measurements are shown on figure below for hydrophilic surface (left) and superhydrophobic (right) and an example of recorded film.

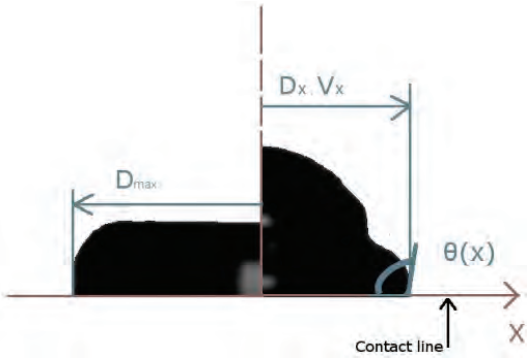

The measurements are performed both for the advancing as well as for the receding phases of the droplet impingement. The results are compared with traditional static and quasi-static measurements (sessile drop, Wilhelmy technique) showing significant and systematic differences.

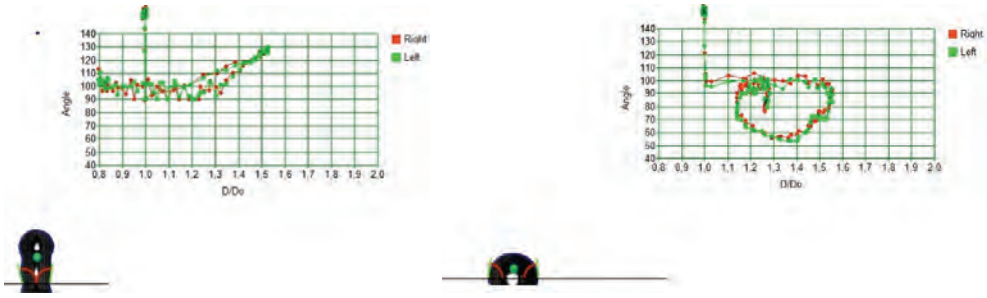

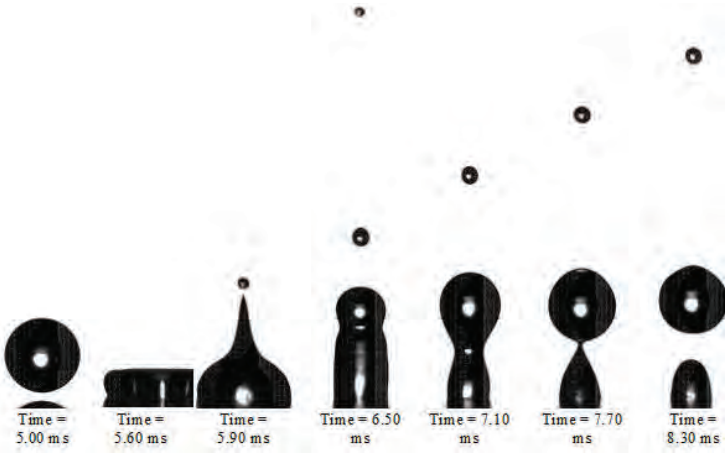

References

[1] BOBIŃSKI T., SOBIERAJ G., GUMOWSKI K., ROKICKI J., PSARSKI M., MARCZAK J., CELICHOWSKI G., *Droplet impact in icing conditions – the influence of ambient air humidity*, Arch. Mech., 2014, 66, 2, 127–142

Simulating the trajectory of droplets in an aircraft wake

T.P. Seredyn[1], R.S. Rowiński[2]

[1] Polish Air Force Academy, Department of Applied Science,
Dywizjonu 303 nr 35, 08-521 Dęblin, Poland
[2] Polish Air Force Academy, Department of Airframe and Engine,
Dywizjonu 303 nr 35, 08-521 Dęblin, Poland. E-mail: t.seredyn@wsosp.pl

The paper presents the so-called "fixed" mathematical models describing the phenomenon of the spread and distribution of liquid droplets using aviation technology. The models treat the undertaken problem as a physical problem of droplets movement in the velocity field of flying aircraft. The influence of vortex wake on the droplets movement is highly genuine and must be precisely recognized and included into theory. It seems, that such influence is underestimated in almost all models describing the process of dispersing droplets from aircraft.

1. Introduction

The spread of various substances by aircraft takes place in many areas of human life: from the military applications, protection of forests to agricultural aviation. However, one of the fundamental limitations of this technique is the possibility of agents drifting [1]. It should be noted, that from the scientific point of view the phenomenon of movement and settling of droplets is very interesting and difficult to describe mathematically. The aim of the work is to present models that describe the physics of the spread of liquid droplets in the air by aircraft. Based on the analysis of models the quality and usefulness of these theories work and possible indication of further directions of research will be considered.

2. Theoretical and mathematical background

The equation of droplets motion in its general form can be written as $\frac{d}{dt}(m\vec{\dot{R}_d}) = m\vec{g} + \vec{F_D} + \vec{F_A} + \vec{F_M} + \vec{F_B}$, with aerodynamic drag force, buoyancy force, Magnus and Basset forces respectively.

2.1. Velocity field after aircraft

The velocity disturbance field after aircraft can be determine as a vector sum of the three velocities: the stream flowing down from the wing, the stream behind the propeller and the wind: $\vec{v} = \vec{v_1} + \vec{v_2} + \vec{v_3}$.

– *Wind* – The influence of area coverage on the velocity profile was adopted by introducing a boundary layer with a logarithmic velocity profile and with the parameter depending on the kind of land cover.

– *Propeller slipstream* – The rotating propeller induces additional velocity field, which can be expressed in the form enabling numerical calculations.

– *Airflow from the wing* – Under the assumption, that near the plane the disturbances velocity field is caused by the horseshoe vortices and in the long distance by the vortex lines [2], the disturbances velocity can be calculated from the appropriate relationships.

In comparison with model proposed by Pietruszka [3], in AGDISP model [4], the flow field after aircraft is very simplified. The majority of the lift is carried by the wings and generates one or more pairs of swirling masses of air downstream of the aircraft. The rollup of this

trailing vorticity is approximated as occurring immediately and the local velocity around each of two vortices is given by the simple formula.

3. Results of droplets motion and their distribution

The whole process of computing should be conveniently divided into four phases: 1. Determination of the circulation distribution along the wingspan. 2. Determination of the vortex wake deformation behind the plane. 3. Solution of the equations of droplets motion. 4. Determination of sprayed agent distribution.

The first implementation of such algorithm was performed in Fortran 77 by Pietruszka [5]. The previous program was rewritten to Fortran 95. The results of calculation are presented below in comparison with experimental data collected during field experiments, which were carried out in the years 1987–1992 on the Academy of Agriculture and Technology in Olsztyn [6]. To verify the model, the distribution of the spray in 30 meter strips was calculated and presented in Figure 1 compared to the field tests in Figure 2. The calculation result shows an underestimation of the mass in the outermost strip and an overestimation of the mass in the strip nearest to the flight axis.

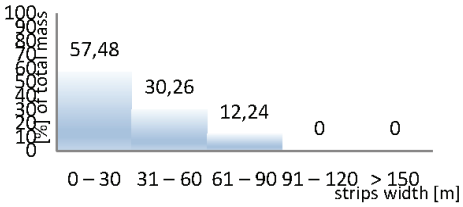

Fig. 1. Percentage distribution of mass in the 30-meter strips according to the model

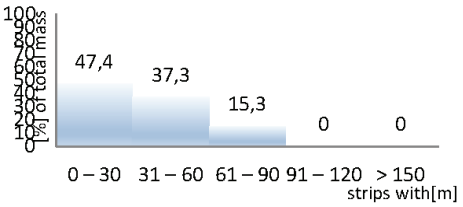

Fig. 2. Percentage distribution of mass in the 30-meter strips according to the field tests

4. Major conclusions

After the recalculations the needs for further considerations are highly visible. First of all, the modeled results, which are obtained from theories are highly consistent with experimental data, but there is still compulsion to implement the physics of flow around aircraft in a more advanced degree. For the second, such models and its improvements provide a low-cost alternative to field experiments aiming to optimize the lateral distribution of the sprayed droplets. And finally, further research, both theoretical and experimental, is needed to produce a higher degree of conformity between results given by the mathematical models and by field tests. The next step in developments of such studies are CFD calculations. This is the subject of subsequent considerations.

References

[1] ROWIŃSKI R.S., FERENC M., *Some Problems Concerned with the Theory of Drift*, Annual Review of Agricultural Engineering, 2000, 2(1), 148–156.
[2] MOORE D.W., *A Numerical Study of the Roll-up of a Finite Vortex Sheet*, Journal of Fluid Mechanics, 1974, 63(2), 225–235.
[3] PIETRUSZKA J., ROWIŃSKI R.S., *Computer Simulation of Aerial Spraying*, Annual Review of Agricultural Engineering, 2004, 3(1), 125–140.
[4] BILANIN A.J., TESKE M.E., BARRY J.W., *AgDisp: the Aircraft Spray Dispersion Model, Code Development and Experimental Validation*, Trans. ASAE, 1989, 32, 327–334.
[5] PIETRUSZKA J., *Symulacja komputerowa procesu opryskiwania z samolotu*, rozprawa doktorska, Politechnika Warszawska, 1987.
[6] SEREDYN T.P., *Experimental Investigations of a Drifting Cloud of Droplets Dispersed from Aircraft*, Archive of Mechanical Engineering, 2014, 3, 393–407.

Cooling intensity influence on shock wave boundary layer interaction region in turbine cascade

P. Kaczynski, R. Szwaba

Institute of Fluid-Flow Machinery, Polish Academy of Sciences,
Fiszera 14, 80-231 Gdańsk, Poland E-mail: Ryszard.Szwaba@imp.gda.pl

The shock wave boundary layer interaction on the suction side of a transonic turbine blade was one of the main objectives of the TFAST project. For this purpose a model of turbine passage was designed, manufactured and assembled in the transonic wind tunnel. The paper presents the experimental investigations concerning the flow structure on the transonic turbine blade. There were investigated a clean case (without cooling system) with normal shock wave interacting with laminar boundary layer and also the influence of blade cooling system with three different coolant blowing intensity on laminar interaction region.

1. Introduction

The shock wave boundary layer interaction (SWBLI) [1] is well known phenomenon in compressible aerodynamics. The increase of blades load in new designed turbines lead to that more often local supersonic flows appears in the turbine passages. Also the phenomenon of the shock wave boundary layer interaction on the suction side of a turbine blade was one of the main objectives of the TFAST project (Transition Location Effect on Shock Wave Boundary Layer Interaction) [2]. In order to investigate the flow structure on the suction side of the blade in a rectilinear test section of the transonic wind tunnel, a model of a turbine passage (Fig. 1) was designed, manufactured and assembled in the wind tunnel. The model can reproduce the flow structure, pressure distribution and the boundary layer development similar to the obtained in a reference turbine cascade profile. The paper presents the experimental investigations concerning the flow structure on the transonic turbine blade. There were investigated a clean case (without cooling system) with normal shock wave interacting with laminar boundary layer and also the influence of blade cooling system with three different coolant blowing intensity on laminar interaction region.

Cooling design process at most takes into account cooling effectiveness and the coolant is introduced to the flow smoothly, at the small angle not to provoke too much mixing losses. These investigations will help to estimate how the increase of the cooling intensity upstream of the interaction region influence on losses downstream of passage. Such study can also cast more light on some phenomena which are not always taken into account during the very complex turbine cascade design process.

2. Experimental Setup and Results

A view of the single passage turbine test section is shown in Fig. 1. Flow structure is investigated on the suction side (upper part) of the lower blade. The lower and upper profiles are located in the similar configuration as in linear cascade in order to keep the similar flow structure as in the reference passage. Both profiles are mounted in the channel at the required inlet Mach number $M = 0.13$. The Reynolds number at the inlet of the passage based on blade cord length is $Re_C = 3 \times 10^5$ and the cord length c is 112.5 mm.

The test section has a possibility to modify the passage geometry to obtain the proper flow pattern similar to reference cascade. There is possibility to change a channel geometry downstream of the passage, changing the setting angle of the tailboard. The following measurement

techniques were used in the experiments: schlieren and oil visualizations, static pressure measurement along the blade, PSP (Pressure Sensitive Paints), Flow Velocity distribution by means of LDA (Laser Doppler Anemometry).

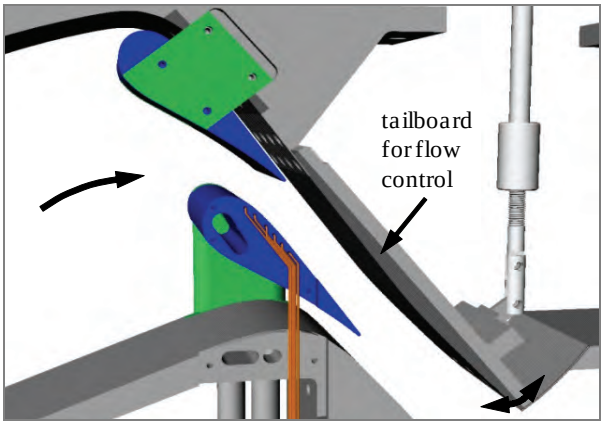

Fig. 1. Scheme of a model of a turbine passage

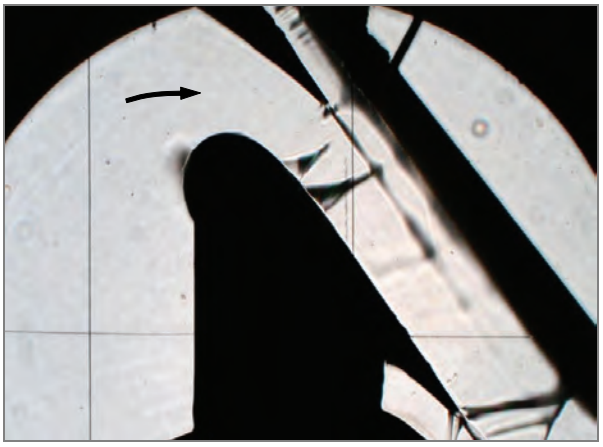

Fig. 2. Schlieren visualization for the clean flow

Schlieren visualization for clean flow case is shown in Fig. 2. This picture show that flow structure is very complex, the local supersonic flow is terminated by two shocks and the change of pressure is realized on relatively long distance. Many other interesting results were obtained from these experimental investigations showing how the blade cooling system influences on the laminar shock wave boundary layer interaction region and those results will be include in a full paper.

References

[1] SHAPIRO A.H., *The Dynamics and Thermodynamics of Compressible Fluid-Flow*, Vol. 2, The Roland Press Company, New York 1954.
[2] http://www.tfast.eu/

Near-blade flow structure modification

T. Kura, E. Fornalik-Wajs

AGH University of Science and Technology, Department of Fundamental Research
in Energy Engineering, al. Mickiewicza 30, 30-059 Kraków, Poland. E-mail: kura@agh.edu.pl

In this paper, the importance of near-blade flow structure influence on the performance of a centrifugal compressor was discussed. The negative effects of eddies appearance were described, together with the proposal of their reduction. Three-dimensional analyses were performed for single channel, focusing on the blade's 3D curvature impact on the efficiency. Proposed modification of blade shape changed the near-blade flow structure and improved the compressor performance.

1. Introduction

Turbomachinery is a field of research since the beginning of modern engineering. Experimental data is widely available, but the researchers are still trying to improve designs of particular units and to reduce negative effects of the swirls, circulations or secondary flows. Progress is possible thanks to CFD methods. Due to them influence of geometry on the flow can be checked with many shape factors which help to obtain flow structure for any examined model. Author has taken the advantage of CFD in [1], where the impact of blades' height, curvature and number on compressor's efficiency was investigated. Results confirmed, that leaks and backflows in compressor's area can cause significant pressure losses. Those backflows were mainly because of the blade-shroud clearance presence. Only a few articles from the last couple of years cover this topic [2], [3]. Moreover many of the equations proposed for evaluation of mentioned losses are empirical, and so they can be used only in particular cases. In following paper, Authors present characteristics of compression rate versus mass flow rate depending on a few geometry types as well as overall performance of proposed rotors.

2. Mathematical and theoretical model

The analyses were based on mass, momentum and energy conservation laws, coupled with an ideal gas law. Three-dimensional analyses were conducted with Ansys 14.5 software, particularly CFX and Turbogrid modules. Results were compared with those coming from theoretical considerations included in [4]. The concept of velocity triangles and Euler's turbomachinery equation were utilized:

$$l = i_2 - i_1 + 0.5(c_2^2 - c_1^2) \tag{1}$$

where: l is energy gained by 1 kg of fluid [J], i is enthalpy [J], c is absolute velocity [m/s], while indexes: 1 is inlet, 2 is outlet from rotor.

3. Analysed geometries

A few various geometries were studied, starting from typical radial compressor and finishing on centrifugal one. Main geometrical transformation was achieved through twisting of the blade, but other modifications were also done. The rotational speed and inlet conditions remained constant.

Results of simulation were compared with the analytical results for the same model. With approximately 1 300 000 elements, overall discrepancy of calculated results was no higher, than 4%, which was relatively good.

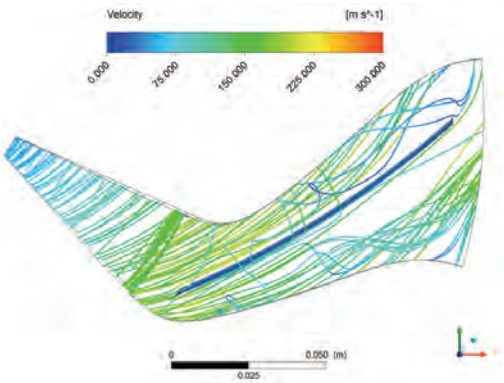

Fig. 1. Streamlines imaging flow eddies in blade-shroud tip, with tip height equal to $2 \cdot 10^{-3}$ m

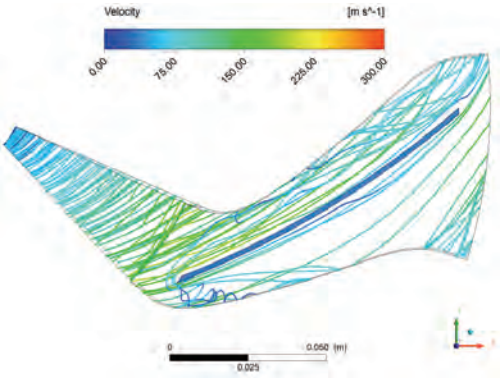

Fig. 2. One of proposed changes, reduction of eddies along blade

4. Results

The first analyzed blade design was basic, with curvature only towards flow direction. Blade-shroud tip clearance resulted in backflows and eddies, as shown in Figure 1. Further investigation and modifications led to reduction of those eddies (see Figure 2). Due to low temperature conditions, no material expansion occurred – so the proposed blade-shroud clearance size could be relatively low.

5. Conclusions

In the paper, the numerical and theoretical analyses of centrifugal compressor were described. The influence of secondary flow on the compressor's performance was presented, for various geometries. Final design proposition led to increase of compressor's total pressure ratio up to 6% and change of isentropic efficiency.

Acknowledgements

The present work was supported by Academic Computer Centre CYFRONET AGH, under award no. MNiSW/IBM_BC_HS21/AGH/021/2015 and by the Polish Ministry of Science (Grant AGH No. 15.11.210.344).

References

[1] KURA T., *Numerical analysis of velocity and temperature fields of compressible fluid flowing through a rotor*, MSc Thesis, 2015 (in Polish).
[2] CHANGHEE K., HORIM L., JANGSIK Y., CHANGMIN S., Int. J. Refrigeration, 2016, DOI: 10.1016/j.ijrefrig.2015.11.008.
[3] SWAMY S.M., PANDURANGADU V., Int. J. of Research in Engineering and Technology, 2013, 2(9), 445.
[4] WITKOWSKI A., *Sprężarki wirnikowe Teoria, konstrukcja, eksploatacja*, Wyd. Pol. Śląskiej, 2013 (in Polish).

Impact of numerical method on a side jets formation in a round jet

K. Wawrzak, A. Boguslawski

Częstochowa University of Technology, Faculty of Mechanical Engineering and Computer Science,
Al. Armii Krajowej 21, 42-201 Częstochowa, Poland. E-mail: wawrzak@imc.pcz.czest.pl

Numerical analysis of a formation of side jets in an externally modulated round jet is presented. The research is performed applying Large Eddy Simulation method and high-order codes based on Cartesian and cylindrical coordinates. The main attention is paid to impact of numerical approach on the formation of the side jets, their number and localisation. The results obtained suggest that on Cartesian meshes the number and directions of the side jets are dependent on the distribution of the mesh nodes.

1. Introduction

Contemporary Computational Fluid Dynamics (CFD) offers a wide range of numerical methods, which are capable to predict complex phenomena occurring in fluid flows with very high accuracy. From the point of view of data validation, knowledge on how a numerical approach influences the physics of the flows and how to exclude such an artificial impact seems to be crucial issues. The present work focuses on Large Eddy Simulation (LES) of an externally excited round jet. A particular attention is devoted to the impact of the numerical approach on the physics of a flow and a possible formation of the side jets. The side jets were observed experimentally in a globally unstable and externally modulated round jet, where very strong vortical structures appeared in the near field of the jet as streams released from the jet at some angle inclined to the jet axis [1–2]. Monkewitz et al. [2] claimed that the primary mechanism of formation of the side jets is an azimuthal instability of the vortical structures, which causes a deformation of vortices. However, a complete mechanism driving this phenomenon is not fully understood so far and needs further analyses. Numerical studies could help to explain and understand this problem but it turns out that the formation of the side jets is very sensitive to even very small disturbances, e.g., errors originating from discretization. Hence, at first a deep and detailed numerical analysis concerning applied numerical approaches need be performed. In this work we compare the results obtained using two different numerical algorithms, the first one is based on the Cartesian mesh and the second one the cylindrical coordinate system.

1.1. Cartesian coordinate system

An incompressible flow problem with the governing equations expressed in Cartesian coordinates is considered. The computations are performed using a high-order solution algorithm based on the projection method for pressure–velocity coupling and a half-staggered mesh arrangement. The time integration is performed by a predictor–corrector (Adams–Bashfort/Adams–Moulton) method and the spatial discretisation is based on 6th order compact difference scheme. The code used in this study was previously verified in isothermal, non-isothermal and exited jets and was precisely described in [3].

1.2. Cylindrical coordinate system

The application of the cylindrical coordinate system for the Navier–Stokes equations introduces the singularity at the polar axis which is due to presence of terms involving the expression $1/r$ where r – radial distance. Moreover, a definition of the computational domain as $(0.2\pi) \times (0, R)$ forces to specify the boundary conditions at $r = 0$, even if there is no physical boundary

at the polar axis. In order to avoid these problems the solution algorithm was formulated applying a coordinate transformation from $(0.2\pi) \times (0, R)$ to $(0.2\pi) \times (-R, R)$ and a series expansion of the Navier–Stokes equations at $r = 0$ [4]. The time integration is performed using a low storage Runge–Kutta method and the spatial discretisation is based on the half-staggered compact difference scheme for the radial and axial directions and the Fourier spectral method for the azimuthal direction.

1.3. Initial conditions

Apart of assessment of the impact of numerical approach on the side jets formation we also analyse their dependence on the boundary conditions. To generate significantly different inlet conditions we apply an externally modulated forcing with a wide range of turbulent intensity $Ti = 0.01\%U_j - 1\%U_j$, amplitude of the excitation $A = 1\%U_j - 10\%U_j$ and frequencies characterized by the Strouhal number $St = 0.4 - 0.6$, where U_j – the jet centreline velocity.

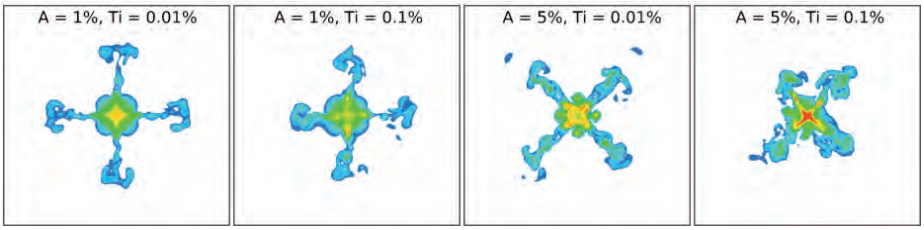

Fig. 1. Axial velocity contours for different initial conditions

2. Results and discussion

Instantaneous velocity contours in a cross-section perpendicular to the jet axis at the distance $y = 8D$ (D – nozzle diameter) from the inflow plane are presented in Fig. 1. These results were obtained using the code based on the Cartesian mesh. Despite the fact that various excitation amplitude and turbulent intensity at the jet nozzle were applied it is seen that the number of side jets does not change. There are always four side jets equally spaced in the azimuthal direction. However, the amplitude of the excitation affects the azimuthal location where the side jets occur. For the case with $A = 1\%\ U_j$ they appear along the mesh line orientation, whereas for the case with $A = 5\%\ U_j$ they lie inline with the diagonal direction of the computational domain. The physical mechanism leading to the formation of side jets seems to be reflected accurately, but the number and direction at which they appear seem to be determined by the Cartesian mesh. In this work we will verify this supposition. We will use a numerical code based on cylindrical coordinate system in which any artificial mesh related disturbances are excluded, by definition.

References

[1] RAGHU S. et al., Proc. 3rd European Turbulence Conference, 1990, 221–226.
[2] MONKEWITZ P.A. et al., Phys. Fluids A, 1989, 1, 446.
[3] TYLISZCZAK A., J. Comp. Phys., 2014, 276, 438–467.
[4] CONSTANTINESCU G.S., LELE S.K., J. Comp. Phys., 2002, 183, 165–186.

High-order hybrid grid generation for simulation of high-Reynolds number flows

P. Szałtys, J. Majewski

Institute of Aeronautics and Applied Mechanics, Warsaw University of Technology,
ul. Nowowiejska 27, 00-665 Warszawa, Poland. E-mail: pszaltys@meil.pw.edu.pl

One of the topic which recently receives much attention in CFD community is related to the high-order (HO) flow simulation. Still an important factor limiting wider application of HO methods is the lack of robust HO mesh generation methods. This is especially true in the case of turbulent RANS simulations, where high resolution of the boundary layer (BL) is necessary. In this paper authors present an approach to the problem of HO hybrid grid generation, which is focused on creation of valid, thin and curved elements, present in BL region.

1. Introduction

In the standard approach, the generator first creates a linear grid, next the grid is enriched by adding new internal HO nodes. Finally such a grid is deformed to conform to the curvilinear boundary [1]. The current algorithm consists of two phases: generation of structured BL grid and second, filling remaining space with unstructured grid. Important modification related to the standard approach lies in the creation of the BL grid. This grid possess the same number of DOFs as the final HO BL grid, or in other words, it corresponds to the grid subdivided into HO sub-cells. Thanks to this approach, the thin structured cells in the BL already fits well to the curved boundary surface. Deformation is only applied to the unstructured grid which is used to fill remaining space. Since the cells outside the BL are significantly less stretched then inside the BL, such process becomes more robust then standard one.

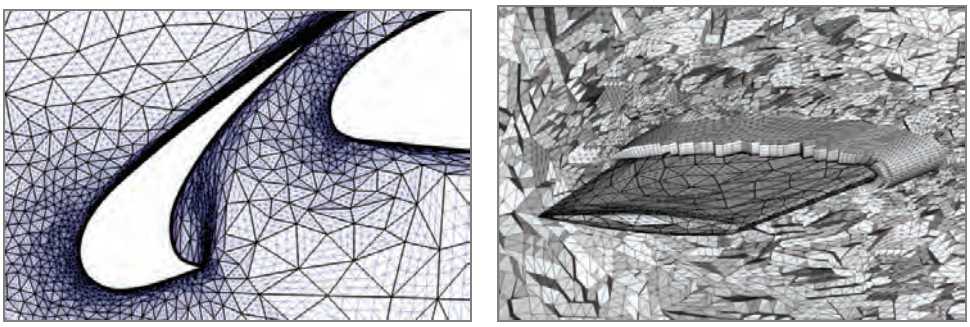

Fig. 1. Examples of high-order hybrid grids for L1T2 airfoil 2D (left) and Onera m6 wing 3D (right)

2. Numerical results

HO order grids generated using presented approach for 2D and 3D testcases (e.g., Onera M6 wing) will be shown together with simulations obtained using the HO solver PADGE developed in DLR [2]. The presented work is continuation of the work started in the frame of the IDIHOM project [3].

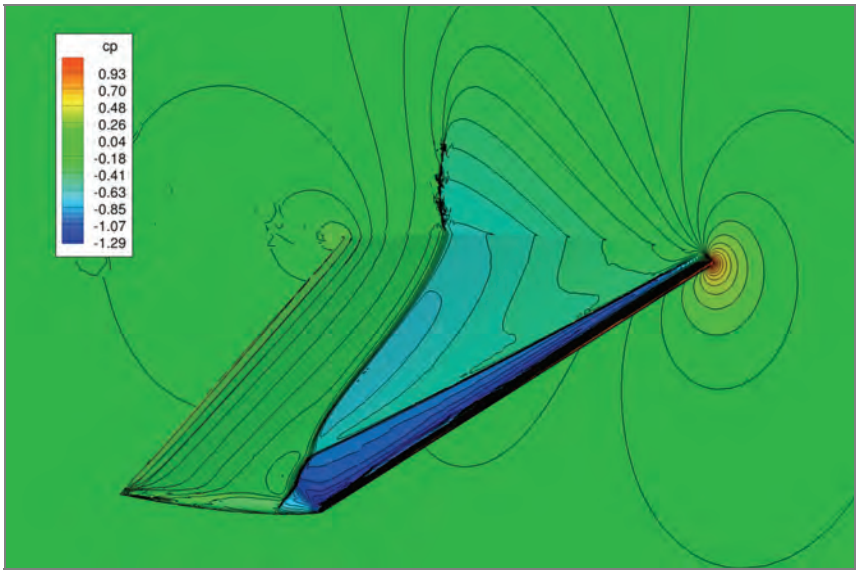

Fig. 2. Pressure coefficient for Onera m6 wing,
third order solution computed with P2 hybrid grid

References

[1] PERSSON P.O., PERAIRE J., *Curved mesh generation and mesh refinement using Lagrangian solid mechanics*, Proc. of the 47th AIAA Aerospace Sciences Meeting and Exhibit, 2009.

[2] HARTMANN R., HELD J., LEICHT T., PRILL F., *Discontinuous Galerkin methods for computational aerodynamics – 3D adaptive flow simulation with the DLR PADGE code*, Aerospace Science and Technology, 2010, 14, 512–519.

[3] KROLL N., HIRSCH C., BASSI F., JOHNSTON C., HILLEWAERT K. (eds.), *IDIHOM – Industrialization of High-Order Methods – A Top Down Approach*, Vol. 128 of Notes on Numerical Fluid Mechanics and Multidisciplinary Design, Springer 2015.

Numerical investigations of flow structure in gas turbine shroud gap

F. Wasilczuk[1,2], P. Flaszyński[1]

[1] Institute of Fluid-Flow Machinery, Polish Academy of Sciences,
Fiszera 14, 80-952 Gdańsk, Poland
[2] Interdepartmental PhD Studies at the Gdańsk University of Technology,
Narutowicza 11/12 80–233 Gdańsk, Poland. E-mail: fwasilczuk@imp.gda.pl

Labyrinth seals are popular mean to decrease the leakage flow in gas turbines. As the first step of the investigations the numerical simulation of the flow through the inter-shroud gap was performed using rotating porous disc instead of turbine blades cascade for simplicity. The results show the pressure drop on each of the fins of the labyrinth. Moreover vortical structure is analysed inside the inter-shroud cavity.

1. Introduction

The use of shrouded blades with the labyrinth seal is one of the most effective ways to combat the excessive tip leakage flow. However such configuration is still not perfect, and can be further improved with flow control techniques. In order to implement them successfully, one must know the detailed structure of the flow in the labyrinth seal to use the appropriate technique in the right location. Therefore, the aim of this study was to perform numerical calculation on the flow in the labyrinth seal and investigate its structure [1, 2, 3].

2. Model

Simplified labyrinth model was used in an investigation. The model was based on an actual labyrinth seal of a high pressure turbine. The ultimate, long term goal of the study is to implement the flow control techniques to influence the mass flow through the shroud gap. Thus, in order to make both numerical calculations and experiment easier, certain simplifications were performed.

Firstly, one of three fins was omitted. Secondly, all curvatures were appropriately replaced with flat surfaces and straight edges. The final approximation was replacing the blade cascade with a rotating porous disc. It allows the bulk flow to pass through, but also provides pressure drop, so part of the fluid is inclined to go through the gap. The pressure drop can be regulated with porosity parameters. Obviously, such model lacks the unsteady periodic effects of a real turbine cascade, but in return offers simplicity of modelling. The whole cross section of the investigated model is presented on Fig. 1. The model was used to perform numerical simulations utilizing Fine/Turbo software.

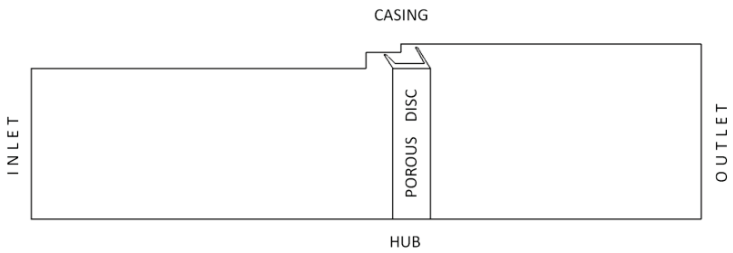

Fig. 1. Model used for calculations of gap flow

3. Results

The porous disc model proved useful for the intended task. It directed part of the flow to the gap, but let the most of the mass flow through. Moreover the pressure drop was obtained. Fig. 2 shows the pressure contour in the labyrinth seal. On the bottom, the pressure drop across the disc can be observed. Furthermore, the pressure drop on each fin is visible, as well as the regions of low pressure close to the edges of the fins, indicating the separation.

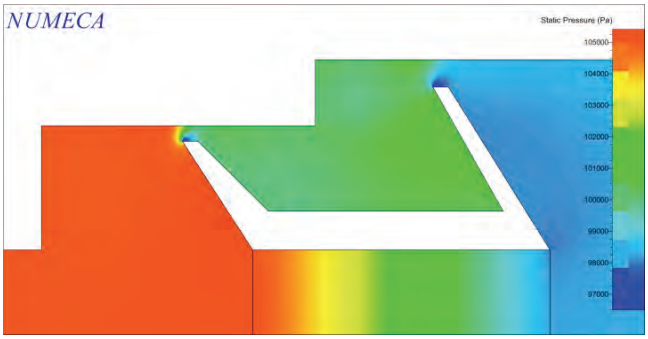

Fig. 2. Pressure contour of the gap flow

The 2-D projection of the streamlines in the labyrinth seal is presented on Fig. 3. One can notice three vortices forming inside the gap, one larger and one smaller in the space between the fins, and one in corner of the casing. In three dimensions those vortices run in the labyrinth seal along the tangential direction, as the seal rotates with the disc.

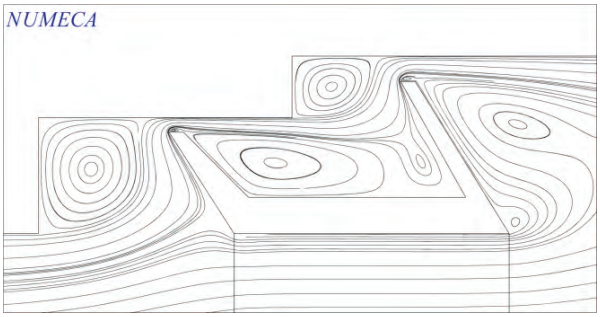

Fig. 3. Streamlines in a gap

The results give an insight into the structure of the leakage flow in an inter-shroud gap. The model can be used as a reference case for the further study on a flow control methods that can be utilized to reduce the mass flow through the gap.

References

[1] LAMPART P., Task Quarterly, 2006, 10, No 2, 139–175.
[2] PFAU A., SCHLIENGER J., RUSCH D., KALFAS A.I., ABHARI R.S., J. Turbomach., 2003, 127(4), 679–688.
[3] PFAU A., TREIBER M., SELL M., GYARMATHY G., J. Turbomach., 2000, 123(2), 342–352.

Analysis of water management at a closed cooling system of a power plant

P. Regucki[1], B. Engler[1], Z. Szeliga[2]

[1] Wrocław University of Technology, Faculty of Mechanical and Power Engineering, Wybrzeże Wyspiańskiego 27, 50-370 Wrocław, Poland
[2] VSB — Technical University of Ostrava, Faculty of Mechanical Engineering, Department of Energy Engineering, 17. listopadu 15/2172, 708 33 Ostrava-Poruba, Czech Republic
E-mail: Barbara.Engler@pwr.edu.pl

The paper presents a mathematical model describing the changes in SO_4^{2-} concentration in a closed system of cooling water circulation in a professional power plant due to the new restrictions posed on industrial emissions by EU and national regulations [1]. Analyzing the behavior of the numerical solutions of the model Authors could determine the optimal volumetric flow rate of wastewater depending on the current configuration of operating power units in a professional power plant.

1. Introduction

The paper presents a mathematical model describing the changes in SO_4^{2-} concentration in a closed system of cooling water circulation in a professional power plant. The analyzed installation consists of: condensers and cooling towers connected by a system of channels. At first, circulating water is heated in the condenser due to condensation of a spent steam from the last stage of the turbine, and next cooled down in the cooling tower. The main mechanism of heat transfer in the cooling tower base on partial evaporation of water, resulting in the increase of concentration of chemical components in the circulating water. This is the unfavorable effect because an excessive increase in the SO_4^{2-} concentration in the system may cause corrosion of the concrete parts of the channels and cooling towers. The only mechanism to decrease concentration of undesirable chemicals in the circulating water is its periodic discharge to the sewage treatment plant. According to the latest Polish government regulations; Regulation of the Minister of Environment dated 18 November 2014 and the Directive of the European Parliament and of the Council 2010/75/EU of 24 November 2010 on industrial emissions [1], from the beginning of 2016 the new limits on the chemical components of a wastewater led to the natural tanks has been accepted what forced planned and cost-effective water treatment in a professional power plants.

2. Mathematical model

Presented mathematical model enables the prediction of the daily increase in the concentration of sulfate ions SO_4^{2-} in the closed cooling water system and determines the optimal volumetric flow rate of wastewater due to the current configuration of operating power units in a professional power plant.

Balancing the SO_4^{2-} ion concentration change in the cooling system the following processes were taking into account: evaporation of water in cooling towers, $q_{v,ct}$, discharge of wastewater to the sewage treatment plant, $q_{v,dw}$ and refilling of fresh water, $q_{v,fw}$. Assuming that the total volume of cooling water V circulating in the system is constant, the change of the current SO_4^{2-} ion concentration $x(t)$ is described by the differential equation (where x_{ct} – SO_4^{2-} ion concen-

tration in water vapour released in cooling tower, x_{fw} – SO_4^{2-} ion concentration in fresh water delivered to the system):

$$V \cdot \frac{d\,x(t)}{dt} = -\,q_{v,dw} \cdot x(t) - q_{v,ct} \cdot x_{ct} + q_{v,fw} \cdot x_{fw} \tag{1}$$

3. Results and comments

Figure 1 presents the different numerical solutions of (1) parametrized by volumetric flow rate of wastewater discharge $q_{v,dw}$ to the sewage treatment plant. Green line indicates a maximum value of SO_4^{2-} concentration in water sewage accepted by EU and national law [1]. This limit may be exceeded if the volumetric flow rate $q_{v,dw}$ will be too small what shows the blue line increasing between 0 and 22 or 42 and 52 days respectively.

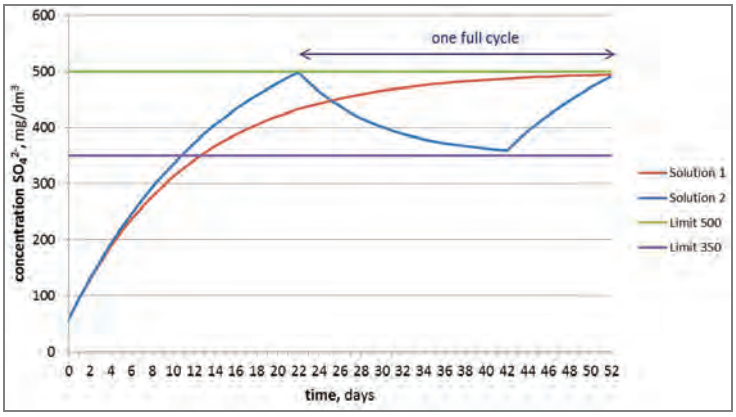

Fig. 1. Example of the numerical calculations presented different solutions of the mathematical model (1)

Analyzing the behavior of the numerical solutions of (1) Authors could determine the optimal volumetric flow rate of wastewater $q_{v,dw}$ due to the current configuration of operating power units in a professional power plant. This knowledge helps operators and decision makers to lead a planned and cost-effective water treatment management in power plants.

References

[1] Council Directive 91/271/EEC of 21 May 1991. Urban Waste Water Treatment (Acts. Office. EC L 135, 05.30.1991, p. 40, as amended. d.; Acts. Office. Polish special edition, ch. 15, v. 2, p. 26), the Directive of the European Parliament and of the Council 2010/75/EU of 24 November 2010 on industrial emissions (integrated pollution prevention and control) (recast) (OJ. office . EC L 334, 17.12.2010, p. 17, as amended. d.

A study of geometrical structure of packed beds using flow simulation with the immersed boundary method

M. Marek

Częstochowa University of Technology, Faculty of Mechanical Engineering and Computer Science,
Institute of Thermal Machinery, Al. Armii Krajowej 21, 42-200 Częstochowa, Poland
E-mail: marekm@imc.pcz.czest.pl

Tortuosity is a geometrical parameter characterising random packed beds and is related to average length of a path followed by a fluid particle in a complex geometry in comparison with such a path in free space. The immersed boundary method is used for simulation of fluid flow through a random packed bed of rings and spheres. Tortuosity is estimated using the obtained flow velocity in two ways: 1) advection of massless particles, 2) directly from velocity components using averaging procedure.

1. Introduction

Random packed beds of various particles are often employed in many areas, e.g., as a porous medium of a large specific surface enhancing the contact between reacting substances. The permeability of such a medium is related to its void fraction (porosity), ratio of volume of empty space to the volume of the whole bed, but also depends on other geometrical parameters like tortuosity. When a fluid flows through a porous medium, the path followed by a fluid particle can be highly distorted and, therefore, the length of such a path is markedly longer then the straight line connecting the same endpoints. In the literature, there is a large number of approximate methods that allow for the estimation of tortuosity using only geometrical information about the bed structure. Some researchers attempted to derive a formula relating porosity to tortuosity, at least for particular types of porous media. Such formulas typically have a rather limited range of validity.

In this work, a direct numerical simulation of a creeping fluid flow through a random packed bed is performed. Full information about flow velocity in the void space at the steady state is obtained and can be used further for calculation of tortuosity either by advection of massless particles (length of their pathlines is found) or by application of a much simpler method proposed by Duda et al. [1]. In the latter approach, the tortuosity can be estimated by the ratio of average flow velocity magnitude to the average value of the streamwise component – the advantage here is that the tortuosity is found directly from the velocity field.

2. Description of the method

The idea of the method is to use a Navier-Stokes equations solver for incompressible flow on structured grids and treat the highly complex domain geometry with the immersed boundary method. In consequence, the flow equations are solved efficiently and it is not necessary to generate a complex computational mesh fitted to the bed particles. The details of the method are described in [2].

The geometry of the bed is obtained in a separate simulation in which particles are dropped one by one into a cylindrical container and move until mechanical equilibrium is reached. This DEM (Discrete Element Method) approach is a slight modification of the method presented in [3].

The fluid enters the container at the top with uniform velocity profile. No-slip boundary conditions are enforced on the container walls and particles' surface. When the steady state

flow velocity field **u**(**r**) is obtained, the pathlines of massless particles are found by integration of equation:

$$\frac{d\mathbf{x}_p}{dt} = \mathbf{u}(\mathbf{r}) \tag{1}$$

Alternatively, the tortuosity T can be estimated as:

$$\mathrm{T} = \frac{\int_V u(\mathbf{r})dV}{\int_V u_y(\mathbf{r})dV} \tag{2}$$

where the integration is taken over the void space and u_y is the streamwise component of the velocity.

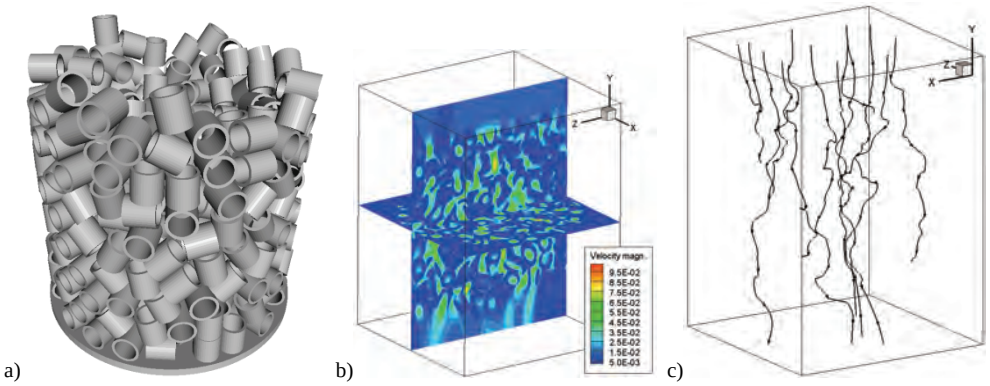

Fig. 1. Random packed bed of rings (a), flow velocity (b) and sample pathlines (c)

3. Sample results

In Fig. 1 sample results are presented concerning: a) bed of Raschig rings obtained in DEM simulation, b) flow velocity through a number of layers of rings taken from the middle part of this bed, c) a few pathlines starting from the top of the domain. In this case, the tortuosity calculated from equation (2) equals 1.23.

Acknowledgements

This work was supported by National Centre of Science, grant no.: DEC-2014/15/B/ST8/04762.

References

[1] DUDA A., KOZA Z., MATYKA M., Phys. Rev. E., 2011, 84, 036319.
[2] MAREK M., Journal of Physics: Conference Series, 2014, 530, 012016.
[3] MAREK M., Chem. Proc. Eng., 2013, 34(3), 347–359.

Particle-fluid interaction inside a beater mill

M.J. Marijnissen, J. Rojek

Institute of Fundamental Technological Research, Polish Academy of Sciences,
Pawińskiego 5b, 02-106 Warsaw, Poland. E-mail: mmarijn@ippt.pan.pl

In this work a trajectory study of copper ore particles through a fan mill was performed with the use of a commercial CFD code, ANSYS Fluent, coupled with DEM (Discrete Element Method). Particles of different sizes were analysed. Results highlight ore behaviour, fluid flow conditions and mark places requiring geometrical improvements.

1. Introduction

Particle-fluid interaction plays a grand role in high speed comminution of ore. Any improvements made into this process have an immense impact on cost reduction. Standard ball mills have been known to take up to 50% of the ore production process's energy requirement [1]. Fan mills on the other hand seem to compete in energy efficiency whilst achieving high internal fluid velocities due to a spinning flywheel with its axis of revolutions normal to the flow. After hitting the flywheel the particles are shed upward into a filter, where particles small enough are passed further on towards the next process. Particles considered too big are recirculated back onto the flywheel. The analysis of particle trajectories allows for insight in the current design of fan mills and provides ground for further improvements. With high internal flow velocities a particle-fluid coupling is required to simulate the appropriate behaviour of the ore. This was achieved with a CFD-DEM coupling which has been used in simulations and validations of particulate flow in a channel [2], fluidized beds [3] and slurry flow [4]. Additionally it has successfully been tested against analytic and experimental data [5].

2. Methodology

The fluid was considered compressible and the flow turbulent. Particle volume fraction were taken into consideration during calculations. Additional required equations of state, turbulence and energy are not presented here.

$$\frac{d\alpha_q\rho_q}{dt} + \nabla\cdot(\alpha_q\rho_q\vec{u}_q) = 0 \tag{1}$$

$$\frac{d\alpha_q\rho_q\vec{u}_q}{dt} + \nabla\cdot(\alpha_q\rho_q\vec{u}_q\vec{u}_q) = \alpha_q\rho_q\rho F_i - \alpha_q\nabla p_r + \nabla\cdot\bar{\tau}_q + \vec{F}_{add,q} \tag{2}$$

$$\frac{d\vec{u}_p}{dt} = \vec{F}_{drag}(\vec{u}-\vec{u}_p) + g\frac{\rho-\rho_p}{\rho_p} + \frac{\vec{F}_{add}}{\rho_p} \tag{3}$$

The equation of continuity and momentum conservation for multiphase flow are shown in (1), (2) while the governing equation for the particle's motion is presented in (3). In these equations α is the phasic volume fractions, $\vec{u}$ is the velocity of the fluid, g gravity, ρ density, p_r pressure and subscript p denotes the particle's equivalent while q denotes the equivalent for a particular phase. Moreover $\bar{\tau}$ is the stress tensor, $\vec{F}_{drag}$ is the approximated drag force and $\vec{F}_{add}$ represents additional forces (ex. contact, coupling, pressure gradient). A two-way CFD-DEM coupling was used.

3. Simulation

The flow calculations were conducted for the full mill. Afterwards boundary condition profiles were passes over to each individual subdomain and particles were added. This was made possible due to a modular geometry connected with interface surfaces. For any particular domain approximately 2000 particles of different size were studied, which were injected after the flow conditions stabilized. Figure 1 shows this for the flywheel domain during operation.

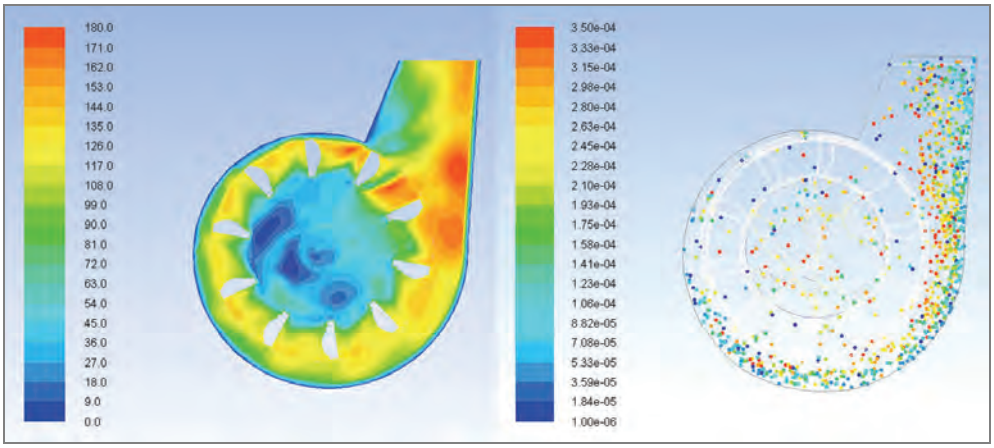

Fig. 1. Result obtained for flywheel domain, fluid velocity (left) [m/s], particles coloured by diameter (right) [m]

4. Results and major conclusions

- Particles tend to leave the flywheel domain with an outer side dominance.
- Bigger particles show a tendency to remain near the inner-middle side of the outlet.

Acknowledgements

The authors would like to acknowledge the financial support from the Polish NCBiR and KGHM granted upon the contract number CuBR/I/3/NCBR/2014.

References

[1] CLEARY P.W., *Predicting charge motion, power draw, segregation and wear in ball mills using discrete element methods*, Minerals Engineering, 1998, 11 (11).
[2] AZIMIAN M., LICHTI M., BART H.J., *Investigation of particulate flow in a channel by application of CFD, DEM and LDAPDA*, The Open Chemical Engineering Journal, 2014, 8, 1–11.
[3] YANG C., DUAN Y., *CFD-DEM model for simulating solid exchange in a dual-leg fluidized bed*, Chemical Engineering and Technology, 2013, 36 (11), 1907–1914.
[4] KUBICKI D., LO S., *Slurry transport in a pipeline Comparison of CFD and DEM models*, 9th International Conference on CFD in the Minerals and Process Industries, 10–12 December, 2012.
[5] KLOSS C., GONIVA C., HAGER A., AMBERGER S., PIRKER S., *Models, algorithms and validation for opensource DEM and CFD-DEM*, Progress in Computational Fluid Dynamics, 2013, 12 (2/3), 140–152.

Application of a single-fluid model for the steam condensing flow prediction

K. Smołka, S. Dykas, M. Majkut, M. Strozik

Silesian University of Technology, Institute of Power Engineering and Turbomachinery,
Konarskiego 18, 44-100 Gliwice, Poland. E-mail: Krystian.Smolka@polsl.pl

One of the results of many years of in-house research conducted in the Institute of Power Engineering and Turbomachinery of the Silesian University of Technology in Gliwice are computational algorithms for modelling steam flows with a non-equilibrium condensation process. In parallel with theoretical and numerical research, works were also started on experimental testing of the steam condensing flow. This paper presents a comparison of the flow field calculations performed by means of a single-fluid model using both an in-house code and the commercial Ansys CFX software package. Additionally, the calculation results are compared with those obtained from in-house experimental testing.

1. Introduction

First attempts to perform two-dimensional numerical modelling of steam flows with homogeneous condensation were made in Bakhtar and Tochai's work [1]. In the last few years a number of new publications concerning the flow of wet steam have appeared, which proves how topical the problem is worldwide. One of the results of many years of research conducted in the Institute of Power Engineering and Turbomachinery of the Silesian University of Technology are computational algorithms for modelling steam flows with a non-equilibrium condensation process [2]. The considered computational models either assume that droplets are small enough to omit the slip between the phases (single-fluid model) or the phenomenon of the slip between the gaseous and the liquid phase is taken into account by solving all conservation equations for the two phases separately (two-fluid model) [3]. In parallel with theoretical and numerical studies, works were also started in the Institute on experimental research on the steam condensing flow [4]. This paper presents a comparison of the flow field calculations performed by means of a single-fluid model using both the in-house TraCoFlow code and the commercial Ansys CFX v16.2 software package. Both codes use the same flow model, i.e., the model based on the Reynolds-averaged Navier-Stokes equations (the RANS model) supplemented with the steam model as specified in the IAPWS'97 standard, the same viscous turbulence model and the same condensation model based on the classical models of nucleation and droplet growth as described in [5] and [6], respectively. Additionally, the calculation results are compared with those obtained from in-house experimental testing performed for the blade channel and Laval nozzle.

2. Flow analysis

The focus of this work is an analysis of the flow field in the blade channel and in Laval nozzle. The blade channel, the experimental facility and the measurement system used in the experimental testing are described in detail in [4]. Laval nozzle was designed for the critical cross section $y^* = 0.04$ m and the outlet Mach number $Ma_1 = 1.8$. Fig. 1 presents an example comparison of pressure distributions obtained for the analysed geometries during the experiment and generated by numerical calculations performed using the in-house (TraCoFlow) and the commercial (Ansys CFX v16.2) codes.

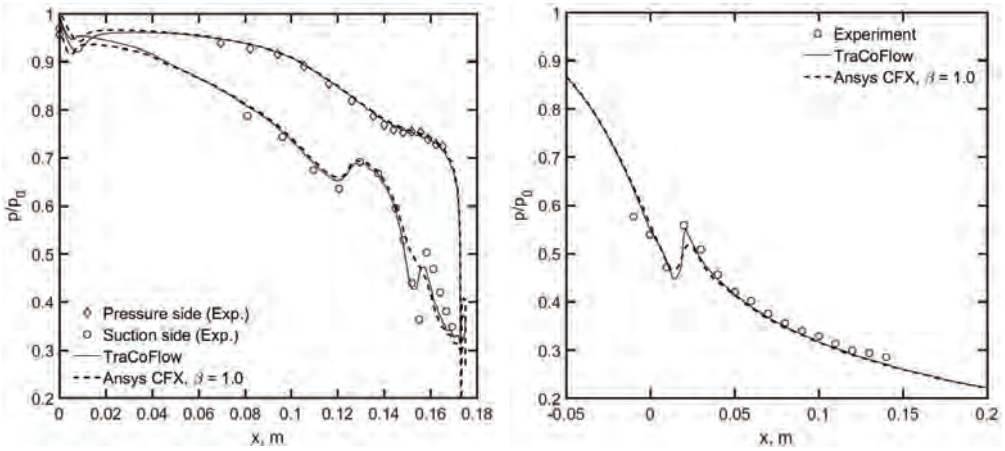

Fig. 1. Static pressure distribution on the blade surface (left) and along the nozzle (right)

3. Conclusions

Comparing the calculation results obtained using the in-house code and the Ansys CFX software with the results of the experiment, it can be noticed that both TracCoFlow and Ansys CFX v16.2 give qualitatively similar results. Among others, they model the location of the condensation wave occurrence correctly. However, quantitative differences can be noticed between the results despite the fact that for both codes identical numerical meshes were used and the same flow and condensation models were applied. Moreover, the same IAPWS'IF97 standard was used for both numerical codes to describe the properties of steam. In order to make a quantitative assessment of the calculation results, distributions of the main parameters of the wet steam flow were compared and a comparison was also made between the results obtained from the experiment and the calculations.

Acknowledgements

The presented work was supported by the Polish National Science Centre with funds within Project UMO-2014/15/B/ST8/00203.

References

[1] BAKHTAR F., MOHAMMADI TOCHAI M.T., *An Investigation of Two-Dimensional Flows of Nucleating and Wet Steam by the Time-Marching Method*, International Journal of Heat and Fluid Flow, 1980, 2(1), 5–18.
[2] WRÓBLEWSKI W., DYKAS S., GEPERT A., *Steam Condensing Flow Modelling in Turbine Channels*, International Journal of Multiphase Flow, 2009, 35(6), 498–506.
[3] DYKAS S., WRÓBLEWSKI W., *Single- and two-fluid models for steam condensing flow modelling*, International Journal of Multiphase Flow, 2011, 37(9), 1245–1253.
[4] DYKAS S., MAJKUT M., STROZIK M., SMOŁKA K., *Experimental study of condensing steam flow in nozzles and linear blade cascade*, International Journal of Heat and Mass Transfer, 2015, 80, 50–57.
[5] FRENKEL J., *Kinetic Theory of Liquids*, Dover Publications Inc., New York 1955.
[6] GYARMATHY G., *Grunglagen einer Theorie der Nassdampfturbine*, Juris Verlag, Zürich 1960.

Modelling of wet fumes condensation process in industrial stacks

P. Konderla[1], K. Patralski[2], J. Lewandowski[1]

[1] Wrocław University of Technology, Faculty of Civil Engineering,
pl. Grunwaldzki 11, 50-377 Wrocław, Poland
[2] Wrocław University of Technology, Faculty of Mechanical Engineering,
Łukasiewicza 5–7, 50-370 Wrocław, Poland. E-mail: Krzysztof.Patralski@pwr.edu.pl

The paper contains numerical analysis of the condensation process in industrial stack. The analysis was carried out for two models which differ by flue inlet geometry. The results show the character of flow and condensate quantity comparison.

1. Introduction

Carbon power plant are obliged by environmental regulations to desulphurize emitted fumes. If Wet Flue Gas Desulphurization installations are applied, physical parameters of the fumes are disadvantageous and fumes condensation on stack walls occur. It leads to two unfavorable effects: wet stack corrosion and pollution of environment by the condensate whose droplets are taken up by the gas stream and spread outside.

For these reasons additional precautions are used separate condenser installation before the flue inlet, proper shaping of stack geometry, particularly installation of the inner slide enforcing a way of gas flow (among other things, it should decrease gas velocity and therefore amount of condensate which is thrown outside) and incorporation of liquid collectors and drains to remove liquid from the duct [1].

In this paper two flue inlet geometries were discussed and analyzed to predict the gas flow and condensation process in the stack and to propose the technical solution which would decrease amount of the condensate.

2. Models of fumes flow and condensation

The analyzed problem is complex and it requires to consider following processes: gas flow in the stack (gas thermodynamics), gas condensation on the stack walls (mass transport) and movement of liquid films and droplets along the wall because of gravity and gas-drag forces and droplets transport (multi-phase flow).

In article [2] results of numerical analyses of thermodynamic gas flow were shown for different stacks' geometries. It is possible to predict intensive condensation zones and consequently to design a proper collectors and drains system. However, this model describes the condensation only in a qualitative but not quantitative manner.

A model describing all three mentioned processes would give more accurate base for design. It is possible but currently ineffective because there is no software allowing to involve such a model. Building of own algorithms is very effective and it seems practical to develop a proper model.

In this paper the authors propose to include not only gas thermodynamics but also condensation process with the assumption of complete condensate absorption by the wall.

3. Numerical analyses of fumes flow and condensation

Two stacks geometries were analyzed The models differ only by flue inlet geometry. Such a model imitates an installation of the slide in a real stack. The slide forces less dissipative rotational gas flow.

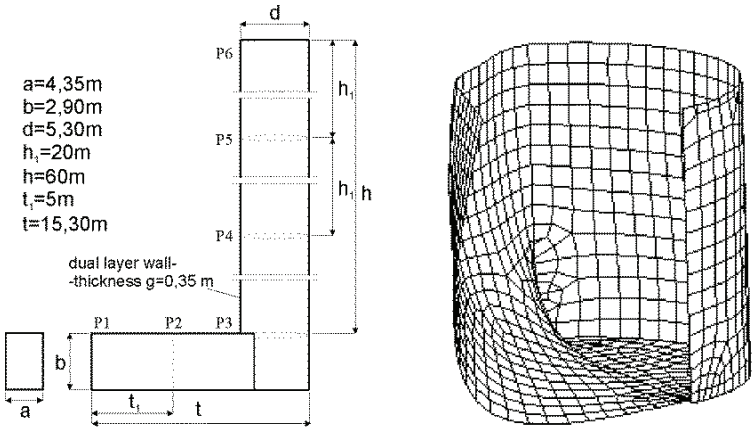

Fig. 1.The geometry of the stack and the part of the second model

For both models same boundary and initial conditions were assumed: outer temperature 10 °C, fumes temperature 60 °C, inlet gas velocity 17m/s, pressure on the outlet 1013 hPa. The gas was defined as a mixture of air (75%) and steam (25%). This data and the stack geometry correspond to real approximate parameters measured for the stack in Turów power plant.

In model 1, the fumes stream is centrally directed from the inlet and it hits the stack wall dividing into two symmetrical streams (2a, P3). In P4 section, irregular flow with two whirl structures is observed. In model 2, due to the slide installation, the fumes stream divides into two parts – one hits the opposite wall (2b, P3) and the second begins its whirl-like movement. In P4 section one can observe the whirl flow of the fumes which central part oscillates around the axis of the duct. Also small parietal flow is noticed. The observations for other sections confirm the one-whirl structure which has the influence for the flow character in the whole stack.

Comparing model 2 to model 1, there is less decrease of average gas speed in respective stack sections. As the result of such a flow, the amount of condensate produced in model 2 is 11% lower than the amount in model 1.

4. Summary

The original achievement of the research is model selection for these processes, as well as creating the algorithm to determine distribution of the condensation intensity on the stack walls which allows to predict quantitatively the liquid film thickness and in future research – the film movement and its interaction with gas. Since there is a strong correlation between the film thickness and the vulnerability of condensate to be taken up by the gas stream, presented results have important practical meaning in terms of environment contamination.

References

[1] EPRI C. DENE, *Revised Wet Stack Design Guide*, Technical Report 2012, P. Alto.
[2] KASPRZAK T., KONDERLA P., PATRALSKI K., WAŚNIEWSKI G., *Modelowanie procesu odprowadzania mokrych spalin w kominach przemysłowych*, Materiały budowlane, 2015, 5/2014.

On the unsteady Reynolds thermal transpiration law

P. Ziółkowski, J. Badur

Energy Conversion Department, The Szewalski Institute of Fluid-Flow Machinery PAS-ci,
Fiszera 14, 18-231 Gdansk, Poland. E-mail: pziolkowski@imp.gda.pl

In the present paper, the phenomenon of unsteady Reynolds thermal transpiration flow is presented. The possible constitutive equations in the transpiration shell-like layer are studied analytically and numerically. There has been examined experimental case of helium flow from cold to hot reservoir in nanopipe.

1. Introduction

Since 1879, when Reynolds has discovered the phenomena of thermal transpiration which can be defined as the macroscopic movement induced in a rarefied gas by a wall temperature gradient. The thermal mobility force, responsible for thermal transpiration, can be classified as a typical Newtonian *vis impressa* which can be able to accelerate any massive substances along the wall [2]. Phenomenological models [3, 4] can be also fitted to thermal transpiration with slip-regime for high Knudsen numbers for the case of gas in highly rarefied conditions.

Note that the *thermal transpiration* is not any pure academic problem and it has been recently used to constructing of very fine MEMS devices. The increased pumping effect could be obtained by a steeper gradient of temperature, extending tube length or making stages of pumping. Other micro-devices which is based on both thermal transpiration and adherence slipping, called accommodation pumping is developed in nanotechnology [4].

2. The boundary forces

The boundary force, responsible for a so-called generalized slip can be separated on two contradictive components: surface friction and surface mobility: $\mathbf{f}_{\partial V} = \mathbf{f}_r + \mathbf{f}_m$. Both forces are the subject of constitutive modeling. For instance, the friction force possesses three known contributions: Duhem, Navier and du Buat [4]:

$$\mathbf{f}_r = \nu_0 (p - \varpi)\mathbf{e}_f + \nu(\mathbf{v} - \mathbf{v}_{wall}) + \nu_2 (\mathbf{v} - \mathbf{v}_{wall})\mathbf{e}_f \tag{1}$$

where slip versor is defined as: $\mathbf{e}_f = (\mathbf{v} - \mathbf{v}_{wall}) / |\mathbf{v} - \mathbf{v}_{wall}|$ and ν_0; ν; ν_2 are three friction coefficients [Duhem, Navier, du Buat, respectively] which dependent simultaneously from the material of fluid and solid surface. However the surface mobility forces, which act usually against a surface friction, describe surface contributions from a numerous transpiration phenomena [2]:

$$\mathbf{f}_m = -c_{mp}\mathrm{grad}_s(p - \varpi) - c_{m\theta}\mathrm{grad}_s(\theta) - c_{mN}\mathrm{grad}_s(N) - .... \tag{2}$$

which depends linearly on surface gradient of surface pressure, surface temperature and surface concentration. In particular, the main goal of the paper is to discuss only Reynolds' contributions to definition of surface mobility modeling ei; $-c_{m\theta}\mathrm{grad}_s\theta$.

3. Results and discussion

Rojas-Cárdenas et al. [5] have applied an original method for thermal transpiration induced mass flow rate measurements conducted via measuring *in situ* the pressure evolution in time at

both ends of the tube using two high-speed response pressure gauges. In the long circular cross-section glass (borosilicate) microtube $D = 2R = 490$ μm; $L = 3.053$ cm is connected to two reservoirs (Fig. 1): cold (no 1, environmental temperature) and hot (no 2, $\theta_2 = 80$ °C, heated by an internal heater) (Fig. 1).

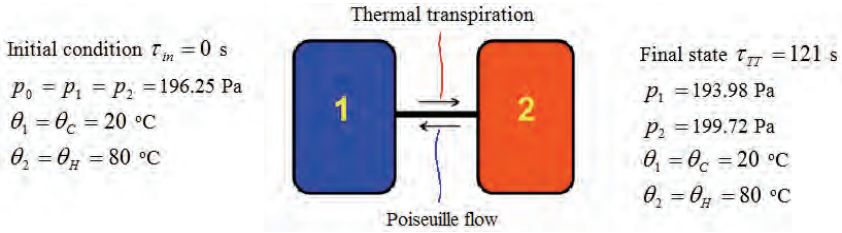

Fig. 1. Scheme of helium flow from cold (1) to hot (2) reservoir Rojas-Cárdenas et al. [5]

After opening a disconnecting valve the flow induced by thermal transpiration is simple – pressure in both reservoirs are equal and flow from cold to hot places is derived only by the wall mobility force (2), that depends on $c_{m\theta}$ value between glass and helium and the wall temperature gradient. The pressure in the cold decrease and at the hot palace increases (Fig. 2a). Now, there is a characteristic time τ_R where thermal transpiration forces achieve maximal value therefore mass flow rate attain pick (Fig. 2b). After that the Poiseuille flow governed by difference of pressure (Fig. 2a) is including, what leads finally, after time τ_{TT} to equilibrated state when the pressure difference arrives to its maximum and the resulting mass flow rate is zero. Therefore, at the stationary state achieves Poiseuille flow in the centre of channel and counter thermal transpiration flow on the surface (Fig. 2c).

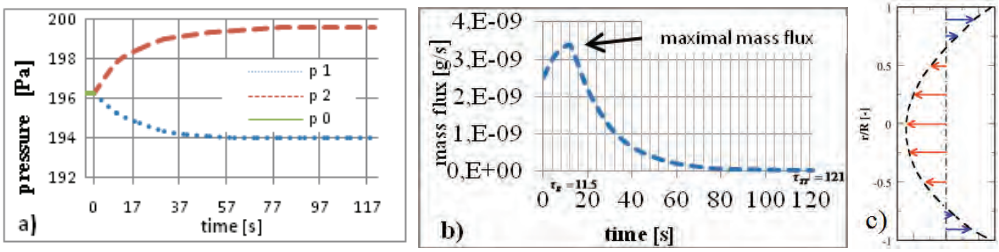

Fig. 2. Results of unsteady thermal transpiration modeling of the Rojas-Cárdenas et al. Benchmark experiment [5] with the thermal transpiration mobility force (eq. (2)):
a) plot of pressure change in (2) and (1) reservoir; b) the plot of mass flux c) stationary velocity profile

4. Conclusions

A numerical implementation of Reynolds model of thermal transpiration and its usefulness for description of an experiment by Rojas-Cárdenas et al. [5] have been performed.

References

[1] REYNOLDS O., Phil. Trans. Royal Society, London 1879, Vol. 170, 727–845.
[2] BADUR J., KARCZ M., LEMAŃSKI M., Microfluid Nanofluid, 2011, Vol. 11, 439.
[3] ZIÓŁKOWSKI P., BADUR J., Journal of Physics: Conference Series, 2014, 530, 1–8.
[4] BADUR J., ZIÓŁKOWSKI P.J., ZIÓŁKOWSKI P., Microfluid Nanofluid, 2015, Vol. 19, 191.
[5] ROJAS-CÁRDENAS M., GRAUR I., PERRIER P., MEOLANS J.G., Phys. Fluids, 2011, Vol. 25, 031702.

Momentum budget of the paramagnetic fluid flow influenced by magnetic force

L. Pleskacz, E. Fornalik-Wajs

Department of Fundamental Research in Energy Engineering,
AGH University of Science and Technology, al. Mickiewicza 30, 30-059 Kraków, Poland
E-mail: pleskacz@agh.edu.pl

The aim of presented analysis concentrated on the understanding of momentum transfer within the paramagnetic fluid flow influenced by the strong magnetic field. Since the changes of temperature and velocity fields were already discussed it is very important to know the mechanisms of phenomena. That is why this paper reported the momentum budget and presented the discussion on significance of its particular terms.

1. Introduction

All elements possesses magnetic properties and they can be divided into three groups: paramagnetics, diamagnetics and ferromagnetics. However, paramagnetics and diamagnetics show lesser magnetic effects than the ferromagnetics. The influence of magnetic field on ferrofluids was broadly discussed in the world's scientific papers. The opportunity to examine paramagnetic and diamagnetic fluids' flows in the magnetic field occurred in the 80's, when the superconducting magnets appeared. From that time the dynamic development of research concerning magnetic field impact on weakly magnetic substances was observed and the new discoveries were reported. From numerous examples the following were chosen: magnetic levitation of weakly magnetic substances and magnetic breath support [1], [2], because they consider moving medium similarly to the topic presented in this paper. The influence of strong magnetic field on natural convection was profoundly discussed numerically and experimentally, i.e., [3]–[5]. However, there were very few papers reporting the topic of weakly-magnetic fluid forced convection in the magnetic field. A gap in the major research direction was distinguished. A first attempt to this problem could be found in [6]. This work was continued by the Authors with the aim of understanding the flow behavior, heat transfer processes and possible future applications.

This paper presents the topic, which has not been previously examined. It concentrated on the detail analysis of momentum transfer in the paramagnetic fluid flow influenced by the strong magnetic field. For this purpose the momentum budget was calculated. The significance of particular terms was discussed.

2. Studied case

The considered case was the straight circular three-dimensional duct (pipe). The circular magnetic coil was placed perpendicularly to the pipe axis dividing it into two equal parts. Its centre was also the centre of the assumed coordinate system. The wall of the first part was adiabatic while the second one was isothermally heated. Parabolic velocity profile was assumed at the duct inlet and the constant value of pressure at its outlet. The analyzed fluid was air and its following properties were introduced in the calculations: density (1.225 kg/m^3), dynamics viscosity ($1.7894 \cdot 10^{-5}$ Pa·s), thermal expansion coefficient ($3.33 \cdot 10^{-3}$ K^{-1}), volumetric magnetic susceptibility ($3.77 \cdot 10^{-7}$ –), magnetic permeability ($4\pi \cdot 10^{-7}$ H/m), specific heat (1006.43 J/(kg·K)) and thermal conductivity ($2.42 \cdot 10^{-2}$ W/(m·K)).

3. Mathematical Model

The mathematical model consisted of three conservation equations: continuity, momentum and energy supplemented by Biot–Savart's law, which was utilized for calculation of magnetic field distribution. The momentum equation in general form can be written as follow:

$$\rho(\vec{u}\cdot\nabla\vec{u}) = -\nabla \mathrm{p} + \mu\nabla^2\vec{u} + \vec{F}_b, \tag{1}$$

where particular terms represent convection, pressure, diffusion and source terms, respectively. As the source terms the magnetic and gravitational buoyancy forces were introduced. The magnetic buoyancy force is represented by the formula:

$$\vec{F}_{mag} = -\left(1+\frac{1}{T_0\beta}\right)\frac{\chi_m\rho\beta(T-T_0)}{2\mu_m}\vec{\nabla}B^2 \tag{2}$$

where: $\vec{F}_{mag}$ is the magnetic force N/m^3, T_0 is the reference temperature K, β is the thermal expansion coefficient K^{-1}, χ_m is the mass magnetic susceptibility in the reference temperature m^3/kg, ρ is the density kg/m^3, T is the local fluid temperature K, μ_m is the magnetic permeability of the vacuum H/m, $\vec{B}$ is the magnetic induction vector T.

4. Results and Conclusions

The performed numerical analyses showed that the strong magnetic field (up to 10 T in the centre of the coil) could significantly influence the flow structure. This impact appeared in the form of maldistribution of temperature and velocity fields. In the case of velocity field the acceleration, deceleration and recirculation zones could be found (Fig. 1). Such changes of the flow structure are strongly connected with the momentum transfer and reorganization of momentum budget.

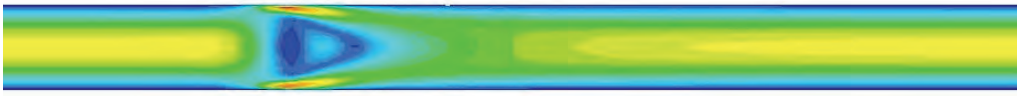

Fig. 1. Velocity field maldistribution for the paramagnetic fluid flow in the strong magnetic field

The performed numerical calculation of the momentum budget could precisely answer the question: which term the most significantly determined the momentum transfer.

Acknowledgment

The present work was supported by the Polish Ministry of Science (Grant AGH No. 15.11.210.327) and Academic Computer Centre CYFRONET AGH, under award no. MNiSW/IBM-BC-HS21/AGH/060/2013.

References

[1] IKEZOE Y., HIROTA N., NAKAGAWA J., KITAZAWA K., Nature, 1998, 393, 749.
[2] WAKAYAMA M., WAKAYAMA N.I., Jpn. J. App. Phys., 2000, 39, 262.
[3] BRAITHWAITE D., BEAUGNON E., TOURNIER R., Nature, 1991, 354, 134.
[4] BEDNARZ T., FORNALIK E., TAGAWA T., OZOE H., SZMYD J.S., Int. J. Therm. Sci., 2005, 44, 933.
[5] WRÓBEL W., FORNALIK-WAJS E., SZMYD J.S., Int. J. Heat Fluid Flow, 2010, 31, 1019.
[6] OZOE H., Magnetic Convection (London: Imperial College Press), 2005, 193.

LBM estimation of the thermal conductivity coefficient in a granular bed

A. Grucelski

Institute of Fluid-Flow Machinery Polish Academy of Sciences, ul. Fiszera 14, 80-231 Gdańsk, Poland
E-mail: agrucelski@imp.gda.pl

Recently, there is a growing engineering interest in more rigorous predictions of effective transport coefficients for multicomponent, geometrically complex materials. We present main assumptions and constituents of the meso-scale model for the simulation of the coal or biomass devolatilisation with the Lattice Boltzmann method. For the results, the estimated values of the thermal conductivity coefficient of a coal (solids), pyrolytic gases and air matrix are presented and compared with available models.

1. Introduction

Coking plants are widely used in coal processing industry to obtain chemically cleaner coal (coke) and other chemical species (generally known as a coal gas) as well as tar. Another motivation for the present study is the pyrolysis of biomass grains (particles) in a gasifiers. Although the process has been used for many years [1], a detailed description of phenomena is of a recent interest of researchers [2, 3, 4]. The number of factors affecting the progress and the final products of the process (type of coal/biomass, including heating rate, maximum temperature, etc.) makes it prohibitively difficult to provide a generalized description of the process unless a multilevel simulation technique is used. Aside of fluid flow and heat transfer in a granular medium, one has to account for chemical compounds release (by heterogeneous as well as homogeneous reactions) with additional shrinking (for biomass) or swelling (for coal) of grains. Facing the level below, meso- or macro-scale analysis has to be supported by the results of modelling at the single grain scale, with detailed description of the phenomena occurring at the micro level [2].

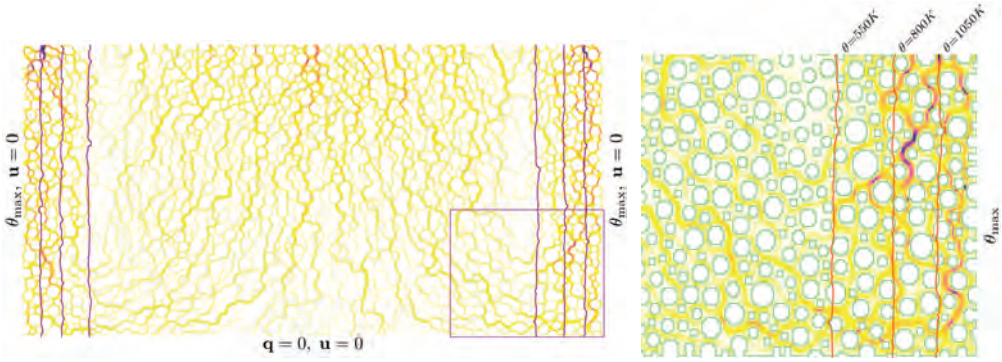

Fig. 1. Results of heat (isolines) and mass transfer (map of mean velocity) with zoomed part of the geometry with presented surface of the grain

One of the key quantities to describe heat transfer (and related phenomena like chemical species release and transport in fluid flow) is the effective heat conductivity coefficient. The rigorous prediction of this coefficient for various materials (mostly of complicated geometry) is of recent research interest [5]. The number of phenomena occurring during the coking process makes it difficult to measure heat conductivity. On the other hand, a physically-sound numerical simulation of the process at the meso-scale (randomly, densely packed bed of coal grains)

has recently become feasible thanks to developing of CFD tools and the increase of computational power. In the work, we present results of heat transfer in the densely packed bed of grains. In the simulation, phenomena of heat transfer (as heating at both sides of the domain), chemical species release (at the surface of grains) and fluid flow (triggered by released light gases and natural convection occurring in the heated volume in the gravity field) are modelled, see Fig. 1. Our longer-term objective is a physically-sound simulation of the coking process in the macroscale (unsteady, one- or two-dimensional formulation), cf. [3].

2. Simulation details

As a modelling approach, we have decided to use the Lattice Boltzmann Method (LBM) based on the Boltzmann equation with a subsequent discretization [6]. The method has proven suitable for simulation of viscous and nearly incompressible fluid flows in simple and complex geometries [7], as well as heat transfer, also with the addition of chemical reactions [8]. The method appears as a promising CFD tool for the multiphysics simulations in complex geometry.

In presented work, the LBM variant for the flow density and velocity is solved in terms of the density distribution function [9]. To account for natural convection, we use the Boussinesq approximation for LBM. The temperature field is found from the additional internal energy density distribution function (IEDDF) [10]. The reactive system is simplified with account to a single specie only (described as pyrolysis product) through the use of a separate distribution function. We present results from LBM modelling on a meso scale (the pore level description) of flow thermomechanics in a granular medium in a representative element of volume (REV) with grains represented by randomly generated circular cylinders.

In the geometry, we use coal grains with the mean diameter d = 3 mm (discretized by a few lattice nodes) in the part of the coking chamber with size $H \times W = 40 \times 80$ cm. The resulting porosity of the bed is $\varepsilon \in [0.45–0.5]$. The sides (see Fig. 1) of the numerical domain are linearly heated from the ambient temperature to $\theta_{max} = 1300$ K. At the bottom of the numerical domain we use the adiabatic condition; at the top boundary we apply the convective outlet condition. Because this is a first step of investigation, boundary condition can be modified to fit more accurately the REV. The no-slip condition is used at the solid-fluid interface. Thermal conductivity is calculated from the Fourier law $k_{eff} = L\int \mathbf{q}\cdot\mathbf{n}/\Delta\theta \int \mathrm{dA}$ where we track in a given time step a heat flux through a part of a domain ($\mathbf{q}\cdot\mathbf{n}|_{dA}$) and reference temperature difference $\Delta\theta$.

Full set of results will contain detailed analysis of the value of conductivity coefficient in a modelled area during the process (and triggered processes of natural convection and chemical compounds release).

References

[1] SERIO M.A., HAMBLEM D.G., MARKHAM J.R., SOLOMON P.R., Energy Fuels, 1987, 1, 138.
[2] LIU X., WANG G., PAN G., WEN Z., Fuel, 2013, 106 667.
[3] POLESEK-KARCZEWSKA S., KARDAŚ D., WARDACH-ŚWIĘCICKA I., GRUCELSKI A., STELMACH S., Arch. Thermodyn., 2013, 34, 39.
[4] MAFFEI T., FRASSOLDATI A., CUOCI A., RANZI E., FARAVELLI T., Proc. Combust. Inst., 2013, 34, 2401.
[5] THIELE A.M., KUMAR A., SANT G., PILON L., Int. J. Heat Mass Transfer, 2014, 73, 177.
[6] AIDUN C.K., CLAUSEN J.R., Annu. Rev. Fluid Mech., 2010, 42, 439.
[7] CHEN S., DOOLEN G.D., Annu. Rev. Fluid Mech., 1998, 30, 329.
[8] DI RIENZO A.F., ASINARI P., CHIAVAZZO E., PRASIANAKIS N.I., MANTZARAS J., EPL, 2012, 98, art. 34001.
[9] GRUCELSKI A., POZORSKI J., Comp. Fluids, 2013, 71,406.
[10] GRUCELSKI A., POZORSKI J., Int. J. Heat Mass Transf., 2015, 86,139.

Stability of flow in a corrugated channel

S. Gepner

Institute of Aeronautics and Applied Mechanics, Warsaw University of Technology,
Nowowiejska 24, 00-665 Warsaw, Poland
E-mail: sgepner@meil.pw.edu.pl

Flow in a corrugated channel has been studied. The analysis is carried out up to Reynolds numbers resulting in the formation of secondary states. The first part of the analysis is based on a two-dimensional model and demonstrates that reducing the corrugation wavelength results in the appearance of an unsteady separation. In the second part a three-dimensional model demonstrates that the flow dynamics are dominated by the centrifugal instability over a large range of geometric parameters, resulting in the formation of streamwise vortices.

1. Introduction

It is known that presence of grooves results in the appearance of two instability modes. The first one is the travelling wave mode [1] which, in the smooth channel limit, connects to the classical Tollmien-Schlichting (TS) wave. This mode is responsible for the transition from stationary to oscillatory states and, eventually, to aperiodic states [2]. The second mode has the form of streamwise vortices [3]. It is attributed to the centrifugal forces associated with the groove-imposed changes of the stream direction. This mode connects in the smooth channel limit to a Squire mode [3]. This instability becomes critical in channels with a certain class of grooves.

2. Problem specifcation

The main focus of this work is mapping of the dynamics of fow in a converging-diverging channel with the groove wave number varied from $\alpha = 10$ (short wavelength grooves) to $\alpha = 0.5$ (long wavelength grooves) which covers the full range of wavelengths of practical importance. The analysis is limited to moderate groove amplitudes, i.e., $S < 0.2$, and relies on DNS based on the spectral finite-element method in the (x, y)-plane combined with the Fourier decomposition in the spanwise direction, as implemented in NEKTAR++ [4].

The analysis is divided into two steps, with the first one focused on the two-dimensional dynamics and presenting flow properties up to the formation of secondary states. Issues of particular interest are the onset and growth of the separation zone (see Figure 1b, c), particularly the unsteady separation (Figure 1d) and the drag penalty associated with the grooves.

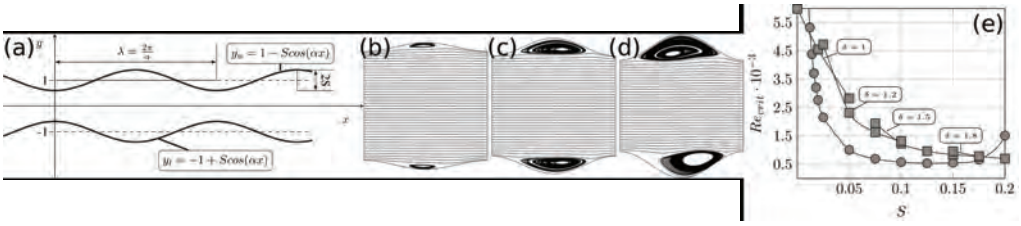

Fig. 1. Geometry of the channel (a). Development of the recirculation zone for $\alpha = 3$, $Re = 2300$, at corrugation amplitudes $S = 0.075$ (b), $S = 0.150$ (c) and $S = 0.225$ (d). Variation of critical the Reynolds number necessary for the onset of a 3D vortices and a competing 2D wave instability with various wavelengths δ as a function of the groove amplitude S for $\alpha = 3$

The second step involves analysis of three-dimensional dynamics and identification of conditions when it precedes the two-dimensional dynamics (see Figure 1e). Determination of conditions leading to the onset of streamwise vortices is of particular interest. The process of vortex creation can be interfered with by the travelling waves. It is thus important to establish conditions where such vortices are likely to dominate the system dynamics. Figure 1e displays variations of the critical Reynolds number as a function of the groove amplitude required for the onset of the travelling waves (of various wavelengths δ) and for the onset of the vortices for $\alpha = 3$. At small amplitudes it is the travelling wave that dominates having a smaller Re_{crit}. For both instabilities an initial monotonic decrease in Re_{crit} is observed as S increases, with the centrifugal instability quickly becoming dominant i.e. having smaller Re_{crit}. Further increase of S eventually reverses the character of variations of Re_{crit} for vortices with Re_{crit} increasing as growing recirculation prohibits the flow from producing enough of the centrifugal effect. As a result, the travelling wave becomes dominant again.

3. Conclusions

Both two- and three-dimensional flow dynamics at previously uninvestigated flow conditions have been studied. Formation of various possible secondary states has been considered, respective critical conditions have been determined and compared. Obtained results provide basis for the identification of the most effective geometric configuration for the generation of the vortices and possible application in designing efficient mixing devices operating at low Reynolds number regimes.

References

[1] FLORYAN J.M., FLORYAN C., *Travelling wave instability in a diverging-converging channel*, Fluid Dynamics Research, 2010, 42 (2).

[2] GUZMÁN A.M., AMON C.H., *Transition to chaos in converging-diverging channel fows: Ruelle-takens-newhouse scenario*, Physics of Fluids, 1994, 6 (6).

[3] FLORYAN J.M., *Vortex instability in a diverging-converging channel*, Journal of Fluid Mechanics, 2003, 482, 17–50.

[4] CANTWELL C.D., MOXEY D., COMERFORD A., BOLIS A., ROCCO G., MENGALDO G., GRAZIA D. DE, YAKOVLEV S., LOMBARD J.-E., EKELSCHOT D., JORDI B., XU H., MOHAMIED Y., ESKILSSON C., NELSON B., VOS P., BIOTTO C., KIRBY R.M., SHERWIN S.J., *Nektar++: An open-source spectral/ element framework*, Computer Physics Communications, 2015, 192, 205–219.

Streamwise vortex generator for separation reduction on wind turbine profile

J. Martinez Suarez, P. Flaszynski

Aerodynamics Department, The Szewalski Institute of Fluid-Flow Machinery (IMP PAN),
14 Fiszera Street, Gdańsk 80-231, Poland. E-mail: javier.martinez@imp.gda.pl

High angles of attack on the wind turbine blades induce severe flow conditions which lead to flow separation and, consequently, aerodynamic performance reduction. Implementation of Rod Vortex Generators (RVGs) on S809 wind turbine profile in order to control and decrease the flow separation is presented. Validation of the numerical model is carried out and the agreement with experimental data is satisfactory. A study of chordwise location and spanwise distribution of RVGs for different inflow conditions is performed. Applied RVGs provide an increased aerodynamic performance and reduction of flow separation.

1. Introduction

Large rotor dimensions of the modern wind turbines operate at non-uniform inflow conditions along the whole blade span, which usually leads to flow separation. In order to reduce the effect of the boundary layer separation flow control techniques are developed and implemented. Present study is focused on the investigation and application of a new type of VGs, called Rod Vortex Generators (RVGs) [1], on wind turbine profile. RVGs are defined by 5 parameters: diameter (D), height (h), skew angle (θ), pitch angle (α) and spacing (W) (Figure 1).

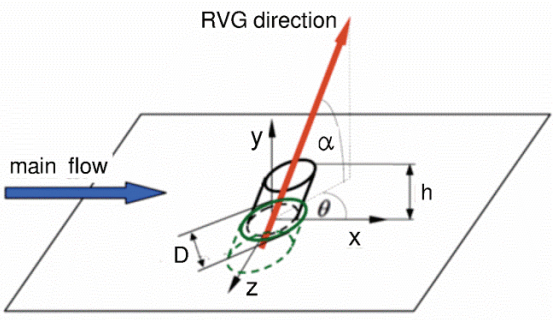

Fig. 1. Rod Vortex Generator configuration

2. Flow solver

The numerical simulations have been carried out by means of FINE^{TM}/Turbo Numeca. The compressible, mass-weighted equations are solved adopting a preconditioning scheme. From the different turbulence closures implemented in the code, the two-equation, low-Reynolds Explicit Algebraic Reynolds Stress Model (EARSM) was chosen [2]. Spatial discretization is based on a finite volume, 2nd order central difference scheme. A full multigrid technique is applied in order to increase the convergence rate.

3. The S809 aerofoil

Designed for wind turbines applications, the S809 aerofoil was chosen for research and it has been favorably validated against the experimental data of Somers [3] and Ramsay [4]. Nu-

merical predictions for the basic flow configuration have been applied to the Rod Vortex Generators dimensioning (h, D) and for the investigation of their chordwise location (x_{RVG}/c) and spanwise distribution (W/D).

Four high inflow angles (Angles of Attacks, AoA: 11.2º, 12.2º, 13.3º and 13.9º), five chordwise RVGs locations (x_{RVG}/c = 0.35, 0.40, 0.45, 0.50 and 0.55) and four spacing scenarios (W/D = 7.5, 10, 15 and 20 were taken into account for flow control investigations. RVGs were dimensioned in relation to the local boundary layer thickness at AoA = 13.9º, where the most severe conditions exist.

Implementation of these devices on the S809 profile results in reduction or even complete removal of the separation and increase of aerodynamic performance. Figure 2 depicts the skin friction coefficient contour maps on the S809 aerofoil suction side at AoA = 11.2º for the clean case and for a chordwise location of rods x_{RVG}/c = 0.50 and spacing between rods, W/D = 7.5. One can easily notice that the detached flow region presented in the clean case is removed.

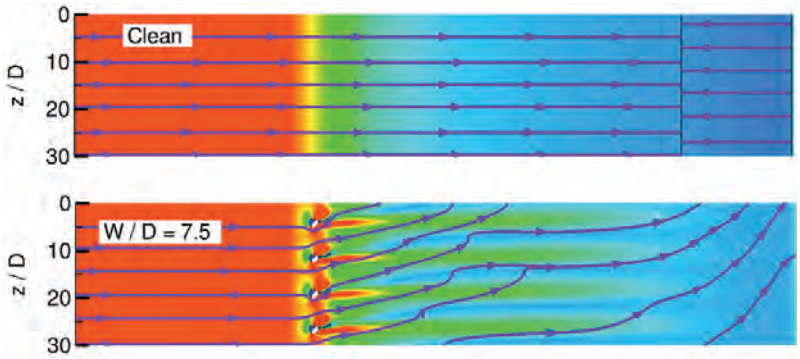

Fig. 2. Skin friction coefficient C_f and streamlines ($Re = 1 \cdot 10^6$, AoA = 11.2º)

References

[1] DOERFFER P., FLASZYNSKI P., SZWABA R., Polish Patent P.38968, 2009.
[2] MENTER F.R., GARBARUK A.V., EGOROV Y., Progress in Flight Physics, 2012, 3, 89–104.
[3] SOMERS D.M., *Design and experimental results for the S809 airfoil*, NREL Report: NREL/SR-440-6918, 1997.
[4] RAMSAY R.R., HOFFMAN M.J., GREGOREK G.M., *Effects of grit roughness and pitch oscillations on the S809 airfoil*, NREL Report: NREL/TP-442-7817, 1995.

Study of Reynolds number effect on turbulent boundary layer near the separation

A. Dróżdż, W. Elsner

Częstochowa University of Technology, Faculty of Mechanical Engineering and Computer Science,
ul. Armii Krajowej 21, 42-200 Częstochowa, Poland. E-mail: welsner@imc.pcz.czest.pl

The paper deals with the experimental analysis of strong decelerated turbulent boundary layer developed at the flat plate. The special design of the test section equipped with perforated, movable upper wall allow to generate on the bottom wall turbulent boundary layer, which is at the verge of separation. The objective of the work is to examine the effects of varying Reynolds number on non-equilibrium boundary layer and the emphasis is on the analysis of the streamwise Reynolds stress and mean velocity profiles.

1. Introduction

Although a significant amount of research has been devoted to understanding canonical flat plate zero pressure gradient boundary layer, it is not the case for adverse pressure gradient boundary layers and even more when the flow is approaching separation. The most common problem in the similarity analysis is the Reynolds number effect [1]. It is important due to nonlinear *Re* impact, what is seen by the rapid decrease of near wall viscous length scale and week variation of the outer length scale with Reynolds number. This is particularly important when trying to predict the separation location on curved surface with adverse pressure gradient (APG).

In the most available experimental research with APG flows there is a lack of canonical setup [2]. The current experiment was performed in an open-circuit wind tunnel, where the turbulent boundary layer developed along the flat plate, which is 7 m long. The special design of the test section equipped with perforated, movable upper wall allow to generate on the bottom wall the turbulent boundary layer, which is at the verge of separation. By playing with the shape and position of the upper wall as well the suction flux it is possible to generate wide range of pressure gradient conditions, while at the inlet channel the zero pressure gradient conditions were secured.

2. Results

Measurements were performed for three different Reynolds number and perfectly matched distributions of pressure coefficient $C_p = 1 - \left(\frac{U_\infty}{U_{\infty_0}}\right)^2$, where $U_{\infty 0}$ is the maximal mean velocity for inlet zero pressure gradient conditions. Flow parameters determined in core flow at the inlet plane to test section (i.e., 5000 mm downstream the leading edge), located in the zero pressure gradient area, are the mean velocity $U \approx 10$, 15 and 20 m/s and turbulence intensity $Tu < 1\%$. The inlet Reynolds number based on friction velocity and boundary layer thickness was equal 2000, 2600 and 3300 respectively.

Figure 1 shows C_p and shape factor $H = \delta^*/\theta$ distributions for analysed flows. It is seen that, irrespective of different Reynolds number both pressure coefficient and shape factor have the same shape of distributions. It confirms similarity of obtained flow conditions from the point of view of pressure gradient. One can noticed also the strong rise of shape factor above $x = 800$ mm indicating development of turbulent boundary layer towards separation.

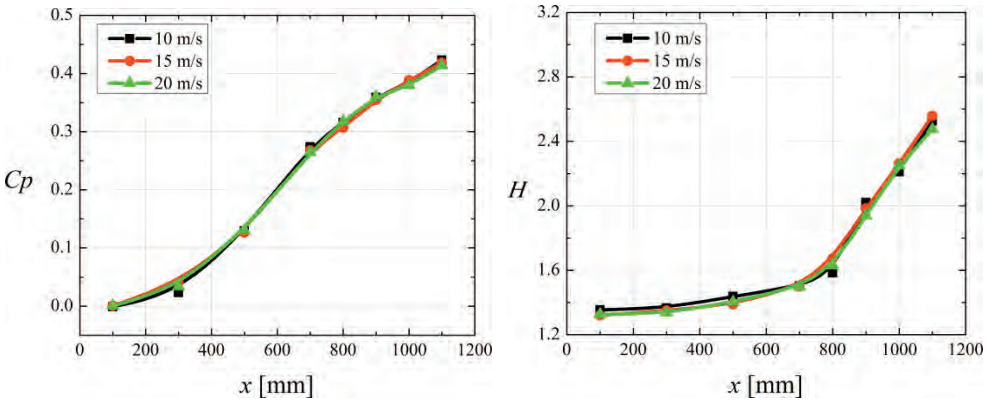

Fig. 1. Pressure gradient parameter C_p and shape factor H distributions

Figure 2 shows the development of the mean streamwise velocity profiles a) and streamwise Reynolds stresses b) for a chosen test case. The velocity is normalized by the local freestream velocity U_∞ and Reynolds stress by outer scale velocity $U_0 = 2(U_\infty - U_{y=0.5\delta})$, while the y coordinate is scaled by the boundary layer thickness δ. In downstream direction a strong deformation of velocity profile and the disappearance of near-wall maximum of streamwise Reynolds stress can be noticed. In the full paper the comparison between consecutive cases will be presented. It is observed that independent of identical pressure coefficient much stronger enhancement of the outer peak of u' is observed with the rise of Reynolds number what confirms the dominant role of the outer length scale and it is different to the observation for canonical zero pressure gradient flows.

a) b)

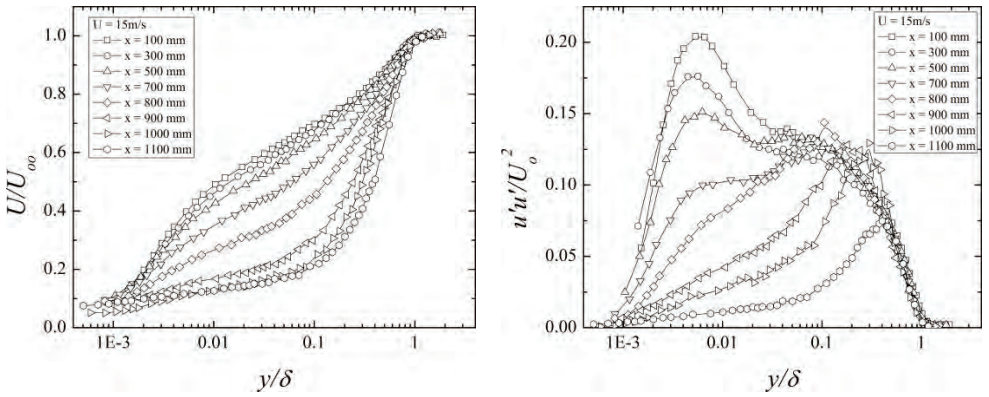

Fig. 2. Mean velocity profiles a) and streamwise Reynolds stress distributions b) for $Re = 2600$

Acknowledgment

The investigations presented in this paper have been obtained with funding from Polish National Centre of Science within the grant DEC 2011/03/B/ST8/06401 as well as statutory fund BS 1-103-301/2015

References

[1] DEGRAAFF D., WEBSTER D., EATON J., Exp. Thermal and Fluid Sicence, 1999, 18, 341–346.
[2] GUNGOR A., MACIEL Y., SIMENS M., SORIA J., J. of Physics: Conf. Series, 2014, 506, 012007.

An attempt to scale streamwise velocity fluctuations near turbulent boundary layer separation

A. Dróżdż, W. Elsner

Częstochowa University of Technology, Faculty of Mechanical and Computer Engineering,
ul. Armii Krajowej 21, 42-200 Częstochowa, Poland. E-mail: arturdr@imc.pcz.czest.pl

The paper is concerned with the issue of scaling of velocity fluctuations profiles u' in turbulent boundary layer subjected to adverse pressure gradient and intermittent separation region. The difficulty in such a scaling is disappearance of near-wall peak and enhancement of the outer peak of u'. The outer peak of velocity fluctuations compels to reject the constant scale across boundary layer thickness. The Reynolds number effect was analysed for precisely matched distributions of pressure gradient parameter C_p using hot-wire technique.

1. Introduction

The need for better description of near wall phenomena and the required input for verification of numerical methods result in rising interest in scaling not only of first, but also of second order statistics [1, 2]. The paper deals with the scaling proposed by Dróżdż et al. [3], which extends the applicability of AOS scaling [2] to pressure gradient turbulent boundary layers by means of additional scaling factor that is the shape factor H. The proposed scaling is based on the following equation:

$$\frac{u'}{UH^{\frac{1}{2}}} = A + B\frac{U}{U_\infty} \tag{1}$$

where: u' is the streamwise velocity fluctuation, U is local streamwise mean velocity, U_∞ is the local maximal mean velocity, and A and B are the constants defined in Table 1. The scaling by the shape factor is valid for boundary layers with pressure gradient because H depends weakly on Reynolds number and strongly upon pressure gradient. The modified scaling procedure introduced by Dróżdż et al. [3] corrects the streamwise Reynolds stress profiles in the outer region, which becomes especially important for APG conditions.

The paper is an attempt to apply the scaling proposed by Dróżdż et al. [3] on flows with strong adverse pressure gradient conditions leading to separation on a flat plate. In particular the purpose of the analysis is to define the local equilibrium regions i.e., regions of constant A and B, for separated turbulent boundary layers.

2. Experimental setup

The experiment was performed in an open-circuit wind tunnel, where the turbulent boundary layer developed along the flat plate, which is 7 m long. The test section located at the end of the wind-tunnel is equipped with perforated, movable upper wall enabling to generate flow conditions for the separation of turbulent boundary layer at the bottom flat plate. The profile of the upper wall and suction flux was adjusted to have, for different Reynolds number, matched distributions of pressure coefficient $C_p = 1 - \left(\frac{U_\infty}{U_{\infty 0}}\right)^2$, where $U_{\infty 0}$ is the maximal mean velocity for inlet zero pressure gradient conditions. Flow parameters determined in core flow at the inlet plane to test section (i.e., 5000 mm downstream the leading edge), located in the zero pressure gradient area, are the mean velocity $U \approx 10$, 15 and 20 m/s and turbulence intensity $Tu < 1\%$.

The inlet Reynolds number based on friction velocity and boundary layer thickness was equal 2000, 2600 and 3300 respectively.

3. Results

The results of applied scaling for analyzed flows are shown in Figure 1. The Figure 1a) shows that the flow in the first part of the test section follows local equilibrium states documented in Dróżdż et a. [3]. A different situation occurs further downstream near separation region (Fig. 1b). The analysis of reduced *u*' profiles reveals that in the region from ID (Incipient Detachment) to ITD (Intermittent Transitory Detachment) [4] profiles deviate from straight line for relaxing APG described as for Case 3 (Table 1). It means that the flow is out of the equilibrium state. The next local equilibrium state is reached at the ITD point. For that location the positive deviation is not occurring close the wall as it has been observed for previous profiles. It means that the flow is controlled only by the outer region of the turbulent boundary layer, i.e., by the large scales.

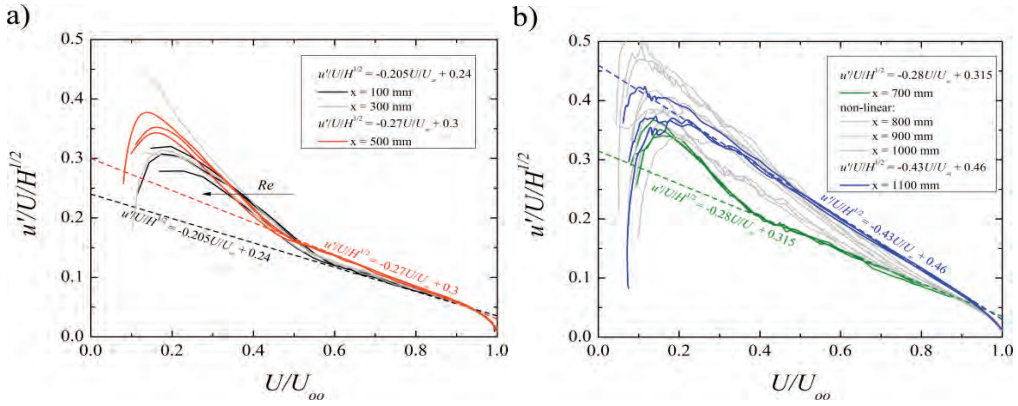

Fig. 1. Streamwise turbulence intensities scaled on shape factor $u'/U/H^{1/2}$ versus U/U_∞: a) profiles in equilibrium states defined by [3]; b) profiles near separation

Table 1. Parameters of the linear function

Case	d*p*/d*x*	d^2p/dx^2	*x* [mm]	*B*	*A*
1	ZPG, APG [3]	≥0	0÷300	–0.205	0.24
2	relaxing APG [3]	<0	500	–0.27	0.30
3	relaxing APG	>0	700	–0.28	0.315
4	APG ID-ITD	>0, <0	800÷1000	non-linear	
5	APG ITD	<0	1100	–0.43	0.46

Acknowledgment

The investigations presented in this paper have been obtained with funding from Polish National Centre of Science within the grant DEC 2011/03/B/ST8/06401 as well as statutory fund BS1-103-301/2015

References

[1] MARUSIC I., KUNKEL G.J., Phys. Fluids, 2003, 15, 2461–2465.
[2] ALFREDSSON P.H., ÖRLÜ R., SEGALINI A., Eur. J. Mech. B/Fluids, 2012, 36,167–75.
[3] DRÓŻDŻ A., ELSNER W., DROBNIAK S., Eur. J. Mech. B/Fluids, 2015, 49,137–45.
[4] SIMPSON R.L., *Turbulent Boundary-Layer Separation*, Annu. Rev. Fluid Mech., 1989, 21,205–34.

Instability in a channel with grooves parallel to the flow

N. Yadav, S. Gepner, J. Szumbarski

Institute of Aeronautics and Applied Mechanics, Warsaw University of Technology,
ul. Nowowiejska 24, 00-665 Warsaw, Poland. E-mail: nyadav@meil.pw.edu.pl

Direct Numerical Simulation of a flow in a channel with grooves parallel to the flow direction has been studied. Analysis is performed up to the Reynolds numbers resulting in the formation of secondary instability states. The analysis includes investigations of the drag reducing properties of the transversely-oriented wall corrugation. Linear stability is investigated by direct simulation of the Navier–Stokes equations resulting in identification of two possible types of hydrodynamic instabilities. The presentation is concluded with presentation of flows resulting from the non-linear saturation of the unstable modes.

1. Introduction

Design of compact mixing devices such as heat exchangers, cooling systems in microelectronics, small bioreactors, oxygenators or dialisators is an important technical problem. The operational efficiency of such devices depends strongly on mixing intensification which is especially difficult to achieve in the low-Reynolds-number laminar flow regimes. One possible approach to improve mixing is to take advantage of hydrodynamic instabilities naturally occurring in the flow.

Corrugated or wavy flow boundaries may lead to the formation of secondary states (steady or oscillatory), as well as they can influence the drag experienced by the channel flow, as shown in [1–5]. Two forms of instabilities have been identified in grooved channel flows. The first one is the travelling wave mode which, in the smooth channel limit, connects to the classical Tollmien–Schlichting (TS) wave. The second form originates from the least attenuated Squire modes and may lead to either stationary or traveling wave disturbance patters, dependently on the spatial orientation of the wall corrugation.

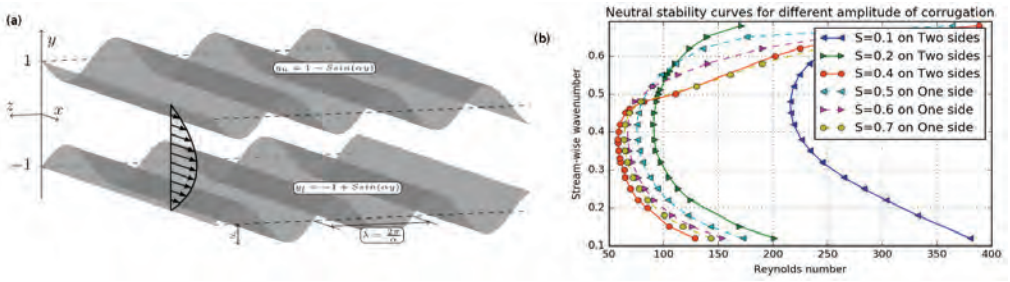

Fig. 1. (a) Geometry of the channel with corrugation amplitude and wave number, $\alpha = 1$ (b) Neutral stability curves of the unstable mode for the corrugation wave number $\alpha = 1$ and different amplitudes

Most attention has been given to the analysis of flows perpendicular to the corrugation. This work is focused on still less investigated case of flow directed parallel to the grooves (see Fig. 1a). The channel geometry is characterized by the corrugation wavenumber α, and corrugation amplitude S. Such configuration is known to become unstable due to two families of traveling waves [3–4]. Depending on geometric parameters of the channel, the dominant instability connects in the limit of vanishing amplitudes to the classical Tollmien-Schlichting wave and – for long corrugation wavelengths – it gets stabilized with increasing the amplitude in

creases, or – for shorter corrugations wavelengths – becomes less stable. According to [3], the threshold value of the corrugation wave number where this change of the stability response to wall corrugation occurs is $\alpha_{cr} = 4.22$. The other possible instability originates as a Squire mode and becomes dominant for smaller values of α and larger corrugation amplitudes. In the paper [2], Szumbarski reports that this mode can become unstable for Reynolds as low as 100 or lower, with remarkable minimal value around 58 attained for the corrugation wave number 1.0, the amplitude S = 0.4 and the streamwise wave number $\beta \approx 0.38$.

2. Problem Specification

The current work is focused on systematic investigation of the dynamics of flows in corrugated channels with grooves parallel to the flow direction. The analysis relies on DNS results obtained with the spectral finite-element method in the (y, z)-plane combined with the Fourier decomposition in the direction of the flow, as implemented in NEKTAR++ [5]. Linear stability is assessed by tracking the growth of a selected form of perturbations over a range of geometric and flow parameters. Figure (1b) illustrates neutral stability curves obtained for the case of one and two sided wall corrugations at different amplitudes. The obtained results much very well with the results of classical stability analysis based on linearized Navier–Stokes equations. Additionally, the DNS analysis provides valuable information about the patterns of nonlinearly saturated states and corresponding flow resistance, clearly not available from purely linear theory.

3. Conclusions

The most destabilizing corrugation amplitude for the Squire-like unstable mode has been found to be around 0.4. The same mode causes flow destabilization for corrugation amplitudes as low as 0.1, but at the Reynolds number exceeding 220. The ongoing research includes evaluation of the nonlinear saturation of disturbances on flow resistance and mixing capabilities.

References

[1] SZUMBARSKI J., *Instability of viscous incompressible flow in a channel with transversely corrugated walls*, Journal of Theoretical and Applied Mechanics 2007, 45(3), 659–683.
[2] SZUMBARSKI J., BLONSKI S., *Destabilization of laminar flow in a rectangular channel by transversely-oriented wall corrugation*, Archives Mechanics, 2011, 63(4), 393–428.
[3] MORADI H.V., FLORYAN J.M., *Stability of flow in a channel with longitudinal grooves*, Journal of Fluid Mechanics, 2014, 757, 613–618.
[4] MOHAMMADI A., MORADI H.V., FLORYAN J.M., *New instability mode in grooved channel*, Journal of Fluid Mechanics, 2015, 778, 691–720.
[5] FLORYAN J.M., FLORYAN C., *Traveling wave instability in a diverging – converging channel*, Fluid Dynamics Research, 2009, 42.2, 025509.
[6] CANTWELL C.D., MOXEY D., COMERFORD A., BOLIS A., ROCCO G., MENGALDO G., GRAZIA D. DE, YAKOVLEV S., LOMBARD J.-E., EKELSCHOT D., JORDI B., XU H., MOHAMIED Y., ESKILSSON C., NELSON B., VOS P., BIOTTO C., KIRBY R.M., SHERWIN S.J., *Nektar++: An open-source spectral/element framework*, Computer Physics Communications, 2015, 192, 205–219.

Influence of holding on second onset of instability for a sphere

P. Regucki[1], S. Goujon-Durand[2]

[1] Wrocław University of Science and Technology, Faculty of Mechanical and Power Engineering,
Wybrzeże Wyspiańskiego 27, 50-370 Wrocław, Poland
[2] PMMH-ESPCI, CNRS UMR 7636, 10 Rue Vauquelin, 75231 Paris Cedex 05, France
E-mail: Pawel.Regucki@pwr.edu.pl

There are presented results of an experimental study about flow around a sphere in a range of $250 < Re < 400$. In this regime occurs the significant change in the character of vortex structures generated behind a sphere – so called second transition. The critical Reynolds number indicating the onset of the above-mentioned transition is well recognised in literature and estimated on $Re_{II} = 273$. Despite this fact, the experiments done in water tunnel indicated the potential influence of a shape and length of the holding on the onset of this instability. Depending on the length of a holding and a diameter of the sphere a threshold of the second transition could be shifted up to $Re_{II} = 377$.

1. Introduction

Investigation of the vortex structures generated in the wake behind a sphere is described in numerous experimental and numerical studies [1–4]. Due to the fact of simple geometry of the sphere, an analysis of the flow around it could be a fundamental prototype for further studies of flows around much more complex three-dimensional bodies. The pattern of flow behind the sphere changes significantly with Reynolds number in the range of (0, 400). Special attention is put on the regime where two steady vortex structures, so called counter rotating vortices, start to be unstable transforming to hairpin vortex shedding [4]. This phenomenon is called second transition and appears in the range of $Re_{II} \in (273, 285)$ [3, 5–6]. Analysis of this transition could help to understand the global problem of instabilities in inhomogeneous flows and to solve many applicable problems in aviation (like formation and destruction of trailing vortices created behind landing aircrafts).

Recently Chrust et al. [7] considered an influence of an inclination of a disk on transition scenario suggesting that the precision in orientation of the object has significant influence on the onset of instability. Besides the exact orientation of the investigated object to the flow, very important, but often neglected, problem is connected with the way of the installation of the body in the research area. Shape and length of a holding could have significant influence on the moment of instability appearance. In the paper, Authors report their investigations related to the influence of the length of the holding on a second onset of instability for different diameters of the sphere. It was noticed that long holding causes a significant modification of the velocity profile in the neighborhood of the obstacle what could result in shifting of the second instability threshold Re_{II}.

2. Measurement methodology

All experiments were carried out in low velocity water tunnel (1.0 to 3.0 cm/s) with square cross section $S = 10 \times 10$ cm^2 and 86 cm long what gives, for the diameter of the sphere $d = 24$ mm, more than 35 sphere diameters. The diameters of investigated spheres change from 14 up to 24 mm.

The sphere was held from upstream by rigid bent tube ($\phi = 2.0$ mm, $H = 50.0$ mm) with different lengths L (Fig. 1). The vortex structures visualization was performed by laser induced fluorescence (LIF) injected to the flow by a hole in the middle of the sphere without any significant influence on the shape of recirculation zone. Particle image velocity (PIV) technique was applied to measure the velocity field in cross section behind a sphere.

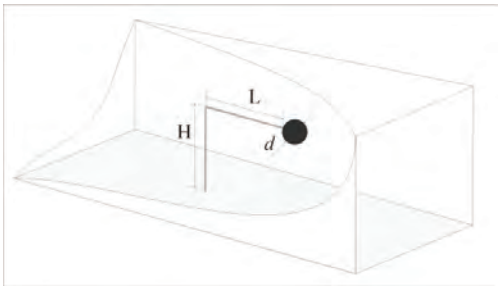

Fig. 1. Scheme of a holding

3. Results and comments

Experimental results, presented in Table 1, show different values of Reynolds numbers Re_{II} obtained for various diameters of the spheres d and lengths of the holdings L. One can notice that Re_{II} describing the transition between two steady counter rotating vortices and unsteady hairpins shedding for L = 25 mm is almost constant and located in the range of the literature values (273, 285). Increase of holding length L causes that Re_{II} is shifted to larger values what is clearly seen for all values of d. In case of holding length L = 500 mm only for diameters d = 20 and 24 mm results are close to Re_{II} = 300.

Table 1. Reynolds numbers Re_{II} obtained for various diameters of the spheres d and lengths of the holdings L

	d = 14 mm	d = 15 mm	d = 16 mm	d = 20 mm	d = 24 mm
L = 25.0 mm	279.5 ± 0.9	282.4 ± 1.1	281.2 ± 1.4	280.6 ± 1.6	280.1 ± 1.2
L = 500.0 mm	376.6 ± 1.3	369.7 ± 1.9	355.6 ± 1.1	308.9 ± 0.9	301.9 ± 1.5

The trend shows, that for L = 500 mm, decreasing of the sphere diameter causes increase of value Re_{II}. It could be explained by the larger thickness of boundary layer created along the holding what modifies the velocity profile in the flow. The thickness of the boundary layer for L = 500 mm and Re_{II} = 376.6 is δ = 21.6 mm what means that the whole sphere d = 14 mm is inside the boundary layer. For Re_{II} = 301.9 and d = 24 mm boundary layer is δ = 31.5 mm. On the other side, if Re_{II} ~ 280 and L = 25 mm the thickness of boudary layer changes for d = 14 and 24 mm between δ = 5.6 and 7.3 mm respectively. It means that for a small length of holding L the edge of the sphere is still in the external flow and "feels" mean velocity u_∞ calculated from a volumetric flow rate for a tunnel cross section S. This explains why for L = 25 mm and for all diameters d Re_{II} is approximately equal 280. With increase of the length of the holding Reynolds number Re_{II} also increase with decreasing values of d.

References

[1] JOHNSON T.A., PATEL V.C., J. Fluid Mech., 1999, 378, 19.
[2] SCHOUVEILER L., PROVANSAL M., Phys. Fluids, 2002, 14, 3846.
[3] GUMOWSKI K., MIEDZIK J., GOUJON-DURAND S., JENFFER P., WESTFREID J.E., Phys. Rev. E, 2008, 77, 055308(R), DOI: 10.1103/physRevE.77.055308.
[4] THOMPSON M.C., LEWEKE T., PROVANSAL M., J. Fluids Struct., 2001, **15** 575.
[5] ORMIERES D., PROVANSAL M., Phys. Rev. Lett., 1999, 83, 80.
[6] TOMBOULIDES A.G., ORSZAG S.A., J. Fluid Mech., 2000, 416, 45.
[7] CHRUST M., DAUTEUILLE C., BOBIŃSKI T., ROKICKI J., GOUJON-DURAND S., WESFREID J.E., BOUCHET G., DUŠEK J., J. Fluid Mech., 2015, 770, DOI: http://dx.doi.org/10.1017/jfm.2015.133.

Reconstruction of three-dimensional velocity vector maps from two-dimensional PIV data

D. Pavlík[1], P. Procházka[2], V. Kopecký[1]

[1]Institute of New Technologies, Technical University of Liberec, Studentská 2, Liberec, Czech Republic
[2]Institute of Thermomechanics, Academy of Sciences of the Czech Republic
E-mail: david.pavlik@tul.cz

In this paper is presented three-dimensional reconstruction of flow field in tunnel with the Hump profile. The reconstruction is always performed for pair of 2D vector maps obtained by 3D PIV with two cameras which records measurement area from different location. Three-dimensional reconstruction can be obtained in various ways, this paper summarizes two: reconstruction based on known correspondence between images, reconstruction based on knowledge of inner and outer parameters of cameras. The methods can be used in cases when it is impossible to use calibration pattern or when failed reconstruction by commercial software.

1. Introduction

The 3D PIV method is advisable to use for the comprehensive description actions inside the tunnel. It is a non-contact measuring method which is based on the records displacement of seeding particles carried by the fluid stream. Satiating particles are very small and their ideal size, properties are determined by many experiments. To measurement is used pulsed lasers, which illuminate particles in predetermined measuring zone. For recording of the particle images are mostly used two cameras, where angle between axis of the cameras lens is optimal 90° [1]. From images of particles recorded at the time *t* and images recorded by several microseconds later are computed two-dimensional vector maps of flow field corresponding to each cameras. The calculation is based on correlation methods. Subsequently, there are reconstructed 3D vector maps from the two-dimensional vector maps, which characterize fluid flow in the measurement area.

Reconstruction can be done in several ways. The basis is to obtain perspective matrices of cameras used for the measurement. Two approaches were used.

2. Experimental setup

Measurement, were carried out in cooperation with Institute of Thermomechanics of the Academy of sciences of the Czech Republic. Experimental setup with Hump profile is shown in

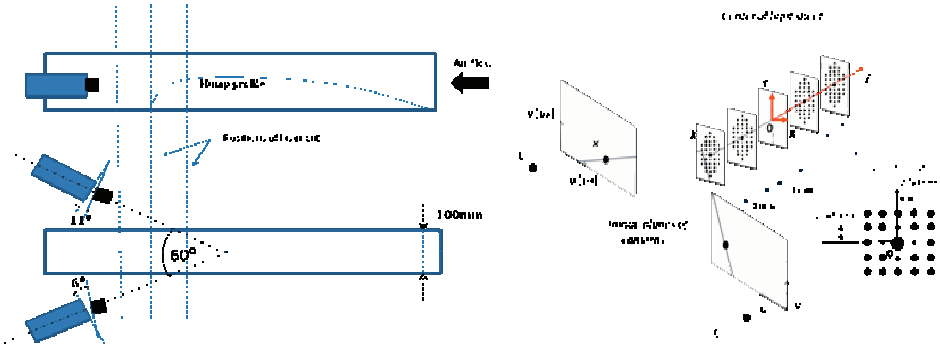

Fig. 1. Experimental setup (left), recording of calibration pattern and coordinate system (right)

Fig. 1. The cameras Nano HISENSE MkIII have a very small depth of field. There must be fulfilment of the Scheimpflug condition in the case we want to have a focused measuring area (object) in the whole field of view in the image plane (CCD detector). Condition is met if the image plane, object plane and cameras lens plane are cross each other at a common straight line in space.

3. Reconstruction based on known correspondences between images

For reconstruction was needed to determine projection matrix of both cameras [2]. The matrices were calculated from the knowledge of the point positions in the scene (X, Y, Z) and the positions of their projections (correspondence) in the image planes (u, v). For that were used calibration patterns and their recordings. The first step of measurement was to place calibration pattern into the tunnel. Black dots form a pattern on a white background. The calibration pattern was recorded in five position: before and behind the laser sheet. Pattern movement was along axis perpendicular to the plane of the measurement area, see Fig. 1. Images of calibration patterns were distorted by perspective projection, before reconstruction was needed to "straighten" images (convert to metric space). The calibration pattern was removed after recording and the air was saturated by particles. The measurement was performed at three position in the tunnel with air flow speed: 5, 10, 20 m/s. The last step was the reconstruction of three-dimensional flow model from vector maps pairs. Reconstruction was resolved by triangulation [2].

4. Reconstruction based on knowledge of cameras inner and outer parameters

Second method is based on calculation of the projection matrices P from outer (orientation R, position t of camera coordinate system in world coordinate system) and inner (focal length, principal point and more in matrix K) parameters. The inner parameters was calculated from several records of chessboard with defined grid. The reconstruction of three-dimensional flow model was resolved by triangulation, just like in previous approach.

$$P = KR[I|-t] \tag{1}$$

5. Results

The paper describes two approaches to the reconstruction. The benefits of these approaches is independence from commercial software which isn't robust enough in some cases. The accuracy of the second reconstruction method was approximately +/– 0.1 m/s compared with results from the first method. The second method can be used when isn't possible put the calibration target into research tunnel.

References

[1] KOPECKÝ V., *Laser anemometri in fluid mechanics*, Brno: ed. TRIBUN EU s.r.o., 2008, 204, ISBN 978-80-7399-357-3.
[2] TUROŇOVÁ B., *3D reconstruction of scene from stereo*, Charles University in Prague, Prague 2008, 48.

Combined Differential Interferometry and long-range µPIV measurements of a temperature driven boundary layer flow

S. Kordel, T. Nowak, R. Skoda, J. Hussong

Ruhr-Universität Bochum, Chair of Fluid Machinery, Universitätsstraße 150, 44801 Bochum, Germany
E-mail: Stephan.Kordel@ruhr-uni-bochum.de

Differential Interferometry and Long-range µPIV are combined in a novel manner for simultaneous temperature and velocity field measurements. The technique is verified by means of a temperature driven boundary layer flow. Systematic, diffraction-induced evaluation errors are avoided by an in-situ calibration procedure. The measurement uncertainty, repeatability and sensitivity will be discussed and results will be compared with numerical simulations.

1. Introduction

Different optical measurement techniques are available nowadays that have been used for simultaneous measurements of velocity and temperature or concentration distributions. Praisner et al. [1] for example combined a liquid crystal sensing system and PIV to determine the convective heat transfer and the flow-field of a turbulent water channel flow. In flow situations where transient scalar fields such as density or pressure distributions have to be determined, interference methods have been the first choice for many decades. The most common interference techniques for flow studies are Mach–Zehnder Interferometry (MZI) and Differential Interferometry (DI) [2]. Early studies on simultaneous density and velocity field measurements were utilized by Skarman et al. [3]. They combined holographic interferometry with 3D-PTV measurements to capture temperature and flow-fields. While interference techniques are often used to measure density fields in gas flows, applications to weakly compressible liquid flows are scarce [4]. Iben et al. [5] performed pressure field measurements in cavitating liquid flows by means of Mach-Zehnder Interferometry.

In the present work simultaneous velocity and temperature field measurements were successfully performed, combining for the first time Long-range µPIV and Differential Interferometry with a standart double-pulsed Nd:YAG laser. To verify the technique, the time dependent temperature and velocity fields are determined in a benchmark experiment, in which a temperature driven circulation flow is created in a cuvette by a heated side wall.

2. Experiment

Benchmark measurements are done in an optically accessible cuvette shown in Figure 1a. One sidewall is replaced with a brass plate. The plate is heated by a 10 Ω resistor with a 4 W power supply. Selected measurement volumes for temperature and velocity field measurements are indicated in green and red in the 3D sketch, covering a region of interest of 2.277 × 1.593 mm² and a measurement depth for temperature measurements of 10 mm and for velocity measurement of 1.6 mm, respectively.

A time series of 60 s was recorded during the heating process. While the commercial software DaVis 8.2.2 (LaVision GmbH) was used for the PIV evaluation, a self-written Matlab algorithm was employed to evaluate recorded interferograms. The interferometric measurement principle utilizes the Lorenz–Lorentz relation to link refractive index gradients to spatial density gradients in the fluid. Refractive index gradients lead to phase changes between light rays passing the measurement section. In a differential interferometer these appear as displacements

from the original interference fringe location in the image plane. Density gradient fields can be directly deducted from extracted fringe displacements. Assuming constant pressure, these density gradients can be converted to a temperature field.

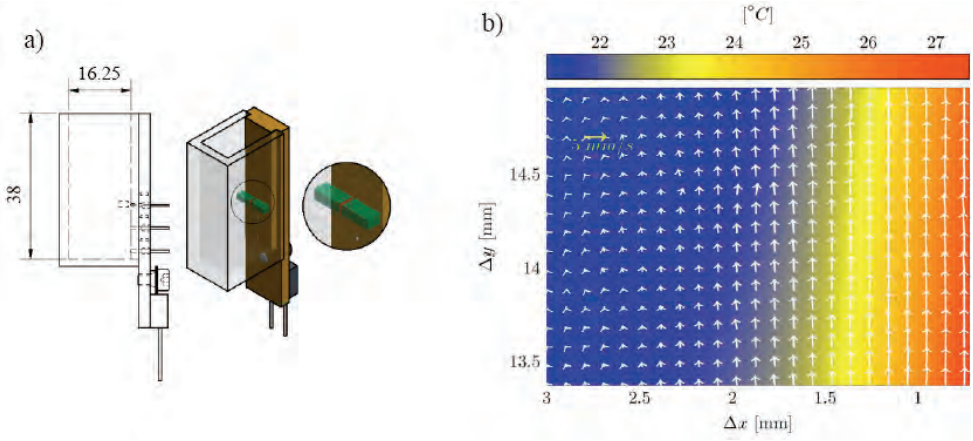

Fig. 1. a) Cuvette with heated side wall; b) Simultaneous measured temperature and velocity field

With the help of an in-situ calibration procedure systematic errors caused by refraction could be excluded, leading to a final uncertainty of ±0.19 K for the temperature measurements. Fig. 1b shows a representative result of simultaneous long-range µPIV and DI measurements 58 s after the plate's heating was started. An overall measurement sensitivity of 0.029 K and spatial resolution of 405 µm could be achieved. Numerical simulations are compared to experimental results, showing a local deviation of less than 6 percent in both temperature and velocity fields.

Overall, we show that DI and µPIV can be combined with a single standard PIV Laser to quantify transient scalar and velocity fields with sub-millimetre resolution. The measurement technique is applicable to various flow problems and will be used in the future for studies of simultaneous pressure and velocity field measurements in weakly compressible, cavitating flows.

References

[1] PRAISNER T.J., SABATINO D.R., SMITH C.R., *Simultaneously combined liquid crystal surface heat transfer and PIV flow-field measurements*, Experiments in Fluids, 2001, 30(1), 1–10.
[2] EGBERS C., BRASCH W., SITTE B., IMMOHR J., SCHMIDT J.-R., *Estimates on diagnostic methods for investigations of thermal convection between spherical shells in space*, Measurement Science and Technology, 1999, 10(10), 866–877.
[3] SKARMAN B., BECKER J., WOZNIAK K., *Simultaneous 3D-PIV and temperature measurements using a new CCD-based holographic interferometer*, Flow Measurement and Instrumentation, 1996, 7(1), 1–6.
[4] WOISETSCHLÄGER J., PRETZLER G., JERICHA H., MAYRHOFER N., PIRKER H.P., *Differential interferometry with adjustable spatial carrier fringes for turbine blade cascade flow investigations*, Experiments in Fluids, 1998, 24(2), 102–109.
[5] IBEN U., MOROZOV A., WINKLHOFER E., WOLF F., *Laser-pulse interferometry applied to high-pressure fluid flow in micro channels*, Experiments in Fluids, 2011, 50(3), 597–611.

Three-dimensional structures behind Glauert–Goldschmied profile under control of plasma actuation

P. Prochazka, V. Uruba

Institute of Thermomechanics, Czech Academy of Sciences,
Dolejškova 5, Praha 182 00, Czech Republic E-mail: prochap@it.cas.cz

The effect of plasma dielectric barrier (DBD) discharge to developed boundary layer was investigated previously. It has been shown that plasma actuation can stabilize the flow near to the surface. In the case of streamlined profile, the plasma actuation is able to shift the point of separation and hence to supress the extent of separation area. This will lead to decrease of the form drag and increasing the total efficiency. An experimental approach is suggested for investigation and time-resolved Particle Image Velocimetry (PIV) is considered as a main measurement technique.

1. Introduction

The plasma actuators belong to the group of active flow control devices. They are relatively new in this group since theirs fully integration among research group is not older than one or two decades. These devices need the electric current for running, no matter whether DC or AC. Nevertheless the actuators, which are supplied by AC power, enable to operate in unstable regimes given by modulation of power signal. The laminar-to-turbulent transition (e.g., [1]) can be affected by DBD actuators as well as the shifting of the separation point (e.g., [2]) and other flow field features.

The presenting DBD actuator has slightly different geometry which favours it to produce sufficient strong plasma-induced flow (ionic wind). This flow affects close to the surface (up to 1 mm) and is able to stabilize or destabilize the boundary layer as it was described in [3]. This actuator can be placed in streamwise orientation also resulting in perpendicularly produced ionic wind with respect to the channel flow. Consequently, the powerful longitudinal vortex is created inclined to the boundary layer which parameters are strongly dependent on electrical parameters of power supply.

The Glauert–Goldschmied type profile (HUMP) is a test case commonly used by actuator testing strategy. This profile was chosen since many studies whether experimental or computational are available in the literature and will help to compare the results. The approach of the investigation is experimental, both Particle Image Velocimetry and Hot Wire Anemometry will be used.

2. Experimental layout

The experiment was carried out in a test section of the blow-down wind tunnel. The test section is a narrow channel with length of three meter and cross-section dimension of 100 × 250 mm. The channel velocities were varied from 5 to 20 m/s resulting in developed turbulent boundary layer in the aforementioned place. The turbulence intensity level is 0.1% behind the contraction. The HUMP profile is wall-mounted with the bottom side of the channel so that the distance from the contraction to the leading edge is 1800 mm. There are two profiles with different size. The height of the first profile is 50 mm (20% of cross-section) and second on is 25 mm high (lower level of congestion).

The actuator is placed on the profile surface as close as possible to the point of separation (Table 1) in spanwise orientation with co-oriented ionic wind. The base case is referred when

the actuation is off. To control the flow behind profile, a steady regime and an unsteady regime can be used. The unsteady regime is characterized by rectangular modulation of voltage signal.

Three-dimensional structures are captured by stereo PIV apparatus in three cross-section positions from leading edge: z/L = 0.89; 1.28; 1.66. From both sides of the channel, there are two fast CCD cameras that meet Scheinpflug criterion. The laser sheet is illuminating the concerned area so that the investigated plane is perpendicular to the bottom side and to side walls. The double head laser NewWave Pegasus has wavelength of 527 nm and repetition rate is 10 kHz.

Table 1. The separation point location, the re-attachment location

5 m/s	z/L = 0.7	z/L = 1.16
10 m/s	z/L = 0.7	z/L = 1.01
20 m/s	z/L = 0.7	z/L = 0.96

3. Results and conclusion

There is the wake behind the HUMP profile in 89% of the chord length in the Figure 1. The flow is not perfectly symmetrical and is shifted to one side. The solid thick line denotes the boundary of the wake. The flow field was affected by DBD actuator very positively. The recirculation area is reduced significantly (about 20%) although the point of separation does not show any major changes. The effect of steady actuation has become weaker for higher channel velocities. It proved that the plasma actuator should be placed as close as possible to the natural separation point to gain optimal control.

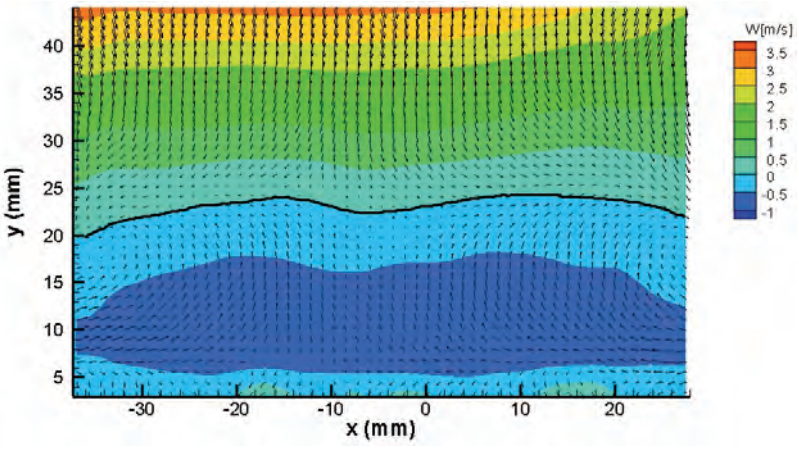

Fig. 1. Cross-section of the flow downstream the leading edge z/L = 0.89

References

[1] KURZ A. et al., Journal Aerospace Lab., 2013, Issue 6 Al06-02.
[2] HE CH., CORKE T.C., PATEL M.P., AIAA, 45th Aerospace Sciences Meeting, 2007, Paper 2007–0935.
[3] PROCHAZKA P., URUBA V., EPJ Web of Conferences, 2015, Vol. 92, Article number 02074.

Numerical and experimental investigations of flow within a pressure exchanger with rotating valves

K. Kurec, J. Piechna

Warsaw University of Technology, Faculty of Power and Aeronautical Engineering,
Nowowiejska 24, 00-665 Warsaw, Poland. E-mail: kkurec@meil.pw.edu.pl

Analysis of flow within a pressure wave exchanger was performed by means of CFD calculations, as well as experiments. Purpose of this research was to assess ability of CFD calculations to predict flow in a pressure wave exchanger, and to shed light on some of the features of the flow. Results of CFD calculations were validated by experimental data, it was concluded that an acceptable level of compliance between experiments and CFD calculations was achieved. Numerical results were used to visualize features of the flow that couldn't be observed due to restrictions of the experimental set-up.

1. Introduction

Pressure wave exchangers utilize unsteady inertial forces that develop during unsteady flow phenomena while a compression of a compressible fluid takes place. This class of machines has a broad range of application [1], such as: topping devices in gas turbine cycles, car engine superchargers, stand alone pressure gain combustors, as well as in refrigerating cycles. However up to present date, only one device of this kind achieved a commercial success, it was Comprex [2], a supercharger for the internal combustion engine mounted in cars manufactured by Mazda in 1980s. Despite several interesting and potentially beneficial features of this technology it still awaits to be widely recognized and utilized in the most efficient way.

Device that was under investigation, was constructed at the Aerodynamics Division at Warsaw University of Technology and holds some unique features that make possible to obtain wide range of experimental data, which is especially useful in order to perform validation of CFD calculations. The presented results of experiments were obtained with the use of PIV measurements, while the test rig was specially adapted for this purpose. This kind of data acquisition was possible due to use of a configuration, in which main part of the device (flow channel) is stationary, and enables application of optical method techniques, as opposed to more common configurations where channels are rotating.

2. Experimental set-up and CFD simulations

Scheme of the pressure wave exchanger is shown in Fig. 1, it shows how the flow passage (located at the center of the pressure exchanger) can be connected with volumes of different pressures and temperatures. Periodic exposition of the flow passage to volumes of different parameters is the essence of the pressure wave exchanger principle of work, and source of pressure waves that are initiated within it, process that occurs during each of the working cycle of the device.

Photograph of the actual device is presented in Fig. 2, it shows that access to the flow channel can be enabled, and with use of see through material like acrylic glass, optical method of flow visualization can be applied. Particle image velocimetry data acquisition was performed, velocity field as well as position and shape of contact gases were recorded, and later used to perform validation of CFD calculations. As it can be seen in Fig. 2, while we can gain access to the central part of the pressure wave exchanger, it is not possible to see what is happening within rotating valves which are mounted in aluminum casings. With aid of numerical calcula-

tions, it was possible to show how initiation of pressure waves occurs and how the mixing takes place during inflow of gases within the rotating valve. One time frame from numerical simulations of this phenomena is depicted in Fig. 3. Performance of a pressure wave exchanger depends in great extent on efficiency of pressure wave phenomena that are taking place during its operation, so it is important to be able to accurately simulate them. CFD calculations were performed with ANSYS Fluent v.15. in unsteady state. Out of the tested turbulence models, SST-Scale-Adaptive Simulation turbulence model proved to be adequate for this kind of simulations.

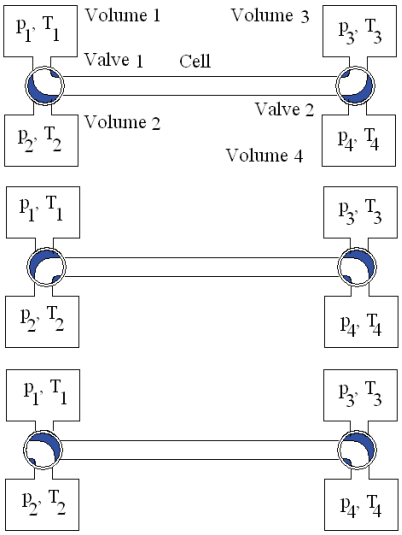

Fig. 1. Scheme of the pressure exchanger, focusing on various configurations of rotating valves

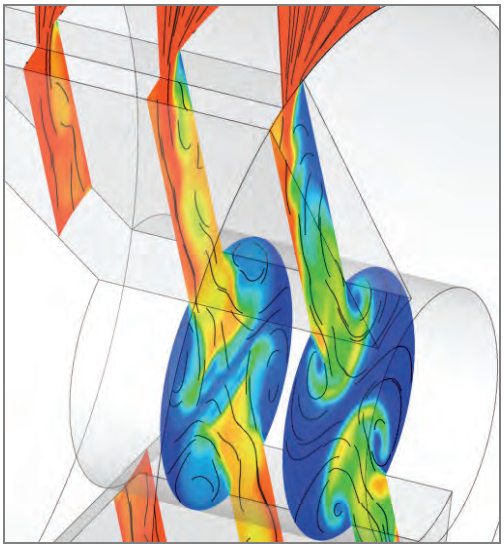

Fig. 3. Contours of high pressure inlet gas Mass Fraction with streamlines, during gradual opening of the rotating valve

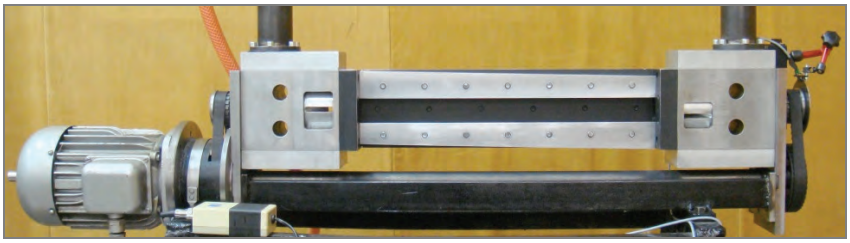

Fig. 2. The examined pressure wave exchanger with revealed flow channel

References

[1] AKBARI P., NALIM R., MUELLER N., *A review of wave rotor technology and its applications*, Journal of Engineering for Gas Turbines and Power, 2006, 128, 4, 717–735.
[2] GYARMATHY G., *How Does the Comprex® Pressure-Wave Supercharger Work?*, SAE Technical Paper, 1983, No. 830234,

Modelling water hammer in viscoelastic pipelines. Short brief

M. Firkowski, K. Urbanowicz, Z. Zarzycki

West Pomeranian University of Technology Szczecin, Faculty of Mechanical Engineering and Mechatronics, Al. Piastów 19, 70-310 Szczecin, Poland.
E-mail: mateusz.firkowski@zut.edu.pl, kamil.urbanowicz@zut.edu.pl, zbigniew.zarzycki@zut.edu.pl

1. Introduction

The increasing of popularity of plastic pipelines in water supply systems caused new problems for engineers and designers of those systems. In compare with old installations (mainly built from steel or brass pipes) there are physics phenomenon which were neglected before, e.g., viscoelasticity of pipe material. To protect newly build systems before unpleasant consequences, one need to analyze a proper mathematical model on design stage.

In presented work a detailed summarize of the current level of knowledge for modelling water hammer in viscoelastic pipelines will be present. In the final mathematical model a new simplified unsteady friction is used [1]. Additionally a set of numerical simulations which results are compared with collected data from experiments (widely described in research papers) are discussed.

2. Mathematical model of viscoelastic water hammer

The classical model of water hammer is described by two partial differential equations (e.g., [2]): continuity equation

$$\frac{\partial H}{\partial t}+\frac{a^2}{gA}\frac{\partial Q}{\partial x}=0 \tag{1}$$

and momentum equation

$$\frac{\partial H}{\partial x}+\frac{1}{gA}\frac{\partial Q}{\partial t}+h_f=0 \tag{2}$$

with the frictional head loss per unit length

$$h_f=f\frac{Q|Q|}{2gDA^2} \tag{3}$$

where f during transient flow is a sum of quasi-steady coefficient f_q and a time dependent one f_u

$$f=f_q+f_u \tag{4}$$

and the wave speed a

$$a=\sqrt{\frac{\frac{K}{\rho}}{1+\alpha\left(\frac{K}{E}\right)\left(\frac{D}{e}\right)}}, \tag{5}$$

where A is the cross-sectional area flow area, D is the internal pipe diameter, E is Young's modulus of elasticity of pipe-wall material, e is the pipe-wall thickness, f is the friction coeffi-

cient according to Darcy–Weisbach, g is the gravitational acceleration, K is the bulk modulus of elasticity of liquid, and α is the axial pipe-constrain parameter dependent on Poisson's ratio v and relative wall thickness e/D.

When taking into account viscoelastic behavior of pipe material, then the continuity equation (1) takes form [3]

$$\frac{\partial H}{\partial t} + \frac{a^2}{gA}\frac{\partial Q}{\partial x} + \frac{2a^2}{g}\frac{\partial (\varepsilon_\varphi)_{ret}}{\partial t} = 0 \tag{6}$$

where $\varepsilon_{\varphi_{ret}}$ is the retarded strain.

3. Exemplary results

The following are examples of simulation results after introducing of viscoelastic effects. In the classical model on Fig. 1 the quasi-steady friction assumptions were made $f = f_q$.

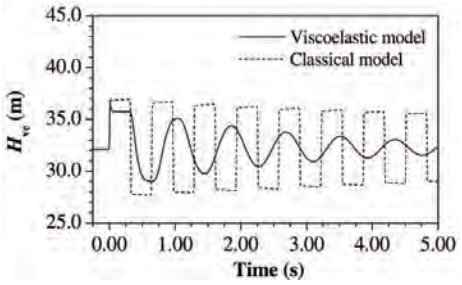

Fig. 1. Comparison of the heads at the valve from [2]

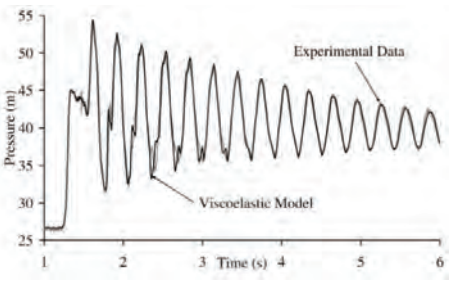

Fig. 2. Numerical results of viscoelastic transient solver vs. transient pressure data from [4]

References

[1] URBANOWICZ K., *Simple modelling of unsteady friction factor BHR Pressure Surges conference Proceedings*, Dublin, Ireland, November 18–20, 2015, 113–130.

[2] BERGANT A., TIJSSELING A., VITKOVSKY J., COVAS D., SIMPSON A., LAMBERT M., *Parameters affecting water-hammer wave attenuation, shape and timing – Part 2: Case studies*, J. Hydraul. Res., 2008, 46 (3), 373–381.

[3] WEINAROWSKA-BORDS K., *Viscoelastic Model of Waterhammer in Single Pipline. Problems and Questions*, Arch. Hydro-Eng. Environ. Mech., 2006, 53 (4), 331–351.

[4] SOARES A., COVAS D., REIS L.F., *Analysis of PVS Pipe-Wall Viscoelasticilty during Water Hammer*, J. Hydraul. Eng., 2008, 134, 1389–1394.

Ground vehicle dynamics in the presence of unsteady aerodynamics loads

J. Broniszewski, J. Piechna

Warsaw University of Technology, Faculty of Power and Aeronautical Engineering,
Nowowiejska 24, 00-665 Warsaw, Poland. E-mail: jbroniszewski@meil.pw.edu.pl, jpie@meil.pw.edu.pl

The purpose of this work is to study car dynamics in the presence of unsteady aerodynamics loads. Co-simulation approach was used during research. A unique connection between Fluent – CFD (Computational Fluid Dynamics) solver, control system (Matlab/Simulink) and multi body dynamics (MSC. Adams) was created. Obtained results show importance of aerodynamics effects on vehicle behaviour. Additionally, influence of active aerodynamics was showed.

1. Introduction

Car body is a rigid object connected in flexible way with the road. Due to flexibility of tires and suspension system position and inclination of the car body varies in time. Variable position of the car in relation to the road, and especially its inclination, influence aerodynamic forces generated on the car body during fast drive. Aerodynamic forces generation is coupled with different modes of car body motion. Simulation of car dynamics considering aerodynamic forces forms a typical problem of Fluid Structure Interaction (FSI). For solution, different types of solvers had to be used in synchronized way. Control system (Matlab/Simulink) was used for coupling the multi body dynamics solver (MSC, Adams) with CFD solver Fluent.

Having system of software simulating FSI problems, it was possible to add elements of active control, utilizing unsteady generation of aerodynamic forces.

The aim of this work is to present a unique co-simulation approach for analyzing ground vehicle dynamics. Unsteady loads were obtained using commercial CFD code Fluent. For determining vehicle dynamics the leading edge multi body dynamic (MBD) solver – MSC. Adams – was used. Matlab/Simulink was acting as an interface and control system for the whole simulation.

Proposed approach allows to include effect of the unsteady aerodynamics load on vehicle dynamics. As an object of interest Honda CRX delSol was chosen. The main reason for this choice is a unique aerodynamics configuration of this car.

2. Methodology

Connection between Fluent and Matlab was established via COM port. This was possible because Fluent can be run in the “as-a-server” mode. In such case it can have more than one client. Connection between Matlab and MSC. Software Adams is well documented in the literature. Dedicated UDF (User-Defined-Features) were developed to calculate forces and moments about a specific point (which can vary with the time). Another UDF was responsible for controlling body motion in the CFD computational domain. Matlab S-functions were required in the process of reading and writing data from and for Fluent. The same functions were responsible for control of running CFD solver.

3. Elements of active aerodynamics

The model contains movable airfoil-spoiler on the back of the car. The angle of attack can be modified to increase or decrease drag and/or lift force depends on velocity and manoeuvre.

This has significant impact on global behaviour of the car because magnitude of the force generated on the airfoil is comparable to the force generated by the rest of the car.

4. Results

Obtained results show importance of unsteady aerodynamics loads on ground vehicle dynamics. 3D effects play a key role in pressure distribution around the car. Using airfoil-spoiler to increase drag force during breaking can reduced velocity in the significant way-especially in the first stage of braking. Further work is required to study more complicated cases including control mechanism in active aerodynamics to stabilized road vehicle driving.

References

[1] ANSYS.Inc 2015, ANSYS Fluent as a Server User's Guide.
[2] MUNTEANU S., How To Make MATLAB Apps For Fluent, 2013, (http://www.ansys-blog.com/).
[3] MSC Software, Getting Started Using ADAMS/Controls, 2014.

Vehicle wheel drag coefficient in relation to travelling velocity – CFD analysis

P. Leśniewicz, M. Kulak, M. Karczewski

Łódź University of Technology, Faculty of Mechanical Engineering, Institute of Turbomachinery (IMP Łódź), Wolczanska Street 219/223, 90-924 Łódź, Poland. E-mail: lesniewicz.pawel@gmail.com

In order to understand the aerodynamic losses associated with a rotating automobile wheel, a detailed characteristics of the drag coefficient in relation to the applied velocity is necessary. Single drag coefficient value is most often reported for the commercially available vehicles, much less is revealed about the influence of particular car components on the energy consumption in various driving cycles. However, detailed flow loss curves are desired for performance estimation. To address these needs, the numerical investigation of an isolated wheel is proposed herein.

1. Introduction

Current global situation together with environmental regulations related to the emissions of greenhouse gases, force car manufactures to look for solutions able to reduce energy consumption of vehicles. One of the paths is related to the development of electric or hydrogen-powered cars, but another one focuses on modifying the existing gasoline-powered vehicles in order to continuously create more ecological and economical automobiles. To facilitate these changes, nowadays, much of the attention of car companies is focused on previously underexplored vehicle areas such as the wheel region.

Aerodynamics of the vehicle wheels was not a topic of many research projects in the past mainly due to the complexity of the flow inside a wheelhouse, but also, as it was believed, because of its limited influence on the vehicle's total drag. However, in the recent years the topic of wheel aerodynamics was refreshed. Basing on the work done by car companies and research institutions, it can be now stated that the contribution of the wheels in the total drag of the vehicle can vary from even up to 30% for vehicles in which wheels are located inside the wheel arches up to around 40% in case of an exposed wheel car [1, 2, 3].

Present article focuses on the characteristic of drag coefficient taking into consideration a selected range of motion velocities. It is an extension of research previously conducted by the aerodynamicists at IMP Łódź, where both, isolated and shrouded wheel impact on energy consumption was studied.

2. Results

For the current study isolated wheel with a grooved tyre was analysed. Detailed description of the numerical model can be found in [4]. Flow simulations were conducted at different values of velocity in the range from 13 m/s to 70 m/s. Over 20 different cases were simulated with the velocity step of 2.8 m/s. Results point out that a single drag coefficient value would not be representative enough to describe the energy consumption trend. This suggests that such loss characteristics might be of value for the designer responsible for the performance analysis of the entire vehicle.

Figure 1 presents the characteristic of the drag coefficient in relation to the applied velocity. It can be observed that with the increase of the velocity the values of drag decrease. In the automotive world, it is assumed that a single value of drag coefficient is often used to describe the aerodynamic performance. In other words, it can be said that the Cx is "assigned" to a car

body. However, as results show, differences in drag force coefficient values depend on the velocity. The variations are relatively small and happen to be the biggest at lower velocities.

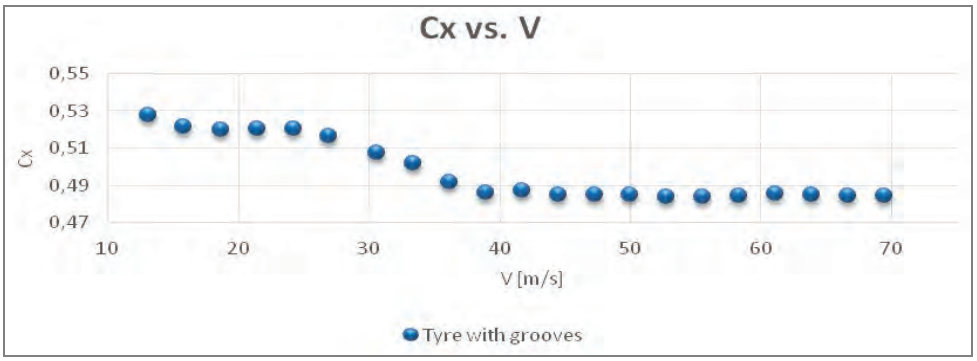

Fig. 1. Relation between applied velocity and drag coefficient

What is more, the relation between aerodynamic resistance and rolling resistance depends on the speed, since with the increase of travel velocity, the impact of aerodynamics is decidedly more significant. In spite of the present tendencies in the car industry to focus on lower velocities as the ones more frequently occurring in the urban traffic (see the driving cycles introduced such as NEDC – New European Driving Cycle and WLTP – Worldwide Harmonized Light Vehicles Test Procedures), it is continuously expected that small urban cars can be and will be environmentally friendly, efficient and economical, while reaching the price availability and performance measures of contemporary gasoline-powered vehicles. Therefore, even the smallest improvements in reducing the aerodynamic drag are worth investigating.

3. Conclusions

In order to perform the investigation described in this paper over 20 cases were simulated to illustrate dependency between the value of drag coefficient and the motion velocity. After bringing the results together the detailed characteristics of Cx was obtained.

References

[1] QUI Z., LANDSTRÖM C., LÖFDAL L., JOSEFSSON L., *Wheel aerodynamic developments on passenger cars by module-based prototype rims and stationary rim shields*, Proc. FISITA World Congress, 2010, F2010-B-034.
[2] MERCKER E., BREUER N., BERNEBURG H., EMMELMANN H.J., *On the aerodynamic interference due to the rolling wheels of passenger cars*, SAE-Paper 1991, 910311, 63–79.
[3] DIMITRIOU I., KLUSSMANN S., *Aerodynamic Forces of exposed and enclosed rotating wheels as an example of the synergy in the development of racing and passenger cars*, SAE Technical Paper, 2006, 2006-01-0805.
[4] LEŚNIEWICZ P., KULAK M., KARCZEWSKI M., *Aerodynamic analysis of an isolated vehicle wheel*, J. of Physics Conf. Series, 2014, 530 012064 ISSN: 1742-6596.

Application of anelastic and compressible EULAG solvers for limited-area numerical weather prediction in the COSMO Consortium

D.K. Wójcik, Z.P. Piotrowski, B. Rosa, M.Z. Ziemiański

Institute of Meteorology and Water Management – National Research Institute,
ul. Podleśna 61, 01-673 Warszawa, Poland. E-mail: Damian.Wojcik@imgw.pl

Research results in the area of nonhydrostatic anelastic/compressible EULAG fluid solver application for numerical weather prediction (NWP) are presented. They include an assessment of solver capabilities for idealized and realistic experiments. A number of idealized simulations, involving also convective and orographic flows, allows to gain confidence in solver accuracy and robustness and opens the way for realistic NWP tests. The positive outcome from them paves the way to transform our research code from laboratory to the production environment.

1. Introduction

Research conducted at Polish Institute of Meteorology and Water Management – National Research Institute, in collaboration with Consortium for Small Scale Modeling (COSMO) have resulted in the development of a new prototype nonhydrostatic anelastic NWP model COSMO-EULAG (CE-A). The dynamical core of the CE-A model is based on the anelastic set of equations and numerics adopted from the EULAG [1] fluid solver. The core is coupled to the COSMO physical parameterizations involving turbulence, friction, radiation, moist processes and surface fluxes. A special coupler allows for seamless communication between the two distinct cods. The CE-A model turned out to be capable to compute weather forecast in convection-permitting limited-area regional domains and to provide competitive forecasts with respect to the operational COSMO model setup. Furthermore, it allowed to perform very high resolution simulations of realistic flows (up to 0.1 km grid size) in mountainous areas with slopes reaching 82 degree of inclination (see Figure 1).

Recently, the research framework has been equipped with a new compressible EULAG solver. The compressible solver was developed in ECMWF [2, 3]. Preliminary results obtained with the new model (CE-C) are accurate and promising. However, the development work is still in progress. We believe, that the CE-C model will provide an even more accurate forecast and keep the advantages already provided by the CE-A model.

The continuous improvement in the numerical methods for NWP and the availability of high-performance supercomputers is expected to allow employing sub-kilometer grid spacing for operational forecasting in the coming decade. It is expected that this advance will allow to better represent deep moist convective processes in the atmosphere. Ultimately, our research may add value to the forecasting of extreme weather phenomena like, e.g., supercell thunderstorms, intense mesoscale convective systems, prefrontal squall-line storms or heavy snowfall from wintertime mesocyclones.

2. Idealized tests

The idealized tests of: (i) cold pool propagation [4], (ii) mountain flows [5] and (iii) deep moist convection [6] play a key role in examining the consistency of theoretical solver formulation and in checking the correctness of source code implementation. Careful analysis of the idealized test cases leads to the conclusion that CE-A and CE-C models provide results in very good qualitative and quantitative agreement with the reference solutions.

3. Realistic tests

The success of idealized tests allows extending the model testing to realistic weather simulations. For them, an Alpine domain is chosen as it imposes additional challenges for numerical stability of terrain-following vertical model coordinates. A number of simulations is carried out for horizontal resolutions ranging from 2.2 km to 0.1 km, for convective and stable weather regimes (see Fig. 1 for simulation with horizontal resolution of 0.1 km) in order to check the performance of CE-A and CE-C. The tests have a form of case studies as well as verification comparisons. They demonstrate very good model performance (verification scores are competitive with standard operational COSMO model) and lack of numerical stability problems (as demonstrated by case studies with 0.1 km resolution).

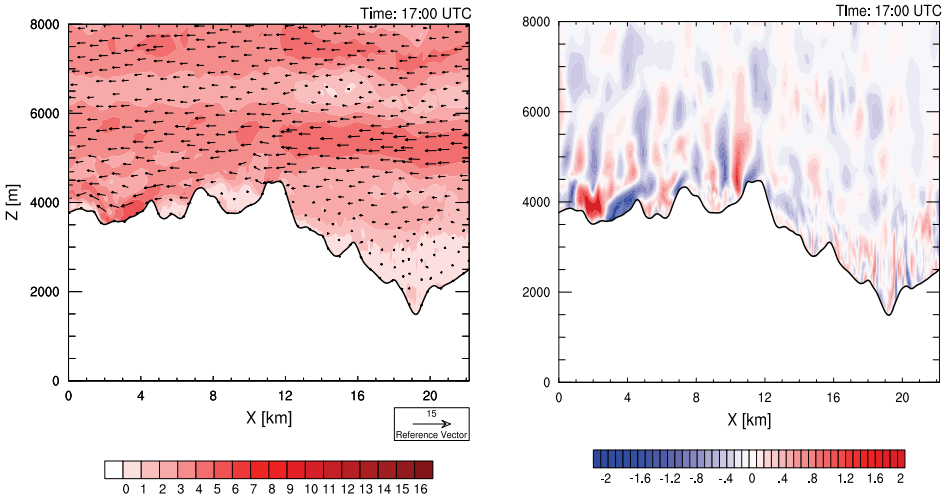

Fig. 1. Horizontal (left) and vertical (right) velocity field in the vicinity of Monte Rosa (CE-A model; grid size 0.1 km; 19 July 2013)

That opens the way for further work on operational implementation of the model.

References

[1] PRUSA J.M., SMOLARKIEWICZ P.K., WYSZOGRODZKI A., Computers and Fluids, 2008, Vol. 37, 1193–1207.
[2] SMOLARKIEWICZ P.K., KÜHNLEIN C., WEDI N., J. Comput. Phys., Vol. 263, 185–205.
[3] KUROWSKI M.J., GRABOWSKI W.W., SMOLARKIEWICZ P.K., J. Atmos. Sci., 2014, Vol. 71, 3767–3787.
[4] STRAKA J.M., WILHELMSON R.B., WICKER L.J., ANDERSON J.A., DROEGEMEIER K.K., Int. J. for Num. Meth. in Fluids, 1993, Vol. 17, 1–22.
[5] PINTY J.-P., BENOIT R., RICHARD E., LAPRISE R., Month. Wea. Rev., 1995, Vol. 123, 3042–3058.
[6] WEISMAN M.L., KLEMP J.B., Month. Wea. Rev., 1982, Vol. 110, 504–520.

Bio-aviation

R.S. Rowiński, T. Seredyn

Wyższa Szkoła Oficerska Sił Powietrznych, Wydział Lotnictwa,
ul. Dywizjonu 303, 08-521 Dęblin, Poland. E-mail: robert.rowinski@op.pl

The paper presents the development of bio-aviation. The name Bio-aeronautics was given by Southwell (1975), and the definition is "application of different types of aviation to the development of useful living organisms on the Earth". A patent received by Alfred Zimmermann, a forester from Detershagen (DE), on 21th of March 1911 is considered as the origin of this field of aviation. The patent belongs to the problem of Lymantria Monacha L control in German forests. Development of aerial constructions applied in Poland and abroad was addressed.

1. Introduction

Before the II World War the use of aircraft in agriculture and forestry treatments had limited range because of technical problems of new aeroplanes and low cost of man power. After the II World War the situation has changed fundamentally, because airplanes used in the war were easy adopted for agricultural and forestry treatments.

However, the problems of flight security and quality of aerially dispersed chemicals as well as attempts to reduce the drift and cost of treatments, forced people to design the production of new aeroplanes and helicopters – the second generation, made specially for these purposes, like Polish aircraft: PZL M-18 "Dromadery", PZL-106 „Kruk", PZL M-15 "Belphegor", Mi-2R (helicopter for agricultural and forestry treatments).

2. The possibilities of the Bio-aviation

In spite of its small actual operating range on the world scale, the bioaeronautics can play very important role in improving the nutritional world situation, especially for countries of Asia, Africa, South and Central America. In those regions a feeble infrastructure, a very poor agricultural mechanization and a shortage of specialists make the bioaeronautics the only practical alternative in some fields of activities.

The main field of activity of Bio-aviation:

- control of human and animal disease vectors (tsetse fly, onchocerciasis),
- control of mass infestations (Locust, Qu ilea),
- plan protection treatment (cereals, cotton, rice, maize, root crops and others),
- application of fertilizers,
- reclaiming, erosion control, ground stabilisation,
- delivery of agricultural and others products,
- health control.

3. Main advantages of Bio-aviation

3.1.Quick acting

- To give possibilities to quickly access the territories showing anomalies,
- to patrol and treat a big area, in a relatively short time. It is very important in forest and to pest control in monoculture area,

- to control a pesto or forest fire at a first phase of growth, thus limiting the area of action and level of losses. Use of aviation in forest fire control in France on the turn of 1980 years decreased the average area of burn down 5.7 times.

3.2. Biological efficiency

- Gives us possibility to do the treatment strictly in an agricultural time to ensure the highest biological effect,
- aircrafts do not compact the most fertile soil layer and can be used when it is not possible to involve ground machinery (water logged soil, high forest),
- induced velocity by slowly flying helicopters gives an "helicopter effect" which allows a good penetration of droplets into canopy. From this point of view helicopters are commonly used in vine-shoots.

3.3. Economic efficiency

- Quick acting enables receiving high efficiency. During pest control in forest, with small dose, efficiency was about 380 hectares/hour or 1330 hectares/day. Efficiency of An-2r and helicopter Mi-2R in agricultural and forest treatments is presented,
- labour, energy and consumption of fuel for low doses is lower in aerially treatments compared to ground sprayers,
- aircrafts can be active in regions with poor infrastructure, and for this reason they are especially useful in large areas of Africa, South America, Asia and others (Akesson, Yates 1974).

4. Negative elements

- Cost of aeroplanes, apparatus and treatments,
- cost of the insurance,
- big influence of meteorological conditions,
- drift as a possibility of pollution of other crops, water, urban area.

Production of aeroplanes, helicopters and an area of treatments in Poland and in the world will be presented.

References

[1] AKESON N.B., YATES W.E., *The use of Aircrafts in Agriculture*, FAO, Roma 1974.
[2] *Development of Airborne Equipment to Intensity World Food Production*, UN, Economic Commission for Europe, New York 1981.
[3] PIETRUSZKA J., ROWIŃSKI R.S., *Computer Simulation of Aerial Spraying*, Annual Review of Aerial Spraying, 2004, 3(1), 125–1404
[4] RYANS D., GERBER A.G., HOLLOWAY G., *Acomputational Study on Spray Dispersal*, Tran. of the ASABE, 2013, 56(3), 847–868

Index of authors

Contents

SPONSORS' ADVERTISEMENT

Municipal Water and Sewage Company S.A. in Wroclaw (MPWiK) is one of the biggest municipal water utilities in Poland. Its uninterrupted operations have continued since 1871 when the water treatment plant "Na Grobli" was first commissioned.

New Technologies Center MPWiK S.A

Wastewater Treatment Plant in Wrocław S

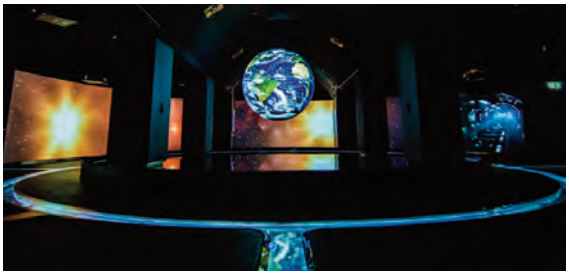

Planet of water zone in Hydropolis - Environmental Education Centre

The utility operates two water treatment plants "Na Grobli" and "MokryDwor" as well as the Water Treatment Station "Lesnica". It operates and maintains nearly 2,000 km of water network and almost 1,500 km of sewage network. For the last few years the utility has operated one of the most modern treatment plants: Wroclaw's Wastewater Treatment Plant "Janowek" and 30 wastewater pumping stations. The utility serves almost 620,000 residents of Wroclaw and neighboring municipalities of Olawa, Siechnice and Dlugoleka which are supplied with mountain water drawn from, among others, the Nysa Klodzka River with its spring in the Sudety Mountains. Customer satisfaction and trust, high water quality and environmental protection through continuous wastewater service and treatment are three main pillars of the company's activities in Wroclaw.

The utility is relentless in its efforts to become a well-respected regional leader who can be characterized by the care for the quality of services offered, natural resources, natural environment, as well as for ensuring career development opportunities for its employees.

MPWiK places a great deal of emphasis on ecological education. An example of such activity is creating a center for the knowledge about water 'Hydropolis' in a historical 19th century structure which in the past served as a drinking water reservoir.

HOW DID THE WATER GET TO EARTH?

YOU WILL FIND THE ANSWER AT **HYDROPOLIS**

Photograph taken in the PLANET of WATER zone

LET'S MEET AT THE WROCŁAW GROBLA

In the one-and-only in Poland centre of knowledge about water you will find, amongst many other things:

- a room with projections showing the origin of water,
- a replica of the Trieste bathyscaphe in scale 1:1,
- an installation with a shark and shoal of tuna,
- a transparent copy of Michelangelo's sculpture "David"
- operating inventions of ancient water engineering ... and dozens of other interactive and multimedia devices.

hydropolis.pl | +48 71 34 09 515

mpwik WROCŁAW HYDROPOLIS

INTEL'S SCALABLE SYSTEM FRAMEWORK

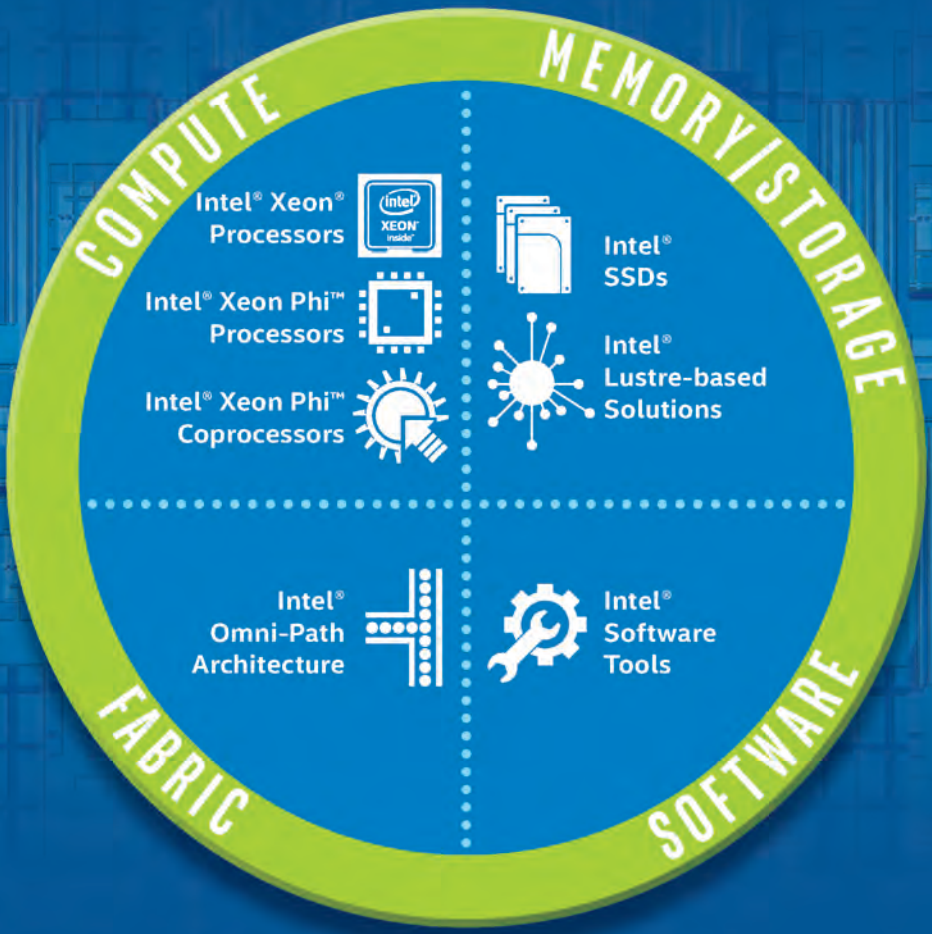

- **Small clusters through Supercomputers**
- **Compute and Data-Centric Computing**
- **Standards-Based Programmability**

intel experience what's inside™

Intel® IoT Platform

Secure, Scalable, Interoperable

The Intel® IoT Platform is an end-to-end reference architecture and family of products from Intel, that works with third-party solutions, to provide a foundation of seamlessly and securely connecting devices, delivering trusted data to the cloud, and delivering value through analytics.

intel XEON inside
intel QUARK inside
intel CORE i3 inside
intel Security
Zephyr™
WIND AN INTEL COMPANY
intel SoFIA

intel experience what's inside™

Symulacja kluczem do SuKcesu

SymKom

Oferta kompleksowa :

- **Sprzedaż oprogramowania**
- **Wsparcie techniczne**
- **Konsultacje**
- **Szkolenia**

Wizualizacja linii prądu wokół samochodu Arrinera Hussarya GT (analiza CFD)

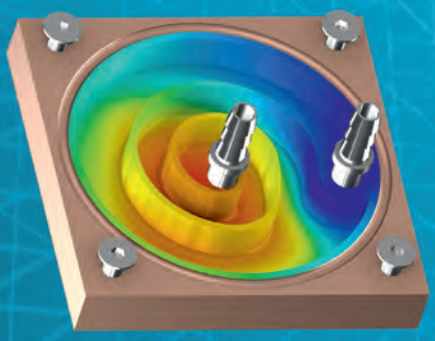

Chłodzenie CPU

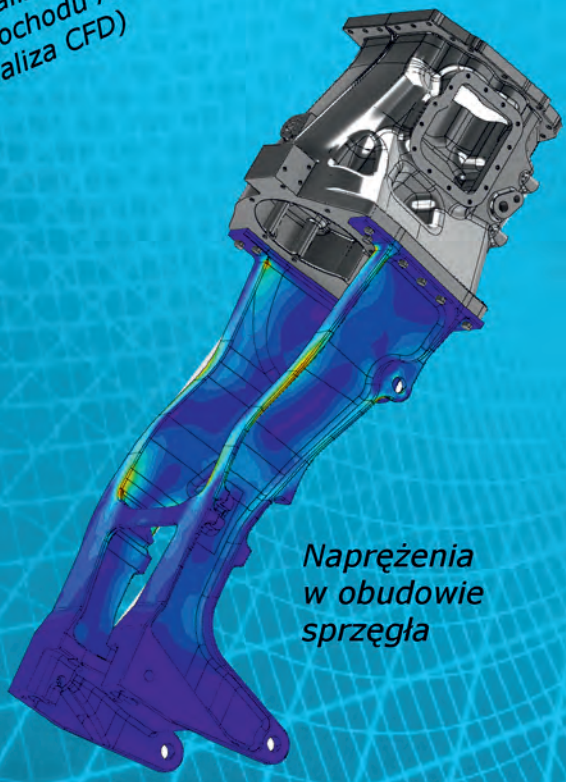

Naprężenia w obudowie sprzęgła

SymKom ANSYS Channel Partner
biuro handlowe:
ul. Głogowa 24, 02-639 Warszawa
tel.: (22) 849 13 92
faks: (22) 856 90 40
www.symkom.pl

Symulacja kluczem do SuKcesu

SymKom

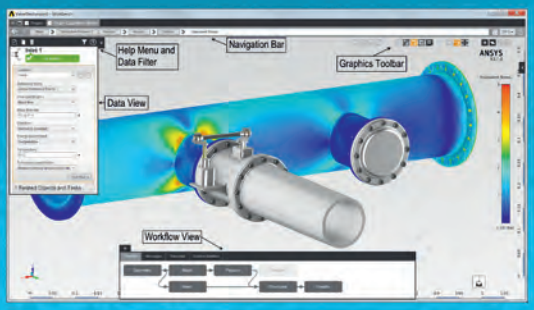

Oferujemy bogaty wybór szkoleń, podstawowych oraz zaawansowanych. Wszystkie szkolenia są prowadzone przez doświadczonych i certyfikowanych przez ANSYS trenerów.

- Przygotowanie modelu

- Design Modeler
- SCDM
- ANSYS Meshing
- Fluent Meshing
- ICEM CFD
- Gambit

- Analizy strukturalne

- MES wprowadzenie
- Budowa i upraszczanie geometrii
- Meshing
- Analizy nieliniowe i kontakt w MES
- Wymiana ciepła
- Analizy sprzężone: przepływowo-mechaniczne
- Modelowanie kompozytów
- Optymalizacja konstrukcji

- Analizy przepływowe

- Wymiana ciepła
- Przepływy burzliwe
- Spalanie
- Przepływy wielofazowe
- Funkcje użytkownika w programie Fluent (User Defined Functions)
- Maszyny wirnikowe
- Poruszająca się i odkształcająca się siatka
- Akustyka

- Analizy elektromagnetyczne

- Modelowanie rdzeni magnetycznych
- Modelowanie magnesów trwałych
- Analiza silników elektrycznych
- Wyznaczanie strat mocy oraz sił elektrodynamicznych
- Analizy sprzężone (elektromagnetyczno - przepływowa, elektromagnetyczno - mechaniczna)
- Analiza parametryczna oraz optymalizacja konstrukcji

SymKom ANSYS Channel Partner
biuro handlowe:
ul. Głogowa 24, 02-639 Warszawa
tel.: (22) 849 13 92
faks: (22) 856 90 40
www.symkom.pl

Casp System Sp. z o.o. and LaVision GmbH

Casp System Sp z o. o. offers LaVision's GmbH diagnostics instruments based on optical techniques as an authorized and certified distributor in Poland since the year 2008.

LaVision was founded in 1989 as a spin-off from Max Planck Institute and Laser Laboratory in Goettingen, Germany. LaVision cooperates with leading scientists, research institutions and companies around the globe.

Casp System is authorized to offer LaVision's standard and dedicated customer designed Laser Imaging Systems for:

- reactive and non-reactive flow field analysis and fluid mechanics applications,
- Intelligent Imaging Systems for non-destructive material testing,
- a range of high-performance cameras and smart optical sensor systems.

The LaVision has extensive professional experience in Laser Imaging Spectroscopy and optical techniques such as:

- Laser Induced Fluorescence (LIF),
- Absorption and Emission Spectroscopy,
- Raman, Rayleigh and Mie Scattering,
- Particle Image Velocimetry (PIV),
- Spray Analysis,
- Digital Image Correlation (DIC) techniques,
- as well as ultra-fast time-resolved imaging and high-speed image recording.

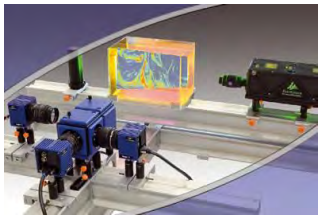

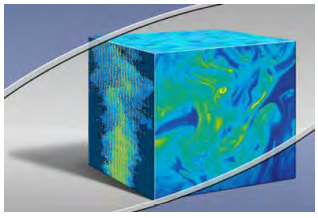

Fluid Dynamics applications

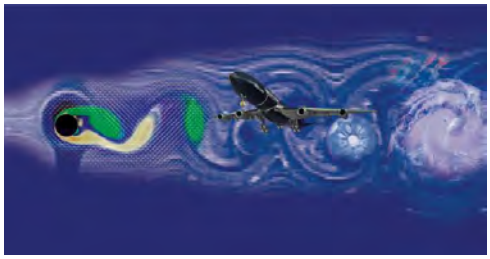

Laser imaging is recognized as the most valuable diagnostic tool in fluid dynamics applications.

Instantaneous 2D and 3D flow images are measured with high spatial and temporal resolution.
Even time-resolved 3D imaging is possible for a comprehensive characterization of for example turbulent flow structures.

Laser Induced Fluorescence (LIF) is the most versatile and practical laser imaging technique for measuring scalar flow parameters such as concentration, mixture fraction, fluid composition and temperature.

Particle Image Velocimetry (PIV) is the established and most powerful method for flow field imaging.
Laser imaging is applied in all kinds of fluid flows such as laminar, turbulent, reactive and multiphase flows and is used for the investigation of e. g. thermal flows, mixing processes and detailed flow field analysis.

Digital Image Correlation (DIC) for surface deformation imaging can be simultaneously applied with PIV measuring the interacting flow field for the investigation of Fluid-Structure Interaction (FSI) phenomena.

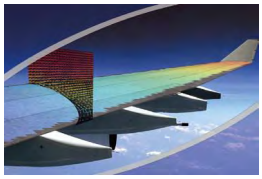

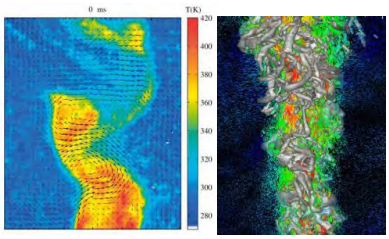

Example results: Thermal flow field imaging and 3D flow field of a large scale convective air plume

Advantages of laser imaging

- instantaneous, non-intrusive and quantitative flow imaging,
- excellent spatial and temporal resolution,
- 2D, 3D and even 4D flow imaging,
- versatile technology supporting multi-parameter flow measurements.

Fluid Master System

FluidMaster is a complete laser imaging system family for the quantitative visualization of thermal flows and mixing processes in fluids.
Instantaneous concentration and temperature fields are measured with high spatial and temporal resolution.

Applications
investigation of fluid mixing, thermal flows and flow structures, flow visualization in wind tunnels and turbomachinery applications, air film cooling, hydrodynamics.

Information

- quantitative visualization of concentration and temperature fields in fluids,
- pH-imaging and degree of reactive mixing in liquids,
- gas density measurements in thermal flows.

System Features

- integrated turnkey laser imaging systems based on application matched best selection of laser and camera,
- complete hardware control using DaVis software,
- accurate hardware and signal calibration,
- most effective LIF excitation techniques,
- Rayleigh thermometry package for thermal gas flows,
- oxygen (O2)-LIF imaging module.

Specials

- 3D-imaging setups,
- time resolved imaging, digital film recording.

Imaging Techniques

- LIF, Raman, Rayleigh

Eurotek International is an added value reseller and solution provider. Eurotek represents in Poland Dantec Dynamics company – the world famous producer non invasive, point, planar and volumetric technics. Our activity divides into two major areas: optical / laser based measurements and laser based machines and devices.

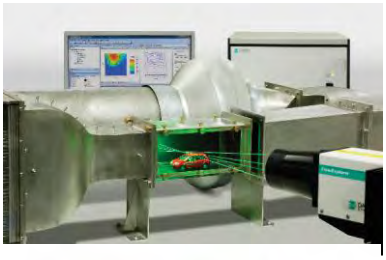

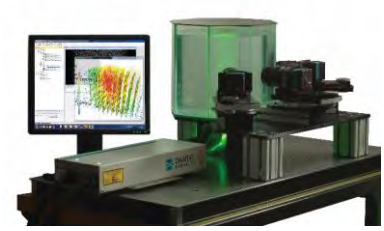

During 20 years of continuous activity we acquired the expertise in:

- point and field measurements of liquid flow (anemometry and imaging)
- optics, photonics
- laser technology.

Delivering and installing optical equipment to hundreds of customers allowed us to gain the necessary experience to answer some demanding challenges and deliver solutions. Below we compiled the major application fields, where the products we carry, are being used.

Application	Technique	Key components
High velocity wind tunnels	LDA	• High power lasers • large FL optical probes • High yield seeding generators • dedicated travers systems
	PIV / TR PIV	• High energy pulsed lasers • Dedicated light sheet optics and • beam delivery • High yield seeding generators • dedicated travers systems
	CTA	• Specialty CTA probes for high velocity • dedicated travers systems
Laser induced fluorescence. Combustion Multi – phase flows	LDA / Point LIF	• Blue/green TEM00 laser • Color filters
	Fluorescence Imaging	• Tunable dye lasers / OPO • Intensified (gated) cameras

Eurotek International Sp. z o.o., Al. Lotników 32/46, 02-668 Warszawa
tel. +48 22 843 79 40

Application	Technique	Key components
	PIV/LIF	• Tunable UV nanosecond dye lasers / OPO with narrow line • Intensified (gated) cameras
Microfluidics	Microscopic PIV	• Microscope coupled pulsed lasers / LEDs • CW lasers / gated cameras
	Optical Coherent Tomography	• OCT systems
	Doppler	• OCT systems with Doppler

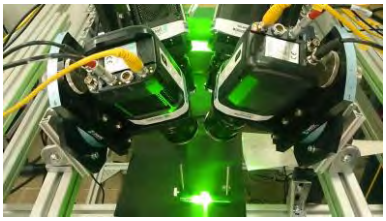

Volumetric PIV, 4 cameras, I kHz real-time

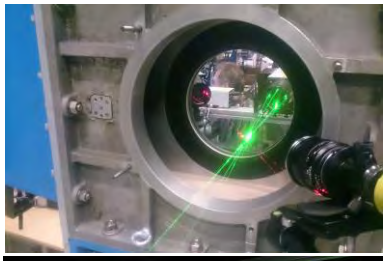

3D LDA setup at supersonic flow with 3D traversing mechanism

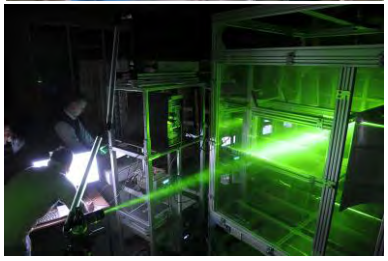

High energy Stereo-PIV for large area flow mapping

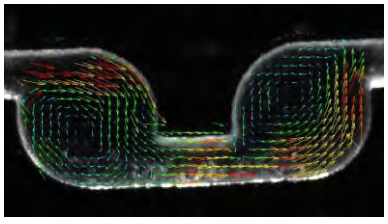

Micro-flow study. Flow channel with superimposed measured vector map. Channel size: 500 micrometers.

Eurotek International Sp. z o.o., Al. Lotników 32/46, 02-668 Warszawa
tel. +48 22 843 79 40

unisens.pl

Gdy każdy punkt się liczy

WIELOKANAŁOWE SKANERY CIŚNIENIA

- wielopunktowy pomiar ciśnienia różnicowego **od 4 cali H_2O do 850 psi**
- dla pojedynczego urządzenia **od 16 do 2048 kanałów**
- częstotliwość próbkowania **do 2000 Hz**
- wersje miniaturowe i w zabudowie przemysłowej
- pomiar rozkładu ciśnienia w tunelach aerodynamicznych
- badania silników turbinowych i turbin energetycznych
- funkcje:
  - przedmuchu kanałów
  - sprawdzania szczelności
  - re-zerowania
  - kalibracji

Gdy rozmiar ma znaczenie ›

unisens.pl

Gdy rozmiar ma znaczenie

MINIATUROWE CZUJNIKI CIŚNIENIA

- pomiar ciśnienia szybkozmiennego **od 0,35 bar do 70 bar**
- częstotliwości rezonansowe **od 40 kHz do 1,7 MHz**
- kompensacja temperaturowa **od -40°C do +90°C**
- rozmiar **od 1,27 mm**

- kompatybilne z gazami niekorozyjnymi i niektórymi płynami
- obudowy:
  - cylindryczne
  - z płaską membraną
  - z maską zabezpieczającą
  - gwintowane

Gdy każdy punkt się liczy

Politechnika Wrocławska

XXII Fluid Mechanics Conference
Słok near Bełchatów, 11–14 September 2016